Fracture Mechanics Based Lifetime Assessment and Long-term Failure Behavior of Polyethylene Pressure Pipes

("Bruchmechanische Lebensdauerabschätzung und Langzeit-Versagensverhalten von Druckrohren aus Polyethylen")

Andreas Frank

A Dissertation

in Candidacy for the Degree of

Doktor der montanistischen Wissenschaften

University of Leoben, April 2010

STATUTORY DECLARATION

Hereby I state in lieu of an oath, that the presented Dissertation has been written by myself and that no illegitimate aid but the literature cited and the support indicated has been used.

Leoben, April 2010 (Andreas Frank)

ACKNOWLEDGMENTS

I wish to express my gratitude to my Advisor Prof. Reinhold W. Lang for introducing me to the principles of scientific work in material science and testing of plastics and to the subject of fracture mechanics on polymers. His expertise and advice always opened new perceptions concerning the topics of this Dissertation. I am also grateful to the second member of my Doctoral Committee Prof. Nicolai Aust for his interest in my work.

I am also indebted to Prof. Gerald Pinter for his guidance and help during the last years and for numerous discussions frequently going beyond our professional collaboration. His excellent knowledge in the field of polymer physics and testing of plastics and particular his expertise in the slow crack growth behavior in PE-HD under static and cyclic loads have led to major findings and improvements during the development of this Thesis.

The research work of this Dissertation was performed at the Polymer Competence Center Leoben GmbH (PCCL, Austria), within the framework of the K_{plus}-program of the Austrian Ministry of Traffic, Innovation and Technology with contributions by the University of Leoben, AGRU Kunststofftechnik GmbH (Austria), Borealis Polyolefine GmbH (Austria), OMV Exploration & Production GmbH (Austria), the Austrian Association for Gas and Water (ÖVGW, Austria), Rabmer Rohrtechnik GmbH & Co.KG (Austria) and SABIC Europe (Netherlands). The PCCL is funded by the Austrian Government and the State Governments of Styria and Upper Austria. I would like to acknowledge the members of the project partners for their support: Markus Haager, Siegfried Liedauer, Wolfgang Havlik and Karin Thayer, Josef Grafeneder and Klaus Neumann, Abraham Hofmann, Mary McCarthy and Linda Havermans van Beek.

Furthermore, I would like to thank my colleagues of the PCCL for many discussions and help in recent years. Representing all, I would like to mention our business manager Martin Payer and his team Jana Maurer, Ines Petek, Elke Holzer, Kerstin Fischer and Michael Berschl for having always provided help concerning the projects as well as activities going beyond our professional work. Sincere ap-

preciation is also expressed to the team of the Institute of Material Science and Testing of Plastics, especially to Jürgen Föttinger for manufacturing an uncountable number of specimens.

Moreover, I would like to address my gratitude to Gernot Mannsberger, Werner Freimann, Anna Maria Hartl, Anita Redhead and Verena Strecher, who contributed much of the experimental work in this Dissertation in the context of their own Bachelor respectively Master Theses.

My sincere gratitude is expressed to my family which assisted me over so many years. I wish to thank my parents Karin and Peter as well as my sisters Anna-Maria and Angelika, and my brother Alexander for their support and motivation during my path of life. Finally, I am indebted to my girlfriend Barbara for her patience and devoted helpfulness.

ABSTRACT

Polyethylene (PE) has become one of the most important materials for pipe applications in the context of gas and water distribution, which results in required service times of at least 50 years for pressurized PE pipes nowadays. To characterize the resistance against the critical failure mechanisms of crack initiation and slow crack growth, several standardized methods are available for a qualitative ranking of different PE types.

With linear elastic fracture mechanics (LEFM), a tool for lifetime prediction of structures like pressure pipes is available, for which the knowledge of material and temperature specific crack growth laws is of fundamental importance. The primary objectives of this Dissertation therefore were to develop and carry out a test program for the detection of relevant material parameters for crack growth laws for PE pipe grades at application near temperatures of 23 °C and to perform a fracture mechanics prediction of the lifetimes of pressurized PE pipes.

A further aspect in the long-term application of pipes is related to the repair and rehabilitation of existing pipe systems. One of the most important trenchless technologies is the pipe rehabilitation with a Close-Fit-Liner. Within the scope of this method a folded PE pipe has to be inserted into an old pipe and reforms during a temperature controlled installation procedure. Due to the fact that there are no scientific studies on material changes available yet, a further objective of this Dissertation was a comprehensive investigation of the influence of the deformation processes associated with this procedure on relevant material properties.

In order to provide a lifetime prediction methodology for pressurized pipes, a fracture mechanics concept was applied. To determine the creep crack growth kinetics under static loads, the fatigue crack growth kinetics of cyclic tests at different loading ratios (R-ratios) was extrapolated to static loading conditions. To address the issue of technical feasible testing times – especially for fracture mechanics testing of modern PE pipe grades – cracked round bar (CRB) specimens were used. For a direct measurement of the crack growth kinetics in the CRB specimens a system of three extensometers was applied, which detects the crack length by measuring

the specimen compliance. After having created a compliance-calibration curve it was possible to measure the crack growth kinetics in a single CRB fatigue test.

With the mentioned test and extrapolation procedure, so called “synthetic” crack growth curves for static loading were developed for different PE types to obtain the relevant fracture mechanics parameters. To predict the lifetime, different calculations for the stress intensity factor in an internal pressurized pipe from literature and finite element methods were compared. As part of a sensitivity study, the influence of different boundary conditions like the crack front geometry or the initial defect size, which must be considered in lifetime calculations, were investigated.

The predicted lifetimes for the tested PE 80 and PE 100 pipe grades show meaningful results, which indicate lifetimes for pressurized pipes of at least 50 years. A case study, in which two old PE pipes from real field installation were investigated, point out that even after a service period of several decades, a sufficient residual lifetime can be expected to reach the required overall service time. As to the calculation model, all predicted lifetimes were on the conservative side and got an additional safety, as the considerable fraction of crack initiation was not considered. The required times for testing of a given material were up to 2 month for the PE 80 type and approx. up to 4 months for the PE 100 type. Therefore, an enormous advantage in testing time can be considered compared to standardized test methods (i.e. pressurized pipe tests), which do not give information on the potential for quasi-brittle failure, even after 10^4 hours (> 1 year).

The morphological characterization of the Close-Fit-Liner improves the understanding of the interaction between the pipe deformation with the inserted molecular orientation and the memory effect which is essential for the inherent redeformation. Although the material is exposed to considerable thermal treatment during the installation (e. g. 80 °C for two hours), it could be shown that there is no significant thermo-oxidative aging taking place. However, a significant improvement of the finally installed Close-Fit-Liner was detected concerning the residual stresses, which were nearly completely reduced due to the additional heating step during installation. This result seems to cause a positive effect on the crack growth resistance of the material and thus is also considered to positively affect the structural reliability of Close-Fit-Liner pipes.

KURZFASSUNG

In der Gas- und Wasserversorgung hat sich Polyethylen (PE) zu einem der bedeutendsten Rohrwerkstoffe entwickelt, wobei die vorhergesagten Einsatzzeiten innendruckbelasteter PE-Rohrleitungen heute zumindest 50 Jahre betragen. Zur Charakterisierung des Widerstandes gegen die kritischen Versagensmechanismen der Rissinitiierung und des langsamem Risswachstums steht eine Reihe standardisierter Prüfverfahren zu Verfügung, die eine qualitative Reihung unterschiedlicher PE-Typen ermöglichen.

Die Lebensdauer von Strukturen, wie z. B. innendruckbelastete Rohrleitungen, kann mithilfe der Linear-Elastischen Bruchmechanik (LEBM) abgeschätzt werden, wobei die Kenntnis der material- und temperaturspezifischen Risswachstumskinetik bei statischer Belastung von entscheidender Bedeutung ist. Die primären Ziele dieser Dissertation waren daher die Erstellung und Durchführung eines Prüfprogramms zur Bestimmung der relevanten Materialparameter bei anwendungsnahen Temperaturen von 23 °C und die bruchmechanischen Lebensdauervorhersage von PE-Druckrohren.

Ein weiterer Aspekt in der Langzeitanwendung von Rohrleitungen umfasst die Sanierung und Rehabilitierung bestehender Systeme. Eine der wichtigsten grabenlosen Technologien ist die Sanierung mit Close-Fit-Linern, bei der ein werkseitig gefaltetes PE-Rohr in ein bestehendes Altrohr eingezogen und unter Temperatureinfluss wieder rückdeformiert wird. Da zu diesem Thema bisher keine werkstoffkundlichen Daten vorliegen, war ein weiteres Ziel dieser Dissertation, eine umfangreiche Untersuchung des Einflusses der Deformationsvorgänge auf relevante Werkstoffeigenschaften durchzuführen.

Für die Lebensdauerabschätzung von innendruckbelasteten Rohren wurde ein bruchmechanisches Konzept basierend auf den Mechanismen der langsamen Rissausbreitung verwendet, wobei die Wachstumsgeschwindigkeiten von Rissen bei zyklischer Belastung (Ermüdung) unter unterschiedlichen Spannungsverhältnissen (R-Verhältnis) auf die statische Belastungssituation extrapoliert wurden. Um speziell bei modernen PE-Rohrwerkstoffen technisch sinnvolle Prüfzeiten zu gewährleisten, wurden zylindrisch gekerbte Prüfkörper („cracked round bar“, CRB)

verwendet. Eine direkte Messung der Risskinetik mit CRB-Prüfkörpern erfolgte über ein System von drei Extensometern, welches die Risslänge über die Prüfkörpernachgiebigkeit erfasst. Mithilfe einer Nachgiebigkeits-Kalibrierkurve war es möglich, die Risskinetik in einem einzelnen zyklischen CRB-Versuch zu messen.

Mit der beschriebenen Prüf- und Extrapolationsmethodik wurden für eine Reihe von PE-Typen „synthetische“ Risswachstumsgeschwindigkeiten bei statischer Belastung bestimmt und entsprechende bruchmechanische Kennwerte abgeleitet. Für die Lebensdauer-Modellrechnungen wurden verschiedene Berechnungen des Spannungsintensitätsfaktors in einem innendruckbelasteten Rohr aus der Literatur und basierend auf Finite-Elemente-Methoden gegenübergestellt. Im Rahmen einer Sensitivitätsanalyse erfolgte eine Untersuchung von Einflussfaktoren, wie z. B. die Form der Risswachstumsfront oder die Anfangsdefektgröße, welche bei der Lebensdauerabschätzung als Randbedingungen berücksichtigt wurden.

Die für die getesteten Rohrtypen PE 80 und PE 100 berechneten Lebensdauern von innendruckbeanspruchten Rohren ergaben durchaus plausible Ergebnisse, welche auf Versagenszeiten von 50 Jahren und mehr hinweisen. Eine Fallstudie an zwei PE-Rohren aus realen Installationen deutet zudem darauf hin, dass trotz bereits jahrzehntelangem Betrieb die erforderlichen Restlebenszeiten erreicht werden dürften. Die auf derartigen Modellrechnungen basierenden Lebensdauerabschätzungen lagen zudem auf der konservativen Seite, da der beträchtliche Anteil der Rissinitiierung nicht berücksichtigt wurde. Der Zeitaufwand für die Materialprüfung betrug je Werkstoff ca. 2 Monate für PE 80 Rohrtypen und ca. 4 Monate für Werkstoffe vom Typ PE 100, was einen erheblichen Vorteil gegenüber genormten Prüfverfahren (Zeitstandinnendruckversuch) darstellt, wo selbst nach 10^4 Stunden (> 1 Jahr) keine Informationen über das potentielle quasi-spröde Versagen generierbar sind.

Die morphologische Charakterisierung der vorgeformten und rückdeformierten Close-Fit-Liner vertiefte vor allem das Verständnis für die Wirkungsweise der Molekülorientierungen und dem damit verbundenen Memory-Effekt, welcher entscheidend für den Installationsprozess ist. Es wurde gezeigt, dass trotz der erheblichen zusätzlichen thermischen Belastung während der Installation keine signifikanten thermo-oxidativen Alterungsvorgänge stattfinden. Eine wesentliche

Verbesserung des installierten Close-Fit-Liners wurde bei den Eigenspannungen konstatiert, die durch die thermisch begleitete Installation nahezu vollständig abgebaut werden. Dieser Effekt dürfte sich auch positiv auf das Risswachstumsverhalten auswirken, sodass insgesamt eine gute Zuverlässigkeit derart installierter Rohre gegeben erscheint.

TABLE OF CONTENTS

PART II

LONG-TERM FAILURE BEHAVIOR OF A POLYETHYLENE CLOSE-FIT-LINER

PART III

APPENDIX - SELECTED PUBLICATIONS

1 INTRODUCTION AND OBJECTIVES

1.1 Background and motivation

Buried pipes contribute an inconspicuous but very important part to the maintenance of the infrastructure in our modern society and depending on transported goods their applications vary in a wide range. Especially pressurized plastics pipes have been used successfully for several decades, and pipe systems made of polyethylene (PE) have been employed widely in fuel gas and water supply as well as in sewage systems for more than 50 years (Richard et al., 1959; Gaube et al., 1985; Lang, 1997; Lang et al., 1997; Janson, 1999; Brömstrup, 2004). Whereas such pipes were used initially in the low pressure regime up to 4 and 6 bars, respectively, in the case of gas and water pipes, due to advancement in material performance they are now being operated at pressure levels of up to 10 bar (gas pipes) and 16 bar (water pipes).

In 2007, the worldwide demand for pipes made of high density polyethylene (PE–HD) was about 3.7 million tons, and with a growth rate of six percent per year up to 4.9 million tons are expected in 2012 (Brescia, 2008). Turning to Austria, the pipe systems for gas transportation at maximum operating pressures (MOP) above 6 bar for example are clearly dominated by steel, which is also illustrated in Fig. 1.1. Whereas about 6500 km of steel pipes were used in 2008, other materials, like PE with about 53 km in 2008 are of only inferior importance in this field of application.

However, at pressure levels up to an MOP of 6 bar a different distribution of the used materials is found (Fig. 1.2). Whereas the lengths of pipe systems made of materials like steel, ductile cast iron or polyvinylchloride (PVC) remain constant at levels below 4,000 km, PE has become the most important material for pipes in this pressure range. The amount of installed PE pipes for gas transportation in Austria increased constantly from about 16,000 km in 2002 to more than 20,000 km in 2008.

Pressurized pipes made of PE are designed to fulfill operating times of at least 50 years. As a result of improvements of the raw materials, an increase in minimum

service life to possibly 100 years has been proposed most recently for the last generation PE materials of the PE 100 type (Brömstrup, 2004; Hessel, 2007). Due to this extension in operating times as well as due to the fact that repairing and rehabilitation of defect pipes is always associated with high technical efforts and extensive costs, the reliability of these pipe systems is of major significance, and a reliable lifetime prediction with modern methods is essential.

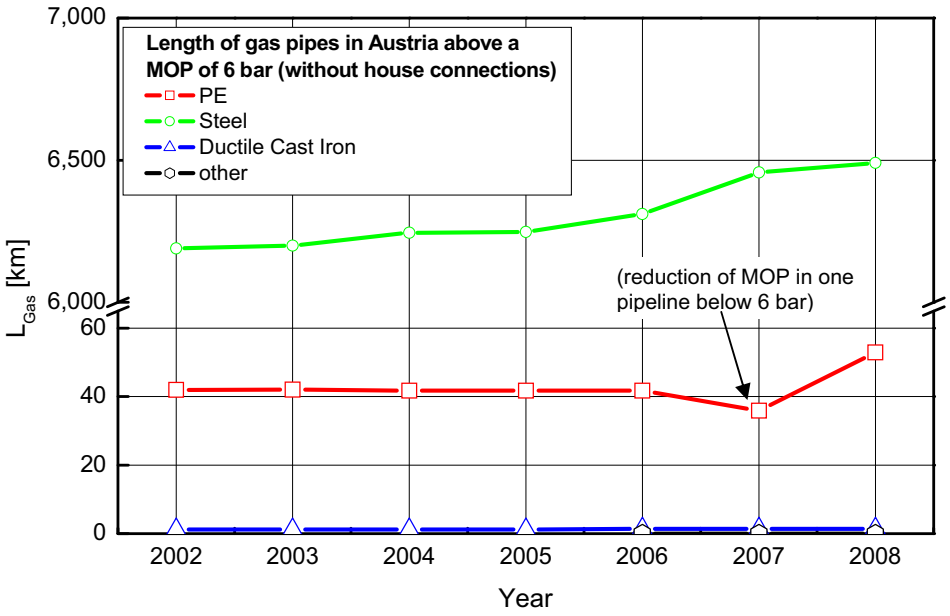

Fig. 1.1: Total pipe lengths of gas pipes at an MOP above 6 bar installed in Austria per material. House connections not considered (Source: ÖVGW, 2009).

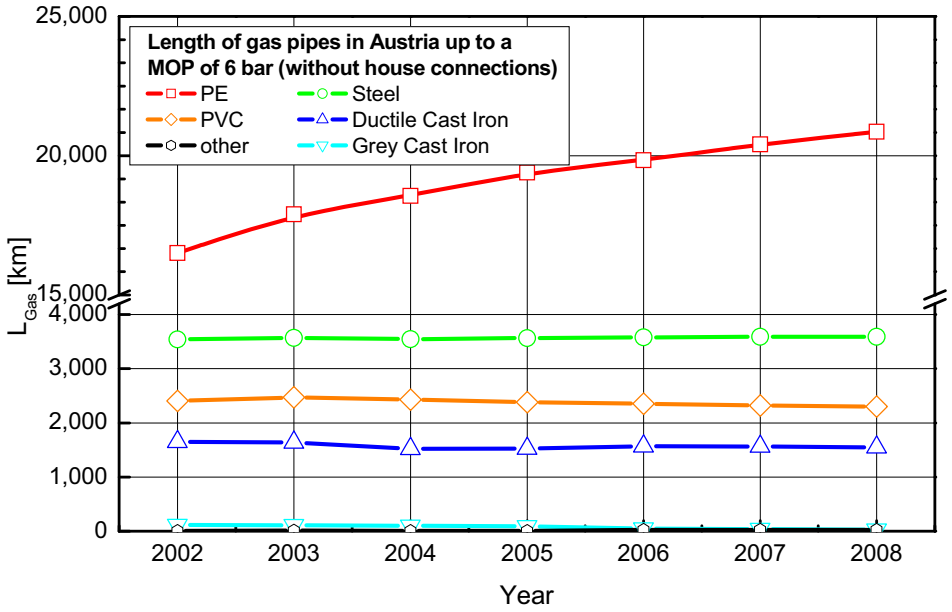

Fig. 1.2: Total pipe lengths of gas pipes at an MOP up to 6 bar installed in Austria per material. House connections not considered (Source: ÖVGW, 2009).

Crack initiation and slow crack growth (SCG) represent the critical failure mechanisms in long-term applications of pressurized plastic pipes (Barker et al., 1983; Gaube et al., 1985; Ifwarson, 1989; Brown and Lu, 1993; Lang et al., 1997). State of the art lifetime predictions, that consider this quasi-brittle failure mechanism, are based on internal pressure tests at different temperatures and a standard extrapolation method described in EN ISO 9080:2003 which classifies PE pipe grade materials by their minimum required strength (MRS) to ensure service times of at least 50 up to 100 years.

Nowadays, modern materials with the classification PE 100 (MRS=10 MPa) are available in such fields, where essential improvements in the raw material, particularly in the bimodal molecular mass distribution and in the controlled implementation of short chain branches, have led to materials with a significant increase in the resistance against crack initiation and SCG (Brown et al., 1992). These improvements indeed shift the critical failure mechanisms in internal pressure tests to unpractical time scales resulting in time consuming and expensive test procedures.

To meet the demand for new accelerated characterization methods to describe the resistance against crack initiation and SCG, different laboratory tests like the Notched Pipe Test (NPT; Kuhlman et al., 1992; Beech et al., 2001; ISO 13479, 2009), the Pennsylvenia Edge-Notch Test (PENT; Beech, et al., 1998; ISO 16241, 2005; ASTM F1473, 2007) or the Full Notch Creep Test (FNCT; Fleissner, 1987, 1998; ISO 16770, 2004) have been developed. Compared to these static tests, a significant acceleration of testing times was achieved by cyclic tests (fatigue) and especially tests with cracked round bar (CRB) specimens have been proposed and have shown a high potential for a quick ranking of different PE pipe grades, even at application near temperatures of 23 °C and without any additional stress cracking liquid (Lang et al. 2005; Haager, 2006; Haager et al., 2006; Pinter et al., 2006; Balika et al., 2007; Pinter et al., 2007).

Although all of the methods mentioned are well established and therefore capable of correlating the resistance against responsible failure mechanisms of different PE pipe grades, a science-based quantitative prediction of the lifetime of pressurized pipes has not been possible yet as they do not provide any or at least not sufficient information concerning the kinetics of slow growing cracks under service-

like conditions. However, the knowledge of the material specific crack growth kinetics is essential for a reliable prediction of the time a crack needs to grow through a structure like a pipe wall until final failure.

A different but nevertheless important aspect of pipe systems with long service times is the rehabilitation of old or defect pipes. Rehabilitation of existing water and gas supply piping systems (e. g. cast iron and asbestos-cement) is expected to be one of the driving forces for a steady growth of the PE pipe market in Europe. Trenchless techniques are increasingly popular and cost effective for the renewal of piping systems using preformed PE pipes. The technology of Close-Fit-Lining is one of the most modern methods and although it has become one of the most important one (Glanert and Schulze, 2002), hardly anything has been published regarding the long-term behavior of preformed pipes. It is expected that the deformation and the thermal exposure during preforming as well as during installation alters the morphology of the pipe and can change the performance compared to the original pipe. Focusing on operating times of at least 50 years, the understanding of material changes and the knowledge of relevant long-term properties of such pipes is of high interest.

1.2 Scope and overall objectives

Based on the problems encountered with the original fracture mechanics approaches, a new concept for an accelerated lifetime prediction of PE pressure pipes has already been proposed by Lang and Pinter (Lang et al., 2005). This concept is based on cyclic tests at different loading ratios and the extrapolation of specific “synthetic” fatigue crack growth rates into the case of static loading. The implementation of CRB specimens to create a test method with relatively short testing times at application near temperatures was one of the major aims of this Dissertation.

The developed test procedure has been used to study the crack growth kinetics in selected pipe grade PE’s: an elder PE 80 material, which represents thousands of kilometers of installed pipes today, and a modern PE 100 material with an improved resistance against long-term failure. To close the gap between theoretical laboratory tests and real pipe applications the concept has also been applied to real pipes already in service for several years to predict their residual life time.

To ensure a realistic fracture mechanics lifetime prediction, different boundary conditions which may affect the calculations have been investigated within a sensitivity study. Parallel to the material investigations, a simulation model based on finite element methods (FEM) has been developed to combine practical test results with modern computational methods (the development of the FEM simulation model itself was not part of this Dissertation). The FEM simulation of pipes under complex loading situations provides the possibility to predict lifetimes for pipes close to real installation conditions.

To focus on the Close-Fit-Lining technology, a comprehensive investigation had to be conducted in order to study the influence of typical deformation and redeformation processes on relevant material parameters and their interaction with structure properties. In this case special attention was paid to the influence of the additional thermal and mechanical treatment on the morphology and on material ageing. Moreover, a further aim was to study the potential influence of this specific prehistory on the resistance against crack initiation and SCG.

1.3 Structure of this Dissertation

This Dissertation has been developed within the scope of the Projects II-3.5 "*A Novel Qualification Concept for Lifetim e and Safety Assessm ent of PE Pressure Pipes for Arbitrary In stallation Conditions*" and II-3.6 "*Long-term behavior of preformed PE-HD pipes* ", which formed part of the K_{plus} research program of the Polymer Competence Center Leoben GmbH (PCCL). Several publications which address different issues of these projects have been published in scientific journals and have been presented at international conferences during the last years.

The structure of this Dissertation is divided into three parts. Whereas **Part I** and **Part II** refer to the two main topics of the development of a fracture mechanics test method and the long-term behavior of PE Close-Fit-Liner, respectively, a selection of publications in **Part III** form the framework of this Dissertation:

Part I: Lifetime assessment of polyethylene pressure pipes based on an accelerated fracture mechanics test procedure

Part II: Long-term failure behavior of a polyethylene Close-Fit-Liner

Part III: Appendix – Selected papers

Following this introduction, **Part I** provides a brief review on the failure behavior of pressurized pipes and a summary of the used basic elements of LEFM. Afterwards, the stress intensity factor concept – an essential part in fracture mechanics investigations on crack growth kinetics and lifetime predictions – will be described. Furthermore, the extrapolation concept for which Lang and Pinter proposed cyclic tests for the accelerated extrapolation of the crack growth kinetics to static loading will be described (Lang et al., 2005).

Based on this concept, a procedure for the direct measurement of SCG in CRB specimens was developed and different PE materials were tested to evaluate the crack growth kinetics for static loading conditions. A sensitivity study investigates the effect of various assumptions in the boundary conditions of the applied fracture mechanics approach. Finally, a lifetime prediction of pressurized pipes based on the generated parameters of the tested materials was conducted.

Part II then focuses on the importance and the demand for pipe rehabilitation in general and provides basic information concerning trenchless pipe rehabilitation with the Close-Fit-Liner technology. A comprehensive investigation of the effects of preforming and redeformation of Close-Fit-Liners will be described. This study primary focuses on the influence of the additional mechanical and thermal treatment during deformation and redeformation of the pipes on changes in morphology, material aging and residual stresses. The changes in these material properties and their effect on the long-term performance of the final state of the redeformed Close-Fit-Liner compared to original pipe are of special interest in this part.

Major findings covering several issues of the described **Part I** and **Part II** have been published yet. Hence, **Part III** of this Dissertation provides a selection of seven publications which are collected in the Appendix and which form the framework of **Part I** and **Part II**, respectively. Whereas **Papers I-1** to **I-5** cover the major aspects of lifetime assessment of polyethylene pressure pipes based on an accelerated fracture mechanics test procedure (**Part I**), the **Papers II-1** and **II-2** refer to the long-term failure behavior of a polyethylene Close-Fit-Liner (**Part II**).

1.4 References

ASTM F1473 (2007). Standard Test Method for Notch Tensile Test to Measure the Resistance to Slow Crack Growth of Polyethylene Pipes and Resins.

Balika, W., Pinter, G., Lang, R.W. (2007). "Systematic investigations of fatigue crack growth behavior of a PE-HD pipe grade in through–thickness direction", Journal of Applied Polymer Science, 103(3), 1745-1758.

Barker, M.B., Bowman, J.A., Bevis, M. (1983). "The Performance and Cause of Failure of Polyethylene Pipes Subjected to Constant and Fluctuating Internal Pressure Loadings", Journal of Materials Science 18: 1095-1118.

Beech, S.H., Mallinson, J.N. (1998). “Slow Crack Growth Performance of Today's Plastics Pipeline Materials”, Plastics Rubber and Composites Processing and App. 27, 418-423.

Beech, S.H., Fergurson, C.R., Clutton, E.Q. (2001). “Mechanisms of Slow Crack Growth in PE Pipe Grades”, in Proc. "Plastics Pipes XI", 401-410, München, Germany.

Brescia, G. (2008). “The changing World of the Chemical Industry and its impact on the Pipe Industry”, Proceedings of Plastics Pipes XIV, Budapest, Hungary (2008).

Brömstrup, H. (2004). Vulkan Verlag, Essen, Deutschland.

Brown, N., Lu, X., Huang, Y., Harrison, I.P., Ishikawa, N. (1992). “The Fundamental Material Parameters that Govern Slow Crack Growth in Linear Polyethylens”, Plastics, Rubber and Composites Processing and Applications 17(4): 255-258.

Brown, N., Lu, X. (1993). "Controlling the Quality of PE Gas Piping Systems by Controlling the Quality of the Resin", Proceedings of the 13th Plastic Fuel Gas Pipe Symposium, San Antonio, Texas, USA.

EN ISO 9080 (2003). Plastics piping and ducting systems - Determination of the long-term hydrostatic strength of thermoplastics materials in pipe form by extrapolation.

Fleissner, M. (1987). “Langsames Risswachstum und Zeitstandfestigkeit von Rohren aus Polyethylen”, Kunststoffe 77, 45-50.

Fleissner, M. (1998). “Experience with a Full Notch Creep Test in Determining the Stress Crack Performance of Polyethylene”, Polymer Engineering and Science 38, 330-340.

Gaube, E., Gebler, H., Müller, W., Gondro, C. (1985). "Zeitstandfestigkeit und Alterung von Rohren aus HDPE", Kunststoffe 75(7), 412-415.

Glanert, R., Schulze, S. (2002). "U-Liner - Der Klassiker für die Sanierung von Druckrohren", 3R International, 41(1), 16-19.

Haager, M. (2006). "Fracture mechanics methods for the accelerated characterization of the slow crack growth behavior of polyethylene pipe materials", Doctoral Dissertation, Institute of Materials Science and Testing of Plastics, University of Leoben, Austria.

Haager, M., Pinter, G., Lang, R.W. (2006). “Ranking of PE Pipe Grades by Cyclic Crack Growth Tests with Cracked Round Bar Specimen”. ANTEC 2006, Charlotte, North Carolina, USA, Society of Plastics Engineers.

Hessel, J. (2007). “100 Jahre Nutzungsdauer von Druckrohren aus Polyethylen - Aussage wissenschaftlich bestätigt”, Vortrag 1, Wiesbadener Kunststoffrohrtage 2007, Wiesbaden, Deutschland.

Ifwarson, M. (1989). "Gebrauchsdauer von Polyethylenrohren unter Temperatur und Druckbelastung", Kunststoffe 79(6), 525-529.

ISO 13479 (2009). Polyolefin pipes for the conveyance of fluids - Determination of resistance to crack propagation - Test method for slow crack growth on notched pipes.

ISO 16241 (2005). Notched Tensile Test to Measure the Resistance to Slow Crack Growth of Polyethylene Materials for Pipe and Fitting Products (PENT).

ISO 16770 (2004). Plastics - Determination of Environmental Stress Cracking (ESC) on Polyethylene (PE) - Full Notch Creep Test (FNCT).

Janson, L.E. (1999). "Plastics Pipes for Water Supply and Sewage Disposal", Borealis, Sven Axelsson AB/ Fäldts Grafiska AB, Stockholm, Schweden.

Kuhlman, C.J., Tweedy, L.K., Kanninen, M.F. (1992). “Forecasting the Long-Term Service Performance of Polyethylene Gas Distribution Pipes”, in Proc. "Plastics Pipes VIII", C2/3-1, Konigshof, Netherlands.

Lang, R.W. (1997). "Polymerphysikalische Ansätze zur Beschreibung des Deformations- und Versagensverhalten von PE-Rohren", 3R International 36, 40-44.

Lang, R.W., Stern, A., Doerner, G. (1997). "Applicability and Limitations of Current Lifetime Prediction Models for Thermoplastics Pipes under Internal Pressure", Die Angewandte Makromolekulare Chemie 247, 131-137.

Lang, R.W., Pinter, G., Balika, W. (2005). "Ein neues Konzept zur Nachweisführung für Nutzungsdauer und Sicherheit von PE-Druckrohren bei beliebiger Einbausituation", 3R International, 44(1-2), 33-41.

Pinter, G., Haager, M., Balika, W., Lang, R.W. (2007). "Cyclic crack growth tests with CRB specimens for the evaluation of the long-term performance of PE pipe grades", Polymer Testing 26 (2), 180–188.

Pinter, G., Haager, M., Lang, R.W. (2006). "Accelerated Quality Assurance Tests for PE Pipe Grades", ANTEC 2006, Charlotte, North Carolina, USA, Society of Plastics Engineers, 2480-2484.

Richard, K., Gaube, E., Diedrich, G. (1959). “Trinkwasserrohre aus Niederdruckpolyäthylen”, Kunststoffe 49(10): 516-525.

PART I

LIFETIME ASSESSMENT OF POLYETHYLENE PRESSURE PIPES BASED ON AN ACCELERATED FRACTURE MECHANICS TEST PROCEDURE

2 GENERAL BACKGROUND AND MATERIAL SELECTION

The long-term failure behavior of pressurized PE pipes is characterized by the determination of the long-term hydrostatic strength with internal pressure tests, regulated in EN ISO 9080. Testing times with this method typically last about 1 year and the testing of pipes that do not fail is usually stopped after a testing period of 10^4 hours (approx. 13.5 months). However, this means that especially for modern PE types of the classification PE 80 and PE 100 nearly no quantitative information concerning the relevant quasi-brittle failure region can be provided.

With the purpose of an accelerated correlation of different materials and their resistance against crack initiation and SCG, several specimen tests for an accelerated data generation have been implemented and compared (Haager, 2006). Although these tests are useful for material ranking and preselection, they do not provide any information concerning the kinetics of quasi-brittle growing cracks, though. However, this information is essential for a fracture mechanics lifetime prediction of pressurized pipes.

The following sections give a brief overview on the failure behavior of pressurized pipes and the applicability of linear elastic fracture mechanics. Especially the concept of the stress intensity factor and a fracture mechanics based lifetime prediction approach are summarized. Furthermore, the fracture mechanics approach based on cyclic tests, which has been proposed used to realize a novel qualification concept for a lifetime and safety assessment of PE pressure pipes, is described (Lang et al., 2005). An overview of the tested materials in context of this Dissertation closes this chapter.

2.1 Failure behavior of pressurized pipes

The standard test method which is generally used to characterize the long-term failure behavior of pressurized pipes is the internal pressure test, standardized in EN ISO 9080. The typical failure behavior of PE pipes that may occur in those tests has already been well investigated (Richard, 1959; Gaube et al., 1985; Lustiger, 1986; Kausch, 1987; Ifwarson, 1989, Lang et al., 1997) and can usually be divided into different characteristic failure regimens depending on the stress level.

Those regimens are schematically illustrated in Fig. 2.1 (Lang, 1997; Lang et al., 2005).

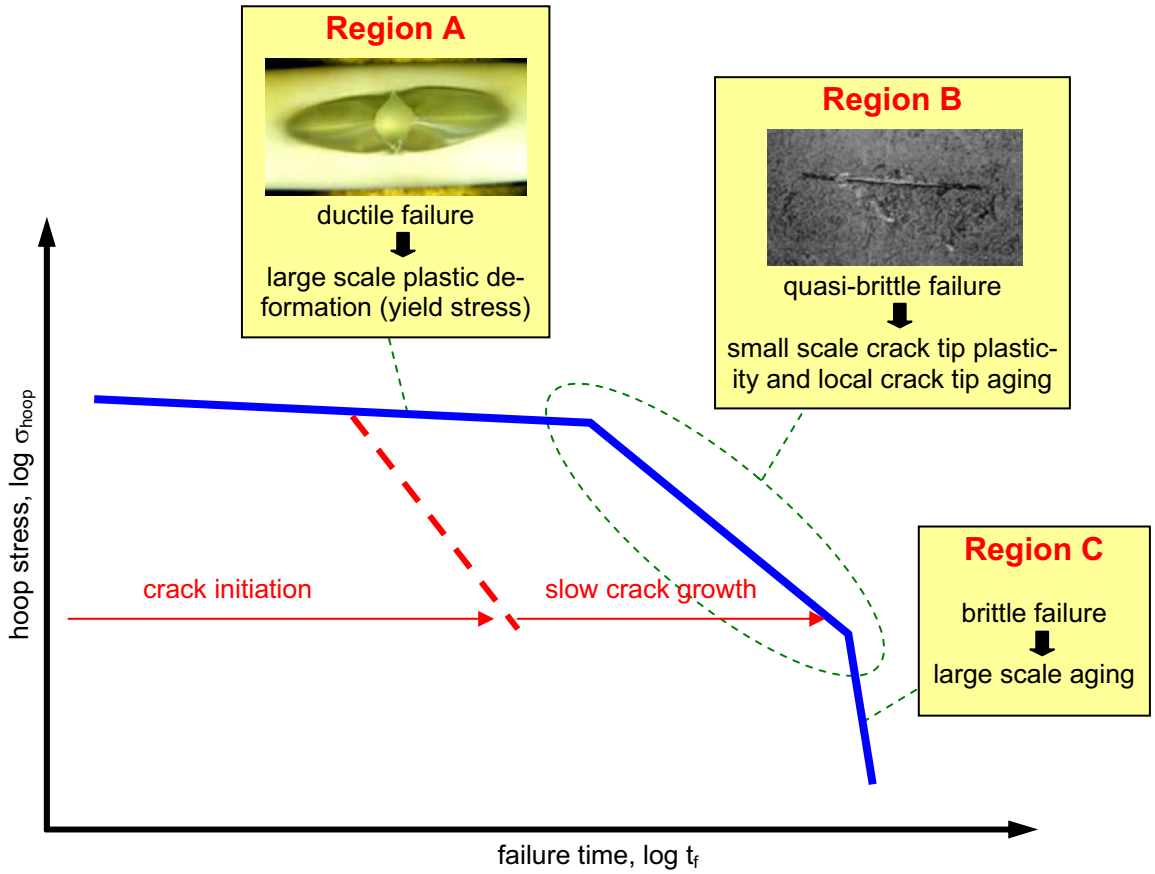

Fig. 2.1: Characteristic failure behavior of PE pressure pipes (Lang et al., 2005).

In Region A (or stage I) at high internal pressures the failure is dominated by ductile deformation with large plastic zones after relatively short times. This region is mainly controlled by the yield stress of the material and failure usually occurs at the smallest wall thickness or at defects (Krishnaswamy, 2005; Zhou et al., 2005).

At lower loads the failure mechanism passes a transfer knee and switches into the quasi-brittle failure Region B (stage II). In this region the failure is caused by crack initiation and SCG with only small scale plastic deformations at the crack tip. In the majority of cases the origins of slow growing cracks turn out to be microscopic defects near the inner pipe wall. Due to stress peaks cracks are initiated which grow continuously through the pipe wall. The total failure time of the pipe consists of both mechanisms: crack initiation time and SCG time (Barker et al., 1983; Stern, 1995; Lang et al., 1997; Pinter, 1999). Slow crack growth is significantly influenced

by the molecular mass of the PE as well as the concentration and length of short chain branches (co-monomer) (Lustiger, 1986; Böhm et al., 1992; Brown et al., 1992; Egan and Delatycki, 1995; Pinter, 1999; Pinter and Lang, 2004; Krishnaswamy, 2005).

The nearly load independent third failure Region C (stage III) becomes relevant after very long times and is the result of aging processes and polymer degradation. Whereas the effect of global aging of the material leads to the forming of a large number of cracks, only small stresses may cause a brittle failure of the pipe. The resistance against this failure is basically controlled by stabilizer systems (Gaube et al., 1985; Doerner, 1994; Stern, 1995; Choi et al., 2009).

For long-term applications of pressurized pipes it is very well accepted, that failure according to Region B represents the critical failure mechanisms. Slow crack growth is always connected to an initial defect which is usually located at or near the inner pipe wall surface (Barker et al., 1983; Stern, 1995; Pinter, 1999). This initial defect creates a stress singularity in which micro-deformations are nucleating local micro-voids simultaneously originating crazes. During the formation of the crazes a combination of local shearing in the amorphous phase and a transformation of the crystalline phase lead to highly drawn fibrils which enlarge the craze. During this time, which is the crack growth initiation time, the size of the initial defect remains essentially constant. Subsequently quasi-brittle crack growth gets initiated. At the same time the stress at the tip of the craze zone increases and continues the craze formation, respectively. This procedure of permanent craze formation and breakdown of fibrils is characteristic for quasi-brittle SCG and has already been investigated in the framework of numerous studies (Dugdale, 1960; Barenblatt, 1962; Friedrich, 1983; Lang, 1984; Lustiger, 1986; Kausch et al., 1999). As part of the described mechanisms of craze breakdown, chain disentanglement and chain rupture may be assumed to have a contribution to the failure of fibrils (Kausch, 1987; Lustiger and Ishikawa, 1991) and also local crack tip aging affects the mechanisms of SCG (Lang et al., 1997; Pinter, 1999; Pinter and Lang, 2003; Pinter et al., 2004).

2.2 Fracture mechanics approach for pipe lifetime assessment under static loads

A large body of scientific work over the past decades has shown, that linear elastic fracture mechanics (LEFM) provides reliable methods to describe and study structural failures of materials (Irwin, 1957; Hertzberg, 1989; Broek, 1986, 1988; Williams 1987; Dieter, 1988; Anderson, 1991). Originally developed for metals, the methods of LEFM may also be utilized for plastics materials (Hertzberg, 1980; Kinloch and Young, 1983; Lang, 1984; Stern, 1995; Stern et al. 1998) as long as the two following basic requirements are met (Lang, 1984):

- The global loading situation of specimen or component is within the range of linear viscoelasticity.
- The formation of plastic deformations at the crack tip is only small.

As already described in Section 2.1, quasi-brittle failure of pressurized PE pipes (Region B) results from small defects or cracks inside the pipe wall. The stress distribution in the vicinity of such a crack tip is described by the stress intensity factor K_I (Equation 2.1) which is a function of the global loading σ, the crack length a and a geometric factor Y that is well known for several specimens and component shapes (Murakami, 1990). It may also be derived from FEM simulation. The index “I” specifies the loading mode I, which refers to pure tensile crack opening and represents the most relevant loading mode for practical applications (Hertzberg, 1989).

$$K_I = \sigma \cdot \sqrt{a} \cdot Y \tag{2.1}$$

The crack growth kinetics da/dt is expected to be a function of K_I and typically results in an S-shaped relationship in a double logarithmic diagram. In Fig. 2.2 the crack growth kinetics (left) and failure times of internal pressure tests of pipes (right) for two different materials are shown schematically. Material 2 is the one with higher resistance against SCG. Hence, compared to Material 1 it fails after longer testing times. Analogously, at a given K_I-value the crack growth kinetics curve for material 2 shows a slower crack growth rate than the curve for material 1.

The region of stable crack growth rate can be described by the equation originally proposed by Paris and Erdogan (Equation 2.2) (Paris and Erdogan, 1963), in which the crack growth rate da/dt is a function of K_I and the constants A and m, which are material parameters depending on the material, the temperature and the loading conditions. Whereas the exponent m is dimensionless, the unit of the parameter A is mm/(sMPam$^{0.5}$), which, however, has no physical significance (Broek, 1988). If the crack growth kinetics for one geometric structure is known (e.g. test specimen), it can be calculated for any other component (e. g. pipe) as long as all geometrical and loading parameters are known.

$$\frac{da}{dt} = A \cdot K_I^{\,m} \tag{2.2}$$

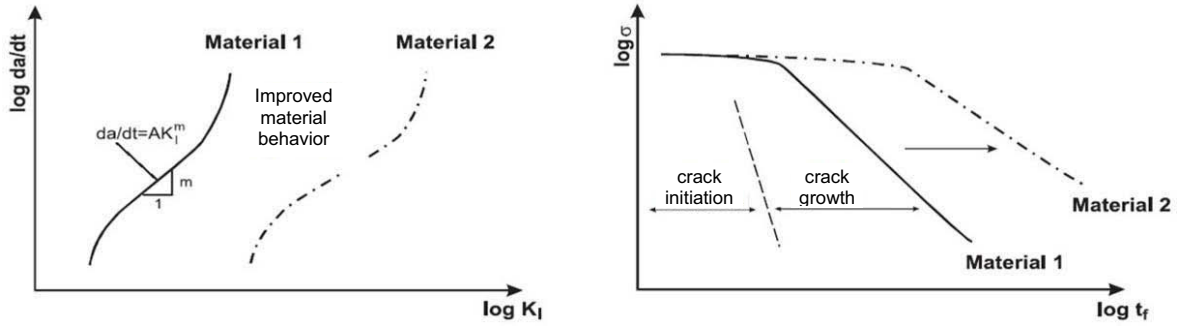

Fig. 2.2: Schematic illustration of the relationship between creep crack growth behavior and failure behavior of internal pressurized pipes (Lang, 1997).

The time a crack needs to grow through a component can be calculated by transforming Equation 2.2, so that the time for creep crack growth t_{CCG} from an initial defect size a_{ini} to a failure crack size of a_f is a function of the component-specific function of the stress intensity factor and the material parameters A and m at static loading conditions (Equation 2.3). The overall failure time t_f consists of the sum of the time for crack initiation t_{ini} and t_{CCG} (Equation 2.4). However, the evaluation of t_{ini} was not part of this Dissertation which implies, that all lifetime predictions are on the conservative side as they only take into account an immediately growing crack.

$$t_{CCG} = \frac{1}{A} \cdot \int_{a_{ini}}^{a_f} \frac{1}{K_I^{\,m}} \cdot da \tag{2.3}$$

$$t_f = t_{tot} \approx t_{in} + t_{CCG} \tag{2.4}$$

2.3 Fracture mechanics approach for pipe lifetime assessment based on cyclic tests

Specimen tests with cyclic loads are an important option to accelerate crack initiation and SCG. Different studies have suggested that within the boundaries of LEFM frequently the same failure mechanisms may be responsible for SCG in fatigue tests as for creep crack growth in static tests. Furthermore, those studies have proposed that the results of fatigue tests are in good accordance to internal pressure tests regarding the purpose of material ranking (Hertzberg and Manson, 1980; Chudnovsky, 1983; Barker et al., 1983; Lang, 1984; Shah et al., 1997, 1998a,b; Parsons et al., 1999; Parsons et al., 2000; Lang et al., 2004; Pinter et al., 2004; Haager et al., 2006; Lang et al., 2006; Pinter et al., 2006, 2007).

To deduce static failure behavior from fatigue tests, an extrapolation concept was proposed by Lang and Pinter, which also forms the base of this Dissertation (Lang et al., 2005, 2006; Pinter et al., 2007). A main objective of this Dissertation is to address and examine the open issues of the proposed extrapolation method and to transform the concept into a laboratory test procedure. Hence, some important parameters for fracture mechanics fatigue testing are defined below, followed by a brief overview of the proposed concept for an accelerated development of CCG curves at application near temperatures.

In contrast to static tests, a cyclic test (fatigue test) is also defined by its loading ratio R (Equation 2.5), which is the ratio of minimum-to-maximum load in a loading cycle. In that case, K_I, which is the driving force for SCG in a static test, changes to the difference of maximum and minimum stress intensity factor ΔK_I in a cyclic test (Equation 2.6).

$$R = \frac{F_{min}}{F_{max}} = \frac{K_{I,min}}{K_{I,max}} \tag{2.5}$$

$$\Delta K_I = K_{I,max} - K_{Imin} = K_{I,max} \cdot (1 - R) \tag{2.6}$$

Several studies show, that for a given value in $K_{I,max}$ a variation of the R-ratio may affect crack growth rates, with crack growth rates increasing as the R-ratio decreases. Thus, the dynamic component of a cyclic test was detected to be an es-

sential factor that may reduce testing times (Lang, 1984; Shah et al. 1997, 1998a,b; Parsons et al., 1999, 2000; Balika et al., 2007).

In cyclic tests the times for crack initiation and SCG are also a factor of the test frequency f, so that crack growth rates are usually defined as changes in the crack length per loading cycle N (Equation 2.7). The material parameters A' and m' in the respective Paris law, however, are unique for every single R-ratio. To correlate and compare the crack growth kinetics of fatigue and static loading, fatigue crack growth rates are multiplied with the test frequency to achieve crack growth rates per time unit (see Equation 2.8; Lang, 1984, Balika, 2003).

$$\frac{da}{dN} = A' \cdot \Delta K_I^{m'} \tag{2.7}$$

$$\frac{da}{dt} = \frac{da}{dN} \cdot f \tag{2.8}$$

To determine the CCG kinetics at static loading at application near temperatures of 23°C, Lang and Pinter proposed an extrapolation concept based on cyclic tests at different R-ratios (Lang et al., 2005). In this concept, static loading conditions are approached by a variation of cyclic test parameters as it is shown schematically in Fig. 2.3.

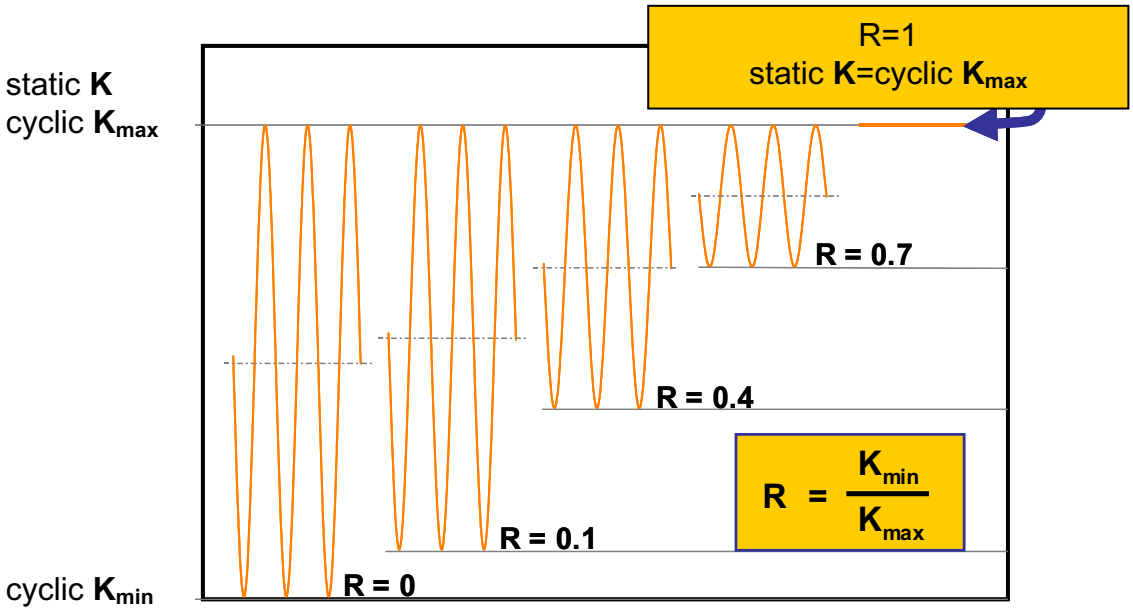

Fig. 2.3: Variation of K_I at various R-ratios (Lang et al., 2005).

For each single R-ratio a specific failure and kinetics curve is measured. Usually, an increasing R-ratio – which means a decrease of the loading range and the crack growth driving ΔK_I, respectively – causes a decrease of the corresponding crack growth rate by a simultaneously increasing failure time. Hence, the longest testing times are required for tests at R=1. If $K_{I,max}$ remains constant at different R-ratios, a mathematical extrapolation of the SCG rates measured at low R-ratios (and relatively short testing times) to the creep crack growth rate at R=1 should be possible, where the static K_I is equal to $K_{I,max}$ of a quasi-cyclic test. The extrapolation procedure proposed by Lang and Pinter for the generation of creep crack growth curves with cyclic tests includes up to four key steps, which are illustrated in Fig. 2.4 (Lang et al., 2005):

- First, fatigue tests with suitable specimens at different R-ratios (e.g. R=0.1, 0.4 and 0.7) and with similar $K_{I,max}$ are performed and analyzed in R-specific Woehler-curves.
- For each R-ratio the generated failure data are converted into “synthetic” FCG curves, using fracture mechanics computational methods and averaged crack growth rates.
- In the next step, the “synthetic” FCG curves at the different R-ratios are transformed into a diagram, in which $K_{I,max}$ is a function of R at constant crack growth rates. These curves are then extrapolated to static loading (R=1).
- Finally, the stress intensity factors for R=1 are transformed back into the crack growth kinetics diagram to generate a “synthetic” creep crack growth curve.

If cyclic crack growths rates are directly determined experimentally via appropriate techniques, it is not necessary to include steps 1 and 2 in the above procedure. From the generated “synthetic” creep crack growth curve the material parameters A and m can be obtained and furthermore be used for the calculation of the creep crack growth time t_{CCG} in any structure like in pipes.

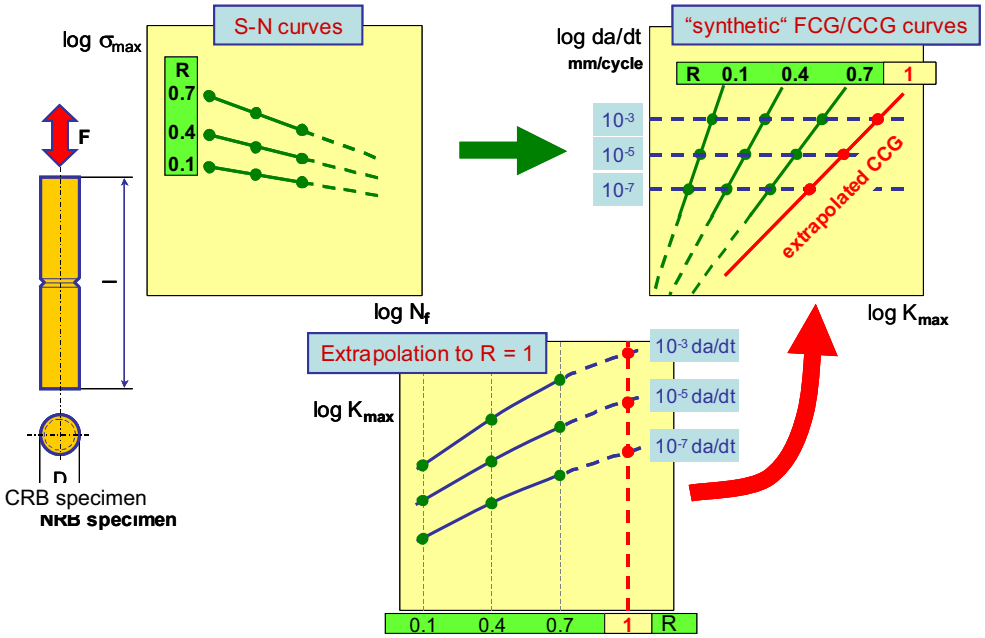

Fig. 2.4: Methodology to generate "synthetic" CCG curves for static loading (R=1) based on cyclic experiments with CRB specimens (Lang et al., 2005).

2.4 Selection of materials

Table 2.1 lists the selected materials used in Part I of this Dissertation and describes the tested R-ratios as well as the condition of the bulk material, from which the specimens were manufactured. Also indicated in the table are those materials for which the extrapolation procedure to R=1 was carried out. The extrapolation was conducted for those materials, which allowed testing of at least three different R-ratios.

All materials tested are commercially available PE types. However, to protect the interests of the involved project partners, only coded material names are used in this Dissertation. To meet the requirements of an academic work in terms of reproducibility, a supplementary sheet which includes the un-coded commercial material names was made available to the project partners.

Table 2.1: Tested materials, pipes and fittings.

Material designation	PE class	CRB specimens prepared from	Tested R-ratios	extrapolation to R=1
PE-BF	non-pipe PE	compression molded plate	0.1, 0.3, 0.5, 0.7	yes
PE-BF-1	non-pipe PE	compression molded plate	0.1, 0.3, 0.5	yes
PE 80	PE 80	compression molded plate	0.1, 0.3, 0.5	yes
PE 100-1	PE 100	compression molded plate	0.1, 0.3	no
PE 100-1F	PE 100	iInjection molded fitting	0.1, 0.3	no
PE 100-2	PE 100	compression molded plate	0.1, 0.3, 0.5	yes
PE 100-2P	PE 100	extruded pipe	0.1	no
PE 100 RC	PE 100 RC	compression molded plate	0.1	no
PE 80-MD	PE 80-MD	compression molded plate	0.1	no
old pipe 1981	PE 80-MD	extruded pipe	0.1, 0.3, 0.5	yes
old pipe 1988	PE 80	extruded pipe	0.1, 0.3, 0.5	yes

The blow-forming non-pipe material PE-BF was used for the development of the extrapolation procedure due to its rather brittle character. A second non-pipe material, PE-BF-1 with higher ductility, which typically is used for extruded films, was selected to evaluate the potential of the lifetime prediction procedure for non-pipe applications.

To study the applicability of the extrapolation procedure for pipe materials, a commercial PE 80 pipe grade was selected, which has been frequently used and still exists in many pipe systems. The characterization of the commercial PE 100 pipe grades was done with PE 100-1, by also taking additional specimens from an injection molded fitting (PE 100-1F), and with PE 100-2 by also testing specimens from a pipe (PE 100-2P). In order to have a modern PE 100 material with improved resistance to cracks, PE 100 RC was selected.

As part of the characterization program of pipes that had been in service for some time, two further pipe materials were selected: a pipe for water supply which has been in service since 1988 (old pipe 1988) and which was identified as a PE 80 pipe grade (Frank et al., 2008), as well as a gas pipe which has been in operation since 1981 (old pipe 1981) and which was found to be a medium density PE 80-MD (Frank et al., 2008). In that case the specimens were directly taken out of the pipes, both of which had the same dimensions of D160 SDR 11 (outer di-

ameter: 160 mm, wall thickness: 14.5 mm). As a reference for this material an additional PE 80-MD pipe grade was selected.

2.5 References

Anderson, T.L. (1991). Fracture Mechanics – Fundamentals and Application, CRC Press Inc., Boca Raton, Florida, USA.

Balika, W. (2003). "Rissausbreitung in Kunststoff-Rohrwerkstoffen unter statischer und zyklischer Belastung", Doctoral Dissertation, Institute of Materials Science and Testing of Plastics, University of Leoben, Austria.

Balika, W., Pinter, G., Lang, R.W. (2007). "Systematic investigations of fatigue crack growth behavior of a PE-HD pipe grade in through–thickness direction", Journal of Applied Polymer Science, 103(3), 1745-1758.

Barenblatt, G.J. (1962). "The Mathematical Theory of Equilibrium Cracks in Brittle Fracture", Advances in Applied Mechanics 7, p 55-129.

Barker, M.B., Bowman, J.A., Bevis, M. (1983). "The Performance and Cause of Failure of Polyethylene Pipes Subjected to Constant and Fluctuating Internal Pressure Loadings", Journal of Materials Science 18, 1095-1118.

Böhm, L.L., Enderle, H.-F., Fleissner, M. (1992). "High-Density Polyethylene Pipe Resins", Advanced Materials 4(3), 234-238.

Broek, D. (1986). Elementary Engineering Fracture Mechanics, Martinus Nijhoff Publishers, Dordrecht.

Broek, D. (1988). The Practical Use of Fracture Mechanics, Kluwer Academic Publishers, Dordrecht, Netherlands.

Brown, N., Lu, X., Huang, Y., Harrison, I.P., Ishikawa, N. (1992). “The Fundamental Material Parameters that Govern Slow Crack Growth in Linear Polyethylens”, Plastics, Rubber and Composites Processing and Applications 17(4): 255-258.

Choi, B.-H., Chudnovsky, A., Paradkar, R., Michie, W., Zhou, Z., Cham, P.M. (2009). "Experimental and theoretical investigation of stress corrosion crack (SCC) growth of polyethylene pipes", Polymer Degradation and Stability 94(5), 859–867.

Chudnovsky, A., Moet, A., Bankert, R.J., Takemori, M.T. (1983). "ffect of damage dissemination on crack propagation in polypropylene",Journal of Applied Physics 54 (10), 5562-5567.

Dieter, G.E. (1988). Mechanical Metallurgy, McGraw-Hill Book Company, London, United Kingdom.

Doerner, G. (1994). "Stabilisatoreinflüsse auf das Alterungs- und Zeitstandverhalten von Rohren aus PE-MD", Doctoral Dissertation, Institute of Materials Science and Testing of Plastics, University of Leoben, Austria.

Dugdale, D.S. (1960). "Yielding of steel sheets containing slits", Journal of the Mechanics and Physics of Solids 8, pp. 100–104.

Egan, B.J., Delatycki, O. (1995). "The Morphology, Chain Structure and Fracture Behavior of High-Density Polyethylene - Part I: Fracture at a Constant Rate of Deflection", Journal of Materials Science 30, 3307-3318.

Egan, B.J., Delatycki, O. (1995). "The Morphology, Chain Structure and Fracture Behavior of High-Density Polyethylene - Part II: Static Fatigue Fracture Testing", Journal of Materials Science 30, 3351-3357.

EN ISO 9080 (2003) Plastics piping and ducting systems - Determination of the long-term hydrostatic strength of thermoplastics materials in pipe form by extrapolation.

Frank, A., Podingbauer, T., Liedauer, S., McCarthy, M., Haager, M., Pinter, G. (2008). "Characterization of the Property Profile of Old PE Gas Pipes in Service for up to 30 Years", Plastics Pipes XIV, Budapest, Hungary.

Friedrich, K. (1983). "Crazes and shear bands in semi-crystalline thermoplastics", Advances in Polymer Science 52/53, 225-274.

Gaube, E., Gebler, H., Müller, W., Gondro, C. (1985). "Zeitstandfestigkeit und Alterung von Rohren aus HDPE", Kunststoffe 75(7), 412-415.

Haager, M., (2006). "Fracture mechanics methods for the accelerated characterization of the slow crack growth behavior of polyethylene pipe materials", Doctoral Dissertation, Institute of Materials Science and Testing of Plastics, University of Leoben, Austria.

Haager, M., Pinter, G., Lang, R.W. (2006). “Ranking of PE Pipe Grades by Cyclic Crack Growth Tests with Cracked Round Bar Specimen”. ANTEC 2006, Charlotte, North Carolina, USA, Society of Plastics Engineers.

Hertzberg, R.W. and Manson, J.A. (1980). Fatigue of Engineering Plastics, Academic Press, New York, USA.

Hertzberg, R.W. (1989). Deformation and Fracture Mechanics of Engineering Materials, John Wiley & Sons, New York.

Ifwarson, M. (1989). "Gebrauchsdauer von Polyethylenrohren unter Temperatur und Druckbelastung", Kunststoffe 79(6), 525-529.

Irwin, G.R. (1957). "Analysis of Stresses and Strains near the End of a Crack Traversing a Plate", Journal of Applied Mechanics 24 , 361-364.

Kausch, H.H. (1987). Polymer Fracture, Springer Berlin-Heidelberg, D.

Kausch, H.H., Gensler, R., Grein, C., Plummer, C.J.G., Scaramuzzino, P. (1999). "Crazing in semicrystalline thermoplastics", Journal of Macromolecular Science, Part B-Physics 38(5&6), 803-815.

Kinloch, A.J., Young, R.J. (1983). Fracture Behaviour of Polymers, Applied Science Publication, London, England.

Krishnaswamy, R.K. (2005). "Analysis of Ductile and Brittle Failures from Creep Rupture Testing of High-Density Polyethylene (HDPE) Pipes", Polymer 46(25), 11664-11672.

Lang, R.W. (1984). "Applicability of Linear Elastic Fracture Mechanics to Fatigue in Polymers and Short-Fiber Composites", Doctoral Dissertation, Lehigh University, Bethlehem, Pennsylvania, USA.

Lang, R.W. (1997). "Polymerphysikalische Ansätze zur Beschreibung des Deformations- und Versagensverhalten von PE-Rohren", 3R International 36, 40-44.

Lang, R.W., Stern, A., Doerner, G.(1997). "Applicability and Limitations of Current Lifetime Prediction Models for Thermoplastics Pipes under Internal Pressure", Die Angewandte Makromolekulare Chemie, Volume 247 Issue 1, Pages 131-145.

Lang, R.W., Balika, W., Pinter, G. (2004). “Applicability of Linear Elastic Fracture Mechanics to Fatigue in Amorphous and Semi-Crystalline Polymers”, The Application of Fracture Mechanics to Polymers, Adhesives and Composites. D.R. Moore. Oxford, England, Elsevier Science Ltd. and ESIS. ESIS Publi¬cation 33: 83-92.

Lang, R.W., Pinter, G., Balika, W. (2005). "Ein neues Konzept zur Nachweisführung für Nutzungsdauer und Sicherheit von PE-Druckrohren bei beliebiger Einbausituation", 3R international, 44(1-2), 33-41.

Lang, R.W., Pinter, G., Balika, W., Haager, M. (2006). A Novel Qualification Concept for Lifetime and Safety Assessment of PE Pressure Pipes for Arbitrary Installation Conditions. Plastics Pipes XIII, Washington DC, USA.

Lang, R.W., Stern, A., Doerner, G. (1997). "Applicability and Limitations of Current Lifetime Prediction Models for Thermoplastics Pipes under Internal Pressure", Die Angewandte Makromolekulare Chemie 247, 131-137.

Lustiger, A. (1986). “Environmental Stress Cracking: The Phenomenon and its Utility”, Failure of Plastics. W. Browstow and R. D. Corneliussen. Munich, Germany, Hanser Publishers: 305-329.

Lustiger, A., Ishikawa, N. (1991). "An Analytical Technique for Measuring Relative Tie-Molecule Concentration in Polyethylene", Journal of Polymer Science - Part B: Polymer Physics 29: 1047-1055.

Murakami, Y. (1990). Stress Intensity Factors Handbook, Pergamon Press, Oxford, Great Britain.

Paris, P.C., Erdogan, F. (1963). "A critical analysis of crack propagation laws", Journal of Basic Engineering 85, p. 528-534.

Parsons, M., Stepanov, E.V., Hiltner, A., Baer, E. (1999). “Correlation of stepwise fatigue and creep slow crack growth in high density polyethylene”, Journal of Materials Science 34, 3315–3326.

Parsons, M., Stepanov, E.V., Hiltner, A., Baer, E. (2000). "Correlation of Fatigue and Creep Slow Crack Growth in a Medium Density Polyethylene Pipe Material", Journal of Materials Science 35, 2659-2674.

Pinter, G. (1999). "Rißwachstumsverhalten von PE-HD unter statischer Belastung", Doctoral Dissertation, Institute of Materials Science and Testing of Plastics, University of Leoben, Austria.

Pinter, G. and Lang, R.W. (2003). "Effect of stabilization on creep crack growth in High-Density Polyethylene", Journal of Applied Polymer Science, 90, 3191-3207.

Pinter, G., Haager, M., Balika, W., Lang, R.W., (2007). "Cyclic crack growth tests with CRB specimens for the evaluation of the long-term performance of PE pipe grades", Polymer Testing 26 (2), 180–188.

Pinter, G., Haager, M., Lang, R.W. (2006). "Accelerated Quality Assurance Tests for PE Pipe Grades", ANTEC 2006, Charlotte, North Carolina, USA, Society of Plastics Engineers, 2480-2484.

Pinter, G., Haager, M., Wolf, C., Lang, R.W. (2004). "Thermo-oxidative degradation during creep crack growth of PE-HD grades as assessed by FT-IR spectroscopy" Macromolecular Symposia, 217, 307-316.

Pinter, G., Lang, R.W. (2004). "Creep Crack Growth in High Density Polyethylene", The Application of Fracture Mechanics to Polymers, Adhesives and Composites, D.R. Moore. Oxford, England, Elsevier Science Ltd. and ESIS. ESIS Publication 33: 47-54.

Pinter, G., Lang, R.W., Haager, M. (2007). "A Test Concept for Lifetime Prediction of Polyethylene Pressure Pipes", Chemical Monthly 138, 347–355.

Richard, K., Gaube, E., Diedrich, G. (1959). “Trinkwasserrohre aus Niederdruck¬polyäthylen”, Kunststoffe 49(10): 516-525.

Shah, A., Stepanov, E.V., Capaccio, G., Hiltner, A., Baer, E. (1997). “Correlation of fatigue crack propagation in polyethylene pipe specimens of different geometries”, International Journal of Fracture 84, 159–173.

Shah, A., Stepanov, E.V., Capaccio, G., Hiltner, A., Baer, E. (1998). “Stepwise fatigue crack propagation in polyethylene resins of different molecular structure”, Journal of Polymer Science Part B: Polymer Physics 36, 2355–2369.

Shah, A., Stepanov, E.V., Klein, M., Hiltner, A., Baer, E. (1998). “Study of polyethylene pipe resins by a fatigue test that simulates crack propagation in real pipe”, Journal of Materials Science 33, 3313–3319.

Stern, A. (1995). "Fracture Mechanical Characterization of the Long-Term Behavior of Polymers under Static Loads", Doctoral Dissertation, Institute of Materials Science and Testing of Plastics, University of Leoben, Austria.

Stern, A., Novotny, M., Lang, R.W. (1998). "Creep crack growth testing of plastics II. data acquisition, data reduction and experimental results", Polymer Testing 17/6, 423-441.

Williams, J.G. (1987). Fracture Mechanics of Polymers, Ellis Horwood Limited, Chichester.

Zhou, W., Chudnovsky, A., Sehanobish, K. (2005). "Evaluation of Time to Ductile Failure in Creep of PEs from Short-Term Testing", ANTEC 2005, Boston, Massachusetts, USA, Society of Plastics Engineers, 3517-3521.

3 FRACTURE MECHANICS TEST METHOD AND DATA REDUCTION PROCEDURE

The following paragraph describes the development of a laboratory test method for the accelerated and reliable fracture mechanics determination of CCG in PE pipe grade materials based on the extrapolation concept by Lang and Pinter (Lang et al., 2005, 2006). Major parts of this research work have been published in **Papers I-1, I-2** and **I-5** in the Appendix and were presented at the Annual Technical Conference of the Society of Plastics Engineers (ANTEC) 2008 and 2009, the Plastics Pipes XIV Conference (Frank et al., 2008) and the 5th International Conference on Fracture of Polymers, Composites and Adhesives 2008.

First, the selection of a suitable specimen geometry and the corresponding calculation of K_I as well as experimental details of the cyclic tests will be outlined briefly. Following a first evaluation of the applicability of simple fatigue tests for the extrapolation concept, the development of an advanced test methodology for the direct measurement of crack growth rates in the selected specimen configuration will be described.

3.1 The cracked round bar specimen

Several specimen configurations are available for fracture mechanics testing. To meet the requirements of a significant acceleration of testing times, cracked round bar (CRB) specimens were selected, as this type exhibits several advantages (Lang et al., 2005) and has already showed promising results in previous studies (Haager, 2006; Pinter et al., 2006, 2007a,b). By conducting cyclic tests on CRB specimens it is not only possible to differentiate between different PE grades (PE80, PE100) within a few days, but also to draw a distinction within one grade as to potential process based batch variations. The correlation of CRB failure data with those of time consuming methods like the FNCT opens an interesting potential for product ranking and material development (Haager, 2006; Pinter et al., 2006, 2007a).

A further advantage of CRB specimens is that fatigue tests can be done at application near temperatures of 23 °C and without any additional stress cracking liq-

uid. Due to the very simple geometry that is shown in Fig. 3.1, it is possible to manufacture the CRB specimens either from compression molded plates or even straight out from extruded pipes.

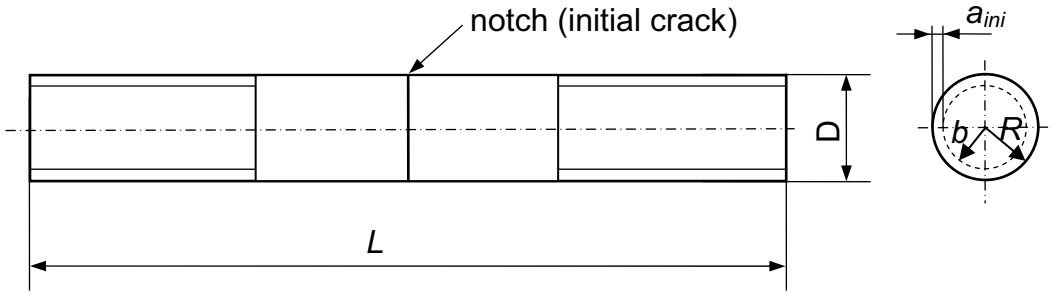

L=100 mm……..... specimen length
D=M14 x 1.25… .. outer specimen diameter (with metric thread):
M14 x 1.25 results in D=13.8 mm
R=D/2…..... outer specimen radius
a_{ini}=1.5 mm… ..... notch depth (initial crack length)

Fig. 3.1: Typical dimensions of the used CRB specimen.

A crucial advantage of the CRB specimens in terms of reduction of testing times are the almost plain strain conditions, which reduce the formation of plastic zones at the crack tip to a minimum. The high constraint in this specimen also ensures an accelerated crack initiation. Finally, the fast raise in K_I with increasing crack length, which occurs after crack initiation, leads to a further acceleration of SCG and a decrease of the testing time, respectively.

In CRB specimens K_I can be calculated with different mathematical formulas. Corresponding to the dimensions depicted in Fig. 3.1, in the calculations presented below F is the applied load, a is the current crack length, R is the radius and b is the ligament radius of the CRB specimen. Equations 3.1 to 3.3 describe the K_I-calculation by Benthem and Koiter (Benthem and Koiter, 1973) that is very accurate for the evaluation of CRB specimens (Murakami, 1990; Scibetta et al., 2000; Haager, 2006).

$$K_I = \frac{F}{\pi \cdot b^2} \cdot \sqrt{\frac{\pi \cdot a \cdot b}{R}} \cdot f\left(\frac{b}{R}\right) \tag{3.1}$$

$$b = R - a \tag{3.2}$$

$$f\left(\frac{b}{R}\right)=\frac{1}{2}\cdot\left[1+\frac{1}{2}\cdot\left(\frac{b}{R}\right)+\frac{3}{8}\cdot\left(\frac{b}{R}\right)^{2}-0.363\cdot\left(\frac{b}{R}\right)^{3}+0.731\cdot\left(\frac{b}{R}\right)^{4}\right] \tag{3.3}$$

More simple calculations for the CRB specimens were presented by G.E. Dieter (Dieter, 1988), which is shown in Equation 3.4, as well as Janssen et al. (Janssen et al., 2004), presented in Equation 3.5. The advantage of these formulas is the ability of solving them analytically in the lifetime calculation model described in Equation 2.3, what is demonstrated in **Paper I-5** in the Appendix.

$$K_I=\frac{F}{D^{\frac{3}{2}}}\cdot\left[1.72\cdot\left(\frac{D}{D-2\cdot a}\right)-1.27\right] \tag{3.4}$$

$$K_I=\frac{0.526\cdot F\cdot\sqrt{D}}{(D-a)^{2}} \tag{3.5}$$

In **Paper I-5**, K_I was also numerically simulated with the FEM simulation program ABAQUS (Vers. 6.91 Standard, SIMULIA, USA). The result of this calculation is presented in Equation 3.6 and was found to follow a polynomial function of fourth order.

$$K_I=\frac{4\cdot F}{D^{2}\cdot\pi\cdot\sqrt{1000}}\cdot\left(1.22-0.09\cdot a+1.80\cdot a^{2}-0.94\cdot a^{3}+0.17\cdot a^{4}\right) \tag{3.6}$$

In Fig. 3.2 the presented definitions of the stress intensity factor, in which K_I is a function of the normalized crack length a/R, are compared. In order to calculate K_I in the CRB specimen, the geometric values of Fig. 3.1 (D=13.8 mm) and a typical maximum load of a cyclic test (F=1340 N) have been used. In CRB specimens typical values for quasi-brittle crack length are between 1.5 mm and 4 mm which correspond to a/R-values between 0.22 and 0.58.

At short crack lengths, up to a/R=0.4, a very good correlation of all three functions exists. Whereas K_I by Dieter shows the lowest values at higher crack lengths at a/R > 0.7, K_I of the ABAQUS simulation clearly has the steepest gradient above a/R=0.5. For all functions, the quick increase of K_I with increasing crack length is well recognizable. At higher K_I the limitations of LEFM are usually violated and the quasi-brittle failure mode at the crack tip turns into a ductile failure mode. In this

Dissertation all CRB tests have been analyzed not exceeding a crack length of 4 mm. An optical evaluation of the fracture surface was combined to evaluate the change in the failure modes. If not mentioned explicitly, all K_I-calculations in this Dissertation were done with Equation 3.1.

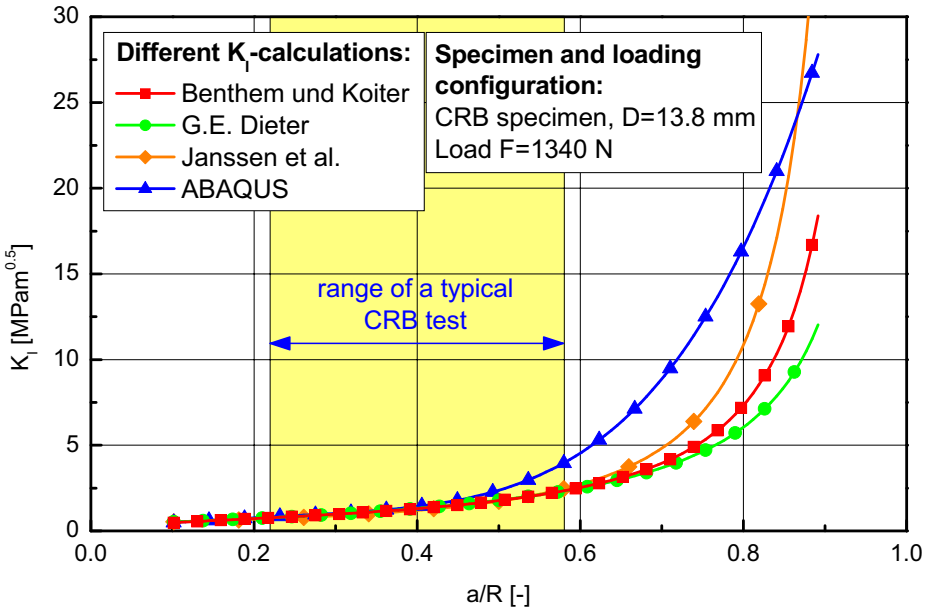

Fig. 3.2: Comparison of stress intensity factors in CRB specimen obtained according to Benthem and Koiter, to G.E. Dieter, to Janssen et al. and to ABAQUS simulation as a function of the normalized crack length a/R.

3.2 Experimental and data reduction procedure

The test methodology was developed with the help of two different types of PE. The first one was a PE high density grade (PE-HD) with the classification PE 80, which is a material that is typically used in many existing pipe systems (Table 2.1). The second one was a non-pipe PE-HD, which is usually employed in blow forming applications and is labeled as PE-BF within this Dissertation (Table 2.1). This material was used due to its rather brittle character that ensured relatively short failure times in the fatigue tests for a quick development of the test procedure. For both materials kinetics data from a previous project were available as a reference, which have been measured with compact type (CT) specimens (Pinter et al., 2002).

For the specimen preparation compression molded plates with a thickness of 15 mm were produced. The CRB specimens with a diameter of 13.8 mm and a

length of 100 mm (Fig. 3.1) were manufactured out of these plates and a circumferential initial crack of 1.5 mm in depth was inserted with a razorblade (Haager, 2006).

All cyclic tests were executed on a servo-hydraulic closed-loop testing system of the type MTS Table Top (MTS Systems GmbH; Berlin, D). The force controlled load was applied sinusoidal with a frequency of 10 Hz. All cyclic tests were conducted at standardized laboratory conditions at ambient temperatures of 23 °C and a humidity of 50 %. The failure cycle number of the fatigue tests was recorded as N_f. In order to provide an exact calculation of the initial K_I, the specimen diameter and initial ligament diameter of the CRB specimen were measured after the test using a light microscope of the type BX51 (Olympus; Vienna, A) and the analyzing software analySIS 3.2 (Soft Imaging Systems GmbH; Munich, D). A detailed description of the determination of the initial K_I from the fracture surface can be found in the Diploma Thesis of Freimann (Freimann, 2008).

3.2.1 Extrapolation method with simple fatigue tests

For a first evaluation of the extrapolation concept (Lang et al., 2005) fatigue tests at the R-ratios of 0.1, 0.3 and 0.5 were executed on CRB specimens of the PE 80 material. In Fig. 3.3 the number of cycles until failure N_f at a temperature of 23 °C for the different R-ratios as a function of the initial $K_{I,max}$ is shown. As expected, N_f increases with increasing R-ratio. For R=0.3 and 0.5 not only the quasi-brittle failure regime was detected but also ductile failure at higher stress intensity factors, which is demonstrated by the open symbols in Fig. 3.3. The illustrated fracture surfaces show eccentric crack growth starting anywhere around the circumference of the specimen, which is typical for this type of specimen (Haager, 2006). Unfortunately, due to this effect it is difficult to directly observe the current crack length and the crack growth rate, respectively.

Although the test configuration with the CRB specimen generally decreases the testing time, N_f at R=0.5 are higher than 10^7 cycles, which amounts to about 12 days of testing at a frequency of 10 Hz. A further increase of the test frequency will lead to hysteretic heating of the specimen, which will influence the failure behavior significantly. For modern PE 100 pipe grades, with an improved resistance against

crack initiation and SCG, it is expected, that cyclic tests at R-ratios of 0.5 need to be tested 4 to 8 weeks per specimen or even more.

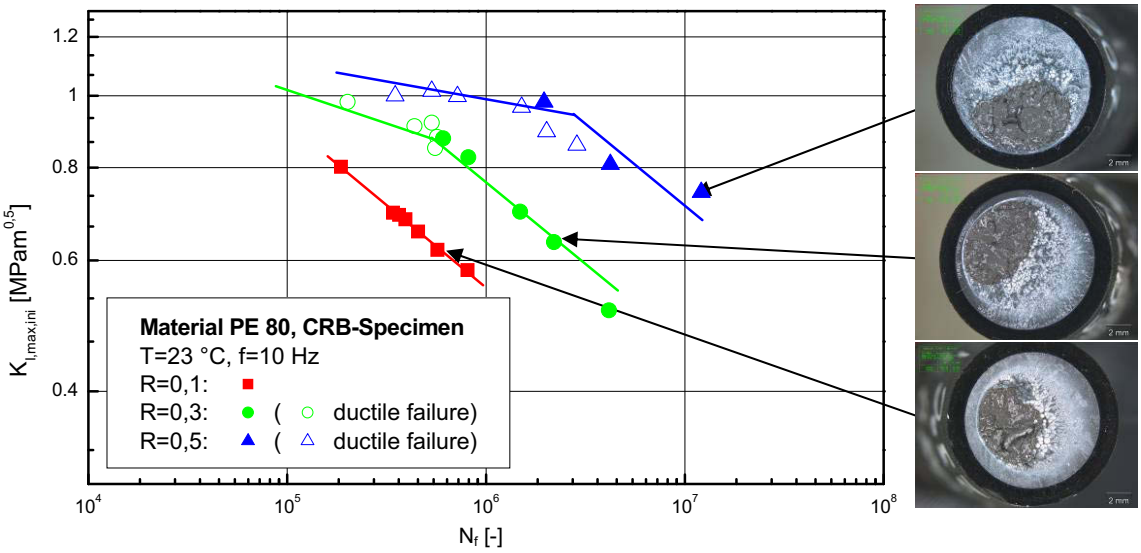

Fig. 3.3: Number of cycles until failure N_f of PE 80 at 23 °C for R-ratios of 0.1, 0.3 and 0.5 and corresponding fracture surfaces of CRB specimens (open symbols refer to ductile failure).

As in the fatigue tests which are presented in Fig. 3.3 a direct measurement of the crack growth kinetics was not possible, the “synthetic” FCG curves were determined with the help of the calculation of averaged crack growth rates based on fracture surface analyses of the single specimens. For this purpose, the length of the quasi-brittle crack was measured from the initial crack length a_{ini} up to the start of the brittle-ductile transition. The “synthetic” FCG curves for PE 80 are summarized in Fig. 3.4, and the data are compared to crack kinetic curves measured with CT specimens of the same material (Pinter et al., 2002). Whereas the reference curves display real kinetic lines of a single test, in which the current crack tip in the CT specimen was observed with a travelling microscope and was correlated to the relevant number of cycles, the “synthetic” FCG curves were calculated on the basis of several cyclic CRB tests and fracture surface analysis. In that case, the cycle number for crack propagation was obtained from the crosshead displacement recorded during the cyclic test. On the other hand, the length of the quasi-brittle crack was estimated from the fracture surface of the failed CRB specimen as the

distance from the initial crack length to the change of the failure mode from quasi-brittle failure to ductile failure. Hence, each single cyclic CRB test results in a single average crack growth rate (see **Paper I-1** in the Appendix).

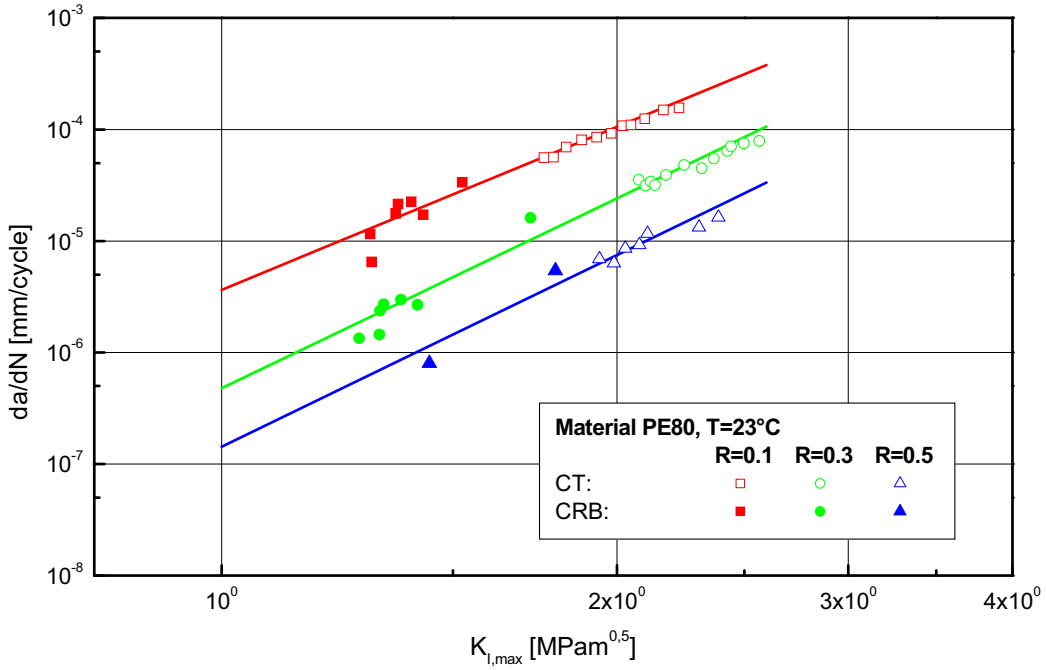

Fig. 3.4: Correlation of "synthetic" FCG in CRB specimens and crack growth kinetics in CT specimens for PE 80 at R=0.1, 0.3 and 0.5 at a temperature of 23°C.

Although the single points of the "synthetic" FCG curves match the kinetic lines of the reference data quite well, a description of crack growth kinetics seems not to be reliable enough with this approach, especially for higher R-ratios. To generate a R-specific "synthetic" FCG curve, at least two CRB tests have to be conducted. The results of Fig. 3.4 show, that a determination of a crack growth laws based on only two points of average crack growth rates is not precise enough. Hence, an acquisition of a representative number of data is necessary, which increases the testing effort significantly. Furthermore, it was detected, that the single-point evaluation is highly dependent on the fracture surface analysis. Especially for higher R-ratios it turns out difficult to detect the brittle-ductile transition. Moreover, the action of detecting it causes uncertainties in the determination of the average crack growth rate, which is a significant source for data scattering. Instead of developing "synthetic" FCG curves, as originally proposed by Lang and Pinter, it was

decided to develop a methodology which allows a direct measurement of the crack growth kinetics in CRB specimens.

3.2.2 Compliance calibration method

Due to the unknown position of the crack initiation around the circumference of the CRB specimen and the eccentric crack growth, the direct measurement of the current crack length is quite difficult for this type of geometry. However, an indirect determination of the average current crack length is possible by using the specimen specific compliance C of a material (Saxena and Hudak, 1978), which is the ratio of the crack opening displacement (COD) of a crack and the applied force F (see Fig. 3.5, left).

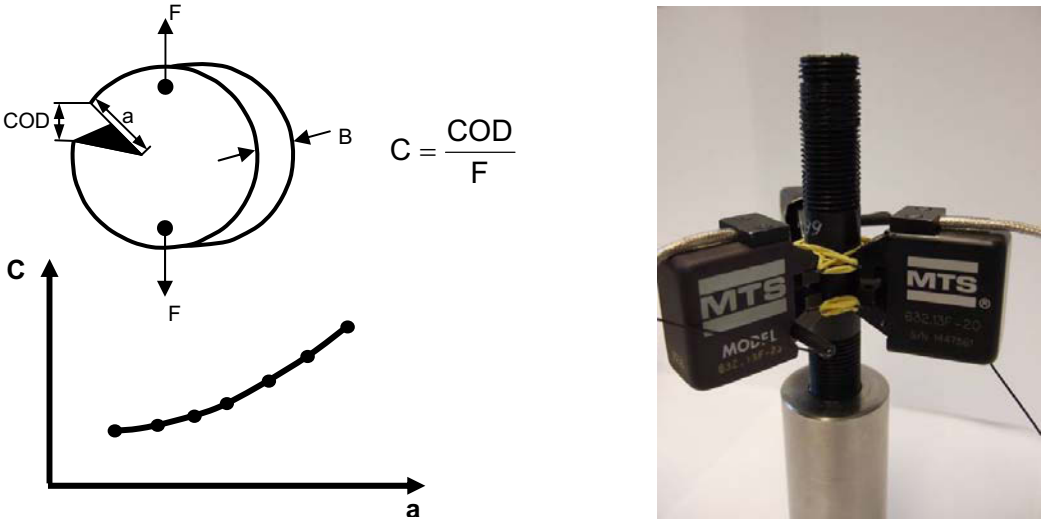

Fig. 3.5: Left: Schematic illustration of the crack opening displacement (COD) and the relationship between the compliance C and the crack length a; Right: CRB specimen with three extensometers for the measurement of the COD.

The application of this technique to CRB-specimens is part of **Paper I-2** in the Appendix and it is also described in the Diploma Thesis of Freimann (Freimann, 2008). Therefore, three extensometers (Type 632.13-20, MTS Systems GmbH; Berlin, D) were positioned at equal distance around the specimen crack (see Fig. 3.5, right). To develop a compliance calibration curve, first the compliance of the CRB specimens was measured at different initial crack lengths from 1.0 to 3.0 mm. As a result of the cyclic loads in the fatigue test, the crack opening dis-

placement was measured as the difference ΔCOD of minimum and maximum COD and the specimen compliance was calculated to ΔC, respectively. The developed compliance calibration curve allows calculating the current crack length in a single CRB specimen at any time of a fatigue test by measuring ΔC.

For both materials, PE 80 and PE-BF, the compliance calibration curve ΔC as a function of the crack length a at a temperature of 23 °C is shown in Fig. 3.6. As a result of the higher material stiffness of the blow forming type the curve for PE-BF is clearly lower than for PE 80. As long as the requirements of LEFM for plastics are met, at a constant temperature the compliance only depends on the material and the specimen geometry but but it does not show any dependency regarding the applied load. This was proven by the results of material PE-BF in which the compliance at different a_{ini} was also measured at R=0.3. The data overlap the calibration curve quite well, indicating load independency.

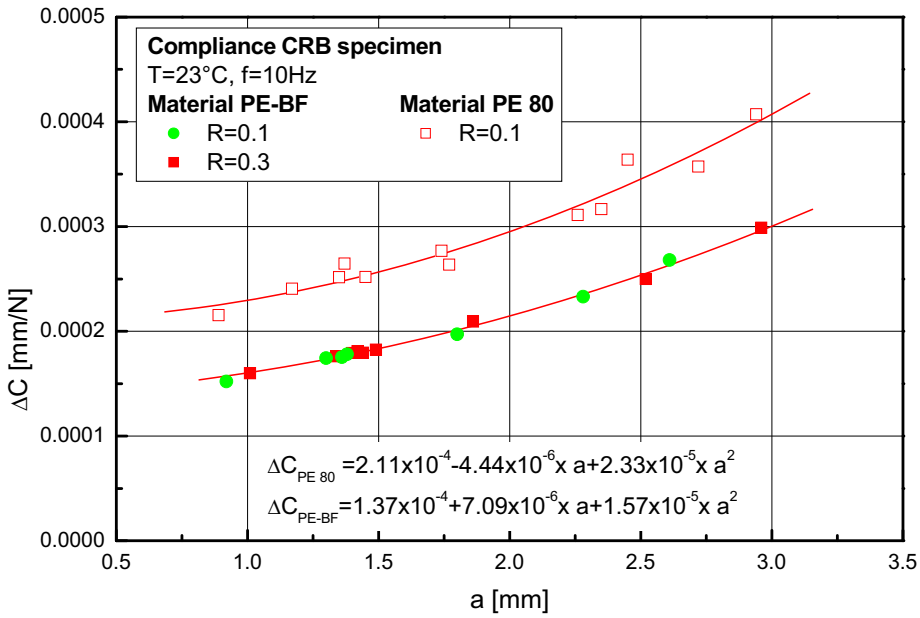

Fig. 3.6: Compliance calibration at 23 °C; ΔC as a function of the crack length a for CRB specimens of PE-BF (R=0.1 and 0.3) and PE 80 (R=0.1).

To avoid starting effects, the values for ΔC were recorded after a few thousand cycles and definitely before crack initiation occurred. The curve fitting was done with a simple polynomial function of 2nd order. By converting this material and specimen specific function into a quadratic equation, it was possible to calculate

the current crack length in a cyclic CRB test from any corresponding measured ΔC.

Another benefit of the system with three extensometers is the possibility to accurately detect the crack initiation. In Fig. 3.7 the extensometer signals of a typical CRB fatigue test show ΔCOD as a function of cycle number N, also indicating N_{ini} and N_{tot}. The crack initiation cycle number N_{ini} is characterized by the first step in these signals. With continuing crack growth a stepwise signal can be recognized, which is very typical of quasi-brittle crack growth in PE, until final failure of the specimen occurs at N_{tot}.

This clear separation of the overall failure time into crack initiation time and SCG time provides new interesting options for material benchmarking. Furthermore, a more reliable estimation of the fraction of crack initiation at static loading conditions is possible with this additional information. A detailed study on the reproducibility of the compliance calibration method on CRB specimens, which is of high precision, is summarized in **Paper I-2** in the Appendix.

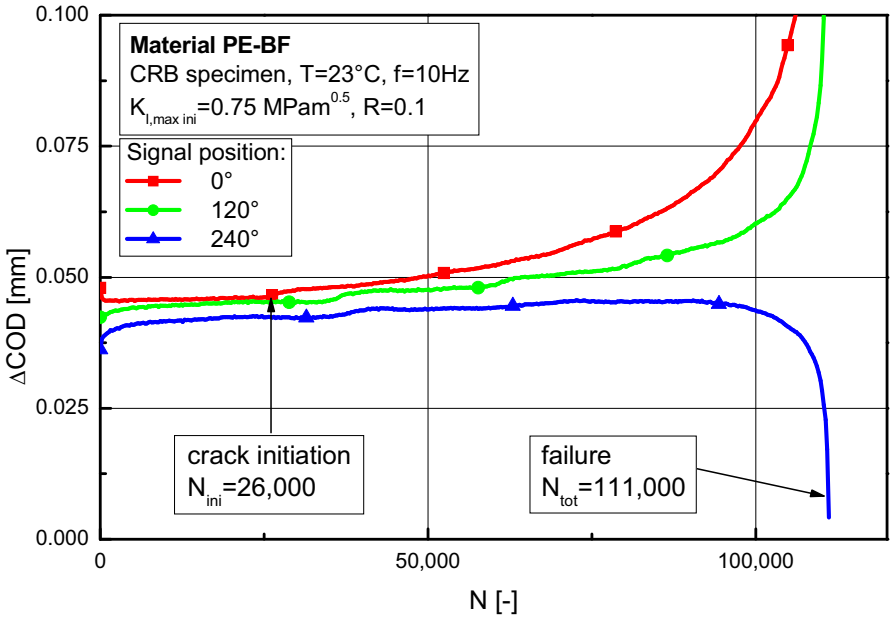

Fig. 3.7: Extensometer signals ΔCOD as a function of cycles N, indicating values for N_{ini} and N_{tot} for a typical CRB fatigue test on PE-BF. The first steps in the curves indicate crack initiation.

3.2.3 Extrapolation procedure

With the direct measurement of the current crack length in a CRB fatigue tests it is possible, to generate real FCG curves at a specific R-ratio with only one single test, which makes the mathematical transformation from several failure data into “synthetic” FCG curves obsolete. Thereby, the extrapolation procedure from Fig. 2.4 is reduced to Fig. 3.8, so that the evaluation of R-specific Woehler-curves is no longer required.

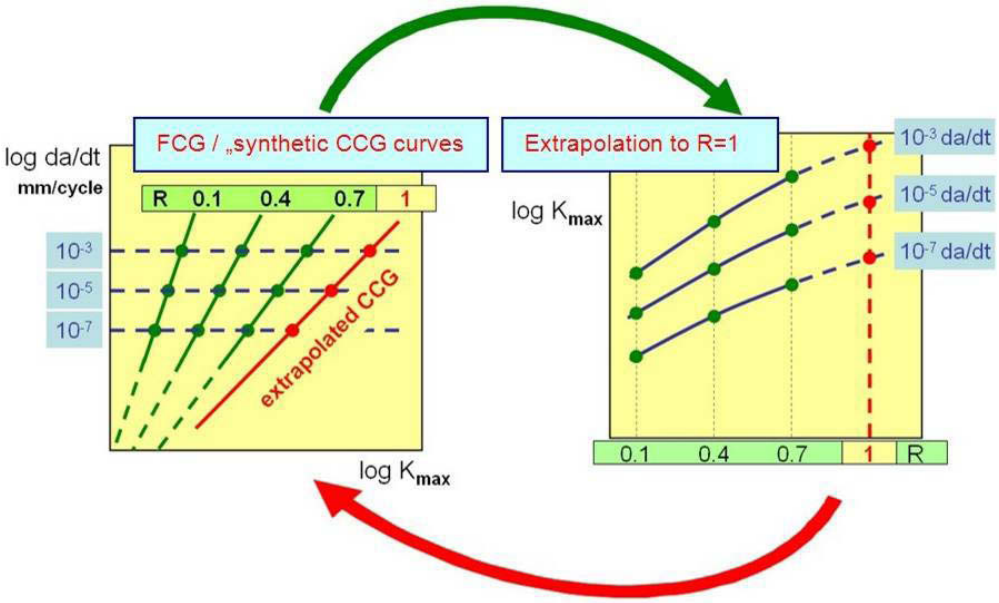

Fig. 3.8: Extrapolation procedure to generate “synthetic” CCG curves for static loading (R=1) based on measured FCG kinetics at different R-ratios in CRB specimens.

The crack growth curves for PE-BF at R=0.1, 0.3, 0.5 and 0.7 at a temperature of 23 °C are shown in Fig. 3.9, left. As expected, for a given $K_{I,max}$ the crack growth rate decreases with increasing R-ratio. This diagram also includes crack growth rates which have been measured with CT-specimens (Pinter et al., 2002). The CT data show somewhat faster crack growth rates which may have been caused by marginal changes in the raw material (different batches). Nevertheless, the functional characteristics of the curves confirm the reliability and the potential of the developed method for a quick measurement of crack growth kinetics with CRB specimens.

As demonstrated schematically in Fig. 3.8, the kinetics of the PE-BF at different R-ratios were cut at lines of constant crack growth rates and transformed into a chart $K_{I,max}$ being a function of R (Fig. 3.9, right). An empirically found logarithmic function was used for the extrapolation to R=1, which represents static loading. Finally, the obtained stress intensity factors at R=1 were transformed back into the kinetics diagram to generate the "synthetic" CCG curve, which is shown in Fig. 3.10 along with the crack growth data obtained for different R-ratios. Having this "synthetic" CCG curve, it was possible to obtain the material parameters A and m for static loading conditions which allow a fracture mechanics lifetime prediction. In the case of PE-BF at a temperature of 23 °C this parameters are A=4.65 x 10^{-5} and m=7.32.

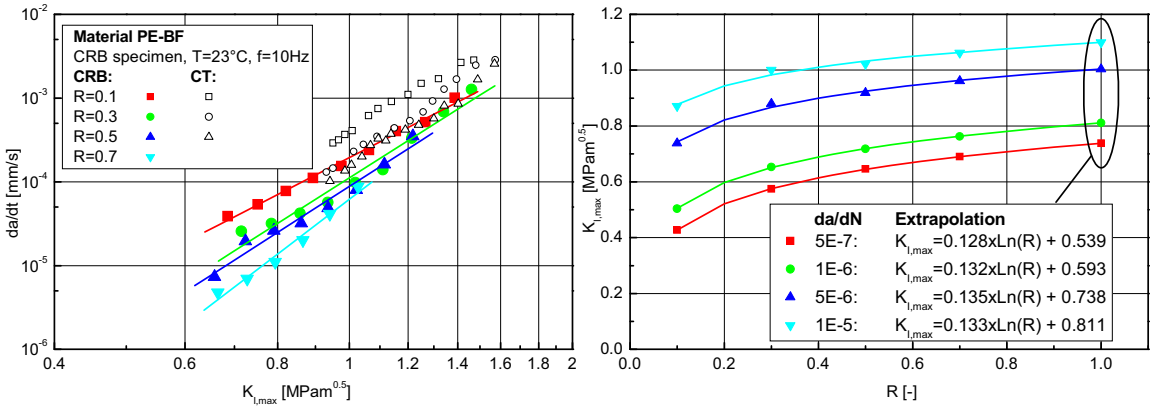

Fig. 3.9: Left: Measured crack growth curves da/dt of PE-BF at different R-ratios. Right: Extrapolation of R-ratio depending $K_{I,max}$ to R=1.0 (static loading).

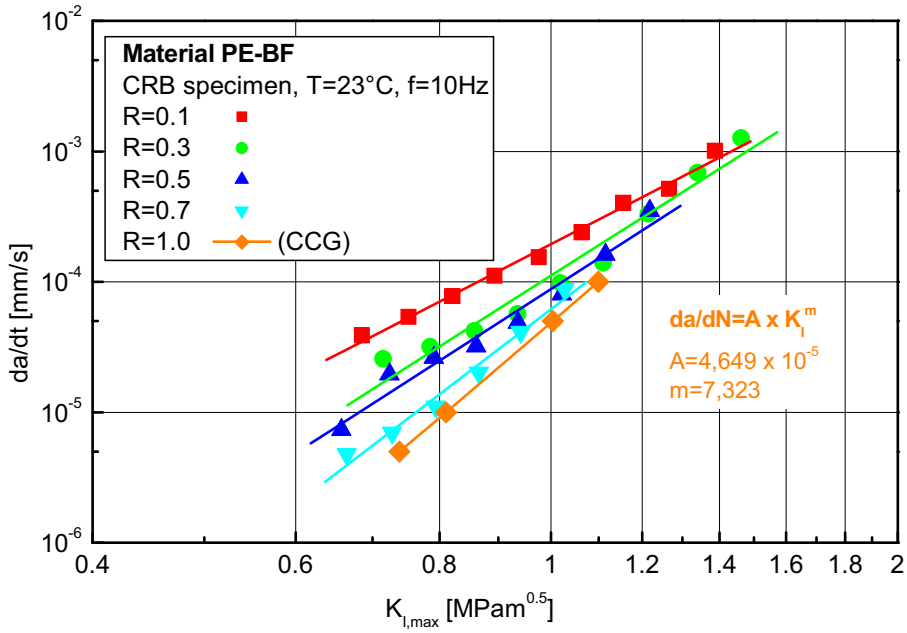

Fig. 3.10: Measured crack growth curves da/dt of PE-BF at different R-ratios and extrapolated "synthetic" CCG curve (R=1.0).

The rather brittle non-pipe material PE-BF was primarily selected to ensure short testing times and for a quick development of the test methodology. To evaluate the applicability of the test procedure for pipe grade PE, the whole procedure was repeated with the material PE 80 from Table 2.1. Results for this material are summarized in Chapter 5.

3.3 References

Benthem, J.P., Koiter, W.T. (1973). “Method of Analysis and Solutions of Crack Problems”, Sih, G.C., ed., 3, 131-178, Noordhoft International Publisching, Groningen, Netherlands.

Dieter, G.E. (1988). Mechanical Metallurgy, McGraw-Hill Book Company, London, United Kingdom.

Frank, A., Pinter, G., Lang, R.W. (2008). "A Novel Qualification Procedure for Lifetime and Safety Assessment of PE Pressure Pipes for Arbitrary Installation Conditions", Plastics Pipes XIV, Budapest, Hungary.

Freimann, W. (2008). "Charakterisierung des Risswachstumsverhaltens von Cracked Round Bar (CRB) Prüfkörpern auf Basis der Materialnachgiebigkeit", Master Thesis, Institute of Materials Science and Testing of Plastics, University of Leoben, Austria.

Haager, M., (2006). "Fracture mechanics methods for the accelerated characterization of the slow crack growth behavior of polyethylene pipe materials", Doctoral Dissertation, Institute of Materials Science and Testing of Plastics, University of Leoben, Austria.

Janssen, M., Zuidema, J., Wanhill, R. (2004). Fracture Mechanics, 2nd Edition, Spoon Press, Oxfordshire, Great Britain.

Lang, R.W., Pinter, G., Balika, W. (2005). "Ein neues Konzept zur Nachweisführung für Nutzungsdauer und Sicherheit von PE-Druckrohren bei beliebiger Einbausituation", 3R international, 44(1-2), 33-41.

Lang, R.W., Pinter, G., Balika, W., Haager, M. (2006). “A Novel Qualification Concept for Lifetime and Safety Assessment of PE Pressure Pipes for Arbitrary Installation Conditions”, Plastics Pipes XIII, Washington DC, USA.

Murakami, Y. (1990). Stress Intensity Factors Handbook, Pergamon Press, Oxford, Great Britain.

Pinter, G., Balika, W., Lang, R.W (2002). "A Correlation of Creep and Fatigue Crack Growth in High Density Poly(Ethylene) at Various Temperatures", Temperature-Fatigue Interaction, REMY, L. AND PETIT, J, Amsterdam, Elsevier Science Ltd. and ESIS, ESIS Publication 29: 267-275.

Pinter, G., Haager, M., Lang, R.W. (2006). "Accelerated Quality Assurance Tests for PE Pipe Grades", ANTEC 2006, Charlotte, North Carolina, USA, Society of Plastics Engineers, 2480-2484.

Pinter, G., Haager, M., Balika, W., Lang, R.W. (2007). "Cyclic crack growth tests with CRB specimens for the evaluation of the long-term performance of PE pipe grades", Polymer Testing 26 (2), 180–188.

Pinter, G., Lang, R.W., Haager, M. (2007). "A Test Concept for Lifetime Prediction of Polyethylene Pressure Pipes", Chemical Monthly 138, 347–355.

Saxena, A., Hudak, S.J. (1978). "Review and Extension of Compliance Information for Common Crack Growth Specimens", International Journal of Fracture, Vol. 14, No. 5, 453-468.

Scibetta, M., Chaouadi, R., Van Walle, E. (2000). “Fracture Toughness Analysis of Circumferential-Cracked Round Bars”, International Journal of Fracture 104: 145-168.

4 APPLICABILITY AND LIMITATIONS OF THE FRACTURE MECHANICS APPROACH TO LIFETIME PREDICTION

In addition to the material parameters A and m, the correct calculation of K_I values in a pressurized pipe is essential for reliable fracture mechanics predictions of lifetimes. The aim of the present chapter is to introduce the selected pipe model as well as to further investigate the calibration of K_I in the pipe. Furthermore, the influence of the initial crack size and variations in the extrapolation from FCG to CCG will be demonstrated within the scope of a sensitivity analysis. Details with regard to the development of the simulation model for an internally pressurized pipe are summarized in **Paper I-3** in the Appendix, which also includes detailed information on more complex loading situations like soil loads or additional bending.

4.1 Stress intensity factor calibration of pressurized pipes

The standard model for fracture mechanics lifetime prediction is an internal pressurized pipe with an initial defect at the inner pipe surface, as shown in Fig. 4.1. This model also describes the loading situation in internal pressure tests based on ISO 9080 in which pipe specimens are tested at different internal pressures but without any additional load. This means that lifetime predictions based on this model can be compared to real test data, if available. If not mentioned explicitly, it is stated that all calculations in this Dissertation were performed for a model pipe of the dimensions D40 SDR 11 (outer diameter: 40 mm, wall thickness: 3.6 mm).

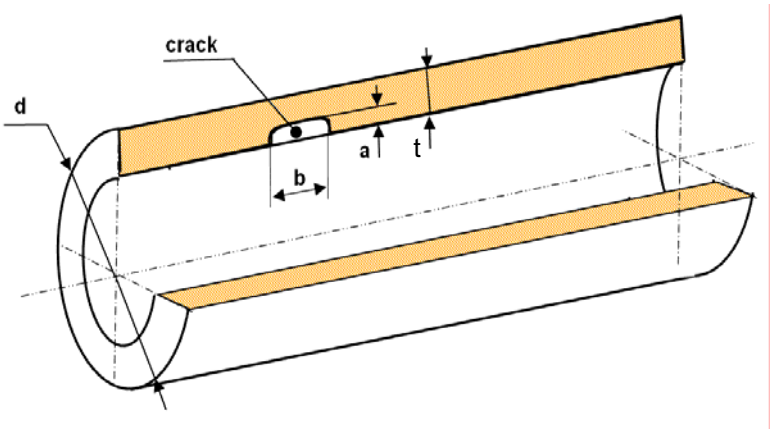

Fig. 4.1: Model of the pipe with a surface crack at the inner pipe wall.

Literary publications provide different solutions for the stress intensity factor in the described pipe model (Murakami, 1990; Anderson, 1991; Krishnamachari, 1993). To verify these solutions and to open the possibility of calculating more complex loading situations (soil load, bending), K_I was also simulated with FEM using ABAQUS (see **Paper I-3** in the Appendix).

A comparison of K_I as a function of the normalized crack length a/t (crack length a divided by pipe wall thickness t) provided by Muarkami, Anderson, Krishnamachari and based on the FEM simulation is shown in Fig. 4.2. The calculations were accomplished for a semi-elliptical surface crack (b=2a), which is usually assumed (Stern, 1995). The different calculations of K_I for semi-elliptical surface cracks show, that the literature formulas proposed by Murakami and Anderson match the characteristics of the FEM simulation quite well, especially at small crack lengths, associated with the initiation of creep crack growth. However, the curve based on the calculation of Krishnamachari is completely different in comparison to the other calculations. Thus, this solution will no longer be considered in this study. The selection of the K_I-calculation in pressurized pipes used in this Dissertation is described in the following section.

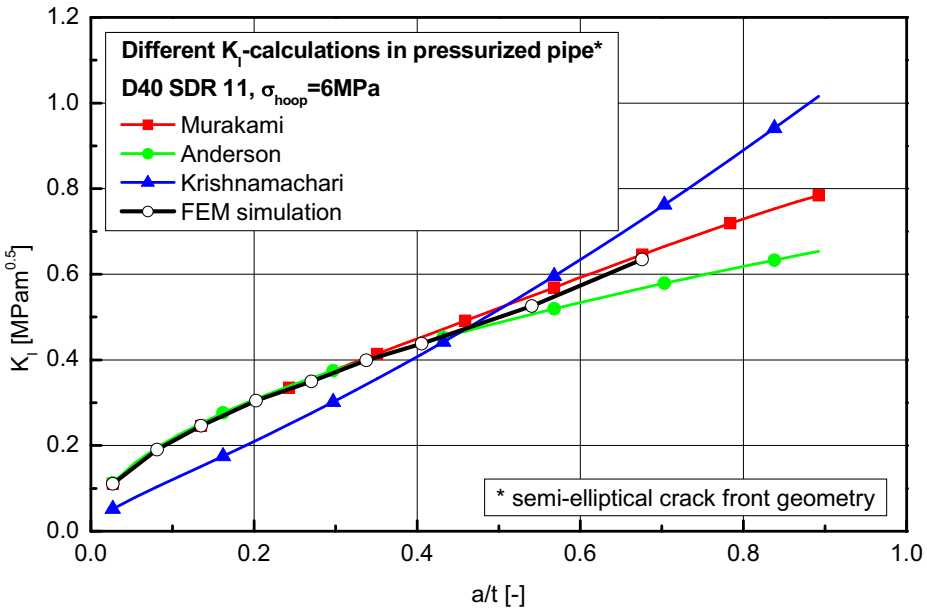

Fig. 4.2: Calculations of K_I in the wall thickness direction as a function of the normalized crack length a/t in an internal pressurized pipe with semi-elliptical crack front geometry.

4.2 The problem of the crack front geometry

The characteristics of the K_I vs. crack length relationship in a pressurized pipe also depend considerably on the crack front geometry and the crack front position (Broek, 1986, 1988; Hertzberg, 1995). A model of a semi-elliptical and a semi-circular crack front geometry of identical initial crack length a_{ini} in the wall thickness direction is shown in Fig. 4.3. As pointed out before, a crack with a semi-elliptical shape and a constant ratio between main axis and minor axis, the main axis (crack width) $2c_e$ being twice the minor axis $2a_{ini}$, was assumed for the calculations illustrated in Fig. 4.2. For this crack front geometry, K_I is higher at point A than at point C_e, which results in a transformation of the semi-elliptical shape into a semi-circular shape as the crack grows (Pinter, 1999). In the second assumption of a semi-circular initial crack shape the radius c_c is equal to the initial crack length a_{ini} in the wall thickness direction. In this situation K_I is only slightly lower at point A than at point C_c, which will result in only a small tendency of the crack front geometry to change from semi-circular to semi-elliptical crack shape.

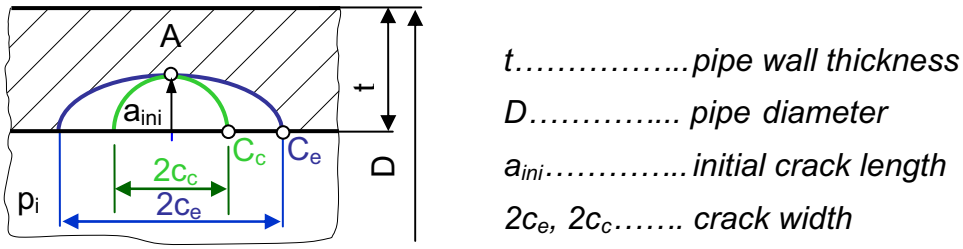

Fig. 4.3: Semi-elliptical and semi-circular surface crack front geometry of identical initial crack length a_{ini} in the thickness direction at the inner pipe wall of an internal pressurized pipe.

Fig. 4.4 to Fig. 4.6 illustrates various fracture surfaces of internal pressure tests on pipe segments. A typical effect of SCG in PE is the discontinuous character of crack propagation which results from the continuous formation of a craze with highly orientated fibrils at the crack tip and the stepwise breakdown of the crack tip craze upon physical crack growth (Barker et al., 1983; Pinter, 1999; Parsons et al., 2000; Favier et al., 2002; Pinter et al. 2005; Balika et al., 2007). This discontinuous mechanism creates markings on the fracture surface indicating the real crack front geometry at various times of crack advance.

Figure 4.4 shows a fracture surface of an internal pressure test on an old pipe which has been used in service since 1988 (Table 2.1) and which was tested in 2009. Slow crack growth starts at an inherent defect at the inner pipe surface. The markings at very small crack lengths confirm a nearly semi-circular crack front geometry. With increasing crack length the plain stress situation at the inner pipe surface allows for larger plastic deformations which retard SCG. In the center of the pipe wall plain strain conditions prevail and ensure a higher constraint with continuing SCG. When the crack front approaches the outer pipe surface the plain stress condition again allows for larger plastic deformations which are crack retarding. Meanwhile, the crack in the center of the pipe wall is still growing in a quasi-brittle manner in the direction of the pipe axis until final breakdown with ductile failure at the outer pipe wall occurs.

This characteristic of a predominantly semi-circular crack front geometry at small and mid-size crack length and the change to a semi-elliptical crack front geometry at large crack lengths can be observed on many fracture surfaces of pipes from internal pressure tests. The examples of fracture surfaces in Fig. 4.5 (Barker et al. 1983) and Fig. 4.6 (Pinter, 1999) also confirm the dominating semi-circular crack front geometry.

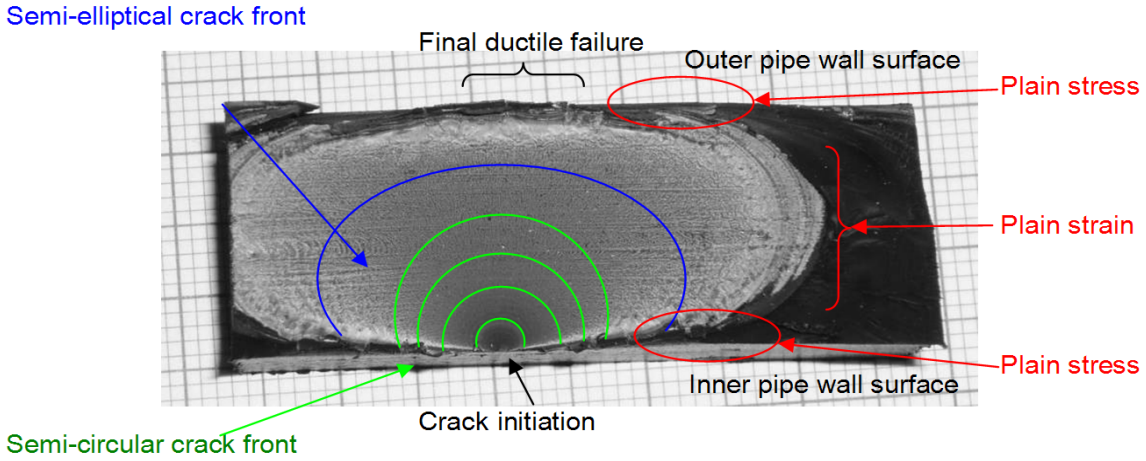

Fig. 4.4: Fracture surface of an internal pressure test on an old pipe installed in 1988 at 80 °C and a hoop stress σ=4.6 MPa. Failure time t_f=1038 h.

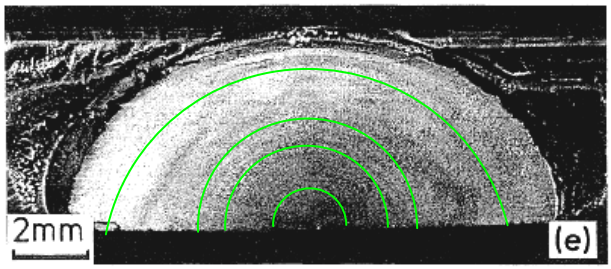

Fig. 4.5: Fracture surface of an internal pressure test on PE-HD (Barker et al. 1983). A semi-circular crack front dominates the fracture surface.

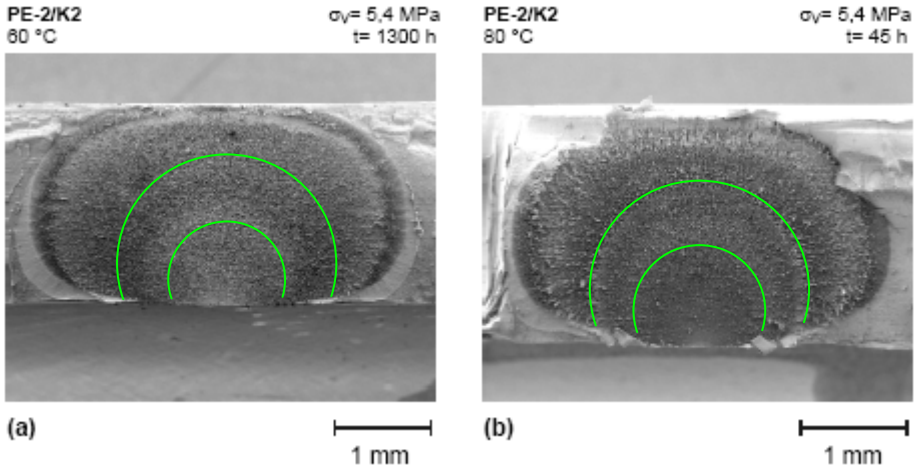

Fig. 4.6: Fracture surface of internal pressure tests on PE-HD (Pinter, 1999).

To take the findings of the real crack front geometry into account, in Fig. 4.7 K_I as a function of the normalized crack length a/t by Murakami and Anderson were re-calculated with the assumption of a constant semi-circular crack front geometry throughout the entire SCG regime. Compared to the semi-elliptical crack shape, a significant decrease in the values of K_I at a constant a/t can be noticed. This chart also includes a FEM simulation of K_I values taking into account the change of the real crack front geometry. At very small and mid-size crack length the FEM simulation matches the literature formulas for the semi-circular crack front geometry quite well, whereas at very long crack length K_I increases faster and approaches the curves of the semi-elliptical crack front geometry of Murakami and Anderson. The mathematical formulation of K_I of the FEM simulation is shown in Equation 4.1, p being the internal pressure of the pipe, a the crack length, and t is the pipe wall thickness. This solution is only valid for a standard dimension ratio (SDR) of 11, which describes the ratio of the outer pipe diameter D divided by the pipe wall thickness t.

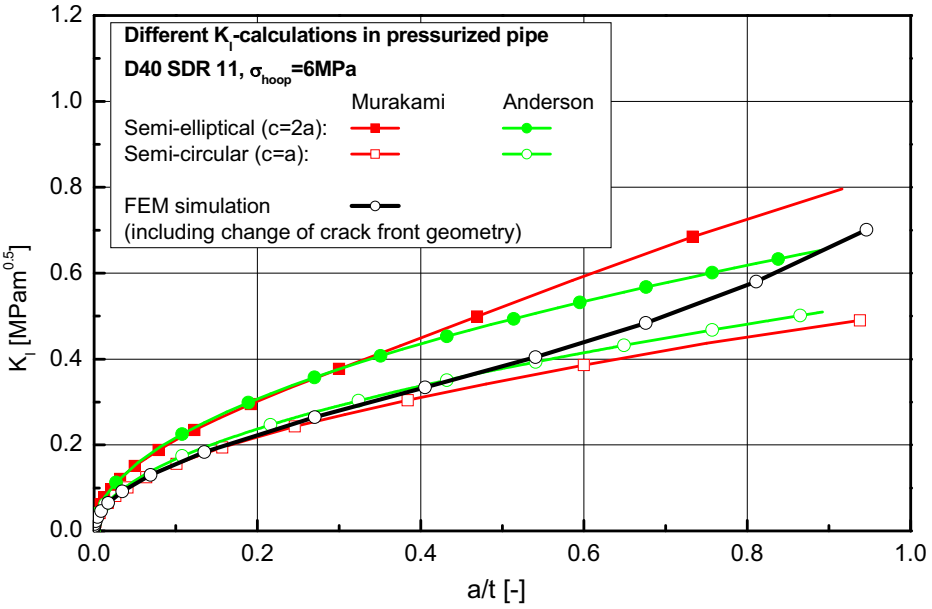

Fig. 4.7: Calculation of K_I in the wall thickness direction as a function of the normalized crack length a/t in an internal pressurized pipe with semi-elliptical, semi-circular and simulated real crack front geometry.

$$K_I = p \cdot \sqrt{\pi \cdot a} \cdot \left[3.74 + 0.36 \cdot \left(\frac{a}{t}\right) - 0.16 \cdot \left(\frac{a}{t}\right)^2 + 1.80 \cdot \left(\frac{a}{t}\right)^3 \right] \qquad (4.1)$$

On the one hand, this K_I study emphasizes the importance of the correct use of literature values and the choice of right assumptions for the crack geometry. On the other hand, the potential of the FEM simulation for K_I calibration was demonstrated. For the fracture mechanics lifetime prediction in this Dissertation, K_I of Equation 4.1 including the change of the real crack front geometry was used, if not mentioned explicitly.

4.3 Assumption of the initial defect size

As shown in Equation 2.3, a fracture mechanics lifetime prediction calculates the time that a crack needs to grow from an initial crack length a_{ini} through the entire pipe wall up to a final failure crack length a_f which corresponds to the pipe wall thickness. Whereas in a test specimen like a CRB specimen a_{ini} is well defined by the sharp notch inserted with a razor blade, in real applications unavoidable inherent defects like impurities, polymer agglomerates, material inhomogeneities or cavities are frequently responsible for the initiation of SCG. For internal pressurized pipes it was shown, that a reasonable assumption of a typical size of such

inherent defects is between 100 and 400 μm (Gray et al., 1981; Stern, 1995; Lang et al., 1997; Pinter, 1999). This variation of inherent initial crack length leads to a scattering of failure times in internal pressure tests. An example of internal pressure test results of a PE 80 pipe grade (a different type to those which were characterized within this Dissertation) based on ISO 9080 is shown in Fig. 4.8, left (Bodycote Polymer, 2009). The material was tested at temperatures of 20, 60 and 80 °C, a distinctive quasi-brittle failure within the test time was only detected at 80 °C, though. At constant hoop stress, the variation of the inherent initial defects led to a distribution of failure times of about one decade. A typical initial defect, that causes SCG, is shown in Fig. 4.8, right (Pinter, 1999). For the lifetime assessment calculations within this Dissertation the initial crack length a_{ini} was assumed to be between 100 and 400 μm, the larger assumption resulting in a more conservative lifetime estimate.

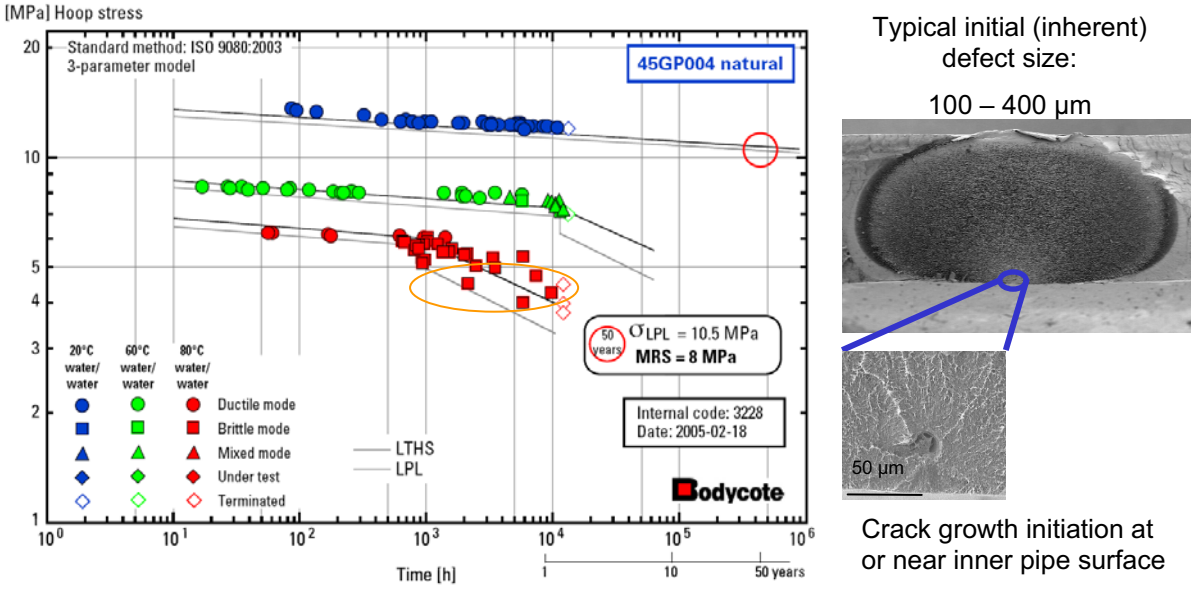

Fig. 4.8: Left: Internal pressure test (ISO 9080) for a PE 80 material (Bodycote Polymer, 2009); Right: Typical inherent defect responsible for the initiation of SCG (Pinter, 1999).

4.4 Generation of "synthetic" creep crack growth laws

An important quantitative influence in the lifetime prediction is linked to the extrapolation procedure to obtain a creep crack growth law for static loading from cyclic experiments (compare Section 3.2.3). In Fig. 4.9, left, the measured da/dt

vs. $K_{I,max}$ at R=0.1, 0.3 and 0.5 are shown for the PE 80 material. The kinetic curves are cut at constant crack growth rates and transformed into the right diagram, by depicting $K_{I,max}$ as a function of R. In this chart the extrapolation of constant crack growth rates to R=1 is conducted to derive a "synthetic" CCG curve.

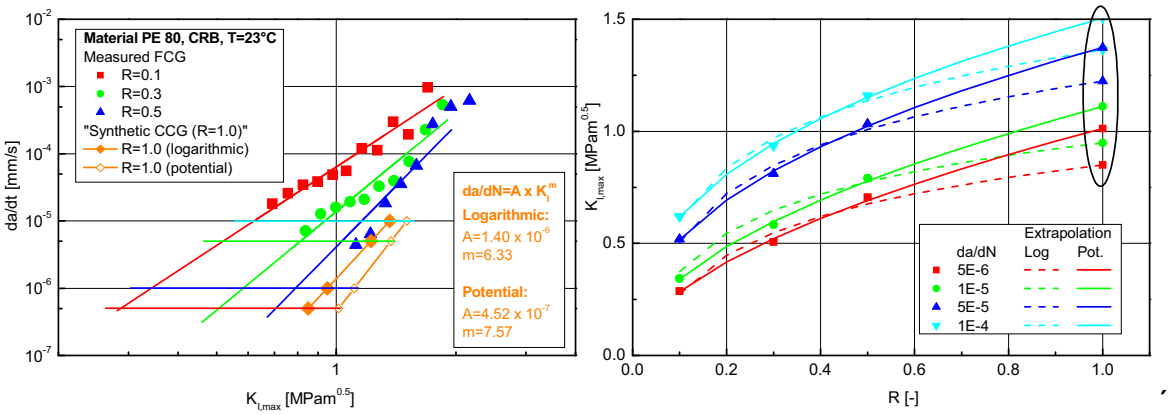

Fig. 4.9: Effect of the extrapolation function for fatigue crack growth data to obtain "synthetic" CCG curves for R=1: logarithmic vs. potential extrapolation.

An uncertainty in this procedure is the fact, that the extrapolation function is based on only three data points, which makes it quite difficult to predict a suitable mathematics correlation. As already mentioned in Section 3.2.3, crack growth data at higher R-ratios like R=0.7 would be desirable. However, due to the higher crack resistance of PE 80 and the exceeding long testing times, such tests are very time consuming. Hence, the extrapolation in Fig. 4.9 was done using two different functional correlations, a logarithmic function (Equation 4.2) and a potential function (Equation 4.3), with a and b being the fitting parameters in these functions.

$$K_I = a \cdot \ln(R) + b \tag{4.2}$$

$$K_I = a \cdot R^b \tag{4.3}$$

Although both functions show a proper fitting within the experimental data range of R=0.1 to 0.5, a significant deviation in the extrapolated $K_{I,max}$ values at R=1 is observed, with the potential extrapolation leading to higher $K_{I,max}$ than the logarithmic extrapolation. When re-transforming $K_{I,max}$ at R=1 back to the kinetics diagram, the potential extrapolation exhibits significantly slower crack growth rates compared to

the logarithmic extrapolation at the same $K_{I,max}$. The obtained crack growth law parameters, $A=1.40 \times 10^{-6}$ and m=6.33 for the logarithmic extrapolation, and $A=4.52 \times 10^{-7}$ and m=7.57 for the potential extrapolation, also differ significantly. To ensure a conservative approach for the lifetime prediction, the logarithmic extrapolation procedure was chosen as the standard procedure in this Dissertation.

4.5 Lifetime prediction and sensitivity analysis

All of the discussed boundary conditions have certain effects on the calculated lifetimes of pressurized pipes, which is demonstrated in Fig. 4.10. In this figure the lifetimes for a pressurized pipe of the material PE 80 were calculated by using the fracture mechanics material parameters A and m at 23 °C from Section 4.4. In this diagram the calculated lifetimes are compared to real failure times of the same material at 20 °C (TGM, 1993; Stern, 1995), although only ductile failure was detectable within 10^4 hours.

In Fig. 4.10, the calculation with the material parameters A and m from the potential extrapolation results in the longest failure times which are more than a decade higher than those of the logarithmic extrapolation. For this extrapolation procedure the predicted lifetime of a pipe at a hoop stress of σ_{hoop}=8 MPa and an initial defect size of a_{ini}=400 μm is about 10^7 hours, which is more than 1,100 years. However, as ageing mechanisms and potential material degradation are unknown for such times, such lifetime estimates raises questions as to their reliability.

The lifetime calculation based on material parameters from the conservative logarithmic extrapolation decreases the predicted failure by more than one magnitude in time. In this case a lifetime of about 70 years is predicted for a hoop stress of 8 MPa and an initial defect size of 400 μm.

In both examples, K_I was calculated for a semi-circular crack with the formula of Murakami (Murakami, 1990), and the strong dependene of the initial crack length a_{ini} can be noticed. The shift in failure times with a_{ini}=100 μm and 400 μm is more than one decade and matches the experience in data scatter of real internal pressure tests (see Fig. 4.8). Using the FEM simulation model for K_I, which also accounts for the change in the real crack front as the crack advances (Equation 4.1), only a slight decrease in the failure times can be observed. At a hoop stress of

8 MPa and an initial defect size of 400 μm a lifetime of about 60 years is estimated with this model.

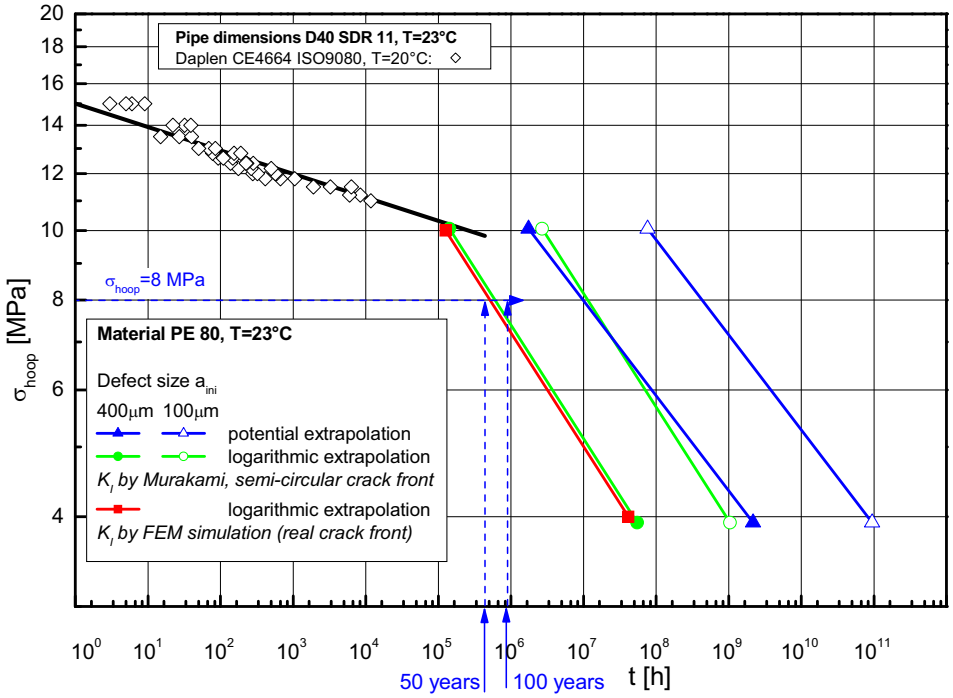

Fig. 4.10: Lifetime prediction of a pipe of PE 80 with the dimension D40 SDR 11 at T=23°C. The calculation are based on parameters A and m from potential and logarithmic extrapolation and on different initial crack length assumptions of a_{ini}=100 and 400 μm in comparison with experimental data from internal pressure tests of pipes at 20 °C (TGM, 1993).

The results presented in Fig. 4.10 emphasize, that some fundamental assumptions are necessary in order to reliably predict the fracture mechanics lifetime. Except for cases with explicit mentioning of deviations, all lifetime calculations within this Dissertation were done for the following boundary conditions and assumptions:

- Logarithmic extrapolation of the FCG curves to “synthetic” CCG curves. This solution will result in conservative results.
- Initial defect size a_{ini}=400 μm.
- FEM model for K_I in a pressurized pipe considering the real crack front geometry according to Equation 4.1. This model also allows for comparisons to real internal pressure tests.

4.6 References

Anderson, T.L. (1991). Fracture Mechanics – Fundamentals and Application, CRC Press Inc., Boca Raton, Florida, USA.

Balika, W., Pinter, G., Lang, R.W. (2007). "Systematic investigations of fatigue crack growth behavior of a PE-HD pipe grade in through–thickness direction", Journal of Applied Polymer Science, 103(3), 1745-1758.

Barker, M.B., Bowman, J.A., Bevis, M. (1983). "The Performance and Cause of Failure of Polyethylene Pipes Subjected to Constant and Fluctuating Internal Pressure Loadings", Journal of Materials Science 18, 1095-1118.

Bodycote Polymer (2009). www.bodycotepolymer.com, Sweden.

Broek, D. (1986). Elementary Engineering Fracture Mechanics, Martinus Nijhoff Publishers, Dordrecht.

Broek, D. (1988). The Practical Use of Fracture Mechanics, Kluwer Academic Publishers, Dordrecht, Netherlands

EN ISO 9080 (2003). Plastics piping and ducting systems - Determination of the long-term hydrostatic strength of thermoplastics materials in pipe form by extrapolation.

Favier, V., Giroud, T., Strijko, E., Hiver, J.M., G'Sell, C., Hellinckx, S., Goldberg, A. (2002). "Slow Crack Propagation in Polyethylene under Fatigue at Controlled Stress Intensity", Polymer 43, 1375-1382.

Gray, A., Mallinson, J.N., Price, J.B. (1981). “Fracture behavior of polyethylene pipes”, Plastics and Rubber Processing and Applications 1, 51-53.

Hertzberg, R.W. (1995). Deformation and Fracture Mechanics of Engineering Materials, John Wiley & Sons, New York.

Krishnamachari, S.I. (1993). Applied Stress Analysis of Plastics – A Mechanical Engineering Approach, Van Nostrand Reinhold, New York, USA.

Lang, R.W., Stern, A., Doerner, G. (1997). "Applicability and Limitations of Current Lifetime Prediction Models for Thermoplastics Pipes under Internal Pressure", Die Angewandte Makromolekulare Chemie 247, 131-137.

Murakami, Y. (1990). Stress Intensity Factors Handbook, Pergamon Press, Oxford, Great Britain.

Parsons, M., Stepanov, E.V., Hiltner, A., Baer, E. (2000). "Correlation of Fatigue and Creep Slow Crack Growth in a Medium Density Polyethylene Pipe Material", Journal of Materials Science 35, 2659-2674.

Pinter, G. (1999). "Rißwachstumsverhalten von PE-HD unter statischer Belastung", Doctoral Dissertation, Institute of Materials Science and Testing of Plastics, University of Leoben, Austria.

Pinter, G., Haager, M., Balika, W., Lang, R.W. (2005). "Fatigue Crack Growth in PE-HD Pipe Materials", Plastics Rubber and Composites 34(1), 25-33.

Stern, A. (1995). "Fracture Mechanical Characterization of the Long-Term Behavior of Polymers under Static Loads", Doctoral Dissertation, Institute of Materials Science and Testing of Plastics, University of Leoben, Austria.

TGM (1993). Gutachten Nr. K 14 450, Technologisches Gewerbemuseum, Wien, Austria.

5 CRACK GROWTH BEHAVIOR AND LIFETIME PREDICTION OF SELECTED MATERIALS

This chapter describes the application of the test methodology and data reduction procedure developed in this Dissertation to different non-pipe and pipe grade PE's, which have been summarized in Table 2.1. First, the discussion of crack initiation and total failure times of CRB specimens emphasizes the applicability and new options of the chosen specimen geometry for a quick and reliable material ranking. After extrapolating fatigue crack growth data to R=1, lifetime predictions for selected materials including specimens from real pipes are described and discussed. **Papers I-1**, **I-2**, **I-4** and **I-5** in the Appendix provide the major results of this chapter.

5.1 Crack initiation and total failure times

The quasi-brittle failure cycle numbers N_f of cyclic CRB tests at R=0.1 at a temperature of T=23°C are shown in Fig. 5.1 as a function of ΔK_I and the initial ligament stress σ_0, respectively. A clear separation of different PE classes is possible, where the two non-pipe grades PE-BF and PE-BF-1 show the shortest failure times. For the pipe grade materials N_f increase continuously from PE 80 to PE 100 and finally to PE 100 RC. Within the PE 100 pipe grades, PE 100-1 shows slightly longer failure times than the specimens made from PE 100-2.

As an effect of the processing history, the CRB specimens of PE 100-1F manufactured from an injection molded fitting show shorter N_f values than specimens obtained from the compression molded plate. However, the PE 100-2P specimens from the pipe have somewhat longer failure times, if there is any difference at all. These results differ from the results of Haager (Haager, 2006), who found an increase of the failure times in the order pipe - compression molded plate - injection molded fitting. These differences point out, that the influence of the processing history (which affects the crystallinity, molecular orientations, residual stresses, etc.) on the long-term failure behavior seems to be significant and even more complex than expected. For this reason, information on the processing history is essential when comparing different materials. Whereas test results obtained from

compression molded plates reflect a pure material behavior, other results from specimens out of extruded pipes or injection molded fittings also include aspects of the specific processing history.

As to the old pipe characterization, the failure cycle numbers of the old pipe from 1988 even match the region of a novel PE 80 material, whereas the crack growth resistance of the old pipe from 1981 is clearly shorter than even the PE 80-MD reference material. Also, the slope of the curves of the old pipes and the PE 80-MD reference material is somewhat lower than the one for the other materials. A more detailed interpretation of the results of the old pipes characterization can be found in **Paper I-4** in the Appendix.

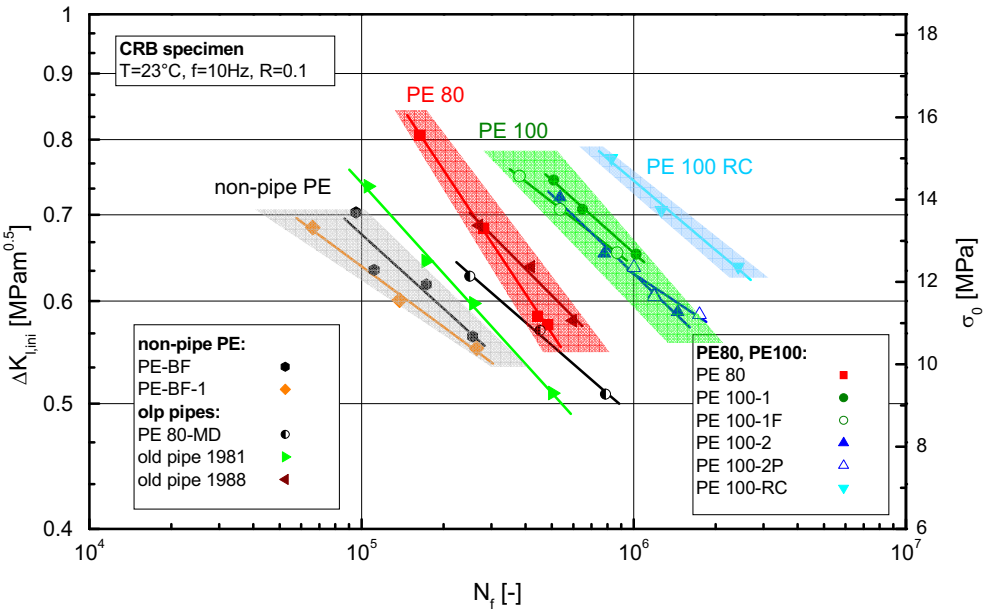

Fig. 5.1: Failure cycle numbers N_f of CRB specimens of different PE types tested at R=0.1 and f=10 Hz at T=23°C.

To obtain values for the testing times, the failure cycle numbers N_f of Fig. 5.1 are transformed into failure times t_f by dividing N_f by the test frequency f (Equation 2.8). Crack initiation cycle numbers or times can also be detected with high precision by using the extensometer system as already mentioned in Section 3.2.2. Thus, the total failure time t_f can be divided into a time for crack initiation t_{ini} and a time for SCG t_{SCG}. Average numbers for the contribution of SCG in percent of the total failure time are provided in Fig. 5.2 for the various materials.

First, values for t_{ini} in Fig. 5.2 for the different PE pipe grades in general show the same ranking as t_f values. However, a change in the ranking can be noticed between the differently processed specimens of PE 100-1 and PE 100-1F. Whereas the total failure times for specimens from the compression molded plates are slightly longer than for specimens from the injection molded fitting, only minor differences were found for crack initiation times. This might signify that there are differences in the morphology influence SCG, whereas crack initiation has not been affected essentially, at least in the investigated case. As a detailed study of processing history effects was beyond the scope of this Dissertation, this topic is recommended for further research.

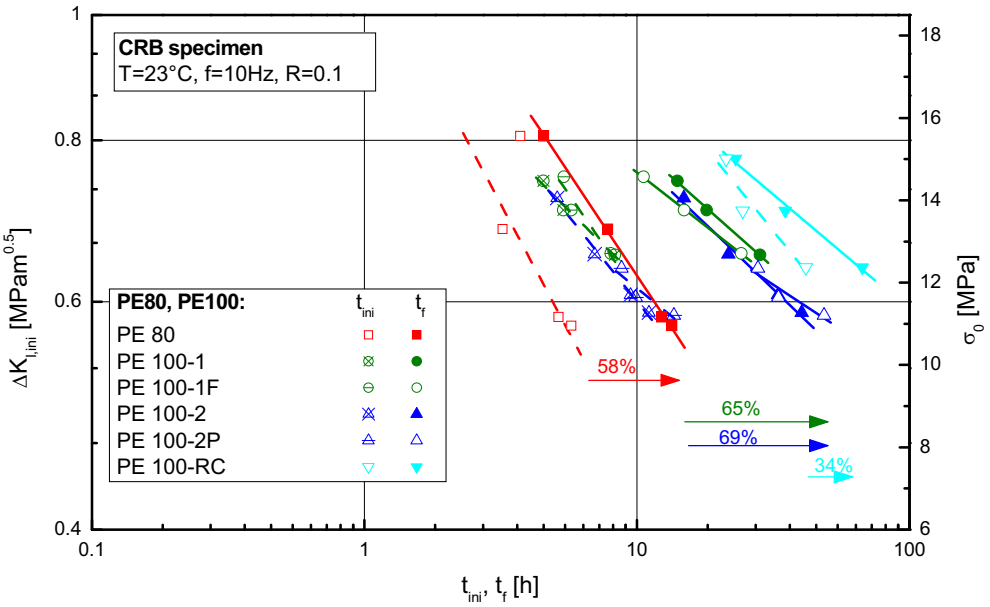

Fig. 5.2: Crack initiation times t_{ini} and total failure times t_f of cyclic CRB specimens at R=0.1 and f=10 Hz of different PE types at T=23°C.

For more information on the contribution of crack initiation and SCG to the total failure time, Fig. 5.3 shows correlation between the applied initial ΔK_I and the ratio t_{ini}/t_{SCG}. For all tested materials the fraction of crack initiation in the CRB specimens decreases with decreasing ΔK_I.

Apparently, at least for the tested CRB specimens, most of the lifetime (i.e. 60 to 70 %) of the PE 100 grades is dominated by SCG. This implies, that, compared to PE 80, the improvements of the raw materials increases the resistance against SCG. On the other hand, most of the lifetime of the PE 100 RC material is domi-

nated by crack initiation (i.e. 66 %) with a significant improvement of the resistance against the mechanisms of crack initiation.

Focusing on the PE 100 materials it can be noticed, that the results for the compression molded plate material state PE 100-2 and the pipe material state PE 100-2P are nearly identical, whereas the material states of the compression molded plate PE 100-1 and the fitting PE 100-1F exhibits significant deviations. The completely different slope of the lines for the injection molded fitting compared to the compression molded plate again indicates a complex influence of the processing history on the mechanisms of crack initiation and SCG.

Comparing the results of each compression molded plate, it becomes evident, that the slope for PE 100-RC is also somewhat different than for PE 80, PE 100-1 and PE 100-2. The special modifications in the morphology of this material (molecular mass distribution, short-chain branches, crystallinity) apparently lead to a higher increase in the resistance against crack initiation at higher stress intensities when compared to the PE 100 materials.

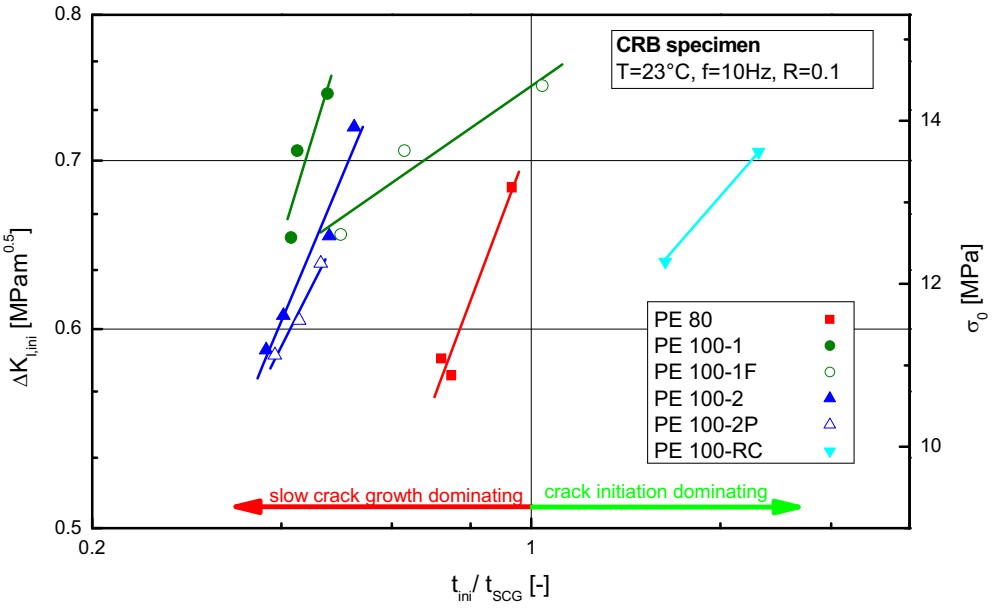

Fig. 5.3: Ratio of crack initiation time t_{ini} and SCG time t_{SCG} in cyclic test on CRB specimens for different PE pipe grades at T=23°C with R=0.1 and f=10 Hz, as a function of the initial ΔK_I value applied.

5.2 Crack growth kinetics under cyclic loads

The primary objective of the developed test method was to determine the crack growth kinetics in CRB specimens. In Fig. 5.4 the fatigue crack growth data da/dt vs. $K_{I,max}$ for R=0.1 are shown. The material ranking in terms of the crack growth rates corresponds to the ranking in terms of failure times in Fig. 5.1 in which a clear separation between the different PE classes is possible. As expected, at a given $K_{I,max}$-level the non-pipe PE's show the fastest growing cracks. At constant $K_{I,max}$ the crack growth rate da/dt decreases in the order of non-pipe PE to PE 80 to PE 100 to PE 100 RC. This result reflects the improvements of the materials in terms of an increased resistance against SCG. The PE 100 RC material clearly shows the best performance of the investigated materials as it exhibits the slowest crack growth rates. However, the crack growth curve of PE 100 RC is also characterized by the highest slope.

The crack growth rates of the old pipes correspond to the failure times of Fig. 5.1. Again, the crack growth kinetics of the old pipe from 1988 is similar to the one of PE 80. Conversely, at equivalent values for $K_{I,max}$, the crack growth rates of the old pipe from 1981 are clearly higher and comparable to the non-pipe PE's.

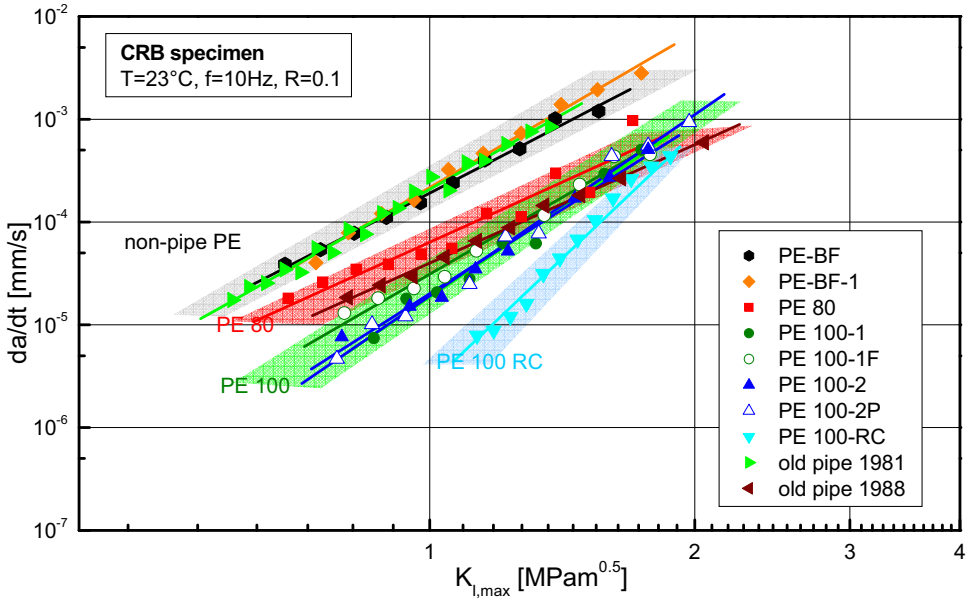

Fig. 5.4: Fatigue crack growth kinetics of different PE types at T=23°C, obtained with CRB specimens at R=0.1 and f=10 Hz.

5.3 "Synthetic" creep crack growth kinetics

As indicated in Table 2.1, for some materials FCG curves obtained at different R-ratios were extrapolated to CCG curves with R=1. The procedure and the result of the extrapolation to "synthetic" creep crack growth curves have already been described in Section 3.2.3 for PE-BF.

The measured crack growth data for PE 80 at the R-ratios of 0.1, 0.3 and 0.5 are shown in Fig. 5.5. The kinetic data from a previous project obtained from CT specimens of the same material are also included into this chart as a reference (Pinter et al., 2002). The compliance calibration based kinetic curves for R=0.1 and R=0.3 show an excellent correlation to the CT data. However, at R=0. 5 the crack growth rates in the CRB specimens are higher than those in the CT specimens, what is probably due to the lower constraint and the larger plastic zones in the CT specimen which are crack retarding. The material parameters for CCG (R=1) for PE 80 were obtained to A=1.40 x 10^{-6} and m=6.33.

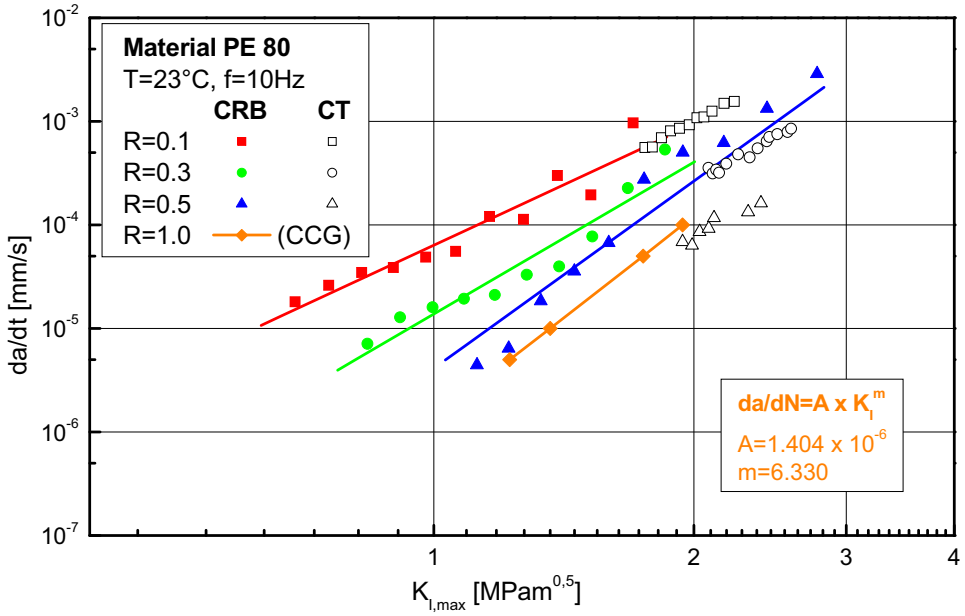

Fig. 5.5: Crack growth data da/dt vs. $K_{I,max}$ for PE 80 at R=0.1, 0.3 and 0.5 and "synthetic" CCG at R=1 (CT data taken from Pinter et al., 2002)

The testing times of the cyclic CRB tests increase significantly for the PE 100 pipe grades, so that the cyclic crack growth data were only measured at R=0.1 and 0.3, except for PE 100-2, which was also tested at R=0.5. In the latter instance, the testing time amounted to about eight weeks. In Fig. 5.6 the results for PE 100-2 at

R=0.1, 0.3 and 0.5 are shown. The extrapolation to "synthetic" CCG results in terms of fracture mechanics parameters yields values for A=8.45 x 10^{-7} and m=6.83.

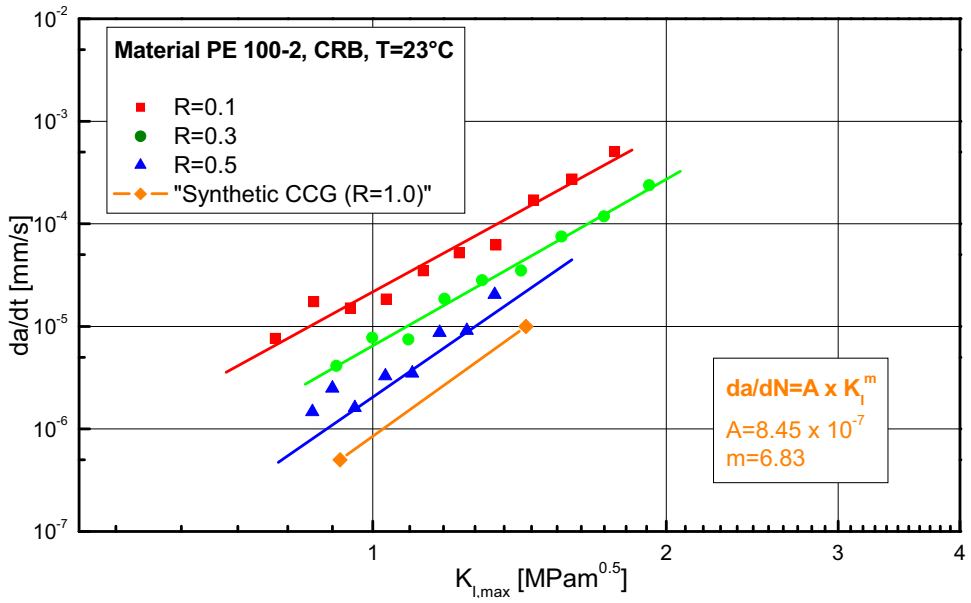

Fig. 5.6: Crack growth data da/dt vs. $K_{I,max}$ for PE 100-2 at R=0.1, 0.3 and 0.5 and "synthetic" CCG at R=1.

The measured FCG data for the non-pipe material PE-BF-1 at R=0.1 and 0.3 are shown in Fig. 5.7. The crack growth curve for R=0.5 had to be estimated as testing was not possible due to the high ductility and the low yield stress of this material. However, the extrapolation to R=1 results in a "synthetic" creep crack growth curve from which the fracture mechanics material parameters were obtained as A=4.68 x 10^{-6} and m=6.82.

In Fig. 5.8 the crack growth behavior for the old pipes from 1981 and 1988 which were investigated at R=0.1, 0.3 and 0.5 is shown. In contrast to the materials discussed so far, in this case the CRB specimens were manufactured from the pipe walls to be loaded in axial pipe direction. The extrapolation to the static loading conditions of R=1 resulted in the material parameters A and m for CCG with A=6.41 x 10^{-8} and m=5.02 for the old pipe from 1981 and A=4.49 x 10^{-8} and m=4.68 for the old pipe from 1988.

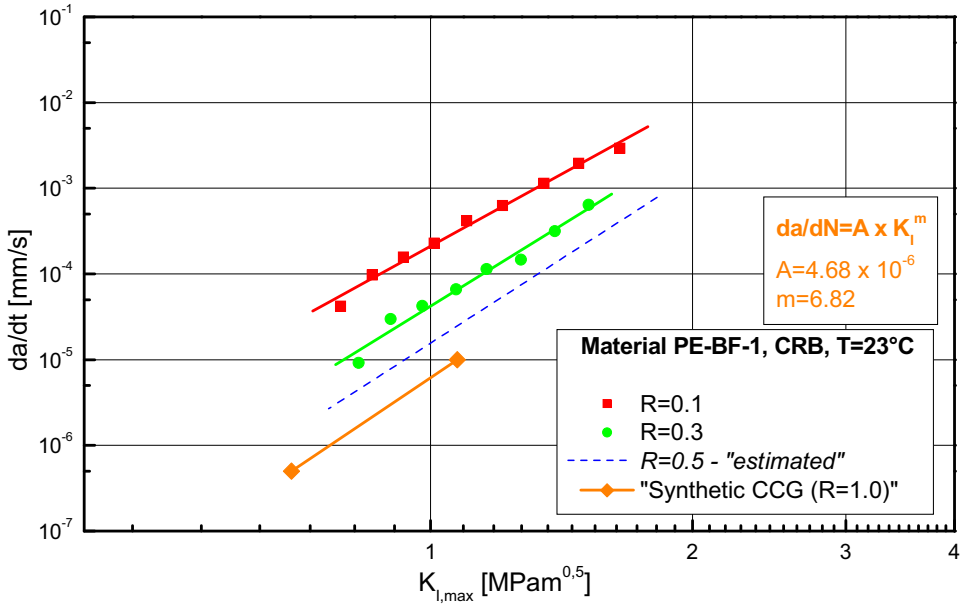

Fig. 5.7: Crack growth data da/dt vs. $K_{I,max}$ for PE-BF-1 at R=0.1, 0.3 and 0.5 (estimated) and "synthetic" CCG at R=1.

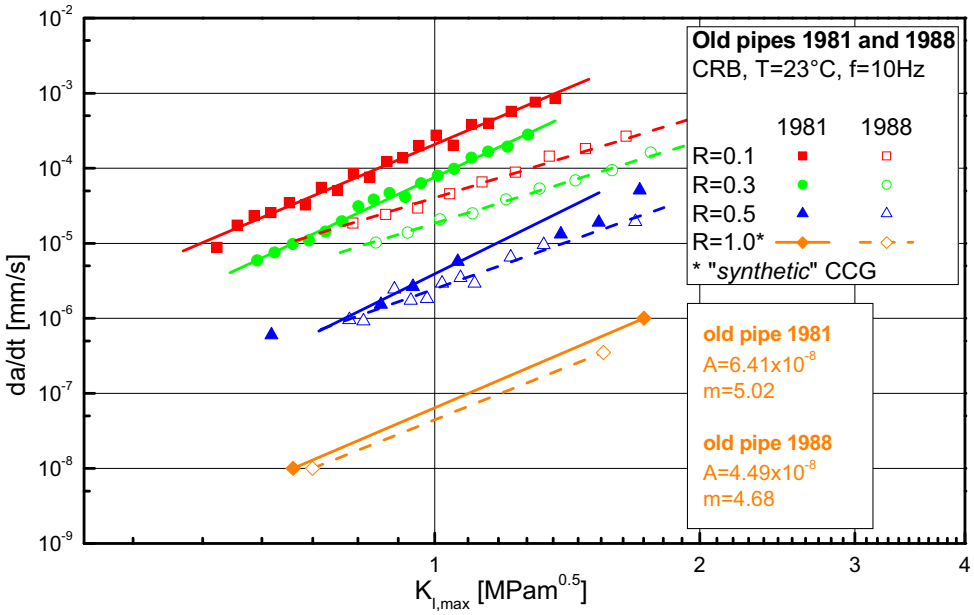

Fig. 5.8: Crack growth data da/dt vs. $K_{I,max}$ for pipes from 1981 and 1988 at R=0.1, 0.3 and 0.5 and "synthetic" CCG at R=1.

Table 5.1 summarizes the material parameters A and m for the extrapolated "synthetic" CCG curves of the various materials investigated at T=23°C. With the help of these parameters the fracture mechanics lifetime prediction based on Equation 2.3 can now be performed.

Table 5.1: Fracture mechanics parameters A and m of "synthetic" CCG curves for selected materials at 23°C.

Material PE	class	Condition	A $\left[\frac{mm}{sMPam^{0.5}}\right]$	m [-]
PE-BF	non-pipe PE	compression molded plate	4.65×10^{-5}	7.32
PE-BF-1	non-pipe PE	compression molded plate	4.68×10^{-6}	6.82
PE 80	PE 80	compression molded plate	1.40×10^{-6}	6.33
PE 100-2	PE 100	compression molded plate	8.45×10^{-7}	6.83
old pipe 1981	PE 80-MD	pipe	6.41×10^{-8}	5.02
old pipe 1988	PE 80	pipe	4.49×10^{-8}	4.68

5.4 Lifetime prediction for PE 80 and PE 100 pipes

The lifetime prediction for the material PE 80 at a temperature of 23 °C is shown in Fig. 5.9. This figure also presents a comparison between the predicted results and real data which have resulted from internal pressure tests according to ISO 9080 (TGM, 1993). In the pressurized pipe tests, significant quasi-brittle failure was only detected at a temperature of 80 °C. Whereas the ductile-brittle transition was reached for tests at 60 °C, the measurements at 20 °C only showed ductile failure within the maximum testing time of 10^4 hours.

The prediction of the pipe lifetime, that neglects the crack initiation time and assumes SCG immediately after the pressurization of the pipe, was done with Equation 2.3 using K_I from the FEM simulation model considering the change of the crack front geometry (Section 4.2) and the fracture mechanics parameters A and m from Table 5.1. The calculation was done for a pipe of the dimension D40 SDR 11, which means an outer pipe diameter of 40 mm and a pipe wall thickness of 3.6 mm. To demonstrate the influence of the initial crack length a_{ini}, the prediction was done for a_{ini}=400 μm and 100 μm, respectively (Gray et al., 1981;

Stern, 1995; Lang et al., 1997; Pinter, 1999). The two different assumptions result in a deviation of the failure times of more than one decade in time. Although there is a lack of data in internal pressure tests of about one decade to the conservative fracture mechanics failure estimation with the initial defect size of 400 μm, the slope and the values of the predicted SCG curve show reasonable characteristics.

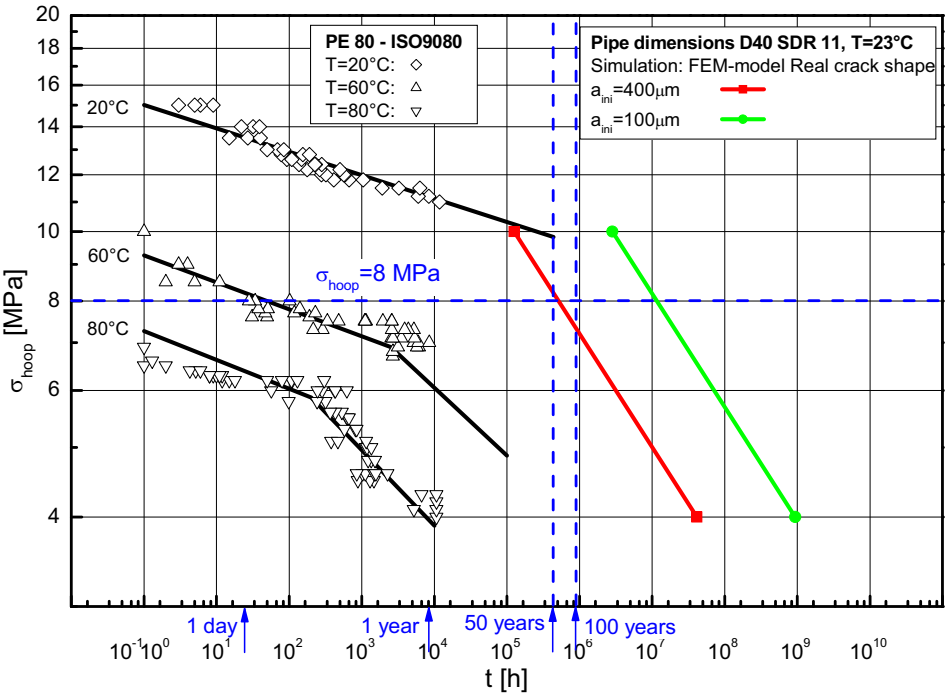

Fig. 5.9: Fracture mechanics lifetime prediction for PE 80 pipes at 23°C in comparison to experimental data from internal pressure tests of pipes at 20, 60 and 80°C (TGM, 1993).

In Fig. 5.10 the predicted lifetimes of the materials PE 80 and PE 100-2 at 23°C and real test data from internal pressure tests based on ISO 9080 at 20°C (TGM, 1993; Bodycote Report, 2002) are compared. At a given hoop stress, the experimental failure times of PE 100-2 are approximately one magnitude higher than for PE 80, although only ductile failure was detectable at this temperature within 10^4 hours. The prediction of quasi-brittle failure by SCG via the fracture mechanics method shows analogous results with a significantly higher failure time for SCG for PE 100-2 than for PE 80.

Based on the predicted failure times, both materials seem to fulfill the requirements of ISO 9080, which demands a resistance against failure of at least

50 years at MRS values of 8 MPa and 10 MPa for PE 80 and PE 100, respectively. Whereas the predicted failure time at σ_{hoop}=8 MPa is in the range of 60 years for the PE 80 material, the failure time for the PE 100 material at σ_{hoop}=10 MPa is about 55 years. As pointed out before, crack initiation times, which have not been taken into account in the fracture mechanics lifetime calculation, will provide a significant additional safety.

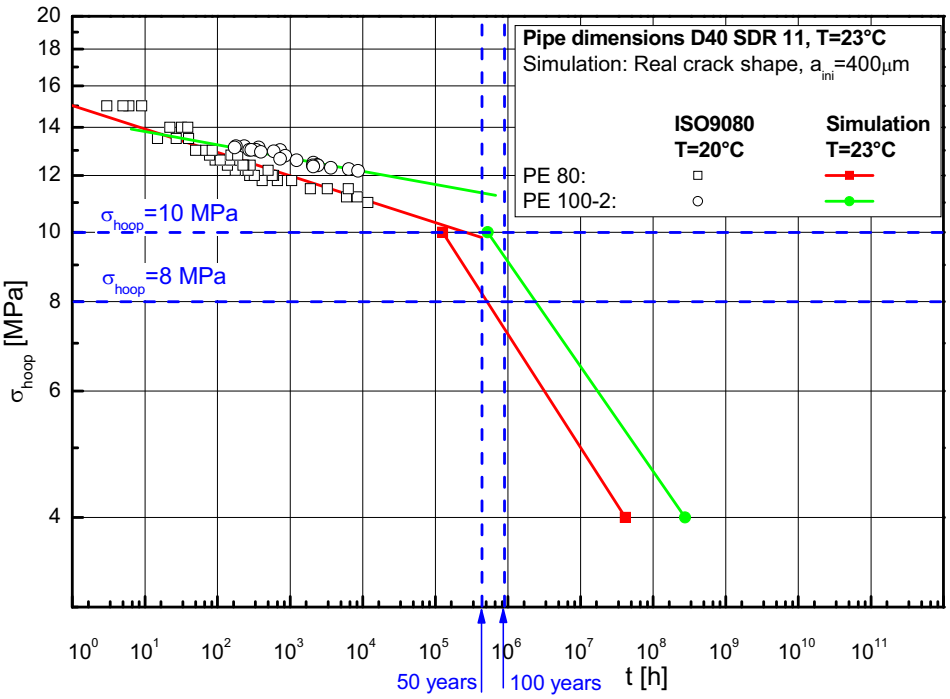

Fig. 5.10: Fracture mechanics lifetime prediction for PE 80 and PE 100-2 pipes at 23°C in comparison to experimental data from internal pressure tests of pipes at 20°C (TGM, 1993; Bodycote Report, 2002).

5.5 Prediction of the residual lifetime of old pipes

The prediction of the residual lifetime of the old pipes is shown in Fig. 5.11. The calculation was done for a pipe of the dimensions D160 SDR 11 (outer diameter: 160 mm, wall thickness: 14.5 mm), as those were the original nominal pipe dimensions. To achieve an overall operating time of 50 years, the old pipes of years 1981 and 1988 need a resistance against quasi-brittle failure for further 22 respectively 29 years. In this calculation it was assumed, that a quasi-brittle crack of an initial size of a_{ini}=400 µm had started immediately at the beginning of the pipe service in 1981 and 1988, respectively, and has been growing continuously until to-

day. Under this assumption, at a hoop stress of 8 MPa and a temperature of 23 °C, additional crack growth of about 0.195 mm and 0.129 mm until the year 2009 was calculated in the pipe from 1981 and 1988, respectively. Afterwards, the current crack length in 2009 (0.595 mm and 0.529 mm, respectively) served as new initial crack length for the prediction of the residual CCG time.

For both pipe materials the predicted failure times at σ_{hoop}=8 MPa are long enough to fulfill the requirements of a total lifetime of 50 years. The old pipe of 1988 requires a minimum residual lifetime of 29 more years and 37 years are predicted. The predicted residual lifetime of 28 years for the old pipe of year 1981 is somewhat lower than for the old pipe of 1988. Nevertheless, the required residual lifetime of 22 years should be sustained as well. However, it should be emphasized again, that it tends to be difficult to provide an exact prediction of lifetimes as many aspects may lead to significant scattering of the data. And yet, the simulated failure times do not appear unfeasible, and as already mentioned before, the neglected time for crack initiation will provide additional safety. The demonstrated lifetime prediction and a comprehensive material characterization on the old pipes has been published in **Paper I-4** in the Appendix.

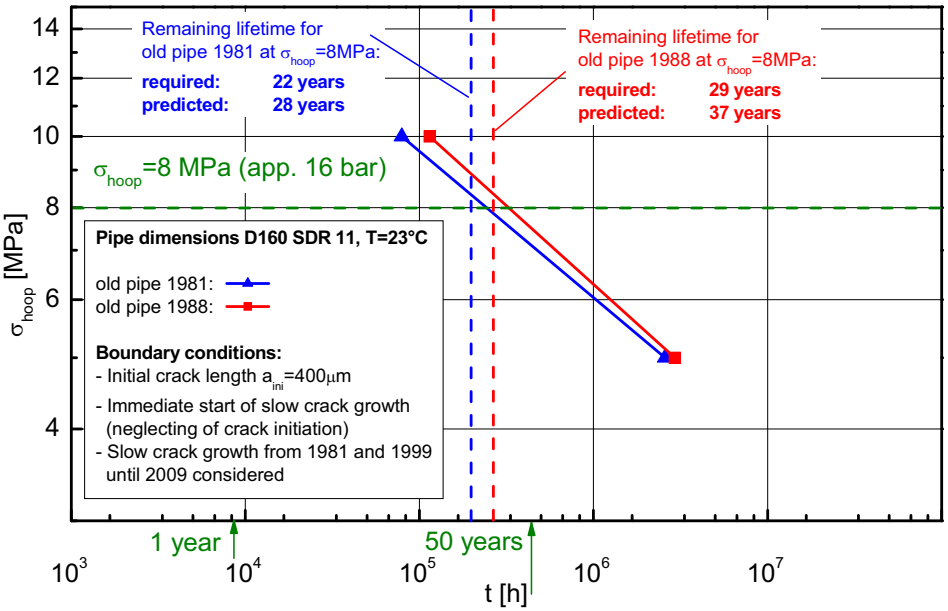

Fig. 5.11: Fracture mechanics prediction for the residual lifetime old pipes from 1981 and 1988 at 23°C.

5.6 References

Bodycote Report (2002), Bodycote/P-02/142, Nyköping, Sweden.

Frank, A., Podingbauer, T., Liedauer, S., McCarthy, M., Haager, M., Pinter, G. (2008). "Characterization of the Property Profile of Old PE Gas Pipes in Service for up to 30 Years", Plastics Pipes XIV, Budapest, Hungary.

Gray, A., Mallinson, J.N., Price, J.B. (1981). “Fracture behavior of polyethylene pipes”, Plastics and Rubber Processing and Applications 1, 51-53.

Haager, M. (2006). "Fracture mechanics methods for the accelerated characterization of the slow crack growth behavior of polyethylene pipe materials", Doctoral Dissertation, Institute of Materials Science and Testing of Plastics, University of Leoben, Austria.

Lang, R.W., Stern, A., Doerner, G. (1997). "Applicability and Limitations of Current Lifetime Prediction Models for Thermoplastics Pipes under Internal Pressure", Die Angewandte Makromolekulare Chemie 247, 131-137.

Pinter, G. (1999). "Rißwachstumsverhalten von PE-HD unter statischer Belastung", Doctoral Dissertation, Institute of Materials Science and Testing of Plastics, University of Leoben, Austria.

Pinter, G., Balika, W., Lang, R.W. (2002). "A Correlation of Creep and Fatigue Crack Growth in High Density Poly(Ethylene) at Various Temperatures", Temperature-Fatigue Interaction, REMY, L. AND PETIT, J, Amsterdam, Elsevier Science Ltd. and ESIS, ESIS Publication 29: 267-275.

Stern, A. (1995). "Fracture Mechanical Characterization of the Long-Term Behavior of Polymers under Static Loads", Doctoral Dissertation, Institute of Materials Science and Testing of Plastics, University of Leoben, Austria.

TGM (1993). Gutachten Nr. K 14 450, Technologisches Gewerbemuseum, Wien, Austria.

6 SUMMARY AND CONCLUSIONS

For a fracture mechanics lifetime prediction of internally pressurized pipes the knowledge of the material specific kinetics of CCG is essential. The development and implementation of a new methodology for an accelerated prediction of lifetimes of PE pipes at application near temperatures of 23°C, which was already proposed within a fracture mechanics extrapolation concept by Lang and Pinter, was the major objective of this Dissertation.

To guarantee a quick data acquisition, CRB specimens were selected as they ensure a high reliability and relatively short testing times. The generation of “synthetic” FCG curves based on single Woehler-type fatigue tests with CRB specimens combined with a post-failure fracture surface analysis results in average crack growth rates for individual tests. However, the uncertainty in the optical detection of the transition from a brittle failure mode to a ductile failure mode was too high, resulting in a large scatter and low reproducibility of the data. Due to this fact, the final intention was to develop a new test procedure that allows for a direct measurement of crack growth rates in CRB specimens.

For this purpose a compliance methodology was used to determine a crack length depending continuously compliance calibration curve for CRB specimens. With this compliance curve it was possible to detect the current crack length during a single fatigue test. To measure the specimen compliance, a system of three extensometers was used to detect the crack opening displacement around the circumference of the cracked specimens. With the knowledge of the crack length as a function of the number of cycles, it was possible to calculate crack growth rates. This direct measurement of the crack growth kinetics helped to modify the original extrapolation concept by Lang and Pinter, as the development of Woehler curves at different R-ratios was no longer necessary. Much rather the FCG curves could be determined directly and more reliably.

With the measured FCG kinetics at different R-ratios, an extrapolation to static loading with R=1 was carried out to derive a “synthetic” CCG curve which served

to obtain the fundamental material constants A and m for a fracture mechanics lifetime assessment.

An additional option of the test procedure with three extensometers was the high sensitivity in the detection of crack initiation. The fact, that the ranking of the various PE types investigated in terms of crack initiation was the same as in terms of total failure times, opens the potential for a further acceleration of the test procedure for material ranking or even for scientific investigations on the mechanisms which are responsible for crack initiation.

To get reliable fracture mechanics lifetime predictions, a proper calculation of the stress intensity factor K_I, which describes the stress field in the vicinity of a crack tip, and the definition of suitable boundary conditions are also necessary. To emphasize the importance of relevant assumptions, different solutions for K_I in an internally pressurized pipe were studied. It was shown, that the literature formulas by Murakami and Anderson provide results of sufficient accuracy concerning the standard model of an internally pressurized pipe without any additional loading and the assumption of a semi-circular crack front geometry. However, in reality the crack front geometry first having a semi-circular shape usually turns into a semi-elliptical one, which was considered in a finite element method (FEM) simulation model. This FEM model of a pressurized pipe represents the loading situation in the internal pressure test according to EN ISO 9080 and may also be used to calculate more complex loading situations like sand embedding, as well as superimposed bending or point loads for the prediction of lifetimes for pipes under arbitrary loading situations.

The described test method and the extrapolation procedure were successfully applied to different PE types. A blow-forming PE (PE-BF) was used to develop the test procedure, as its brittleness results in short testing times. To ensure a high reliability in the extrapolation to R=1, the crack growth kinetics of the PE-BF grade was measured up to R=0.7. To apply the test procedure to PE pipe grade materials, a typical PE 80 material, which has been used widespread in existing pipe systems and several modern PE 100 pipe grade materials, were characterized.

The predicted lifetimes at a temperature of 23 °C of the PE 80 and PE 100 pipe grade materials were compared to available real test data of internal pressure

tests based on ISO 9080 at 20 °C. The position and the slope of the calculated failure times indicate reasonable results and underline the potential of the developed test procedure for a fracture mechanics lifetime calculation of pressurized pipes, even with modern pipe grade PE types.

To emphasize a more practical application of the developed test procedure, two old pipes, which have already been in use for more than 20 years, were characterized to predict their residual lifetimes. The CRB specimens for the characterization were prepared from the pipe walls to be loaded in axial pipe direction. Although it was estimated that immediately after the pressurization a crack has started to grow, the fracture mechanics lifetime prediction seem to confirm a sufficient residual lifetime for both pipes to fulfill an overall service time of 50 years. The overall testing time in this study was less than three months per pipe.

Although one of the aims of the developed test method was to ensure an accelerated material characterization, testing times at higher R-ratios are in the range of several weeks. Especially testing times at R=0.5 require at least 8 weeks for each specimen of PE 100 pipe grades, and modern PE 100 RC materials with especially improved resistance against crack initiation and SCG even need to be tested several months. However, compared to the standard extrapolation method by EN ISO 9080, in which internal pressure tests on pipes of modern PE pipe materials are stopped after 10^4 h (approx. 13.5 month) without any information on quasi-brittle crack growth kinetics or even crack initiation, the developed test method still offers more comprehensive information on these phenomena. Furthermore, the methodology presented opens the opportunity for a modern fracture mechanics lifetime assessment of pipe systems within a time which is significantly lower than the one currently needed according to EN ISO 9080. Especially in combination with the FEM model it is possible to predict the lifetime of pipes under arbitrary loading situations.

For all demonstrated lifetime predictions it always has to be remarked, that the lifetime estimates are conservative, as they only take CCG times into account. Crack initiation claims a significant fraction of the total failure time. Neglecting this part of the total failure time always gives additional safety as to more realistic lifetime expectations.

Differences in the results of CRB specimens with different processing histories indicate certain effects of the morphology on the mechanisms of crack initiation and SCG. Whereas quasi-brittle crack growth in PE has already been well investigated resulting in a wide range of available studies, the mechanisms and kinetics of crack initiation are still not fully understood. Therefore, this topic is recommended for further scientific research.

PART II

LONG-TERM FAILURE BEHAVIOR OF A POLYETHYLENE CLOSE-FIT-LINER

7 CLOSE-FIT-LINER PRODUCTION AND INSTALLATION

Buried pipes contribute an important part in the maintenance of our modern infrastructure and the high living standard of our society. Depending on the transported goods, the application and materials of buried pipes vary in a wide range. Due to the long service times and the proximity to urban regions, the reliability of pipe systems and the avoidance of pipe failure are fundamentally important for any type of material. However, many pipe systems which have been operating for decades are now approaching the end of their lifetime and need to get renovated or even replaced. Especially in urban regions repair or rehabilitation of old pipes is always connected to high technical efforts and enormous costs. The following chapter outlines the importance of reliable pipe systems and the need for time and cost saving methods for pipe rehabilitation. Furthermore, the technology of Close-Fit-Lining will be introduced as a special application for a trenchless rehabilitation of already installed pipes.

Some of the essential results of the investigations have already been published in two papers available in the Appendix. Whereas **Paper II-1** mainly focuses on changes of the thermomechanical material behavior, **Paper II-2** will also describe the long-term failure behavior of Close-Fit-Liner in a rather detailed way.

7.1 Engineering and market importance

Based on the global water supply and sanitation assessment 2000 report (WHO and UNICEF, 2000) the house connection rate in urban regions of Africa (43 %), Oceania (73 %), Asia and Latin America (77 %) is still developable, whereas the largest cities in Europe and North America already dispose of a house connection rate between 96 and 100 %. The essential function of a reliable piping system is to ensure a safe water supply at minimized water loss as well as the prevention of contamination by infiltration. However, the lower the development-standard of a nation, the higher the grade of contamination of potable water. In Africa more than 35 % of the available drinking water does not correspond to national standards with regard to microbiological, chemical, physical or esthetic characteristics (WHO and UNICEF, 2000).

Due to leaking pipes the amount of non-revenue water is higher than 50 % in some regions of the world, and even the large cities of Africa (39 %), Asia and Latin America (42 %) have to face with enormous water loss (WHO and UNICEF, 2000). Based on only few data, the leakage rate of water in North America is also said to be above 15 % (WHO and UNICEF, 2000).

In international comparison, the Austrian pipe network for potable water supply is in good conditions. The regulation W 100 from the Austrian Association for Gas and Water (ÖVGW) indicates a burst frequency of 7 defects per 100 km pipe per year (ÖVGW Richtlinie W 100, 2007; Gangl, 2008). However, hardly no information is available how this number relates to different pipe materials (steel, cast iron, cement, plastics). A high burst rate in Austria is 20/100 km, which is a relatively low level anyway, compared to other international supply areas (Gangl, 2008), such as London Three Valleys with 226/100 km or London Thames Water with 430/100 km (Parker, 2007). The leakage rate in Austria amounts approx. 9.5 % (Schönbäck et al., 2003). However, to keep this high standard of infrastructure in Austria and to improve the situation in other cities and nations, the availability of a sustainable maintenance and rehabilitation program is of essential importance.

The obviously existing defects and the age of pipe systems both indicate the need of rehabilitation (Winkler, 2003; Kaller, 2007). Especially in big cities the infrastructure for water supply is more than 100 years old. In London for example, more than 90 % of the pipes which are in use today have been installed before 1900. This serves as an explanation for the mentioned high burst frequency and a leakage rate of more than 30 % (Kaller, 2007). In Germany, between 1990 and 2001, the need for rehabilitation due to a pipe age of 75 years and more remains constant at rates between 17 and 22 %, which is more than 75,000 km per year (Winkler, 2003). Just for the sake of completeness it is mentioned, that all these mentioned old pipes are made of non-plastics material.

7.2 Close-Fit-Liner technology

For a time and cost efficient, traffic and environmental friendly pipe rehabilitation, different trenchless technologies for plastics pipes have been developed since the 1980's (Glanert and Schulze, 2002). Recently, such technologies have also become more important and due to improvements in standardization, quality assur-

ance and documentation also the acceptance of construction companies increases (Philipp, 2009).

Trenchless pipe rehabilitation with Close-Fit-Liner (CFL) is an established and state of the art technology for the renovation of existing pipe systems. Besides, it is used for significantly extending the service time of old or damaged pipes. Thus, the technology of Close-Fit-Lining with PE pipes has become increasingly important (Glanert and Schulze, 2002).

To manufacture a CFL, usually a conventional extruded pipe gets folded under certain temperature and loading conditions to achieve a reduction of the cross-section of about 30 % (Glanert and Schulze, 2002, Rabmer-Koller, 2007). After this process the folded pipe is cooled and stored on coils.

During a typical installation, which is shown schematically in Fig. 7.1, the CFL is pulled directly off the coil into an already existing pipe system. Afterwards, both ends will be closed. Without a pressurization of the CFL, at the beginning of the pipe, which is called A-station, steam with a temperature of approx. 120 °C is inserted for heating up the material to a temperature of about 80 °C. This temperature is held constant for about 2 hours. To ensure a constant heating of the whole pipe, the temperature is permanently measured at the outer pipe wall position at the end of the CFL, which is called B-station, and controlled at the A-station (Rabmer, 2009).

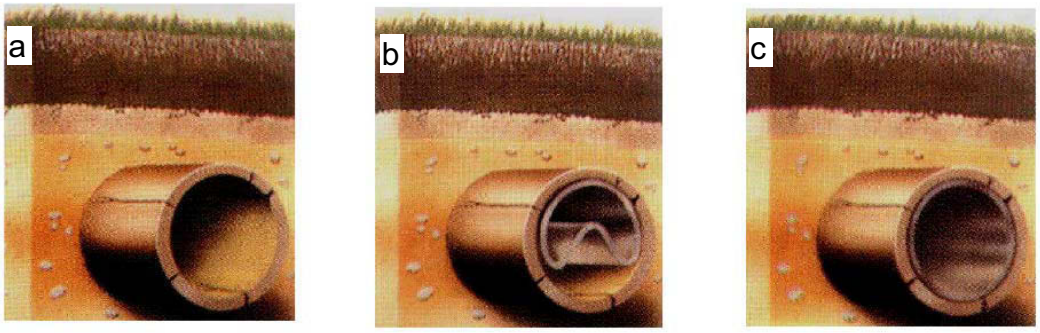

Fig. 7.1: Schematical illustration of the installation process of a CFL: a) old or damaged pipe; b) old pipe with inserted preformed CFL; c) old pipe with redeformed CFL (Rabmer-Koller, 2007).

During this heating, the CFL relaxes and redeforms back to almost its original circular shape due to frozen orientation within the pipe material. This characteristic, which is typical of thermoplastic materials, is called memory-effect (Menges et al., 2002). After this inherent redeformation of the CFL, a dimension specific stepwise pressurization of the pipe ensures a close-fit without any gap to the old pipe. During this process, the pipe is usually not heated anymore. At a specific maximum pressure the installed pipe gets cooled stepwise. According to CFL suppliers, the final installed pipe is supposed to exhibit characteristics of a complete virgin conventional pipe. Depending on the pipe dimensions, it is possible to install lengths of about 950 m in just one step with this sort of technology (Rabmer-Koller, 2007).

7.3 Effects of process steps on the material

In contrast to a conventionally installed PE pipe, the necessary process steps of heating and folding at manufacturing, and reheating during the installation imply a considerable additional thermal and mechanical exposure of the pipe material. However, scientific studies that deal with this topic have not been published so far and appear not to be available. It is assumed, that changes in morphology and properties may occur in the crystallinity, in molecular orientation, in the stabilization of the material against thermo-oxidative aging, or in mechanical properties like residual stresses or the resistance against crack initiation or SCG. Under the aspect of a rehabilitation technology with high sustainability, which ensures operating times of the new installed Close-Fit-Liners of 50 years and even more, the critical questions on changes in the pipe material are more than eligible.

The relatively long thermal exposure at 80 °C for several hours (Rabmer, 2009) is comparable to an annealing procedure, which on the one hand will reduce molecular orientations as well as processing related residual stresses of the pipe (Choi and Broutman, 1997). On the other hand, additional annealing usually influences the crystallinity of the material and also thermo-oxidative aging may change the material behavior. All these characteristics and properties play a fundamental role in the resistance of the material against the critical failure mechanisms of crack initiation and SCG as well as for the long-term properties of the pipe.

For modern pipe applications special pipe grade materials of the classification PE 100 with bimodal molecular mass distribution are used nowadays. Although

there is a huge number of studies on morphological or thermomechanical behavior of PE pipe grades, no information is available on the effects of the deformation and redeformation process on the material properties of CFL.

Therefore, one major goal of this part of this Dissertation was to perform a systematic study of the influence of the additional mechanical and thermal processes on the material properties of the CFL. In particular, morphological changes in crystallinity and molecular orientation were investigated as well as changes in residual stresses of the pipe, the stabilization against thermo-oxidative material aging and the long-term failure behavior.

7.4 Material and specimen preparation

The morphological characterization of the CFL was conducted with a new product of AGRU Kunststofftechnik GmbH (Bad Hall, A). The investigated pipes of the dimension D188 SDR 17 (outer diameter: 188 mm, wall thickness: 11.1 mm) were manufactured using a modern PE 100 pipe grade. The redeformation under laboratory conditions inside a steel pipe was done by the company RABMER Rohrtechnik GmbH & Co.KG (Altenberg, A). This pipe is labeled as “AGRU I” in this Dissertation.

With a different batch of the AGRU pipe a redeformation under laboratory conditions was done by RABMER with the aim of investigating different thermal insulations. Therefore, for one redeformation the steel pipe was used again, another redeformation was done in a steel pipe with an additional insulation of a polypropylene (PP) pipe. The purpose of this procedure was to simulate a more realistic heat balance that normally exists by the surrounding soil at real construction sites. This pipe is labeled as “AGRU II” in this Dissertation.

Other CFL segments from a field installation with the dimensions D150 SDR 15 were manufactured by REHAU GmbH (Guntramsdorf, A) and installed and delivered by RABMER. The exact type of the PE 100 pipe grade was unknown. Because of the fact that the motivation for testing this pipe was a correlation of material properties at the A-station and the B-station of a real installed pipe, it is labeled as “A-B-correlation” in this Dissertation.

To obtain comprehensive information on morphological properties around the circumference of the pipe, five characteristics positions (Pos. 1 to Pos. 5), which are shown in Fig. 7.2, were defined considering the folding process. The strongest changes in the geometry of the pipe in the CFL appear at Pos. 1. The symmetrical positions Pos. 2 and Pos. 3 represent vertices, at which the pipe radius is significantly decreased. The positions Pos. 4 and Pos. 5, which are symmetrical as well, are nearly unaffected by the mechanical folding process. Segments were milled out from all positions, and care was taken to minimize any thermal effects while cutting the samples. Afterwards, these segments were used for further specimen preparation depending on the characterization method. If possible, specimens were also prepared from different pipe wall positions (inner pipe wall, center of the pipe wall, outer pipe wall) (Mannsberger, 2007; Redhead, 2009).

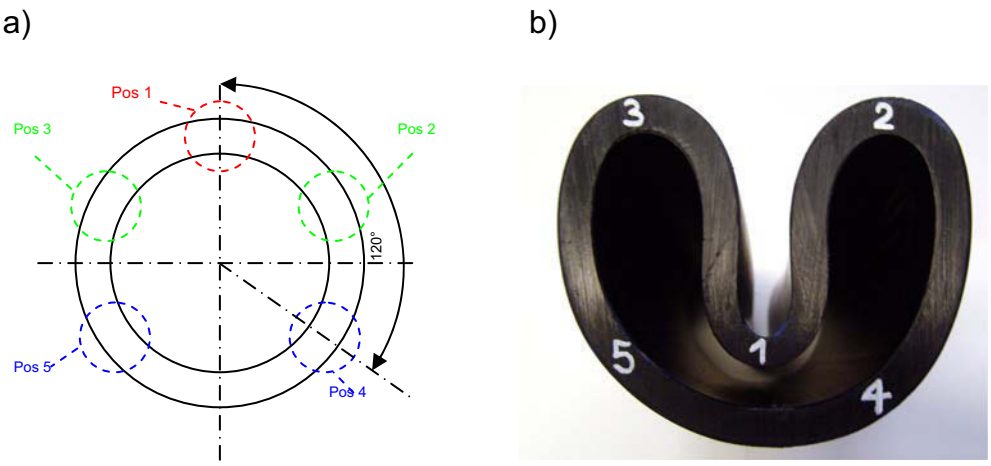

Fig. 7.2: Schematical illustration of the defined positions Pos. 1 to Pos. 5 in a) the undeformed pipe and b) the folded intermediate state of the CFL.

7.5 References

Choi, S., Broutman, L.J. (1997). "Residual Stesses in Plastic Pipes and Fitting IV. Effect of Annealing on Deformation and Fracture Properties." Polymer (Korea) 21(1): 93-102.

Gangl, G., Theuretzbacher-Fritz, H., Kölbl, J., Kainz, H., Tieber, M. (2006). “Erfahrungen mit der Wasserverlustberechnung im ÖVGW Benchmarking-Projekt”, ÖVGW Symposium 2006, Wien.

Gangl, G. (2008). "Rehabilitationsplanung von Trinkwassernetzen", Doctoral Dissertation, Schriftenreihe zur Wasserwirtschaft 53, Technische Universität Graz.

Glanert, R., Schulze, S. (2002). "U-Liner - Der Klassiker für die Sanierung von Druckrohren", 3R International, 41(1), 16-19.

Kaller, R. (2007). “Durstige Megapolen”, FORUM Gas Wasser Wärme 5, 13-16.

Mannsberger, G. (2007). "Morphologische Charakterisierung an vorgeformten und rückdeformierten Polyethylen-Rohren für die grabenlose Rohrsanierung", Master Thesis, Institute of Materials Science and Testing of Plastics, University of Leoben, Austria.

Menges, G., Haberstroh, E., Michaeli, W., Schmachtenberg, E. (2002). „Werkstoffkunde Kunststoffe“, Hanser, München, D, Wien, A.

ÖVGW Richtlinie W 63 (2009). "Wasserverluste in Versorgungsnetzen, Anschlussleitungen und Verbrauchsleitungen".

ÖVGW Richtlinie W 100 (2007). "Wasserverteilungen - Betrieb und Instandhaltung".

Parker, J. (2007). "Analysing London’s Leakage – Experiences of an Expert Witness", in proceedings: Water Loss 2007, Bucharest, Romania, 188-198.

Philipp, A. (2009). “Großsanierungen von Druckleitungen im PE-Close_fit-Verfahren”, in proceedings: ÖGL Symposium Grabenlos 2009, Loipersdorf, Austria, 45-53.

Rabmer-Koller, U (2007). ““Inliner-“ and “Close Fit” Technologies - Potentials and Advantages for Water Pipe Rehabilitation”, in proceedings: Water Loss 2007, Bucharest, Romania, 126-137.

Rabmer Rohrtechnik GmbH & Co.KG (2009). „Arbeitsanweisung, Heizanleitung Close Fit Rohr“, Altenberg, A.

Redhead, A. (2009). "Untersuchungen an einem unter realen Bedingungen rückdeformierten Close-Fit-Reliner aus Polyethylen", Bachelor Thesis, Institute of Materials Science and Testing of Plastics, University of Leoben, Austria.

Schönbäck, W., Oppolzer, G., Kraemer, R.A., Hansen, W., Herbke, N. (2003). "Internationaler Vergleich der Siedlungswasserwirtschaft", Österreichische Bundeskammer für Arbeiter und Angestellte, Informationen zur Umweltpolitik, Nr. 153, Bde. 1-5, 570 S., Wien.

WHO and UNICEF (2000). Global water supply and sanitation assessment 2000 report, World Health Organization and United Nations Children's Fund.

Winkler, U. (2003). “Grabenlos sanieren – Schnell und wirtschaftlich”, wwt awt, Heft 1-2, 8-15.

8 MORPHOLOGICAL INVESTIGATION OF UNDEFORMED A ND REDEFORMED PIPES

The morphological characterization of the CFL is subdivided into three parts. First, a correlation of the properties of an undeformed pipe with those of a redeformed CFL was done. The results of this study have been published in **Paper II-1** and **II-2** in the Appendix. In a second step pipe segments of a real installation were investigated comparing the properties of the A-station to those of the B-station. In a third step the influence of different thermal insulation conditions were studied. Comprehensive details on sample preparation and the development of the characterization methods are available in the Master Thesis of Mannsberger (Mannsberger, 2007) and in the Bachelor Thesis of Redhead (Redhead, 2009).

8.1 Experimen tal

To evaluate the temperature dependent mechanical properties (like storage modulus and damping), dynamic-mechanical analysis (DMA) tests were performed. Therefore, film specimens with a thickness of approx. 30 μm were tested in a force controlled mode at a frequency of 10 Hz within the linear-viscoelastic region of the material. The temperature was increased with a heating rate of 3 K/min from -90 to 130 °C and the storage modulus E' and the loss-factor (damping) tanδ as a function of the temperature were recorded. Testing was accomplished using a device of the type DMA/SDTA861e (Mettler Toledo GmbH; Schwerzenbach, CH).

The degree of crystallinity α was determined with a differential scanning calorimeter (DSC) of the type DSC822 (Mettler Toledo GmbH; Schwerzenbach, CH) between 23 and 180 °C and a heating rate of 10 K/min (ISO 11357-3:1999). The calculation of α was done by using a recommended value for the enthalpy of a PE with theoretically 100 % crystallinity of ΔH_{m0}=293 J/g (Lohmeyer, 1984).

To estimate the degree of molecular orientation which allows to draw conclusions on the thermal and mechanical history, the linear thermal expansion was measured in circumferential direction with specimens of the dimensions 4 x 4 x 6 mm

(with the long side in circumferential direction). Testing was done between 25 and 120 °C and a heating rate of 2 K/min (ISO 11359-2:1999) with a dilatometer of the type TMA/SDTA840 (Mettler Toledo GmbH; Schwerzenbach, CH).

8.2 Dynamic mechanical analysis

The DMA results at Pos. 1 of the pipe AGRU-I, which are presented in Fig. 8.1, show a slightly lower E' value at the outer pipe wall position in the whole temperature range compared to the pipe center or the inner pipe wall position for both pipe conditions, undeformed as well as redeformed. Analogously, tanδ exhibits somewhat higher values at the outer pipe wall position. This effect is related to the processing history of the pipe in which the material gets cooled more rapidly at the outer surface, retarding the formation of the crystalline phase (Ehrenstein et al. 1995). For the redeformed pipe a tendency to an increased E' value can be noticed which may have been caused by a higher crystallinity across the pipe section. However, a significant change in the measured properties due to the additional thermal and mechanical treatment could not be detected. The position Pos. 1 is the section of the pipe with the maximum deformations. The results of Pos. 2 to 5, which are not depicted here, show similar values, so that a strong influence of different degree of deformation on the stiffness of the material can be excluded.

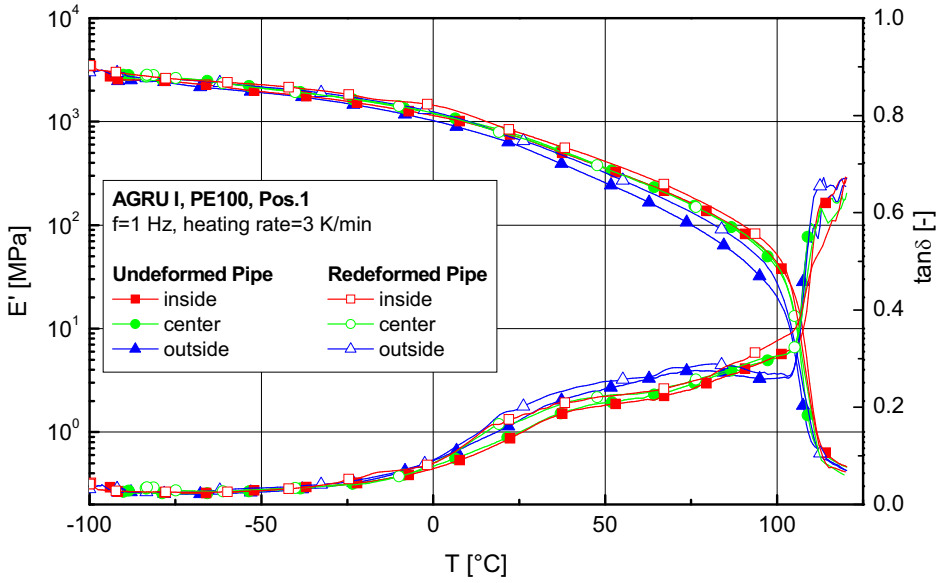

Fig. 8.1: Storage modulus E' and loss-factor tanδ at Pos. 1 of the undeformed and redeformed pipe of AGRU I at different pipe wall positions.

The characteristics of the storage modulus E' and the loss factor tanδ of the A-B-correlation in Fig. 8.2 shows results that are comparable to the AGRU I pipes. Although similar effects across the pipe wall position were noticed, a significant difference between the beginning and the end of the pipe was not detected.

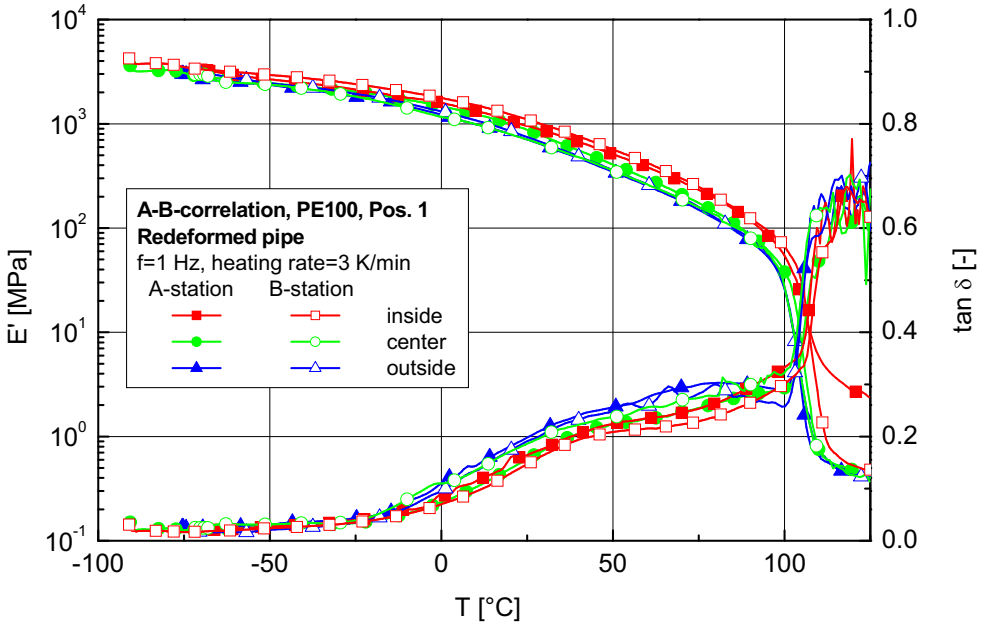

Fig. 8.2: Storage modulus E' and loss-factor tanδ at Pos. 1 of the A-station and the B-station of the redeformed pipe; A-B-correlation at different pipe wall positions.

To summarize, the characterization of dynamic-mechanical properties (Mannsberger, 2007; Redhead, 2009) shows no significant influence of the deformation of the pipe to the CFL and the later deformation to the final pipe on the investigated material properties. Solely the tendency of a somewhat higher stiffness in the redeformed CFL indicates an increase in crystallinity as a result of the additional thermal treatment.

8.3 Changes in the degree of crystallinity

The degree of crystallinity α of AGRU I is shown in Fig. 8.3 ascertaining a clear dependence on the pipe wall position. The lowest value for α with approx. 53 % was found at the outer pipe wall position of the undeformed pipe, and increases to about 57 % in the center and the inner pipe wall position. This gradient confirms

the results of the DMA in which the lower crystallinity results in a somewhat lower storage modulus due to the higher cooling rate at the outer pipe wall.

After the redeformation process of the CFL, α increases constantly by about 4 to 5 % across the whole pipe wall up to a maximum of about 62 % and without any significant differences in the circumferential positions. This post-crystallization is a clear hint for morphological changes within the pipe material as a result of the additional heating during the installation. Usually, a higher degree of crystallinity relates to higher material stiffness and hardness, however, the fracture toughness and crack growth resistance of the material can potentially be affected negatively.

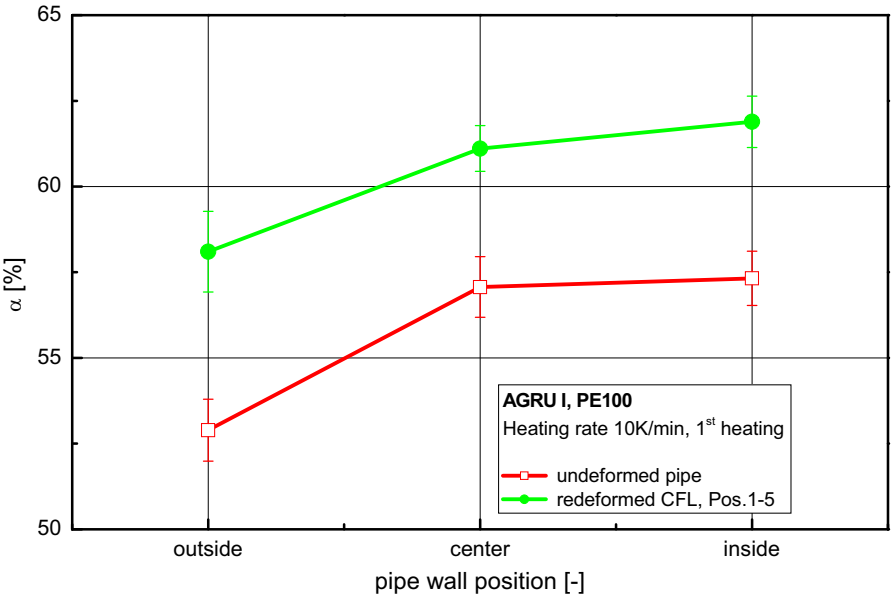

Fig. 8.3: Crystallinity α for the undeformed pipe and the redeformed CFL of AGRU I at different pipe wall positions.

Whereas α shows similar results for the A-station and the B-station in the redeformed pipe of the A-B-correlation, different shapes of the enthalpy curves at the inner pipe wall position were observed (Redhead, 2009). The heat flow as a function of the temperature for these two positions is shown in Fig. 8.4. For the signal at the A-station a significant shoulder with a peak at a temperature of approx. 120 °C can be recognized. During the installation and redeformation process of the CFL, steam with a temperature of about 120 °C is inserted at the A-station to hold a temperature of about 80 °C at the outer pipe wall position at the B-station for at least two hours. As distance between the A-station and the B-station was

about 100 m, the amount of heat energy to hold a constant temperature along the whole CFL was higher at the A-station. This apparently resulted in the detected temper-shoulder. Due to the fact of similar overall crystallinity and stiffness at both pipe ends, the temper-shoulder may not expected to have a significant effect on the behavior of the final pipe.

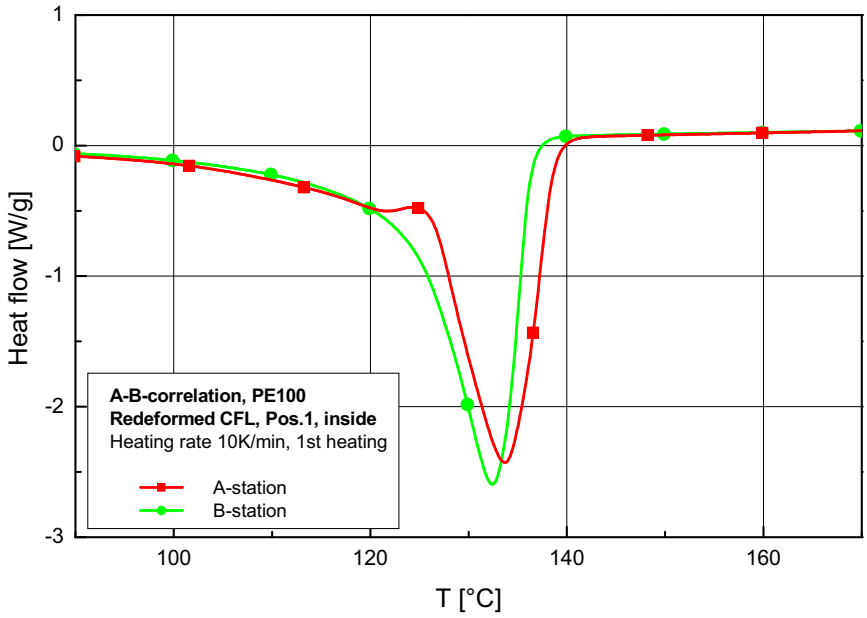

Fig. 8.4: Heat enthalpy at the inner pipe wall position of the A-station and the B-station of the A-B-correlation.

8.4 Molecular orientation and memory-effect

During the mechanical deformation in the folding process of the pipe to the CFL, high molecular orientations are inserted into the material, which are essential for the inherent redeformation during the installation of the pipe. This entropy-elastic effect is called memory-effect (Menges et al. 2002). One way to determine molecular orientations is by measuring the linear thermal expansion of the material.

A simplified model of the coherency of molecular orientation and thermal expansion is shown in Fig. 8.5. Macromolecules always tend to take a shape of highest entropy, which means the highest level of disarrangement. While processing, the macromolecules are usually orientated in a preferred direction. After a very quick cooling they get frozen with a high degree of orientation (Fig. 8.5 a). If the material is heated to or above the temperature at which the orientations were frozen, the thermal mobility allows for a rearrangement of the macromolecules to increase

their entropy and disorientation. As a result of this process the thermal expansion is affected as it is illustrated in Fig. 8.5 b.

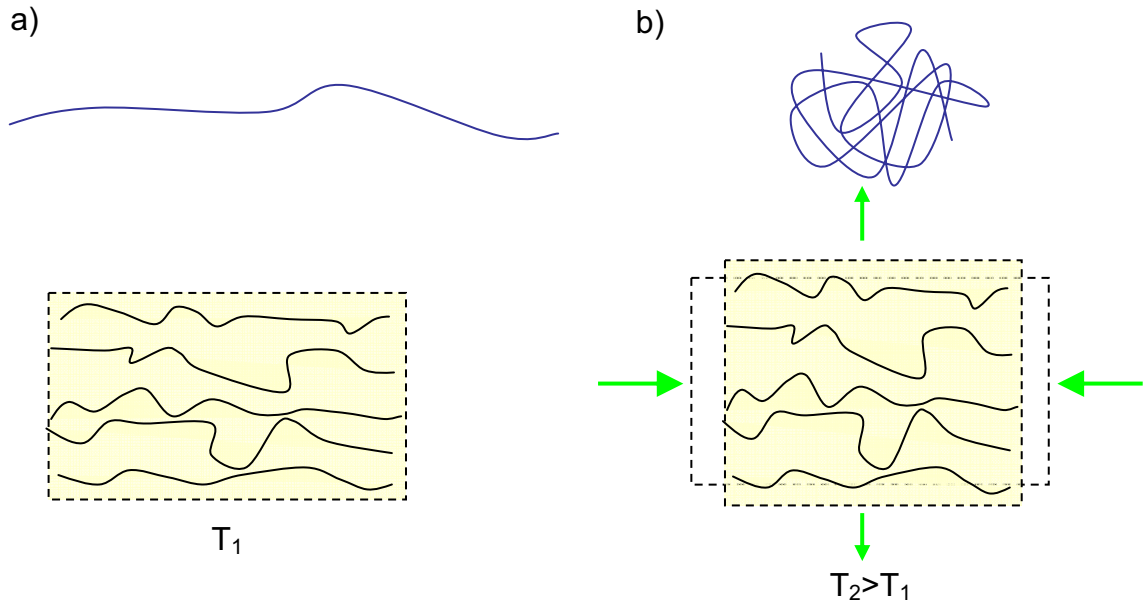

Fig. 8.5: Schematically illustration of molecular orientation: a) most unlikely shape with lowest entropy; b) most possible shape with highest entropy.

The measurements in axial direction of AGRU I in Fig. 8.6 only show a significant change at the outer pipe wall position, where the linear thermal expansion Δl in the undeformed pipe is clearly higher than in the redeformed CFL. In the undeformed pipe a high extent of orientation was frozen in circumferential direction that leads to a relatively high Δl in axial direction. In the redeformed pipe the orientations have been removed and the thermal expansion in axial direction shows lower values. Hardly any difference between the positions Pos. 1 to 5 could be detected, which leads to the conclusion that a dependency of the extent of mechanical deformation on molecular orientation in axial direction can be excluded.

A completely different behavior was found for the linear thermal expansion in circumferential direction, where a strong dependency of Δl on the extent of mechanical deformation was detected (Fig. 8.7). The thermal expansion curves for the outer pipe wall at the positions Pos. 4 and 5 of the redeformed CFL, which are nearly unaffected by the folding process of the pipe, show a good agreement in data for the undeformed pipe. However, at the vertices of the redeformed CFL at Pos. 2 and 3, a lower linear thermal expansion was measured, and at Pos. 1 even

a negative gradient of the curve was detected at higher temperatures. The different Δl values indicate a strong correlation between the degree of mechanical deformation of the material during the action of folding and installation and the molecular orientation.

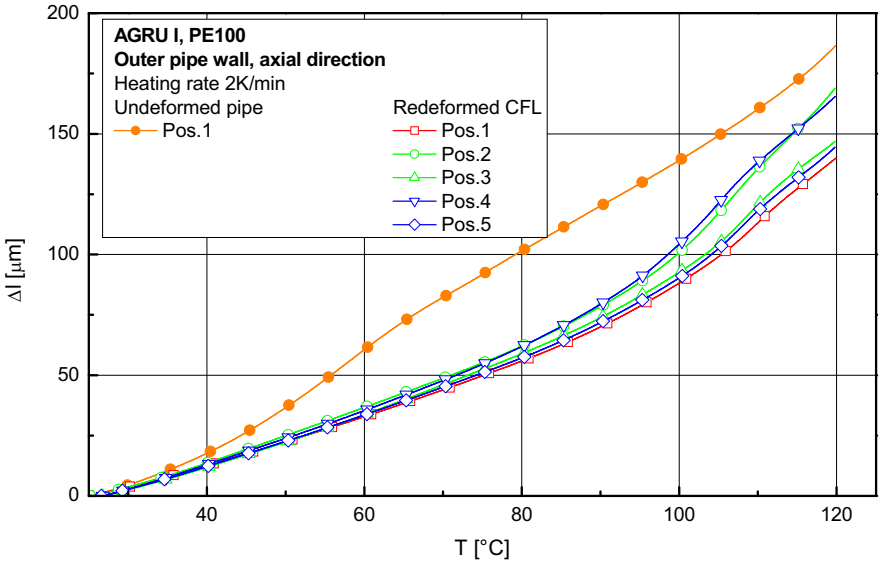

Fig. 8.6: Linear thermal expansion Δl in axial direction at the outer pipe wall position of the undeformed pipe and the redeformed CFL of AGRU I.

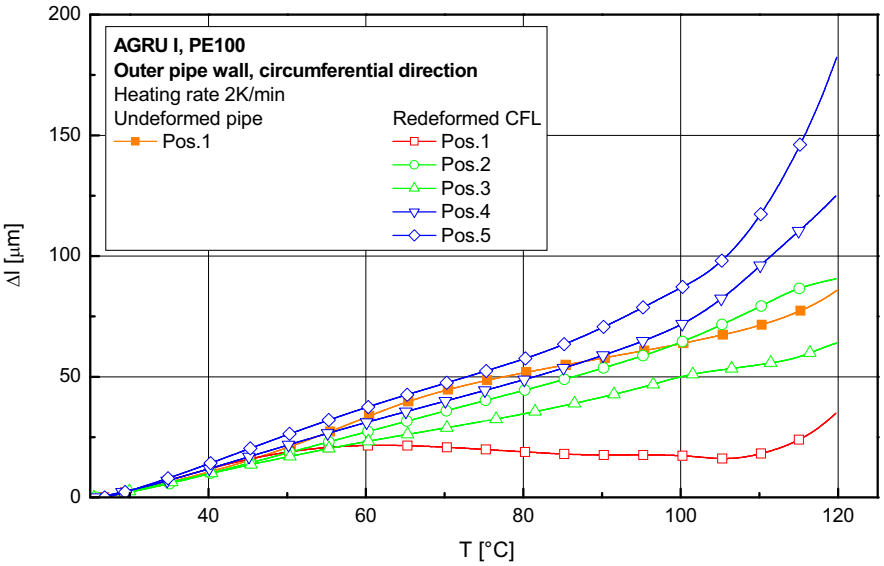

Fig. 8.7: Linear thermal expansion Δl in circumferential direction at the outer pipe wall position of the undeformed pipe and the redeformed CFL of AGRU I.

Higher values for Δl were noticed at the A-station in the A-B-correlation in Fig. 8.8. During the installation of the CFL, the exposure of the A-station to heat is considerably higher than at the B-station. This higher thermal treatment increases the occurrence of relaxation processes within the material, which in turn decrease the degree of molecular orientation.

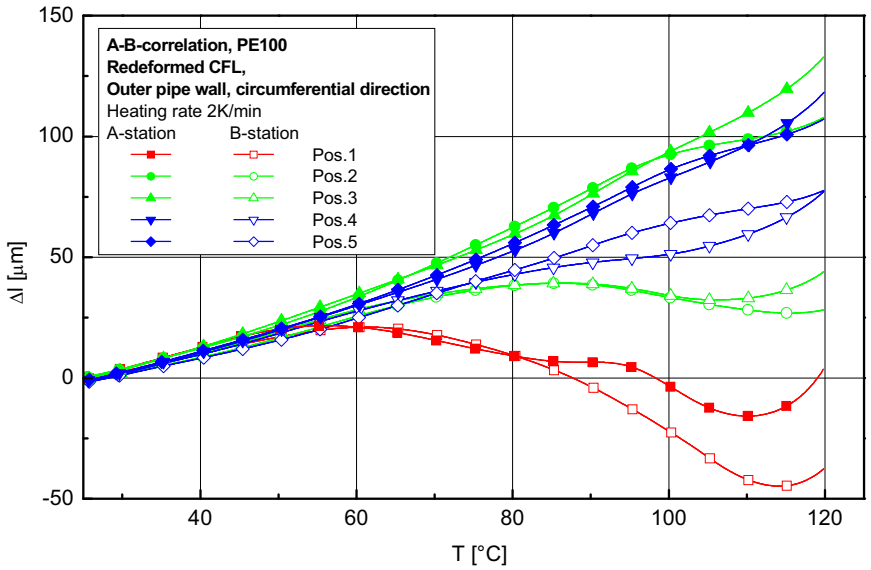

Fig. 8.8: Linear thermal expansion Δl in circumferential direction at the outer pipe wall position of the redeformed CFL of the A-B-correlation.

A more detailed investigation of the changes in molecular orientation was performed for the pipes of AGRU II. In addition to investigations of the undeformed pipe and two redeformed CFL pipes under different insulation conditions during the redeformation process, special attention was also paid to the intermediate state of the deformed CFL. The results for Pos. 1 are shown in Fig. 8.9, which points to a significant change of the linear thermal expansion between the undeformed pipe and the redeformed CFL to the deformed CFL. At the outer pipe wall position of the deformed CFL Δl increases rapidly, whereas even a negative thermal expansion was measured at the inner pipe wall position. For the folded pipe, this tendency of an expansion at the outer pipe wall and contraction at the inner pipe wall at Pos. 1 leads to the inherent redeformation of the CFL into its origin shape during heating at the installation process.

The high gradient of the entropy-elastic effect emphasizes the importance of a proper redeformation temperature during installation. At a typical installation tem-

perature of 80 °C the thermal expansion of the tested specimens at the outer pipe wall is about 490 μm and about -140 μm at the inner pipe wall, respectively. If this temperature decreases by only 5 K to 75 °C, the thermal expansion will be reduced by 16 % (410 μm) at the outer and 18 % (-115 μm) at the inner pipe wall, a redeformation temperature of 70 °C will reduce the inherent redeformation by 33 % (330 μm) at the outer and 36 % (-90 μm) at the inner pipe wall. A similar effect of this entropy-elastic memory-effect was found at Pos. 2 and 3. However, due to the folding of the pipe wall in the opposite direction, the outer pipe wall pipe wall tended to contract whereas the inner pipe wall expanded during the process of heating.

The different insulation conditions, which are also displayed in Fig. 8.9, only show a little effect on Δl in the final redeformed CFL. If at all, the additional insulation with a PP-pipe results in somewhat lower thermal expansion which probably may be caused by a lower cooling rate.

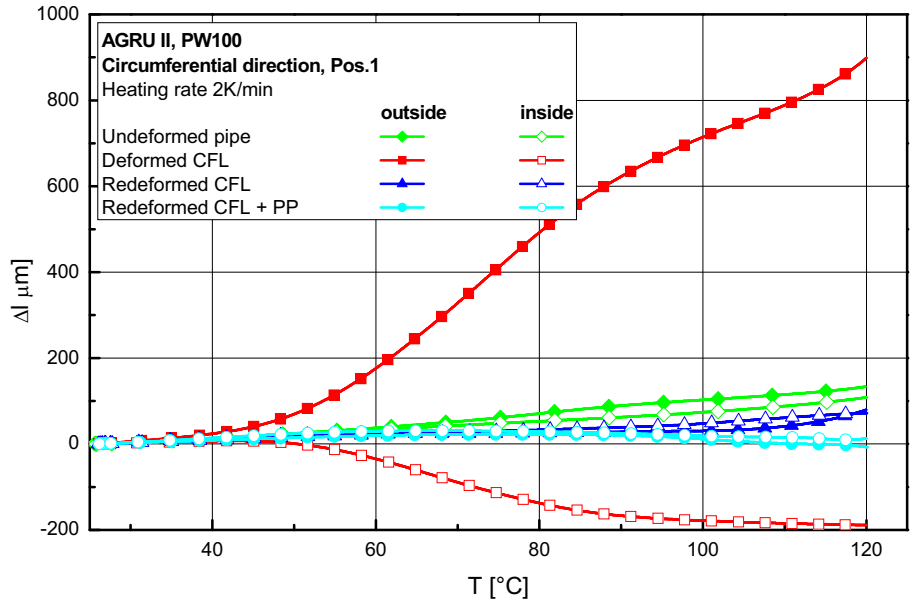

Fig. 8.9: Linear thermal expansion Δl in circumferential direction of the undeformed pipe, the deformed and two redeformed CFL of different insulations at the inner and outer pipe wall position of AGRU II, Pos. 1.

8.5 References

Ehrenstein, G.W., Riedel, G., Trawiel, P. (1995). Praxis der Thermischen Analyse von Kunststoffen, Hanser, München, D.

ISO 11357-3 (1999). Plastics - Differential scanning calorimetry (DSC) - Part 3: Determination of temperature and enthalpy of melting and crystallization.

ISO 11359-2 (1999). Plastics - Thermomechanical analysis (TMA) - Part 2: Determination of coefficient of linear thermal expansion and glass transition temperature.

Lohmeyer, S. (1984). Die speziellen Eigenschaften der Kunststoffe, Expert Verlag, Grafe-nau, Germany.

Mannsberger, G. (2007). "Morphologische Charakterisierung an vorgeformten und rückdeformierten Polyethylen-Rohren für die grabenlose Rohrsanierung", Master Thesis, Institute of Materials Science and Testing of Plastics, University of Leoben, Austria.

Menges, G., Haberstroh, E., Michaeli, W., Schmachtenberg, E. (2002). Werkstoffkunde Kunststoffe, Hanser, München, Germany.

Redhead, A. (2009). "Untersuchungen an einem unter realen Bedingungen rückdeformierten Close-Fit-Reliner aus Polyethylen", Bachelor Thesis, Institute of Materials Science and Testing of Plastics, University of Leoben, Austria.

9 MATERIAL AGING AND R ESIDUAL STRESSES OF UNDEFORMED AND REDEFORMED PIPES

In contrast to conventional PE pipes the folding to a CFL and the redeformation during the installation process implies a considerably additional mechanical and thermal treatment of the material. Changes in the material stabilization against thermo-oxidative aging may be expected as well as an influence on residual pipe stresses. The following sections focus on these properties and essential findings of this study have been published in **Papers II-1** and **II-2** in the Appendix. Details on the specimen preparation and development of the test methods are described in the Master Thesis of Mannsberger (Mannsberger, 2007) and in the Bachelor Thesis of Redhead (Redhead, 2009).

9.1 Experimen tal

The thermo-oxidative material aging was evaluated by determining the oxidation-induction time (OIT) and via infrared (IR)-spectroscopy. The OIT measurements were carried out according to ISO 11357-6 with a differential scanning calorimeter of the type DSC822 (Mettler Toledo GmbH; Schwerzenbach, CH). The samples of about 7 mg, which were taken from stripes of different pipe wall positions, were weighed in aluminum cups with a volume of 40 µl and heated up to 210 °C in an atmosphere of nitrogen with a heating rate of 10 K/min. This temperature was held constant, and afterwards the atmosphere was switched to atmospheric air. The time until exothermic oxidation of the material was measured as OIT.

For IR-spectroscopy a device of the type Spektrum GX (Perkin Elmer, Überlingen, D) in attenuated total reflection (ATR) mode was used. As the highest temperature exposure occurs inside the pipe during the redeformation process, stripes were prepared from the inner pipe wall position. To avoid possible surface effects, the specimens were taken from the inner pipe surface in a distance of 0.5 mm. Special focus on the characterization was on regions between wave numbers ν of 1700-1740 cm^{-1}, as they indicate carbonyl groups as typical aging products.

Residual pipe stresses are typically determined by the measurement of the deformation of cut free pipe samples (König, 1989; Choi und Broutman, 1997; Janson,

1999; Pilz, 2001). Residual stresses in circumferential direction $\sigma_{R,c}$ were measured with ring deformation tests, for which cut free ring segments of 80 mm in length had previously been prepared. The residual stresses in axial direction $\sigma_{R,a}$ were detected by the deformation of stripes with a thickness of 5 mm and a length of 250 mm, which were taken from the pipe parallel to the pipe axis (strip deformation test). At different times after cutting the contours of the specimens were plotted on millimeter paper to determine the deformation. The necessary time dependent creep modulus in bending $E_b(t)$ was taken from the material data sheet, the time dependent Poisson's ratio $\mu(t)$ was assumed to remain constant at μ=0.48. A detailed description of the ring and strip deformation test and the corresponding calculations can be found in Pilz (2001).

9.2 Thermo-oxidative material aging

Thermoplastics like PE are already exposed to high temperatures during the granulation process. Especially high shear rates and long dwell times, as they occur in extrusion, are critical as they may induce thermo-oxidative degradation of macromolecules. Moreover, the exposure to atmospheric oxygen supports the creation of radicals which accelerate this effect (Pinter, 1999). In addition to material stabilization against these short-term processing effects, a long-term stabilization is essential, too. As a result of molecular diffusion, atmospheric oxygen is always present in polymers so that oxidative reactions may also take place, even if aging is activated by different mechanisms (Pinter, 1999). A usual ageing reaction is the saturation of radicals with oxygen, so that typical carbonyl groups are formed (Gächter and Müller, 1990, Jin et al., 2006). Climatic influences cause an additional contribution to aging by a combination of several mechanisms (Kelly and White, 1997; Turton and White, 1999; Jin et al., 2006). To prevent or retard thermo-oxidative material aging as long as possible, different stabilizer systems have been developed. Today, complex systems of processing stabilizers, antioxidants and UV-absorber are available for a comprehensive material stabilization.

9.2.1 Oxidation-induction time

The detection of the OIT is a widespread used methodology to characterize the stabilizing conditions of PE pipe grades. However, it is important to point out that

different stabilizer systems vary in their activity, which also depends on the morphology of the material. Thus, a qualitative comparison of the effects of a stabilizer system by OIT is only allowed for identical polymer/additive systems. Comparing different polymers and a quantitative evaluation of the long-term resistance and lifetime is not possible (Ehrenstein, 1995; Schulte, 2004; Grob, 2005).

The OIT's for the undeformed pipe and redeformed CFL at different pipe wall positions of AGRU I are shown in Fig. 9.1. In the undeformed pipe OIT values of 25 up to 37 min were measured, with the longest times in the center of the pipe wall. This result, which had already been expected, can be attributed to a consumption of stabilizers at the surfaces, e. g. during extrusion. The higher amount of stabilizers inside the pipe wall resembles the function of a reservoir, from which stabilizer systems diffuse out to the surfaces over the time to inhibit material aging. No dependency of the positions Pos. 1 to 5 on the OIT was detected. It is remarkable, that longer OIT values of 42 up to 53 min were detected in the redeformed CFL of AGRU I, which signifies an increase of about 50 %.

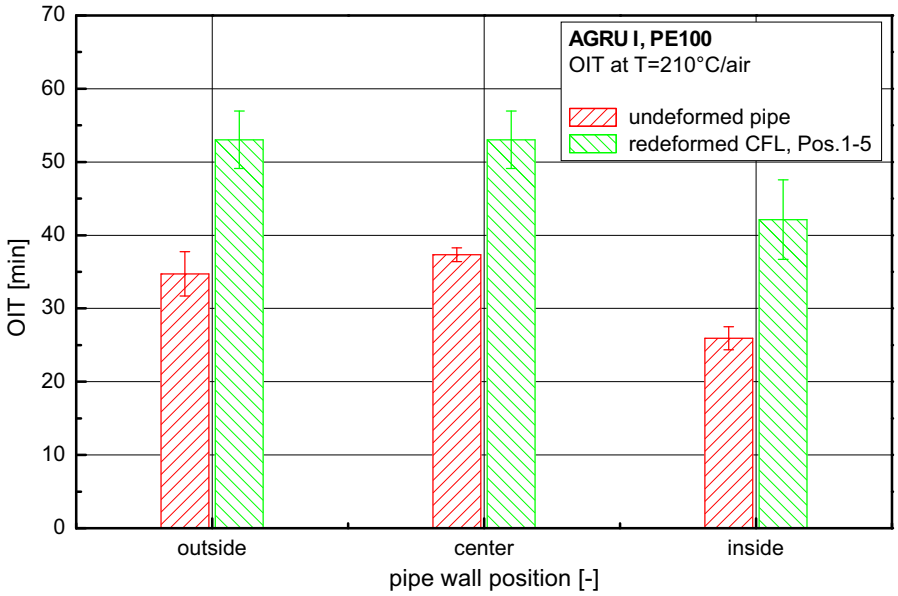

Fig. 9.1: Oxidation-induction time OIT at a temperature of 210 °C for the undeformed pipe and the redeformed CFL of AGRU I.

As this unexpected increase in the OIT values presented in Fig. 9.1 shows paradoxical results, reproducibility experiments were conducted with samples available, which again confirmed these findings. Since no convincing explanation of this phenomenon can be offered at this point, further systematical investigation of

the functionality of stabilizer systems in CFL are proposed to elucidate potential mechanisms. One possibility of this increase in the resistance of the material against thermo-oxidative degradation may be a higher mobility of the stabilizer systems. The additional heating during the folding and redeformation process may allow a rearrangement of the stabilizers, which lead to an increase of the local efficiency of stabilizers. However, a deeper investigation of this phenomenon was beyond the scope of this Dissertation. In any case, focusing on material stabilization as an effect of the additional thermal and mechanical treatment, the detected OIT values at least indicate that no significant stabilizer consumption takes place during the deformation processes.

The measurements of the A-B-correlation are shown in Fig. 9.2 which also provides a comparison between the OIT values of the redeformed CFL at the A-station to those of the B-station. No significant dependence of OIT values on the two positions of the redeformed CFL was detected. As mentioned before, a comparison of the higher OIT's of the pipe material of the A-B-correlation to the results of the pipes of AGRU I is not allowed, because different raw materials and stabilizer systems have been used for pipe manufacturing. For the practical use of PE pipes it can be assumed, that the thermo-oxidative stabilization at the inner pipe wall is especially relevant, as this side is always in contact with the transported medium and stabilizers may get washed out from the inner surface.

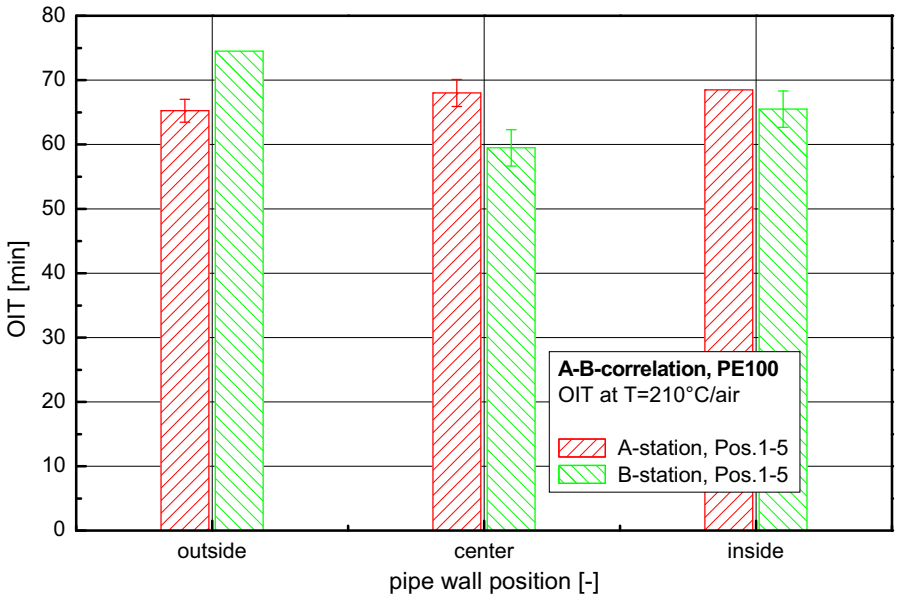

Fig. 9.2: Oxidation-induction time OIT at a temperature of 210 °C for the A-station and the B-station of the redeformed CFL of the A-B-correlation.

9.2.2 Infrared-spectroscopy

The IR-spectrograms for AGRU I are summarized in Fig. 9.3 in which the transmission T is a function of the wave number ν. As the longest and highest temperature exposure happens at the inner pipe wall, specimens were only investigated from this position. The absorption peaks between wave numbers 2925 and 2850 cm^{-1}, at 1470 cm^{-1} and 725 and 720 cm^{-1} are characteristical for PE and are activated by CH- and $(CH_2)_4$-groups. An intact stabilizer system is indicated by the signals of OH-groups at wave numbers between 3000 and 3500 cm^{-1} and phenolic antioxidants between 1500 and 1700 cm^{-1} (Pinter, 1999; Allen et al., 2001; Mendes et al., 2002; Gulmine et al., 2003; Schulte, 2004).

Compared to the undeformed pipe, the signals of the stabilizer systems of the redeformed CFL are more distinctive. The amplitudes of the signals are not significant for the evaluation of the activity of the stabilizer. However, they reflect a higher concentration of the detected elements which is in good correlation to the measurement of the OIT in which an increase of active stabilizers was measured in the redeformed CFL.

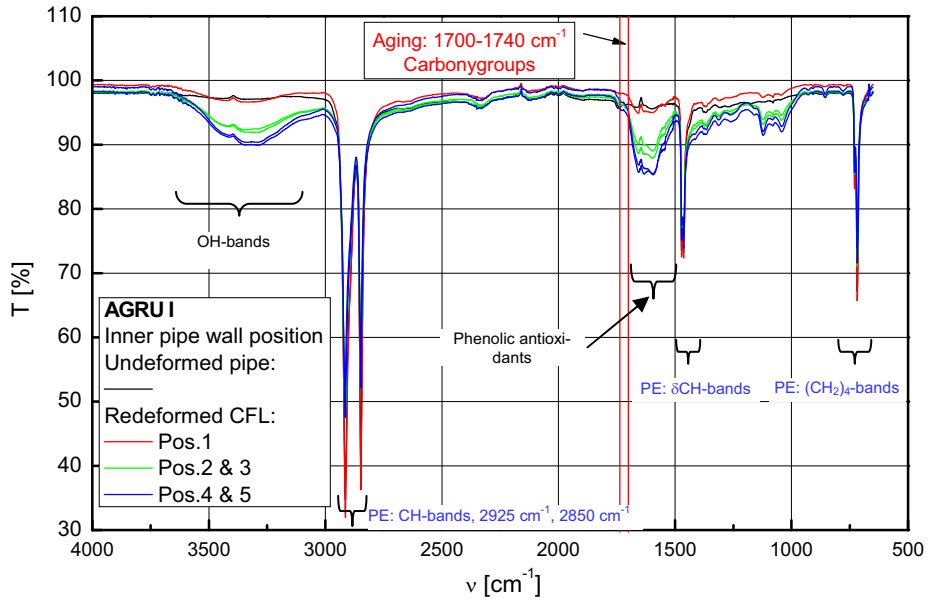

Fig. 9.3: IR-spectroscopy for the undeformed pipe and the redeformed CFL of AGRU I.

As a typical indication for material aging, carbonyl groups are created by thermo-oxidation, which are usually detectable at wave numbers between 1700 and

1740 cm^{-1}. The complete absence of signals in this region, which is also illustrated in Fig. 9.3, confirms that no thermo-oxidative material aging took place during the deformation processes. Similar results were detected for the pipes of the A-B-correlation.

9.3 Residual pipe stresses

Residual stresses in thermoplastics structures are highly dependent on the processing history. As a function of the cooling rate, the degree of crystallinity is not constant across the component. This effect has already been investigated in Section 8 of this Dissertation in which a lower degree of crystallinity was detected at the outer pipe wall surface which was cooled first. Further significant effects of different cooling rates along the cross-section of components are residual stresses. As a rule of thumb, in the last cooled material zone tensile stresses appear whereas in the first cooled zone compressive stresses prevail. For an extruded PE pipe, which is cooled outside, this would mean, that compressive stresses (-σ) develop at the outer pipe wall and tensile stresses (+σ)develop at the inner pipe wall position (Fig. 9.4).

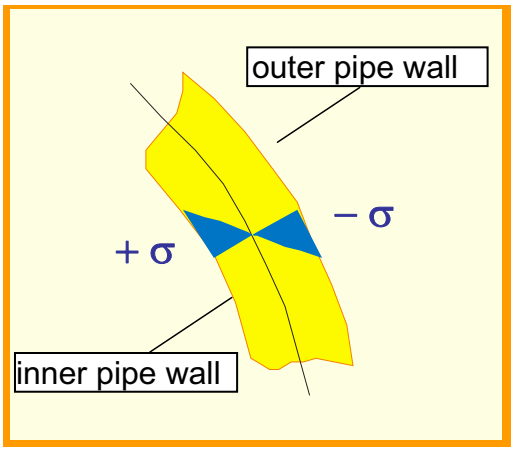

Fig. 9.4: Schematic illustration of residual stresses in extruded plastics pipes: -σ…compressive stress, +σ…tensile stress (Pilz, 2001).

Previous studies have determined, that the amount of residual stresses in PE pipes can be up to 7 MPa and that it may vary depending on the direction (axial vs. circumferential; Clutton and Williams, 1995; Pilz, 2001). With respect to an MRS of 8 MPa for PE 80 and 10 MPa for PE 100 pipe grade materials, residual

stresses contribute a significant additional load which should be considered in the design of pipe systems. Usually it can be expected, that an additional heating of a PE pipe reduces residual stresses significantly which can be seen as an improvement of the component (Choi und Broutman, 1997). Due to economical and technical reasons, manufacturing of plastics pipes usually does not include such a final annealing. However, a significant additional heating of the material takes place during the installation process of CFL and it can be expected, that residual pipe stresses are altered by this process.

In Fig. 9.5 the residual stresses in circumferential direction $\sigma_{R,c}$ and in axial direction $\sigma_{R,a}$ are shown for the undeformed pipe and the redeformed CFL of AGRU I. This chart also includes the range of typical values for $\sigma_{R,c}^{ref}$ and $\sigma_{R,a}^{ref}$ as a reference (Pilz, 2001). For AGRU I, the values of about 2.7 MPa in circumferential and 5.9 MPa in axial direction correspond to the reference values. However, in the redeformed CFL a significant decrease of residual stresses was detected in circumferential as well as in axial direction. On the one hand, the reduction of the residual stresses down to 1 MPa and less increases the gap to the MRS of the material significantly. On the other hand, an improved long-term behavior of the redeformed CFL can be expected (Choi und Broutman, 1997) as the tendency for the crack opening mode I load due to residual stresses is significantly reduced.

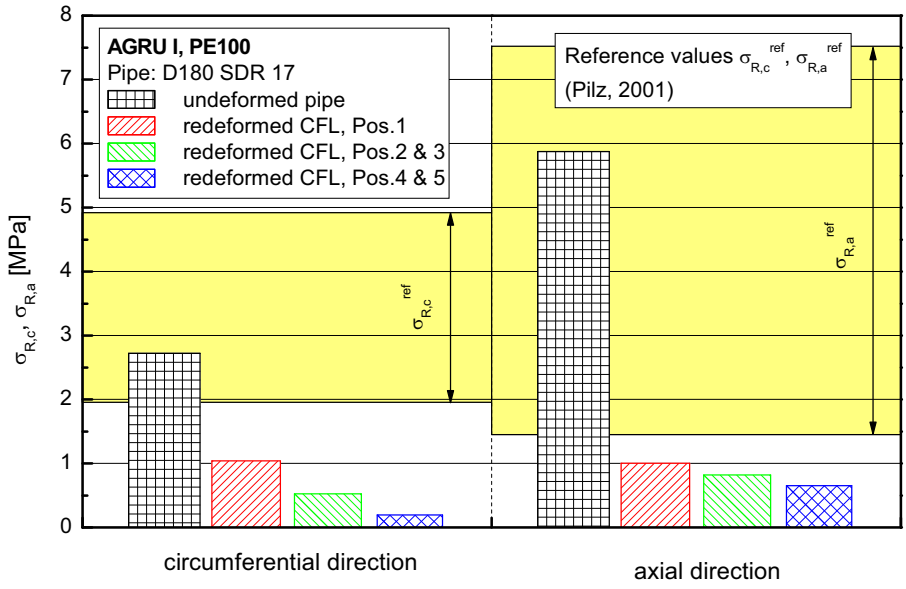

Fig. 9.5: Residual pipe stresses $\sigma_{R,c}$ and $\sigma_{R,a}$ in circumferential and axial direction for the undeformed pipe and the redeformed CFL of AGRU I.

9.4 References

Allen, N.S., Hoang, E., Liauw, C.M., Edge, M., Fontan, E. (2001). „Influence of processing aids on the thermal and photostabilisation of HDPE with antioxidant blends", Polymer Degradation and Stability 72, 367.

Choi, S. and L. J. Broutman (1997). "Residual Stesses in Plastic Pipes and Fitting IV. Effect of Annealing on Deformation and Fracture Properties", Polymer (Korea) 21(1): 93-102.

Clutton, E.Q., Williams, J.G. (1995). "On the measurement of residual stress in plastic pipes", Polymer Engineering & Science 35(17): 1381-1386.

Ehrenstein, G.W., Riedel, G., Trawiel, P. (1995). Praxis der Thermischen Analyse von Kunststoffen, Hanser, München, D.

Gächter, R. and Müller, H. (1990). Kunststoffadditive, Carl Hanser Verlag, Munich, Vienna.

Gulmine, J.V., Janissek, P.R., Heise, H.M., Akcelrud, L. (2003). „Degradation profile of po-lyethylene after artificial accelerated weathering", Polymer Degradation and Stability 79, 385.

Grob, M. (2005). "Moderne Additivierung - ein effektiver Alterungsschutz für Kunststoffe", Korrosion von Kunststoffen, Frankfurt, Deutschland, Gesellschaft für Korrosionsschutz e.V.

ISO 11357-6 (2002). Plastics - Differential scanning calorimetry (DSC) - Part 6: Determination of oxidation induction time

Janson, L.E. (1999). Plastics Pipes for Water Supply and Sewage Disposal, Borealis, Sven Axelsson AB/ Fäldts Grafiska AB, Stockholm, Schweden.

Jin, C., Christensen, P.A., Egerton, T.A., Lawson, E.J., White, J.R. (2006). "Rapid measurement of polymer photo-degradation by FTIR spectrometry of evolved carbon dioxide", Polymer Degradation and Stability 91(5), 1086-1096.

Kelly, C.T. and White, J.R. (1997). "Photo-degradation of polyethylene and polypropylene at slow strain-rate", Polymer Degradation and Stability 56(3), 367-383.

König, G. (1989). Stand der Technik auf dem Gebiet der Eigenspannungsmessungen, Seminar über Eigenspannungsmessungen, Miskolc, H.

Mannsberger, G. (2007). "Morphologische Charakterisierung an vorgeformten und rückdeformierten Polyethylen-Rohren für die grabenlose Rohrsanierung", Master Thesis, Institute of Materials Science and Testing of Plastics, University of Leoben, Austria.

Mendes, L.C., Rufino, E.S., de Paula, F.O.C., Torres Jr, A.C. (2002). „Mechanical, thermal and microstructure evaluation of HDPE after weathering in Rio de Janeiro City", Polymer Degradation and Stability 79, 371.

Pilz, G. (2001). "Viscoelastic Properties of Polymeric Materials for Pipe Applications", Doctoral Dissertation, Institute of Materials Science and Testing of Plastics, University of Leoben, Austria.

Pinter, G. (1999). "Rißwachstumsverhalten von PE-HD unter statischer Belastung", Doctoral Dissertation, Institute of Materials Science and Testing of Plastics, University of Leoben, Austria.

Redhead, A. (2009). "Untersuchungen an einem unter realen Bedingungen rückdeformierten Close-Fit-Reliner aus Polyethylen", Bachelor Thesis, Institute of Materials Science and Testing of Plastics, University of Leoben, Austria.

Schulte, U. (2004). "HDPE Pipes are More Resistant to Oxidation than the OIT Indicates", Plastics Pipes XII, Baveno, Italien.

Turton, T.J. and White, J.R. (1999). "Effect of Stabilizer on Photo-Degradation Depth Profile", Weathering of Plastics, 261-269.

10 LONG-TERM FAILURE BEHAVIOR OF UNDEFORMED AND REDEFORMED PIPES

This chapter describes the results of the fracture mechanics characterization of the long-term failure behavior of the undeformed pipe and the redeformed CFL. As quasi-brittle crack growth always starts at an initial defect, in a first step the consequence of the mechanical deformation processes during the folding and the redeformation of the pipe was investigated by focusing especially on remaining surface deformations, which may act as initial points for creep crack growth. In a second step the long-term failure behavior was characterized with fracture mechanics based cyclic tests using CRB specimens. Details on the practical work and recent findings of this work have been published in **Paper II-2** in the Appendix.

10.1 Experimental

Optical investigations of the inner and outer pipe wall surfaces were conducted with a light microscope of the type BX51 (Olympus; Vienna, A) and an image recording system with the corresponding software analysis 3.2 (Soft Imaging Systems GmbH; Münster, D). Additional investigations of selected specimens were carried out with a chromatographic confocal-microscope of the type FRT MicroProf (Fries Research & Technology GmbH; Bergisch Gladbach, D). Scanning electron microscopy (SEM) was done with a device of the type DSM 962 (Carl Zeiss; Oberkochen, D). Prior to the SEM investigations, the specimens were sputter coated with a 15 to 20 nm thick layer of gold.

A servo-hydraulic closed-loop testing system of the type MTS Table Top (MTS Systems GmbH; Berlin, D) was used for the cyclic testing of CRB specimens with sinusoidal loading at a ratio of minimum to maximum loading of R=0.1 and applying a frequency of 10 Hz. The tests were performed under standard conditions at a temperature of 23 °C and a relative humidity of 50 %.

The CRB specimens were manufactured in axial direction from the undeformed pipe as well as from the deformed and the redeformed CFL at the positions Pos. 1, Pos. 3 (symmetrical to Pos. 2) and Pos. 5 (symmetrical to Pos. 4, see Section 7.4 for positions). Additionally, specimens were manufactured from a compression

molded plate of the same PE 100 pipe grade material. Limited by the pipe wall thickness, the CRB specimens had a diameter of 10 mm and a length of 100 mm. The circumferential initial notch with a depth of 1 mm was inserted on a drilling machine by pressing a razor blade into the rotating specimen.

10.2 Surface features and deformations

Images of the inner and outer pipe surfaces of AGRU II at the positions Pos. 1 and 3 are shown in Fig. 10.1 and Fig. 10.2. The investigations were done for the undeformed pipe, the deformed CFL and the redeformed CFL.

At the intermediate state of the deformed CFL, at Pos. 1 (Fig. 10.1) distinguishable markings in axial direction are visible at the outer pipe surface that are similar to a relief structure caused by squeezed material. However, the inner pipe wall surface shows a smooth surface, comparable to the reference image of the undeformed pipe. After the redeformation process the detected markings at the outer side of Pos. 1 disappear and both the inner and the outer pipe surface show a smooth appearance comparable to the one of the undeformed pipe.

AGRU II, outer pipe wall surface, Pos. 1:

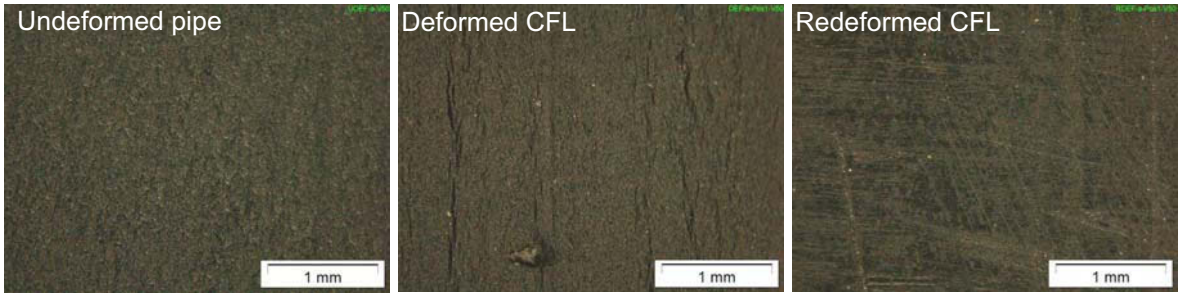

AGRU II, inner pipe wall surface, Pos. 1:

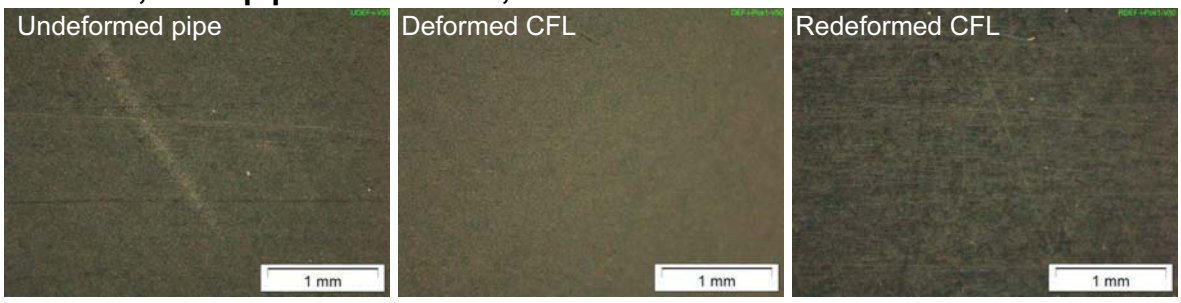

Fig. 10.1: Outer and inner pipe wall surface of the undeformed pipe, the deformed CFL and the redeformed CFL at Pos. 1 of AGRU II.

Similar results were found at Pos. 3 of the deformed CFL (Fig. 10.2). However, in contrast to Pos. 1 the markings were detected at the inner pipe wall. Again, in the final state of the redeformed pipe, the appearance of the surfaces is comparable to the one of the undeformed pipe.

AGRU II, outer pipe wall surface, Pos. 3:

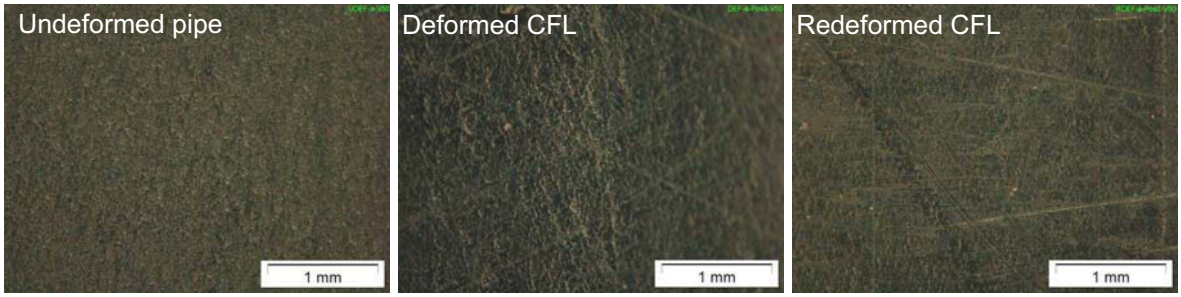

AGRU II, inner pipe wall surface, Pos. 3:

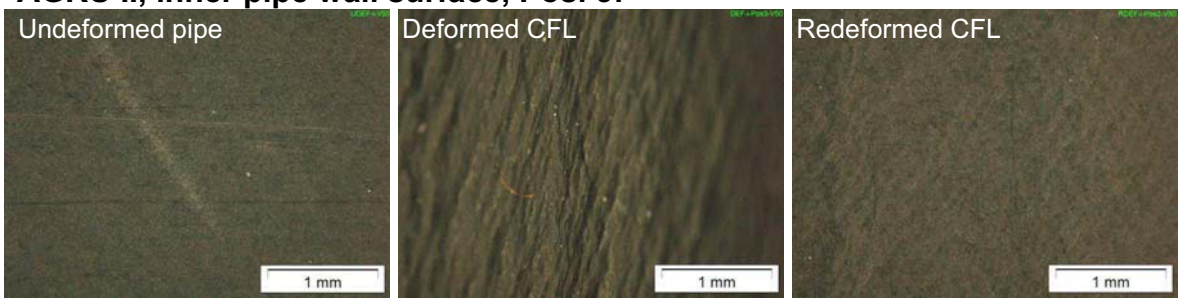

Fig. 10.2: Outer and inner pipe wall surface of the undeformed pipe, the deformed CFL and the redeformed CFL at Pos. 3 of AGRU II.

The relief-like structures oriented in axial directions were detected at the inner side of the folded pipe segment in which material at the surface is squeezed as a result of the mechanical deformation. In this context it is important, that there do not remain any notches or even cracks in the final redeformed CFL that may cause critical stress singularities and moreover act as initiation points for SCG.

For a detailed evaluation of the surface characteristics, the redeformed CFL was also investigated by SEM. The images of Fig. 10.3 show scratch-like crinkles at the inner pipe wall surface of Pos. 1 which were not recognizable with the light microscope. These surface effects may again be assigned to the deformation processes of the CFL. During the action of folding the pipe the material at the inner pipe wall surface of Pos. 1 is stretched and high molecular orientations are created (compare Section 8.4). During redeformation, which is mainly driven by inherent entropy-elastic effects, the stretched material contracts back close to its original

state (memory-effect). For a complete redeformation into a circular shape and to ensure a close fit to the old pipe, the CFL is pressurized. To accomplish a complete redeformation, the pressurization produces a forced bending at Pos. 1 that may cause squeezing of the material layer at the inner pipe surface which may create the crinkles.

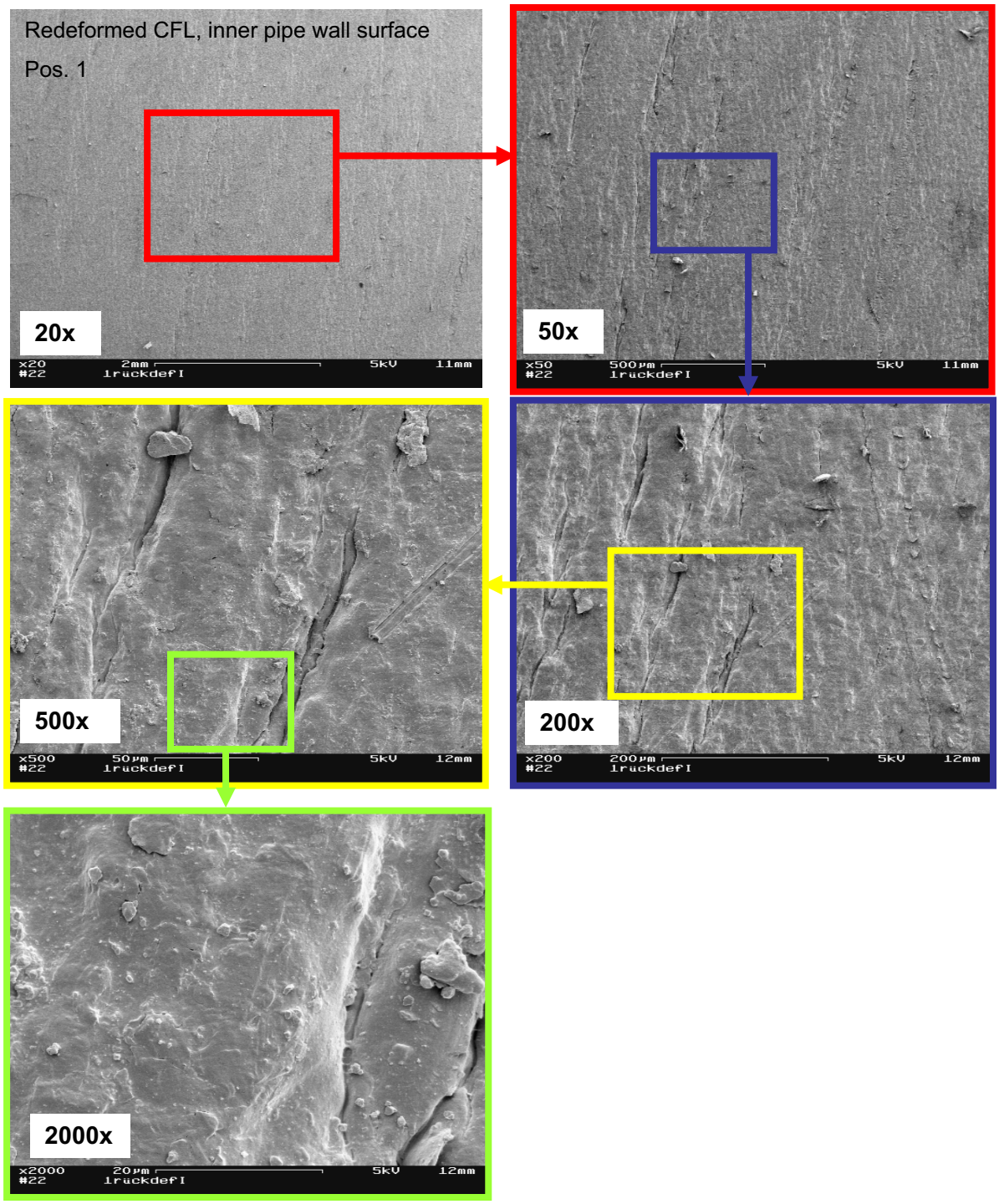

Fig. 10.3: SEM images of the inner pipe wall surface of the redeformed CFL at Pos. 1 of AGRU II.

Since defects at the inner pipe wall surface of the final redeformed CFL may potentially initiate SCG, the dimensions of the detected structures are of special interest. Hence, special topography measurements with a chromatographic confocal-microscope were performed to address this issue. The results are shown in Fig. 10.4 in form of a line-scan and a 3D-image. The analysis of the topography revealed a length of the crinkles of about 120 to 350 μm, a width of approx. 50 μm and a depth of about 15 to 20 μm. Furthermore, the 3D-image reveals an obvious orientation of the surface effects in the direction of the pipe axis.

For initiation of SCG typical defect sizes of 100 to 400 μm are of relevance (Gray et al., 1981; Stern, 1995; Lang et al., 1997; Pinter, 1999). Within this Dissertation a critical defect size of a_{ini}=400 μm was defined to calculate a fracture mechanics lifetime (Section 4.5). As the depth of the detected crinkles is clearly below this critical level, it can be expected, that they may not have a further negative effect on the long-term failure behavior of the CFL.

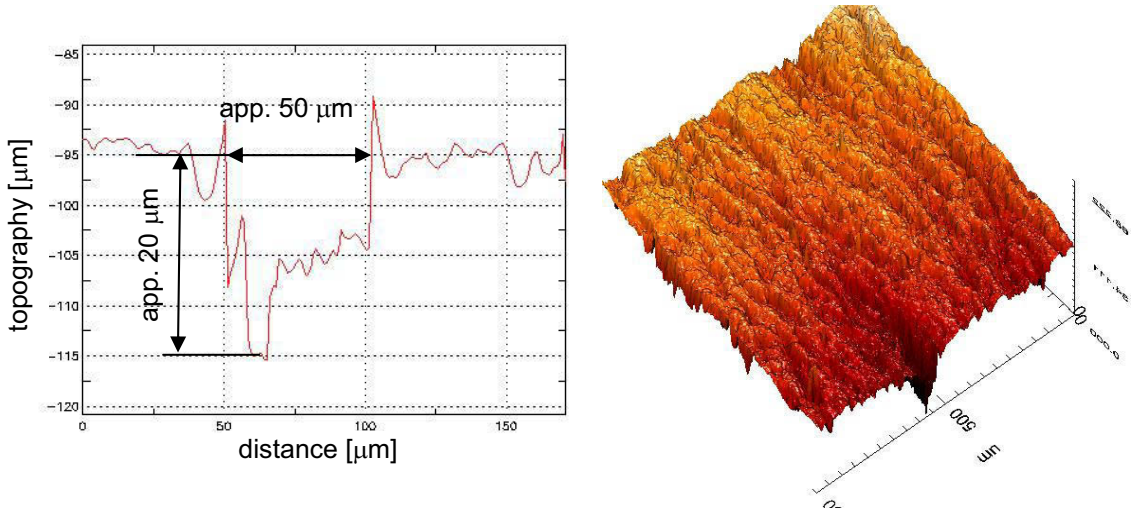

Fig. 10.4: Topography of the inner pipe wall surface of the redeformed CFL at Pos. 1 of AGRU II. Left: line-scan; right: 3D-image.

10.3 Cyclic tests with CRB specimens

The total failure cycle number N_f as a function of ΔK_I for different process stages of the CFL are shown in Fig. 10.5. Although the difference in the determined failure times is only small, the tests with CRB specimens taken from the undeformed pipe in axial direction show the lowest failure cycle numbers when compared to the de-

formed CFL, the redeformed CFL and the compression molded plate. The increase of the failure cycle numbers of specimens from the redeformed CFL compared to specimens from the undeformed pipe is about 20 %. This result can possibly be assigned to residual stresses within the specimens, which are significantly higher for the undeformed pipe than for the redeformed CFL (Section 9.3). Also, the manufacture of compression molded plates results in specimens with low residual stresses.

An influence of the slight increase in the degree of crystallinity, which was detected in Section 8.3, could not be recognized. Moreover, no effects of the different circumferentially located positions Pos. 1, 3 and 5 on N_f were detected and the different insulations during the redeformation process did not show any significant effect on the long-term cyclic failure behavior either.

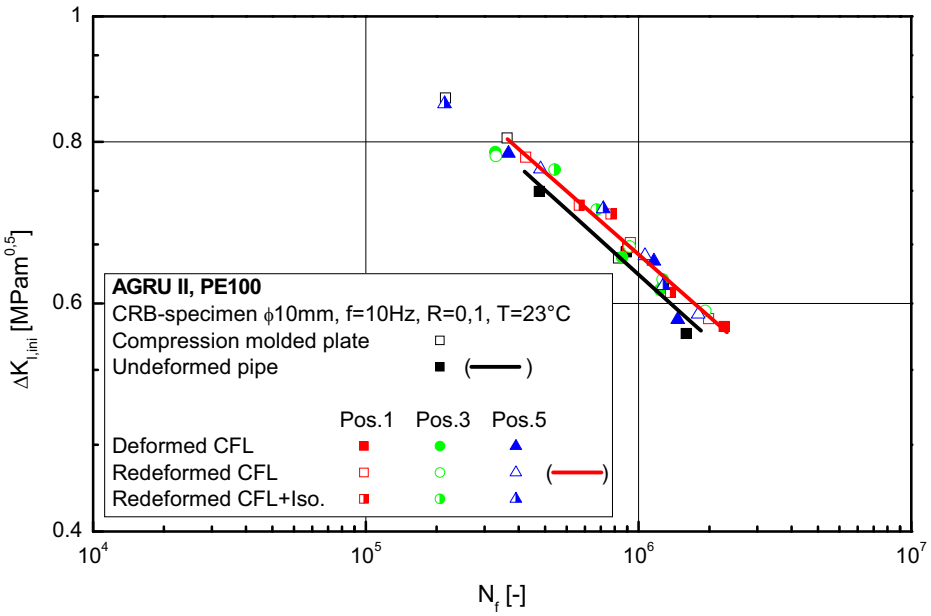

Fig. 10.5: Failure cycle number N_f of CRB specimens at a temperature of 23 °C of the compression molded plate, the undeformed pipe and positions Pos. 1, 3 and 5 of the deformed CFL and different insulations of the redeformed CFL of AGRU II.

Finally it should be emphasized that the above findings are strictly valid only for specimens taken from the pipes in axial direction with cracks in circumferential or radial direction. Further investigations should clarify whether the same trends exist for cracks growing in axial direction.

10.4 References

Barker, M.B., Bowman, J.A., Bevis, M. (1983). "The Performance and Cause of Failure of Polyethylene Pipes Subjected to Constant and Fluctuating Internal Pressure Loadings", Journal of Materials Science 18: 1095-1118.

Gaube, E., Gebler, H., Müller, W., Gondro, C. (1985). "Zeitstandfestigkeit und Alterung von Rohren aus HDPE", Kunststoffe 75(7), 412-415.

Gray, A., Mallinson, J.N., Price, J.B. (1981). “Fracture behavior of polyethylene pipes”, Plastics and Rubber Processing and Applications 1, 51-53.

Ifwarson, M. (1989). "Gebrauchsdauer von Polyethylenrohren unter Temperatur und Druckbelastung", Kunststoffe 79(6), 525-529.

Kausch, H.H. (1987). Polymer Fracture, Springer Berlin-Heidelberg, D.

Lang, R.W., Stern, A., Doerner, G. (1997). "Applicability and Limitations of Current Lifetime Prediction Models for Thermoplastics Pipes under Internal Pressure", Die Angewandte Makromolekulare Chemie 247, 131-137.

Lustiger, A. (1986). “Environmental Stress Cracking: The Phenomenon and its Utility”, Failure of Plastics, W. Browstow and R. D. Corneliussen, Munich, Germany, Hanser Publishers: 305-329.

Pinter, G. (1999). "Rißwachstumsverhalten von PE-HD unter statischer Belastung", Doctoral Dissertation, Institute of Materials Science and Testing of Plastics, University of Leoben, Austria.

Richard, K., Gaube, E., Diedrich, G. (1959). “Trinkwasserrohre aus Niederdruckpolyäthylen”, Kunststoffe 49(10): 516-525.

Stern, A. (1995). "Fracture Mechanical Characterization of the Long-Term Behavior of Polymers under Static Loads", Doctoral Dissertation, Institute of Materials Science and Testing of Plastics, University of Leoben, Austria.

11 SUMMARY AND CONCLUSIONS

The technology of PE Close-Fit-Liners (CFL) is a modern technology which allows cost efficient and quick rehabilitation of old or damaged pipes. However, installing pipes using this method is connected to additional mechanical and thermal treatment of the pipe material. Unfortunately, there are no scientific studies available concerning relevant changes in material properties due to the typical additional process steps. Therefore, the effects of deformation and redeformation of the CFL on the pipe material have been studied comprehensively.

A morphological investigation confirmed that the additional deformation and thermal processes have no obvious negative effect on relevant characteristics of the material, which was a commercial PE 100 pipe grade typically used for CFL. The storage modulus and loss factor, determined by dynamic-mechanical analysis (DMA) show process related differences across the pipe wall thickness, however, no significant changes between the undeformed pipe and the redeformed CFL were detected. If at all, only a slight increase of the storage modulus could be determined as a result of an increase in crystallinity by about 4 to 5 %, verified with differential scanning calorimeter (DSC). This post-crystallization takes place during the additional heating of the pipe which is part of the installation process and causes an annealing of the material. At the inner pipe wall of the beginning of the CFL (A-station), a temper-shoulder was detected in the DSC curve at approx. 120 °C as an effect of the heat treatment during the pipe installation. At the end of the CFL (B-station) no such temper-shoulder was detected. However, in combination with the measured degree of crystallinity and the storage modulus at these positions, this effect probably has no considerable relevance for the final properties of the installed CFL.

The characterization of the memory-effect was done by measurements of the linear thermal expansion in circumferential direction of the pipe, which is linked to molecular orientation. The results have been added to the knowledge of the operating mechanisms within the material, which are responsible for the inherent redeformation of the folded pipe. In the intermediate state of the folded pipe, considerable molecular orientations are frozen in the folding positions. During the

installation process, the action of heating of the material increases the mobility of the macromolecules, and due to entropy-elasticity they relax into a direction which works contrary to the prior folding. In the final state of the redeformed CFL the linear thermal expansion is lower than the one in the undeformed pipe. In the case of a temperature increase during the pipe service, this will cause a lower thermal expansion of the pipe material and a lower degree of residual stresses, respectively.

As a possible effect of the additional thermal treatment, special attention was paid on the characterization of thermo-oxidative material aging via oxidation-induction time (OIT) measurements and infrared (IR)-spectroscopy. Comparing results of the undeformed pipe and the redeformed CFL, an unexpected increase in OIT values of about 50 % was detected. Moreover, the IR-spectroscopical investigations showed a higher concentration of active stabilizers. No indications for a thermo-oxidative material degradation in the redeformed CFL were detected. The increase of active stabilizer systems is surprising, indeed, and may be an effect of a higher mobility and rearrangement processes during the annealing at installation. However, as this increase in the OIT values after the additional thermal and mechanical treatment shows paradoxical results, it is recommended to further investigate the general functionality of stabilizer systems in CFL. The investigation of the A-station and the B-station of an installed pipe did not reveal any significant differences in the OIT and IR-spectroscopy either. In summary, the OIT measurements and IR-spectroscopy indicate, that no significant thermo-oxidative material aging takes place during the additional thermal and mechanical process steps of CFL production and installation.

In conventional extruded pipes residual tensile stresses must be expected at the inner pipe wall, which have a crack opening effect for surface defects. However, a considerable change of residual pipe stresses was found in the final state of the redeformed pipe. In axial as well as in circumferential direction, the annealing reduces the residual stresses down to values of 1 MPa and less. This reduction in internal stresses is certainly considered beneficial in terms of CFL performance.

Moreover, an optical investigation revealed that the redeformation processes during folding and installation does not create any critical defects, which would remain at the pipe wall surface and may act as points for crack initiation. Probably, as a

result of reduced residual stresses, the resistance of CRB specimens against crack initiation and SCG in cyclic tests was found to increase by about 20 % for the final state of the redeformed CFL.

Overall, the performed testing program indicates that the additional process steps of deformation and redeformation do not have any obvious negative effects on relevant material properties. Much rather, the significant reduction of residual pipe stresses may be considered as a significant improvement in the final pipe performance, and may act to even improve the reliability of these pipes in terms of long-term application by retarding potential failure modes such as crack initiation and SCG.

PART III

APPENDIX – SELECTED PUBLICATIONS

APPENDIX – SELECTED PUBLICATIONS

I-1 Accelerated Investigation of Creep Crack Growth in Polyethylene Pipe Grade Materials by the use of Fatigue Tests on Cracked Round Bar Specimens
A. Frank, G. Pinter, R.W. Lang
in proceedings: ANTEC 2008, Milwaukee, Wisconsin, USA (2008), 2435-2439.

I-2 A Fracture Mechanics Concept for the Accelerated Characterization of Creep Crack Growth in PE-HD Pipe Grades
A. Frank, W. Freimann, G. Pinter, R.W. Lang
Engineering Fracture Mechanics 76 (2009), ESIS Publication, 2780–2787.

I-3 Numerical Simulation of the Failure Behavior of PE Pressure Pipes with Additional Loads
P. Hutař, M. Ševčík, L. Náhlík, I. Mitev, A. Frank, G. Pinter
in proceedings: ANTEC 2009, Chicago, Illinois, USA (2009), 2163-2168.

I-4 Prediction of the Remaining Lifetime of Polyethylene Pipes after up to 30 Years in use
A. Frank, G. Pinter, R.W. Lang
Polymer Testing 28 (2009), 737–745.

I-5 Lifetime Prediction of Polyethylene Pipes Based on an Accelerated Extrapolation Concept for Creep Crack Growth with Fatigue Tests on Cracked Round Bar Specimens
A. Frank, G. Pinter, R.W. Lang
in proceedings: ANTEC 2009, Chicago, Illinois, USA 2009, 2169-2174.

II-1 Characterization of the Effects of Preforming and Redeforming on Morphology and Thermomechanical Properties of Polyethylene Close-Fit Liners for Trenchless Pipe Rehabilitation
A. Frank, G. Mannsberger, G. Pinter, R.W. Lang
in proceedings: ANTEC 2008, Milwaukee, Wisconsin, USA (2008), 2251-2255.

II-2 Close-Fit Liner – Verfahrensbedingte Beeinflussung der Werkstoffeigenschaften und des Rohrlangzeitverhaltens
A. Frank, M. Haager, A. Hofmann, G. Pinter
3R international 48 (11) (2009), 639-645.

I-1 Accelerated Investigation of Creep Crack Growth in Polyethylene Pipe Grade Materials by the use of Fatigue Tests on Cracked Round Bar Specimens

A. Frank, G. Pinter, R.W. Lang

in proceedings: ANTEC 2008, Milwaukee, Wisconsin, USA (2008), 2435-2439.

ACCELERATED INVESTIGATION OF CREEP CRACK GROWTH IN POLYETHYLENE PIPE GRADE MATERIALS BY THE USE OF FATIGUE TESTS ON CRACKED ROUND BAR SPECIMENS

Andreas Frank, Polymer Competence Center Leoben, Austria (frank@pccl.at)
Gerald Pinter, University of Leoben, Austria
Reinhold W. Lang, University of Leoben and Polymer Competence Center Leoben, Austria

Abstract

For lifetime and safety assessment of pressurized polyethylene (PE) pipes the knowledge of the crack growth behavior is of essential importance. With common test methods the investigation of creep crack growth (CCG) in modern PE-pipe materials under static loading conditions is not possible in a feasible time. In the present research work fatigue tests on cracked round bar (CRB) specimens at different R-ratios (min. load/max. load) were used to extrapolate to the case of static loading. By comparing these results with already existing data it was verified, that the applied method is qualified to generate CCG-curves at service-near loading and temperature conditions in relatively short times.

Introduction

It is generally accepted, that crack initiation and slow crack growth (SCG) are the critical long-term failure mechanisms of pressurized polyethylene (PE) pipe systems [1-7]. Hence for lifetime prediction of a pipe the knowledge of the crack growth kinetics is of essential interest.

Usually internal pressure tests on pipe specimens and the extrapolation method based on EN ISO 9080:2003 [8] are used to determine the long-term behavior and to ensure operating times of at least 50 years. In addition to these expansive and time-consuming tests in the last years accelerated test methodologies were developed using fracture mechanics considerations, like the Notched Pipe Test (NPT), the Pennsylvania Notch Test (PENT) or the Full Notched Creep Test (FNCT) [9].

On the one hand the further development of modern PE-pipe materials and their improved resistance against crack initiation and crack growth opens a broad discussion about operating times of up to 100 years [5, 10]. On the other hand the improved crack growth resistance poses a challenge to the common test methods regarding feasible testing times. One possibility to reduce testing times are fatigue tests under cyclic loads based on linear elastic fracture mechanics (LEFM).

Several studies show that results of fatigue tests are in good accordance to the internal pressure tests [4, 11 -13]. Especially tests with cracked round bar (CRB) specimens show promising results. With these specimens not only a differentiation of different PE-grades (PE80, PE100) but also a distinction within one grade up to process based batch variations is possible in a few days. The correlation of CRB data with those of time consuming methods opens an interesting potential for product ranking and material development. A further benefit of CRB specimens is that fatigue tests can be done at application orientated ambient temperatures and without the influence of stress cracking liquids [9, 12-13].

However, for a fracture mechanics lifetime prediction of PE pipes the crack growth behavior at static loading is of importance. A methodology how to transfer cyclic fatigue tests to the relevant case of static loading conditions has already been proposed [14, 15]. In the present work this concept was applied to a commercially available PE80 pipe grade.

Background

Basic requirements for the applicability of LEFM concepts in plastics are that global loadings are in the range of linear viscoelasticity and only small plastic deformations at the crack tip appear. The stress distribution near the crack tip is described by the stress intensity factor (SIF) K_I [16-18] that is a function of the global loading σ, the crack length a and a geometric factor Y that is known for several specimens and component shapes (Equation 1).

$$K_I = \sigma \cdot \sqrt{a} \cdot Y \qquad (1)$$

The crack growth kinetics da/dt at static loading and da/dN at cyclic loading, respectively, usually is shown in a double logarithmic diagram as a function of the SIF K_I and the difference of the maximum and minimum SIF $\Delta K_I = K_{I,max} - K_{I,min}$, respectively, and often gives an S-shaped relationship (see Figure 1). Schematically the kinetic curve can be divided into three sections:

- In region 1, the threshold region, the crack growth rate decreases fast at low SIF values. Beneath a threshold K_{th} no crack growth is detectable.

- In region 2 stable crack growth occurs and the crack growth rate under static and cyclic loads can be described by the equation of Paris and Erdogan (Equation 2 and 3) [19]. The constants A and m depend on the material as well as on test conditions like the temperature.
- In region 3 the crack growth rate raises fast and unstable crack growth leads to the failure of the specimen or component.

$$\frac{da}{dt} = A \cdot K_I^{\ m} \qquad (2)$$

$$\frac{da}{dN} = A' \cdot \Delta K_I^{\ m'} \qquad (3)$$

The linear region of the kinetics can be used to compare different materials concerning crack growth resistance. As illustrated in Fig. 1 a higher crack growth resistance shifts the crack growth rate to higher SIF and also a lower slope of the curve can be a result of improved material behavior. Figure 1 also shows the influence of better crack growth resistance in the internal pressure test where the better material has longer failure times.

Compared to static loading failure times can be significantly reduced in cyclic tests. The loading conditions in fatigue test are specified by the R-ratio, the ratio of minimum to maximum loading (see Figure 2). Each R-ratio results in a single failure and kinetics curve. A ratio of R=1.0 describes static loading.

Although the direct measurement of crack growth rates with CRB specimens is rather difficult (asymmetric crack growth, high gradient in K_I), a fatigue procedure for generating crack growth curves for static loading conditions in accelerated tests with this specimen type has been proposed in [12]. The four key steps in this procedure are (see also Figure 3):

- First fatigue tests with CRB specimens at different R-ratios (e.g. R=0.1 to 0.7) are performed and analyzed in R-specific Wöhler-curves.
- For each R-ratio the generated failure data are converted into "synthetic" fatigue crack growth (FCG) curves using fracture mechanics computational methods and averaged crack growth rates.
- In the next step the kinetic curves at different R-ratios are transformed into a diagram, where $K_{I,max}$ is a function of R at constant crack growth rates, and these curves are extrapolated to static loading (R=1.0).
- Finally, the SIF for R=1.0 are transformed back into the crack growth kinetics diagram to generate a "synthetic" creep crack growth (CCG)-curve.

The generated synthetic CCG-curve can be used for lifetime prediction of pipes. The fracture mechanics calculation of lifetimes of pressurized pipes can be done with Equation 4 [20]. The total failure time consist of crack initiation and crack growth times, where A and m are material constants, a_0 is the initiating defect size, σ describes the global loading and Y is a factor of geometry.

$$t_f = t_{tot} \approx t_{in} + \frac{2}{A \cdot (m-2) \cdot Y^m} \cdot a_0^{(2-m)/2} \cdot \sigma^{-m} \qquad (4)$$

Experimental

The CRB specimens were manufactured from compression molded plates made of a commercial PE80 pipe grade. The circumferential initial crack was inserted with a razor blade, so that the whole specimen provides plane strain conditions by high constraint very similar to the conditions in a real pipe.

The fatigue tests were executed at a servo-hydraulic closed-loop testing system MTS 858 Table Top (MTS Systems GmbH, Berlin, GER). The sinusoidal loading at 23 °C and a frequency of 10 Hz was applied with R-ratios of 0.1, 0.3 and 0.5. For determination of the SIF for CRB specimens several equations are available. Usually the SIF by Benthem and Koiter provides proper results at small crack lengths [9, 21-22]. In this work, however, equation 5 was used [18], as it is analytically soluble, where D is the specimen diameter, d the ligament diameter and F the applied load. As shown in Figure 4 for the relevant crack lengths the results of this equation are in good agreement to Benthem and Koiter.

$$K_I = \frac{F}{D^{\frac{3}{2}}} \cdot \left[1.72 \cdot \left(\frac{D}{d} \right) - 1.27 \right] \qquad (5)$$

In the test he number of cycles until crack growth initiation was detected by measuring the crack opening displacement (COD) with an extensometer of the type MTS 632.13F-20. Typically crack growth initiation is characterized by a step in the COD curve.

Results

Figure 5 shows the total failure cycles at 23 °C for R-ratios of 0.1, 0.3 and 0.5. The SIF $K_{I,max}$ was calculated with the precracked initial defect size a_{ini}. The illustrated fracture surfaces indicate two phenomenons, which make a direct measurement of the crack growth kinetics in CRB specimens difficult. On the one hand the effective crack length and the quasi brittle fracture surface is rather small and connected with a fast increase of the SIF. On the other

hand eccentric crack growth occurs that makes an evaluation of the crack length difficult.

As in this work a direct measurement of the crack growth kinetics was not possible, the determination of the "synthetic fatigue crack growth curves was done by calculation of averaged crack growth rates based on fracture surface analyses of the several specimens. The crack growth kinetics was calculated by substitution of Equation 5 in Equation 3 and the following integration from the initial crack length a_{ini} to the final quasi-brittle crack length determined from the fracture surface. Also the crack initiation cycles were considered by subtracting from the total failure cycles. Now for each R-ratio the material constants A and m could be determined so that the crack growth kinetics could be calculated. In Figure 6 these "synthetic" fatigue crack growth curves show a good correlation to already existing data of compact tension (CT) specimens of the same material [23].

In the next step the relationship between the R-ratios and the SIF for constant crack growth rates was worked out. The extrapolation to static loading (R=1.0) was done by exponential functions. In Figure 7 the data for static loading were transformed back into the kinetics diagram to build the "synthetic" creep crack growth (CCG) curve.

With this CCG-curve it was possible to model lifetimes in real pipes using Equation 4. In Figure 8 the predicted lifetime of a pressurized pipe is compared to real data of internal pressure tests. The calculation was done with the assumption that the inherent defect size of an extruded pipe is between 100 and 400 μm. Based on this calculation the generated failure region for a pipe with an internal pressure of 10 bars (hoop stress of 5.4 MPa) clearly lies above 100 years, although crack growth initiation times are still not considered.

Limitations

The determination of the material constants A and m and furthermore the crack growth kinetics is very sensitive to the fracture surface analyses (extent of brittle failure region) of the CRB specimens. Therefore a method for direct measurement of the crack growth kinetics is desirable and for this purpose it is planned to implement a compliance calibration procedure. However, in this respect special consideration has to be given on the effect of the eccentric crack growth on the evaluation procedure.

Although the results of the presented methodology seem to be reasonable it should be pointed out, that the extrapolation to R=1.0 was based on values at R=0.1, 0.3 and 0.5. To ensure the extrapolation method tests at R=0.7 are currently performed but due to their time intensity data are not available for the present work.

As many data from former research works were available the fatigue tests of this work were performed on a PE80 pipe material with the aim to develop the extrapolation method. Modern PE100 and PE100+ pipe grades may increase the testing times.

Conclusion

In the present research work the proposed concept for accelerated lifetime prediction of PE pipes [14] based on fatigue tests on CRB specimens was performed on a PE80 pipe grade. It was shown, that the crack kinetics at the loading ratios of R=0.1, 0.3 and 0.5 could be extrapolated to the case of static loading with R=1.0. With the generated "synthetic" creep crack growth curve it was possible to continue the lifetime prediction of pressurized pipes.

The advantage of this method is that the fatigue tests can be done at temperatures close to the real application and without the help of stress cracking liquids. The testing time requirements per material (or material condition in the pipe) are estimated at a few weeks up to a maximum of a few months.

Acknowledgement

The research work of this paper was performed at the Polymer Competence Center Leoben GmbH (PCCL, Austria) within the framework of the K_{plus}-program of the Austrian Ministry of Traffic, Innovation and Technology with contributions by the University of Leoben, AGRU Kunststofftechnik GmbH (Bad Hall, A), Borealis GmbH (Linz, A), OMV AG (Wien, A), ÖVGW – Österreichische Vereinigung für das Gas- und Wasserfach (Wien, A) and SABIC Polyolefine GmbH (Gelsenkirchen, D). The PCCL is funded by the Austrian Government and the State Governments of Styria and Upper Austria.

Literatur

1. Lang, R.W., Stern, A., Doerner, G., (1997) Applicability and Limitations of corrent Lifetime prediction Models for Thermoplastics Pipes under Internal Pressure, Die Angewandte Makromolekulare Chemie, 247 (1997) 131.
2. Gaube, E., Gebler, H., Müller, W., Gondro, C. (1985). Zeitstandfestigkeit und Alterung von Rohren aus HDPE, Kunststoffe 75(7), 412-415.
3. Ifwarson, M. (1989). Gebrauchsdauer von Polyethylenrohren unter Temperatur und Druckbelastung, Kunststoffe 79(6), 525-529.
4. Barker, M.B., Bowman, J.A., Bevis M. (1983) The Performance and Cause of Failure of Polyethylene Pipes Subjected to Constant and Fluctuating Internal

Pressure Loadings, Journal of Materials Science 18, 1095-1118.
5. Brömstrup, H. (2004) PE 100 Pipe Systems, Vulkan Verlag, Essen, Deutschland.
6. Brown, N. and X. Lu (1993). Controlling the Quality of PE Gas Piping Systems by Controlling the Quality of the Resin. 13th Plastic Fuel Gas Pipe Symposium, San Antonio, Texas, USA.
7. Brown, N. and X. Lu (1991). PENT Quality Control Test For PE Gas Pipes And Resins. 12th Plastic Fuel Gas Pipe Symposium, Boston, Massachusetts, USA.
8. Janson, L.E. (1999) Plastics Pipes for Water Supply and Sewage Disposal, Borealis, Sven Axelsson AB/ Fäldts Grafiska AB, Stockholm, Schweden.
9. Haager, M. (2006). Bruchmechanische Methoden zur beschleunigten Charakterisierung des langsamen Risswachstums von Polyethylen-Rohrwerkstoffen, Institute of Materials Science and Testing of Plastics, University of Leoben, Austria.
10. Hessel, J. (2007). 100 Jahre Nutzungsdauer von Druckrohren aus Polyethylen - Aussage wissenschaftlich bestätigt, Vortrag 1, Wiesbadener Kunststoffrohrtage 2007, Wiesbaden, Deutschland.
11. Parsons, M., Stepanov, E.V., Hiltner, A., Baer, E. (2000). Correlation of fatigue and creep slow crack growth in a medium density polyethylene pipe material, Journal of Materials Science 35, 2659-2674.
12. Pinter, G., Haager, M., Lang, R.W. (2006). Accelerated Quality Assurance Tests for PE Pipe Grades. ANTEC 2006, Charlotte, North Carolina, USA, Society of Plastics Engineers.
13. Pinter, G., Haager, M., Balika, W., Lang, R.W. (2007). Cyclic crack growth tests with CRB specimens for the evaluation of the long-term performance of PE pipe grades. Polymer Testing, Volume 26, Issue 2, April 2007, Pages 180-188.
14. Lang, R.W., Pinter, G., Balika, W. (2006). A Novel Qualification Concept for Lifetime and Safety Assessment of PE Pressure Pipes for Arbitrary Installation Conditions. Plastics Pipes XIII, Washington DC, USA.
15. Lang, R.W., Pinter, G., Balika, W. (2005) Konzept zur Nachweisführung für Nutzungsdauer und Sicherheit von PE-Druckrohren bei beliebiger Einbausituation. 3R international, 44(1-2), 33-41.
16. Anderson, T.L. (1991) Fracture Mechanics – Fundamentals and Application, CRC Press Inc., Boca Raton, Florida, USA.
17. Kinloch, A.J., Young, R.J. (1983) Fracture Behaviour of Polymers, Applied Science Publ., London, England.
18. Dieter, G.E. (1988). Mechanical Metallurgy, McGraw-Hill Book Company, London, United Kingdom.
19. Paris, P.C., Erdogan, F. (1963) A Critical Analysis of Crack Propagation Laws. Transactions of the ASME, Journal of Basic Engineering 85, p. 528-534.
20. Krishnamachari, S.I. (1993) Applied Stress Analysis of Plastics – A Mechanical Engineering Approach, Van Nostrand Reinhold, New York, USA.
21. Benthem, J.P., Koiter, W.T. (1973) in "Method of Analysis and Solutions of Crack Problems", (Sih, G. C., ed.), 3, 131-178, Noordhoft International Publisching, Groningen, Netherlands.
22. Murakami, Y. (1990) Stress Intensity Factors Handbook, Pergamon Press, Oxford, Great Britain.
23. Pinter, G., Balika, W., Lang, R.W. (2002) in Temperature-Fatigue Interaction (L. Rémy and J. Petit, eds.), ESIS Publication 29, 267-275, Elsevier, Amsterdam, Netherlands.

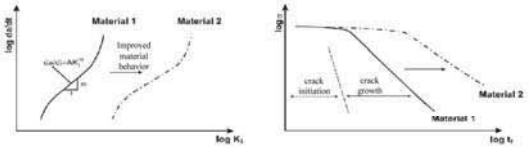

Figure 1: Relationship between creep crack growth behavior and failure behavior of internally pressurized pipes [14].

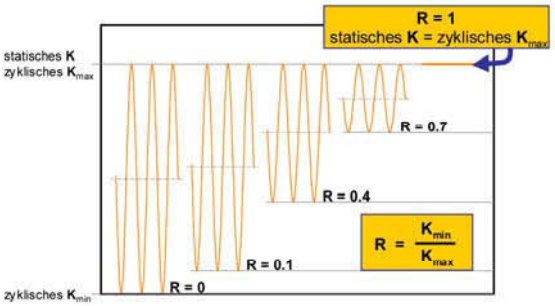

Figure 2: Crack tip stress field for static and cyclic loads at various R-ratios. [14].

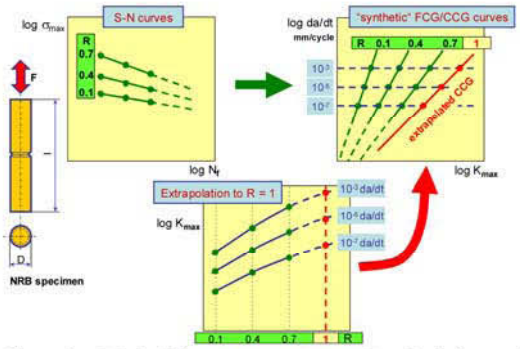

Figure 3: Methodology to generate "synthetic" crack growth curves for static loading (R=1.0) based on cyclic experiments with CRB specimens [14].

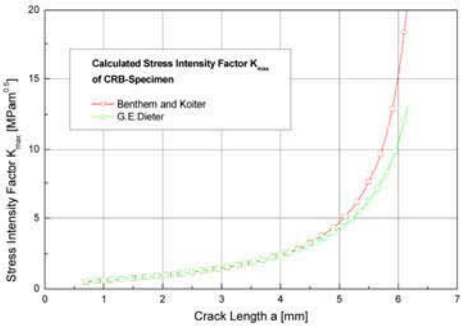

Figure 4: Comparison of the stress intensity factor by Benthem and Koiter [19] and G.E. Dieter [18] a function of the crack length in a CRB specimen.

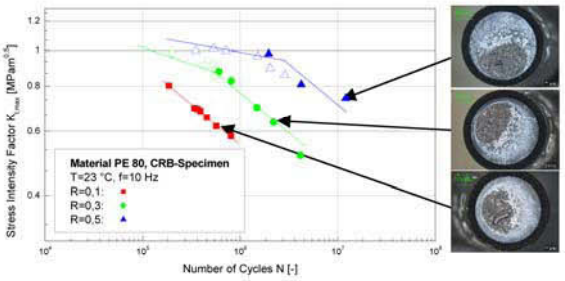

Figure 5: Number of cycles until failure of PE80 at 23 °C for R-ratios of 0.1, 0.3 and 0.5 and fracture surfaces of CRB specimens:
a) R=0.1; $K_{I,max}$=0.61 MPam^{0,5},
b) R=0.3; $K_{I,max}$=0.70 MPam^{0,5},
c) R=0.5; $K_{I,max}$=0.81 MPam^{0,5}.

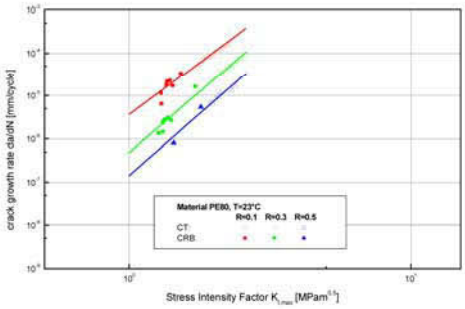

Figure 6: Correlation of "synthetic" crack growth kinetics of CRB specimens with existing data of CT specimens for PE80 and R-ratios of 0.1, 0.3 and 0.5.

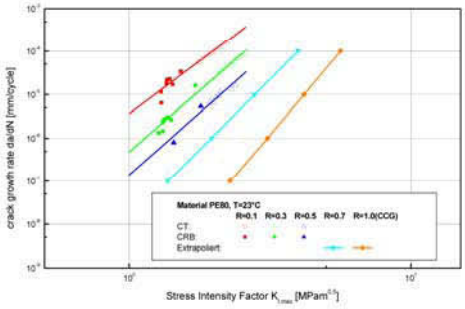

Figure 7: Extrapolation to "synthetic" crack growth kinetics for R-ratios of 0.7 and 1.0 (CCG) based on "synthetic" fatigue crack growth at R= 0.1, 0.3 and 0.5.

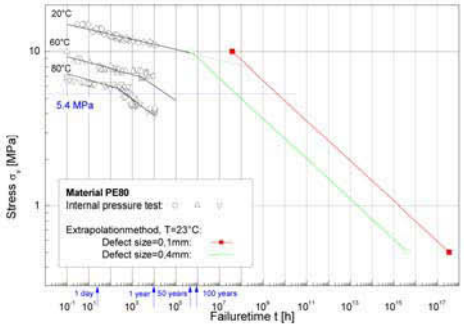

Figure 8: Comparison of real internal pressure tests on PE80 and predicted failure times based on extrapolation methodology with initial defect size of 0.1 and 0.4 mm.

Key Words: Polyethylene, fatigue, pipe, crack growth, lifetime.

I-2 A Fracture Mechanics Concept for the Accelerated Characterization of Creep Crack Growth in PE-HD Pipe Grades

A. Frank, W. Freimann, G. Pinter, R.W. Lang

Engineering Fracture Mechanics 76 (2009), ESIS Publication, 2780–2787.

Engineering Fracture Mechanics 76 (2009) 2780–2787

Contents lists available at ScienceDirect

Engineering Fracture Mechanics

journal homepage: www.elsevier.com/locate/engfracmech

A fracture mechanics concept for the accelerated characterization of creep crack growth in PE-HD pipe grades

Andreas Frank [a,*], Werner Freimann [a], Gerald Pinter [b], Reinhold W. Lang [b]

[a] Polymer Competence Center Leoben GmbH, Roseggerstrasse 12, A-8700 Leoben, Austria
[b] Institute of Materials Science and Testing of Plastics, University of Leoben, Franz-Josef-Strasse 18, 8700 Leoben, Austria

ARTICLE INFO

Article history:
Received 25 September 2008
Received in revised form 8 June 2009
Accepted 15 June 2009
Available online 24 June 2009

Keywords:
Polymers
Pipe
Polyethylene
Fatigue
Slow crack growth

ABSTRACT

For the lifetime prediction of pressurized polyethylene (PE) pipes based on methods of the linear elastic fracture mechanics the knowledge of the crack resistance and the kinetics of creep crack growth (CCG) is essential. In the present work a rather brittle nonpipe material was used to develop a methodology for an accelerated measurement of crack kinetics in fatigue tests on cracked round bar (CRB) specimens at ambient temperatures of 23 °C. A material and specimen specific compliance calibration curve was generated to detect the crack kinetics with only one single CRB test. Based on an already proposed concept the kinetics at different *R*-ratios (minimum/maximum load) was measured and extrapolated to the case of CCG. To demonstrate the transferability of this concept to pipe materials a PE 80 pipe grade was used. Although the necessary testing time increased considerably the concept still has the potential to reduce the overall testing time for new pipe materials to be certified significantly. With the presented procedure a characterization of CCG in modern PE pipe grades at room temperature and without the use of stress cracking liquids is possible within a few months.

1. Introduction

It is generally accepted, that for long-term applications crack initiation and slow crack growth (SCG) are the critical failure mechanisms of pressurized polyethylene (PE) pipes. The knowledge of the long-term failure behavior – especially SCG – of the material is of essential interest for lifetime and safety assessment [1–7]. The standard method for the determination of the long-term behavior and the estimation of lifetimes is based on internal pressure tests on pipe specimens and the extrapolation method by EN ISO 9080:2003 [8]. A number of test methods using fracture mechanics considerations were developed for an accelerated characterization of the resistance against SCG, like the Notched Pipe Test, the Pennsylvania Notch Test or the Full Notch Creep Test [6,9]. A decrease of the failure times in these tests was achieved by increasing temperature or by the influence of stress cracking liquids.

Essential improvements in the raw materials have led to pipe materials with increased crack resistance. Especially the controlled implementation of short chain branches and a bimodal molecular mass distribution result in materials with a minimum required strengths (MRS) of 10 MPa and above that are classified in PE 100 grades [10,11]. However, these modern materials represent new challenges to usual test methods, as their higher resistance against crack initiation and SCG also extends the testing times into unpractical time frames.

* Corresponding author. Tel.: +43 (0) 3842 42962 26; fax: +43 (0) 3842 42962 6.
E-mail addresses: Andreas.Frank@pccl.at (A. Frank), Werner.Freimann@pccl.at (W. Freimann), Gerald.Pinter@mu-leoben.at (G. Pinter), Reinhold.Lang@unileoben.ac.at (R.W. Lang).

0013-7944/$ - see front matter © 2009 Elsevier Ltd. All rights reserved.
doi:10.1016/j.engfracmech.2009.06.009

One possibility to reduce testing times are fatigue tests under cyclic loads and using fracture mechanics concepts for data evaluation [4,12]. Moreover, the choice of suitable specimen geometries influences the testing time and especially cracked round bar (CRB) specimens show very promising results even at temperatures of 23 °C, which are very close to the application temperatures of real pipes, and without any stress cracking liquids [13,14].

An extrapolation concept how to transfer cyclic fatigue tests into the case of static loading conditions to describe SCG has already been proposed [15,16]. One essential step in this concept is the determination of the crack kinetics at several *R*-ratios (ratio of minimum to maximum loading) [15–18]. Hence, the main objective of this work was the development of a technology for a direct measurement of crack kinetics on CRB specimens, which was not previously possible. For this purpose a rather brittle nonpipe PE was used to evaluate the reliability of the measurement of the crack kinetics based on crack length dependent material compliance. Afterwards a PE 80 pipe grade material was used to apply this technology and to demonstrate the transferability of the generated crack kinetics into the proposed extrapolation concept.

2. Background

The long-term failure behavior of pressurized PE pipes is well investigated and can be separated into three characteristic regions (Fig. 1) [1]. In region A at relative high stress levels the failure is dominated by ductile deformation with large plastic zones. At lower loadings the failure mechanism passes a transfer knee and change to quasi-brittle failure region B where the longer failure times of this region can be separated into crack initiation and SCG. The nearly load independent third region C is reached after very long times and is caused by ageing processes, polymer degradation and stress corrosion cracking [19].

The failure mechanism in region B (crack initiation and SCG) can be described with linear elastic fracture mechanics (LEFM) concepts and therefore several laboratory tests have been developed. Basic requirements for the applicability of the concepts of LEFM in plastics materials are that global loadings are within the linear viscoelastic deformation range and the size of plastic zones at the crack tip is only small. The stress distribution in the vicinity of the crack tip is described by the stress intensity factor (SIF) K_I (index I stands for a crack opening load normal to the crack plane) that is a function of the crack length a, the applied stress σ and a geometric factor Y that is known for several specimens and component shapes (Eq. (1)) [20,21].

$$K_I = \sigma \cdot \sqrt{a} \cdot Y \tag{1}$$

The crack growth kinetics da/dt under static loading is plotted in a double logarithmic diagram as a function of the SIF K_I (Fig. 2) [17]. In the region of quasi-brittle crack growth usually a distinct linear correlation is found that can be described by the power law of Paris and Erdogan (Eq. (2)), where the constants A and m depend on the material as well as on test conditions like temperature. The linear region of the crack kinetics can be used to compare different materials concerning crack growth resistance. An improved material shifts the kinetics to higher SIF and also a lower slope can be a result of higher crack resistance. The material parameters A and m are of high importance for a fracture mechanics lifetime prediction.

$$\frac{da}{dt} = A \cdot K_I^m \tag{2}$$

One possibility to reduce testing times are fatigue tests under cyclic loading, where the loading conditions are specified by the *R*-ratio, the ratio of minimum to maximum loading (Fig. 3). Several studies show, that independent of the loading conditions (cyclic vs. static) the mechanism of slow crack growth is very similar and material rankings based on fatigue tests

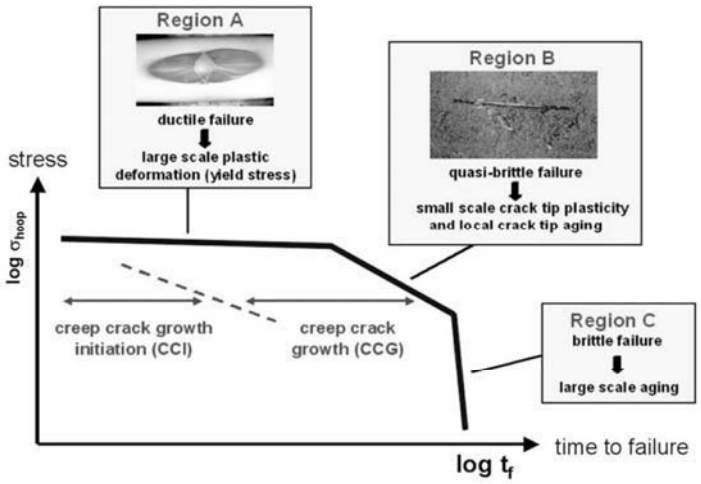

Fig. 1. Schematic illustration of the long-term failure behavior of pressurized PE pipes [1].

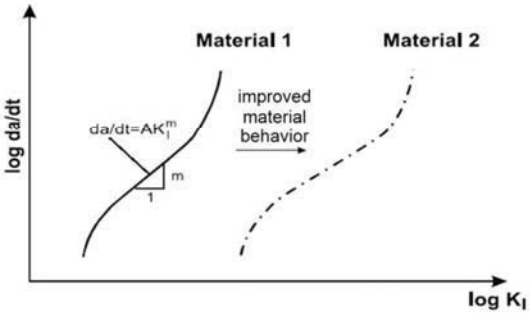

Fig. 2. Crack growth kinetics under static loads [15].

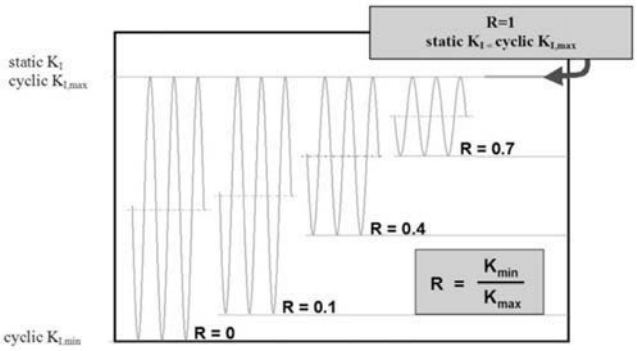

Fig. 3. Crack tip stress field for static and cyclic loads at various *R*-ratios [15].

are comparable to those of static tests [4,12,22–24]. In the case of cyclic loading fatigue crack growth (FCG) is usually depicted in a double logarithmic diagram, where da/dN is a function of the range of the SIF $\Delta K_I = K_{I,max} - K_{I,min}$. A ratio of $R = 1.0$ describes static loading ($K_{I,max} = K_{I,min}$). By decreasing R testing times decrease too and every single R-ratio will result in a specific kinetics curve. According to Fig. 3 the approach from cyclic to static tests in this work was done at an equal maximum SIF, so that all illustrations of this work are related to $K_{I,max}$.

Another possibility for a reduction of testing times is the choice of a suitable specimen geometry. The use of cracked round bar (CRB) specimens provides near plain strain conditions which reduce the formation of the plastic zone size at the crack tip to a minimum [25–28]. The high constraint in this specimen ensures a relatively quick formation of craze zones and an accelerated crack initiation. It was shown that even at ambient temperatures of 23 °C and without any stress cracking liquids a material ranking with fatigue tests on CRB specimens give the same results as time consuming tests like Full Notch Creep Tests [29]. Moreover, not only a differentiation of different PE-grades (PE 80, PE 100) can be done, but also a distinction within one grade up to process related batch variations is possible within a few days. Due to the very simple geometry it is possible to manufacture the CRB specimens either from moulded plates or even from extruded pipes. Therefore these fatigue tests on CRB specimens open an interesting potential for product ranking, quality assurance and material development [9,13–16].

For LEFM lifetime prediction the knowledge of creep crack growth (CCG) is important. Based on an already proposed extrapolation methodology [15,16] the FCG curves at different R-ratios are transformed into a diagram of constant crack growth rates, where $K_{I,max}$ is a function of R (Fig. 4). After the extrapolation of the crack growth rates with appropriate mathematical methods to $R = 1.0$ (static loading) the generated SIF's are transformed back into the kinetics diagram to generate a "synthetic" CCG curve. From this curve the material constants A and m can be determined and furthermore used for a fracture mechanics based lifetime calculation of components like pressurized pipes.

Due to the specimen geometry and the tendency of eccentric crack growth a reliable direct measurement of the crack kinetics da/dN on a CRB specimen is difficult [18]. Nevertheless a determination of the crack kinetics is possible indirectly by using specimen compliance [30]. The compliance C is defined as the ratio of the crack opening displacement COD and the applied load F (Eq. (3)). As displayed in Fig. 5 the specimen compliance also depends on the crack length a, which means, that with increasing crack length C increases, respectively.

$$C = \frac{\mathrm{COD}}{F} \tag{3}$$

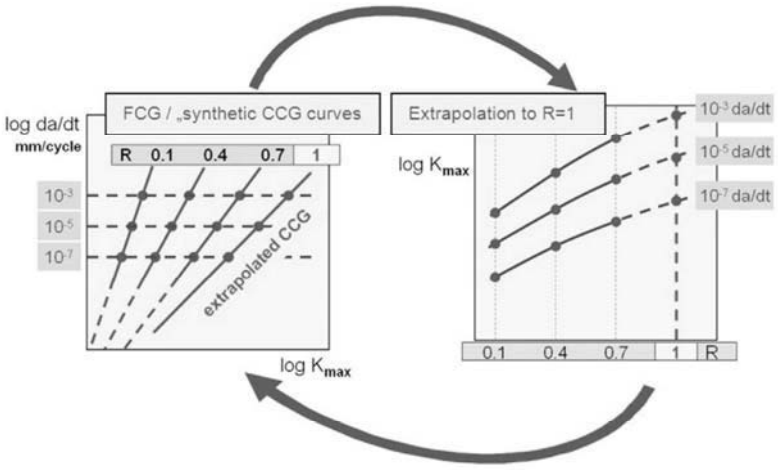

Fig. 4. Methodology to generate "synthetic" creep crack growth curves for static loading (R = 1.0) based on cyclic experiments with CRB specimens [15,16].

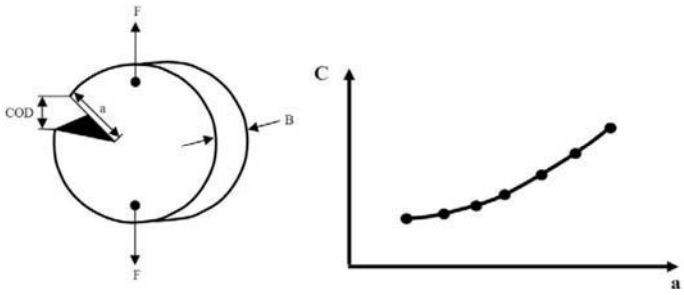

Fig. 5. Left: Schematic illustration of crack opening displacement COD. Right: Dependence of compliance C from crack length.

3. Experimental details

All investigations were performed on commercially available PE materials. First the development of the method for direct measurement of the crack kinetics on CRB specimens was done with a rather brittle blow-moulding type PE-BF at R-ratios of 0.1, 0.3, 0.5 and 0.7. The extrapolation concept for generating CCG was applied to this material. In the following step further investigations were done with a PE 80 pipe grade.

For specimen preparation compression moulded plates with a thickness of 15 mm were produced. The CRB specimens with a diameter of 13.8 mm were manufactured out of these plates and the circumferential initial crack with the depth of 1.5 mm was inserted with a razorblade. All fatigue tests were executed on a servo-hydraulic closed-loop testing system MTS Table Top (MTS Systems GmbH, GER) with a sinusoidal loading at 23 °C and a frequency of 10 Hz.

For the indirect determination of the crack kinetics a crack length depending compliance calibration curve was developed. Therefore the COD of CRB specimens with different initial crack lengths from 1.0 to 3.0 mm was measured with three extensometers (Type 632.13–20, MTS Systems GmbH, GER) that were positioned at equal intervals of 120° around the crack. Important was to guarantee that during these tests no crack initiation took place and the loads were chosen in the linear viscoelastic range. Because the loads F in fatigue tests change between a minimum and a maximum value, the crack opening displacement was measured as the difference ΔCOD of minimum and maximum COD. Analog the specimen compliance was calculated to $\Delta C = \Delta\text{COD}/\Delta F$. Those compliance calibration curves could then be used to calculate crack lengths in the cyclic CRB tests and to generate crack kinetic curves.

4. Results and discussion

Fig. 6 shows the compliance calibration curve for PE-BF and PE 80 at 23 °C where the correlation of ΔC with increasing crack lengths a is displayed. For equal temperature the compliance is only depending on the material and the specimen geometry. This is proven by the results for material PE-BF where the measured calibration curves for the R-ratios of 0.1

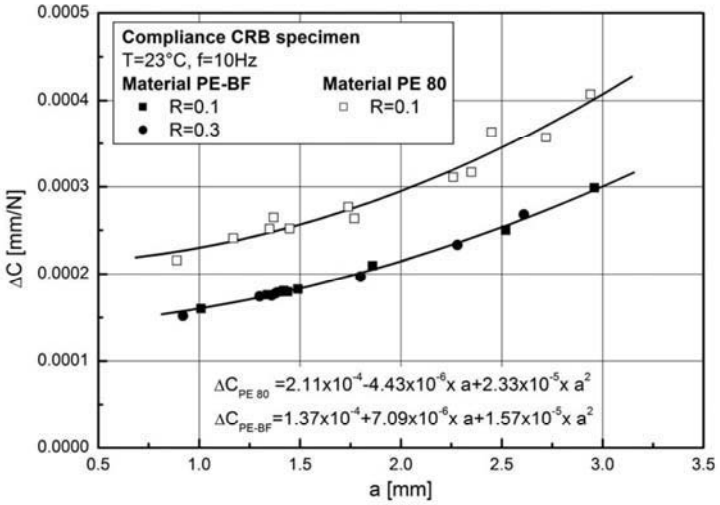

Fig. 6. Compliance calibration curve ΔC at 23 °C as a function of the crack length a for CRB specimens of PE-BF ($R = 0.1$ and 0.3) and PE 80 ($R = 0.1$).

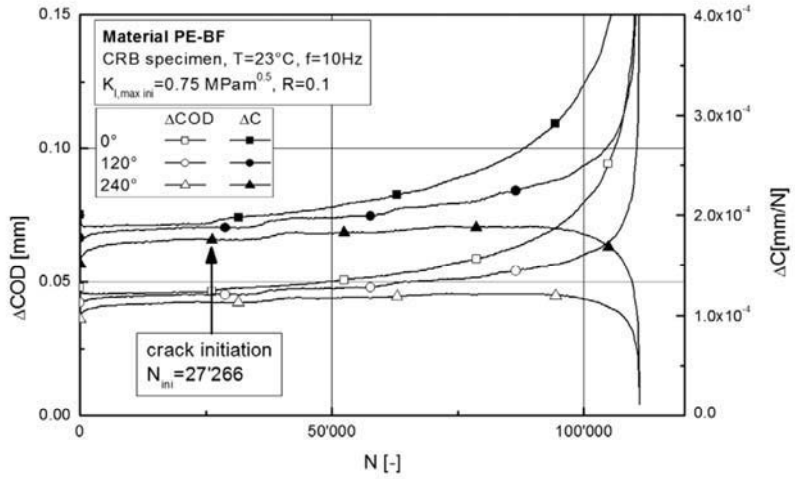

Fig. 7. Extensometer signals ΔCOD and corresponding specimen compliance ΔC as a function of cycles N. The first step in the curves indicates crack initiation.

and 0.3 overlap indicating load independency. The values for ΔC were recorded after a few thousand cycles, so that starting effects (e.g. stabilization of extensometer assembling) are eliminated, and before crack initiation. A curve fitting was done with a simple polynomial function. By converting this material and specimen specific function into a quadratic equation it was possible, to calculate the crack length in a cyclic CRB test from any corresponding measured ΔC.

The results in Fig. 6 show that the compliance curve for PE-BF is clearly lower than for PE 80 what is caused by the comparatively brittle material behavior of the blow-moulding type. A typical characteristic of modern pipe grade materials is the improved toughness against crack initiation and crack growth what lead to a higher compliance of the PE 80 material.

Fig. 7 shows the typical signals of the extensometers ΔCOD and the associated ΔC values of a single fatigue test. After starting effects at very low cycles the values of ΔCOD and ΔC are constant. The deviation of the single signals for the individual extensometers can be assigned to tolerances in specimen preparation and clamping tools that led to diverse crack opening at the surface. The slow crack growth is initiated anywhere around the circumferential initial crack and is clearly detectable at the first step in the extensometer signals. After the initiation the crack grows around the entire notch and with continuing test an increase of ΔCOD and ΔC indicates slow crack growth and the very typical stepwise characteristic of quasi-brittle crack growth in PE can be noticed.

With continuing crack growth and increasing crack length the SIF at the crack tip raises and the failure mechanism changes from slow crack growth into the ductile failure mode, which is reflected by the distinctive raise of the signals.

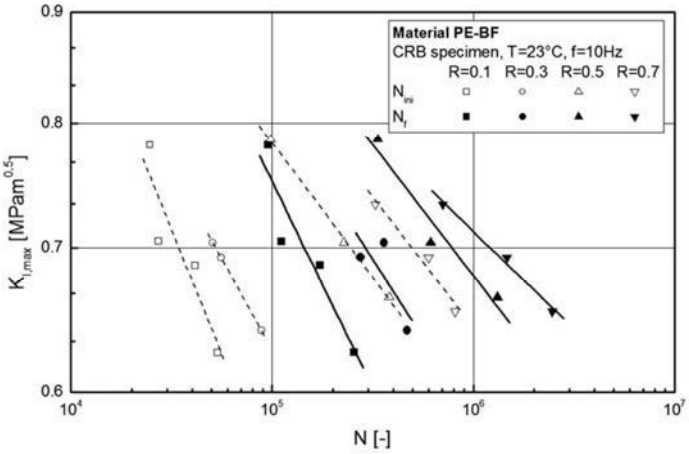

Fig. 8. Cycles until crack initiation N_{ini} and failure N_f at different R-ratios as a function of the maximum stress intensity factor $K_{I,max}$.

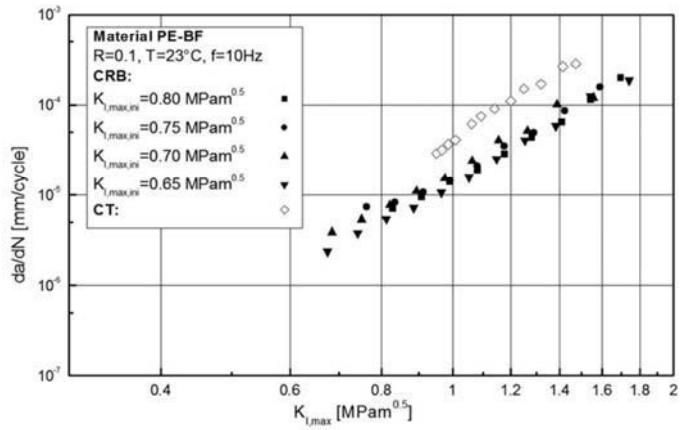

Fig. 9. Crack kinetics da/dN of PE-BF at R = 0.1 from tests started at different initial stress intensity factors $K_{I,max,ini}$. Comparison of CRB and CT specimens.

The fact, that with ongoing test an eccentric crack growth appears causes additional bending in the specimen, which causes a decrease of the signal at 240°. However, the acquisition of the crack kinetic is only permitted within the quasi-brittle failure mode where this effect of eccentric crack growth can be neglected. At the end of the test the specimen approaches its final failure and the signals turn into infinite.

The fatigue tests were varied in the maximum loads for each R-ratio, so that the initial maximum SIF differ between 0.60 and 0.80 MPa $m^{0.5}$. Fig. 8 shows the crack initiation and failure cycle number of PE-BF at different R-ratios as a function of the maximum SIF $K_{I,max}$. The crack initiation cycle number N_{ini} shows the same linear correlation as the failure cycle number N_f, however, at significantly lower testing times. As expected, N_{ini} and N_f increase with rising R-ratios. Several studies prove that fatigue tests on CRB specimens at R = 0.1 are highly reliable as a method for a quick and easy material ranking [9,13–16]. A characterization by crack initiation cycles may have the potential for a further reduction of testing times.

Using the compliance calibration curve in Fig. 6 the crack kinetics can be calculated for the individual fatigue tests. Fig. 9 displays the crack kinetics of PE-BF at R = 0.1 from tests started at different initial SIF's. The results show a very good reproducibility and the characteristic of the crack kinetics is independent of the applied initial load. As a reference the data are correlated to crack growth kinetics measured with compact tension (CT) specimens of the same material. However, this test was performed in a previous project [23]. The CT specimens show slightly faster crack growth rates, what may be a result of marginal changes in the raw material (different batches). Nevertheless, the functional characteristics of the curves confirm the reliability and the potential of the compliance calibration method with CRB specimens for a fast measurement of crack kinetics. Whereas the considerable higher constraint in CRB specimen induces a quick crack initiation, the geometry is responsible for a fast increase in the SIF, what lead to shorter testing times compared to CT specimens.

The crack kinetics for PE-BF at R-ratios of 0.1, 0.3, 0.5 and 0.7 as a function of the maximum SIF $K_{I,max}$ are displayed in the left chart of Fig. 10. With increased R-ratio the kinetic lines are shifted to higher SIF what denotes the decrease in the crack

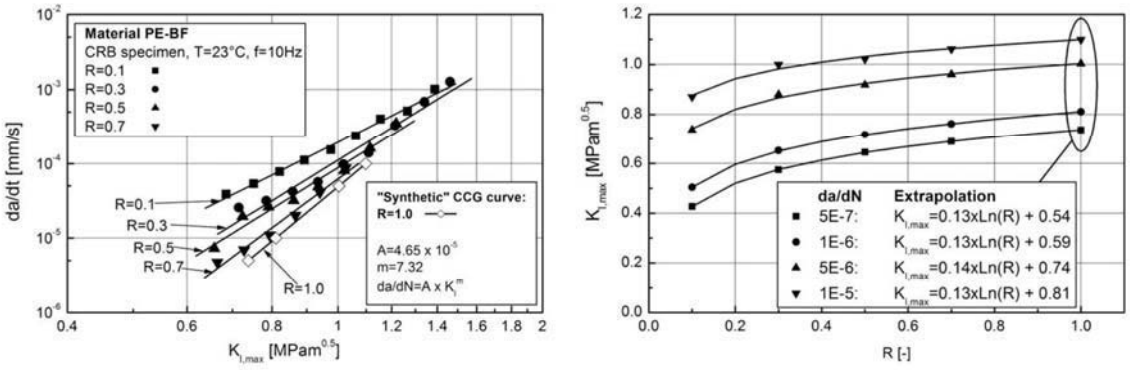

Fig. 10. Left: Fatigue crack kinetics da/dt of PE-BF at different R-ratios and extrapolated "synthetic" creep crack growth curve (R = 1.0). Right: Extrapolation of R-ratio depending SIF to R = 1.0 (static loading).

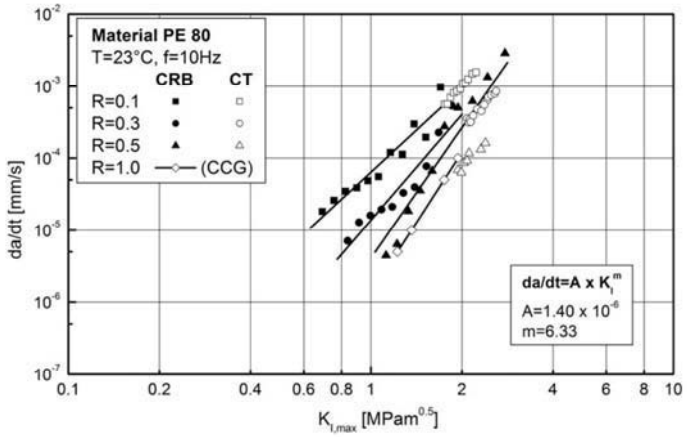

Fig. 11. Crack kinetics da/dN of PE 80 at different R-ratios and extrapolated "synthetic" creep crack growth curve (R = 1.0).

growth rate. Based on the methodology described above (background) for each R-ratio the SIF's at several constant crack growth rates were defined and transformed into a diagram, where $K_{I,max}$ is a function of R (Fig. 10, right). For curve fitting between R = 0.1 to 0.7 different simple calculations like polynomial or logarithmic functions were tested empirical. These functions were used to extrapolate the constant crack growth rate lines to R = 1.0. Finally the associated SIF's at R = 1.0 were transformed back into the kinetics diagram to provide a "synthetic" CCG curve. The logarithmic function shows the best agreement with the existing test data and furthermore this function results in the most conservative approach (which means highest crack growth rate) in the extrapolated crack growth kinetics and is also shown in Fig. 10, left. With this "synthetic" CCG curve it is possible to calculate the important material parameters A and m for static loading conditions and continue with lifetime prediction. In the case of PE-BF this parameters are $A = 4.65 \times 10^{-5}$ and $m = 7.32$.

Fig. 11 shows the measured crack kinetics for the PE 80 pipe grade at the R-ratios of 0.1, 0.3 and 0.5. Data from a previous project measured with CT specimens of the same material are included as a reference [23]. In contrast to the PE-BF material, the compliance calibration based kinetics at R = 0.1 shows an excellent correlation to the CT data. However, at R = 0.3 and 0.5 the crack growth rates in the CRB specimens is higher than in CT specimens. Remembering the low constraint and high plastic zones this could be a reason for retarded crack growth in CT specimens. With increasing R-ratio the material shows slower crack growth rates. The calculation of the "synthetic" CCG curve was again done by extrapolation of SIF with constant crack growth rates to R = 1.0 with logarithmic functions. The material parameters were calculated to $A = 1.40 \times 10^{-6}$ and $m = 6.33$.

5. Conclusions

In the present work a new technique for a direct measurement of crack growth kinetics of polyethylene (PE) on cracked round bar (CRB) specimens in fatigue tests was demonstrated. Fatigue tests under sinusoidal load, a frequency of 10 Hz and at ambient temperatures of 23 °C were performed with two different PE pipe materials at different R-ratios

(minimum/maximum loading). Three extensometers that were positioned at equal intervals of 120° around the crack were used to measure the crack opening displacement (COD) at the specimen surface and to develop crack length depending compliance calibration curves. Those compliance calibration curves were then used to calculate crack lengths in the cyclic CRB tests from COD data and to generate crack kinetic curves. The comparison of the generated kinetics with results form compact tension (CT) tests shows a good comparability.

An extrapolation concept for the estimation of creep crack growth (CCG) was applied for two different PE's. The kinetics of fatigue tests were extrapolated to the R-ratio of 1.0 what represents static loading. With this "synthetic" CCG curves lifetime prediction based on methods of the linear elastic fracture mechanics (LEFM) is possible. As already confirmed fatigue tests on CRB specimens are a reliable method for a quick ranking of PE pipe grade materials. The high sensitivity in the detection of crack initiation by three extensometers opens an interesting option for further acceleration of material comparison.

Acknowledgements

The research work of this paper was performed at the Polymer Competence Center Leoben GmbH (PCCL, Austria) within the framework of the K_{plus}-program of the Austrian Ministry of Traffic, Innovation and Technology with contributions by the University of Leoben, AGRU Kunststofftechnik GmbH (Austria), Borealis Polyolefine GmbH (Austria), OMV Exploration & Production GmbH (Austria), Österreichische Vereinigung für das Gas und Wasserfach (Austria) and SABIC Europe (Netherlands). The PCCL is funded by the Austrian Government and the State Governments of Styria and Upper Austria.

References

[1] Lang RW, Stern A, Doerner G. Die Angewandte Makromolekulare Chemie 1997;247:131.
[2] Gaube E, Gebler H, Müller W, Gondro C. Kunststoffe 1985;75(7):412–5.
[3] Ifwarson M. Kunststoffe 1989;79(6):525–9.
[4] Barker MB, Bowman JA, Bevis M. J Mater Sci 1983;18:1095–118.
[5] Brömstrup H. Essen, Deutschland: Vulkan Verlag; 2004.
[6] Brown N, Lu X. In: 12th Plastic fuel gas pipe symposium, Boston, Massachusetts, USA; 1991.
[7] Brown N, Lu X. In: 13th Plastic fuel gas pipe symposium, San Antonio, Texas, USA; 1993.
[8] Janson LE. Borealis, Axelsson, S. AB/Fäldts Grafiska AB, Stockholm, Schweden; 1999.
[9] Haager M. Institute of materials science and testing of plastics, Austria: University of Leoben; 2006.
[10] Brown N, Lu X, et al. Plast Rubb Compos Process Appl 1992;17(4):255–8.
[11] Pinter G, Lang RW. The application of fracture mechanics to polymers, adhesives and composites. In: Moore DR, editor. vol. 33, Oxford (England): Elsevier Science Ltd. and ESIS. ESIS Publication; 2004. p. 47–54.
[12] Parsons M, Stepanov EV, Hiltner A, Baer E. J Mater Sci 2000;35:2659–74.
[13] Pinter G, Haager M, Lang RW. ANTEC 2006. Charlotte (North Carolina, USA): Society of Plastics Engineers; 2006.
[14] Pinter G, Haager M, Balika W, Lang RW. Polym Test 2007;26(2):180–8.
[15] Lang RW, Pinter G, Balika W. 3R International. 2005; 44(1–2): 33–41.
[16] Lang RW, Pinter G, Balika W, Haager M. Plastics pipes XIII, Washington DC, USA; 2006.
[17] Pinter G, Lang RW, Haager M. Chem Monthly 2007;138:347–55.
[18] Frank A, Pinter G, Lang RW. ANTEC 2008. Milwaukee (Wisconsin, USA): Society of Plastics Engineers; 2008.
[19] Choi B-H, Chudnovsky A, Paradkar R, Michie W, Zhou Z, Cham P-M. Polym Degrad Stab 2009;94(5):859–67.
[20] Kinloch AJ, Young RJ. Fracture behaviour of polymers. London (England): Applied Science Publ; 1983.
[21] Anderson TL. Fracture mechanics – fundamentals and application. Boca Raton (Florida, USA): CRC Press Inc.; 1991.
[22] Haager M, Zhou W, Pinter G, Chudnovsky A. ANTEC 2005. Boston (Massachusetts, USA): Society of Plastics Engineers; 2005.
[23] Pinter G, Balika W, Lang RW. Temperature–fatigue interaction. In: Remy L, Petit J, editors. vol. 29, Amsterdam: Elsevier Science Ltd. and ESIS. ESIS Publication; 2002. p. 267–75.
[24] Lang RW, Balika W, Pinter G. The application of fracture mechanics to polymers, adhesives and composites. In: Moore DR, editors. vol. 33, Oxford (England): Elsevier Science Ltd. and ESIS. ESIS Publication; 2004. p. 83–92.
[25] Duan D-M, Williams JG. J Mater Sci 1998;33:638–52.
[26] Ting SKM, Williams JG, Ivankovic A. Polym Eng Sci 2006;46:763–77.
[27] Ting SKM, Williams JG, Ivankovic A. Polym Eng Sci 2006;46:778–91.
[28] Ting SKM, Williams JG, Ivankovic A. Polym Eng Sci 2006;46:792–8.
[29] Haager M, Pinter G, Lang RW. ANTEC 2006. Charlotte (North Carolina, USA): Society of Plastics Engineers; 2006.
[30] Saxena A, Hudak SJ. Int J Fract 1978;14(5):453–68.

I-3 Numerical Simulatio n of the Fa ilure Behavior of PE Pressure Pipes with Additional Loads

P. Hutař, M. Ševčík, L. Náhlík, I. Mitev, A. Frank, G. Pinter
in proceedings: ANTEC 2009, Chicago, Illinois, USA (2009), 2163-2168.

NUMERICAL SIMULATION OF THE FAILURE BEHAVIOR OF PE PRESSURE PIPES WITH ADDITIONAL LOADS

Pavel Hutař, Martin Ševčík, Luboš Náhlík, Institute of Physics of Materials, Brno, Czech Republic
Ivaylo Mitev, Andreas Frank., Polymer Competence Center Leoben, Austria
Gerald Pinter, University of Leoben, Austria

Abstract

Using linear elastic fracture mechanics concepts a simulation methodology for the assessment of internally pressurized pipe lifetimes was developed. The concept is based on the numerical calculation of stress intensity factors for pipes under different loading conditions and on using experimentally generated creep crack growth kinetics for lifetime calculations. Comparison of simulated lifetimes with experimental data from tests with internally pressurized pipes proved the principal applicability of the concept, but also identified major parameters affecting pipe lifetime.

Introduction

Lifetime prediction of polymeric materials has been subjected to numerous studies [1,2]. A typical requirement for gas or water pipes is a lifetime of at least 50 years. The traditional method to assess the lifetime of plastic pressure pipe materials is based on hydrostatic pressure testing [3]. Hydrostatic rupture tests are conducted in specific environment, at various pressure levels and at different temperatures. The time to failure is usually expressed by a log-log diagram hoop stress versus failure time (see Fig.1).

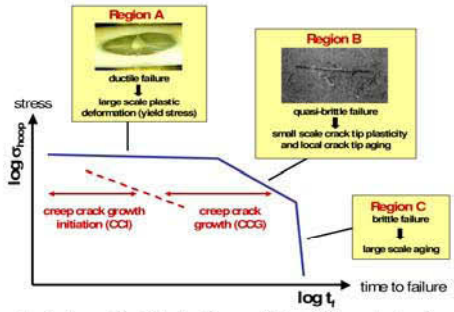

Figure 1. Schematic illustration of the failure behavior of pressurized PE pipes [2]

The hoop stress curve can be generally divided into three regions. After short periods at high internal pressures, region A is characterized by ductile fracture with large plastic deformation (so called fish mouth ruptures). In region B failure is a result of quasi-brittle crack growth. The failure process is determined by crack initiation from local defects and slow crack growth with only local plastic deformation at the crack front. Finally, in region C large scale global ageing of the material leads to nearly stress independent brittle failure. As the failure phenomenon of quasi-brittle crack growth in region B (that is most relevant for real service failure of PE pipes) can be described with fracture mechanics concepts, modern methods of fracture mechanics are used to model the service lifetime of pipes in this work.

Fracture mechanics background

In the service failure relevant region B of the hoop stress diagram plastic deformations are localized just around the crack tip and small scale yielding conditions are valid. Due to this fact linear elastic fracture mechanics (LEFM) can be used for description of the stress field around the crack tip. In LEFM the stress distribution near the crack tip is described by the stress intensity factor (SIF) K_I that is a function of the global loading, the crack length a and geometric factor Y that is known for several specimens and component shapes (see eq. 1) [4].

$$K_I = \sigma \cdot \sqrt{\pi a} \cdot Y \qquad (1)$$

Usually, fracture mechanics creep crack growth curves of polymer materials can be defined by a K_I versus da/dN curve, which is schematically shown in Fig.2 [4].

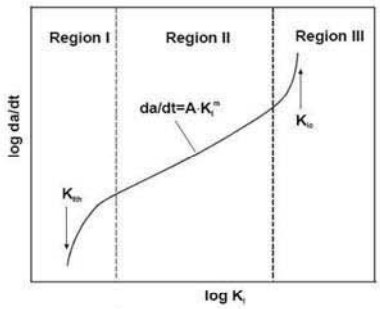

Figure 2. Scheme of creep crack growth rate curve [2]

Based on the schematic illustration in Fig.2., the crack growth behavior can be divided into three regions. In

region I, so-called threshold region, crack growth rates fall sharply to the threshold value K_{Ith}. For stress intensity factors below K_{Ith} the creep crack is arrested. The region of the stable crack growth (region II) can be explained by the exponential relationship:

$$\frac{da}{dt} = A\left(K_I\right)^m \tag{2}$$

where A and m are material parameters. In region III the crack growth rates are rising sharply since the stress intensity factor approaches the critical value K_{IC} [4].

Region 2 of this curve can be used for lifetime estimation of pipes according to equation 3 taking into account the relevant stress intensity factors in a pipe and the relevant initial defect of the size a_0 and final crack length a_f:

$$t = \int_{a_0}^{a_f} \frac{1}{da/dt} da = \int_{a_0}^{a_f} \frac{da}{A \cdot \left[K_I(p,d,s,a)\right]^m}, \tag{3}$$

where p is internal pressure, d is outer diameter of the pipe and s is pipe wall thickness. Crack growth initiation times are neglected in this study.

Numerical model

To predict residual lifetime of a pressured pipe from an initial defect, the FE model of the structure was build (see Fig.3).

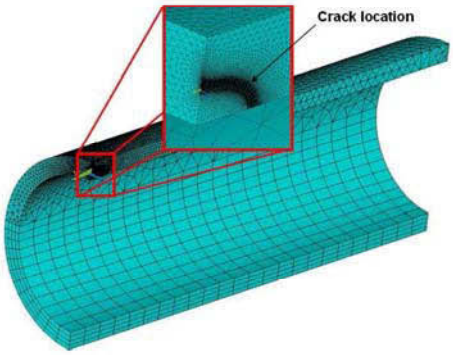

Figure 3. Finite element model of the internally pressured pipe with crack.

The outer diameter of the studied pipe was 40 mm with a wall thickness 3.7 mm. The typical size of the initial defect was estimated on the base of experimental observations as 0.1 mm. Hoop stress level during the simulation was between 4 and 6 MPa. The relation between internal pressure and hoop stress of the material can be obtained in the frame of on linear elasticity as follows:

$$\sigma_{hoop} = p.\frac{d-s}{2s} \tag{4}$$

The finite element model of the pipe was symmetrical containing a small elliptical crack (see Fig.4). Based on experimental observations the ratio between length of the crack a and crack width b was assumed 0.25.

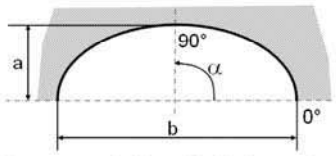

Figure 4. Geometry of the elliptical crack used for calculations

A typical model used for calculation included around 150 000 isoparimetric elements strongly non-homogenously distributed in the structure because of mesh refinement around the crack tip.

Material properties

Measured creep crack growth data representing the stable crack growth range (region II) for the investigated pipe grade PE-HD at 80 °C are shown in Fig. 5. In Fig. 6 results from internal pressure tests at 80 °C for this material are shown [5].

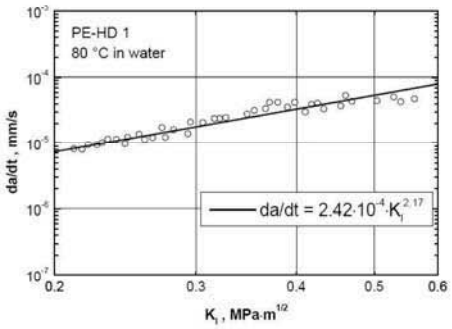

Figure 5. Creep crack growth rates as a function of the stress intensity factor for a pipe grade PE-HD at 80°C [5]

Creep effects of the material and the pipe are not considered in this work and for simulation an elastic isotropic material model is used (corresponding to 80 °C: Young modulus: 180 MPa, Poisson ratio: 0.3).

Residual lifetime estimation

In the following lifetime of the above mentioned PE-HD pipe at 80 °C is simulated using the described LEFM concept with different models and boundary conditions.

As a first simple approximation a two dimensional (2D) model of the pipe with a crack loaded by internal pressure was used. To check the accuracy of the results also a more complicated, three-dimensional (3D) model was developed (see Fig.3). By comparison of the stress intensity factors for these two different models a big discrepancy was found (see Fig.7).

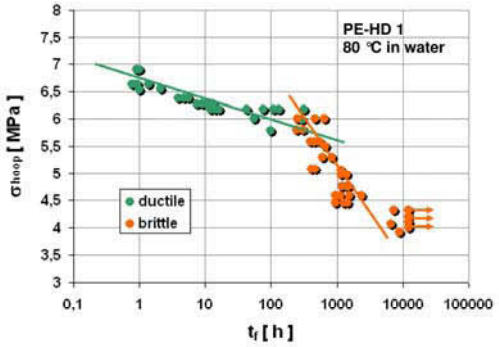

Figure 6. Results from internal pressure tests at 80 °C for a pipe grade PE-HD [5]

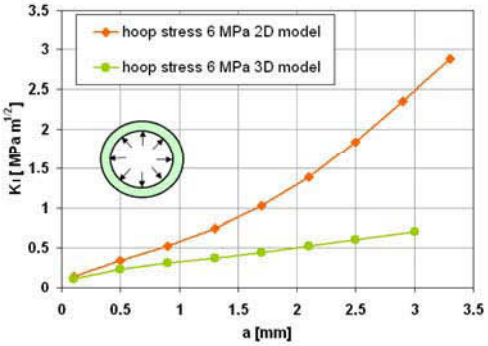

Figure 7. Stress intensity factor as a function of the crack length for 2D and 3D calculation (hoop stress 6MPa)

The completely different results can be explained by the big difference between the 2D representation of the pressure pipe and the more realistic 3D geometry. In the two dimensional model with plane strain conditions, the crack width b is assumed to be similar with a pipe length. This assumption leads to much higher stress intensity factor values than for the 3D model. Therefore, simple 2D approximation is in our case not representative and a complete 3D model is necessary to use.

The values of the stress intensity factor obtained by 3D calculation can be express by the simple relation:

$$K_I = Y\sigma_{hoop}\sqrt{\pi a}$$

where

$$Y = 0.9983 - 0.1146a + 0.1475a^2 - 0,0879a^3 + 0,0334a^4 - 0.0047a^5. \quad (5)$$

Residual lifetime then can be calculated by integral equation 6 from initial defect to wall thickness. In Fig. 8 residual lifetimes for internally pressured pipes for two different hoop stress levels obtained from the 3D model are shown as a function of the crack length. The initial defect size a_o was assumed equal to 0.1 mm.

$$t = \int_{a_o}^{a_f} \frac{da}{A\left(K_I(\sigma_{hoop}, a)\right)^m} \quad (6)$$

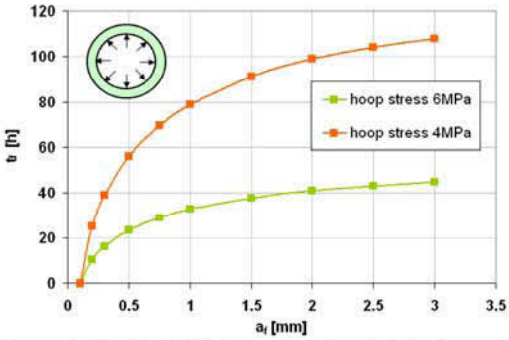

Figure 8. Residual lifetime estimation (t_f) for internally pressured pipe for two different hoop stress levels obtained from 3D model. Initial defect size (a_o) is assumed 0.1 mm.

The estimated residual lifetime considers only the contribution of creep crack growth and the time for crack initiation is not taken into account. This is one reason that numerical results do not perfectly fit the data in the diagram hoop stress versus failure time obtained from internally pressured pipe tests (see Fig.9). In spite of this it is necessary to discuss at least two additional parameters; the first one is the size of the initial defect and the second one is the effect of the threshold area (region I in creep crack growth curve).

The estimation of the defect initial size was based on experimental observations as 0.1 mm; but of course it varies a lot and can significantly influence the residual lifetime of the pipe (see Fig. 10). The decrease of the initial defect size leads to an increase of the residual lifetime of the pipe structure. Therefore, accurate estimation of the initial defect size is necessary to obtain precise time for creep crack growth in the pipe wall.

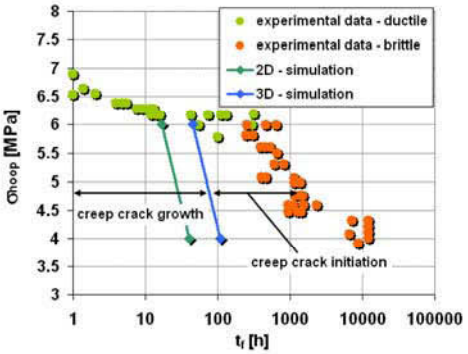

Figure 9. Comparison of the experimental results with numerical simulation of creep crack growth.

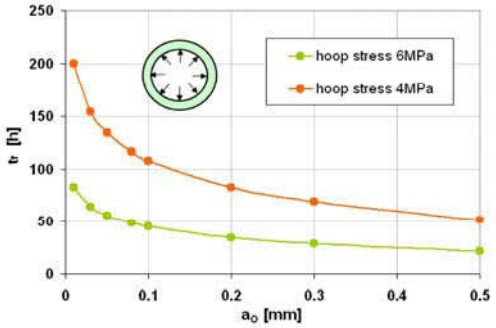

Figure 10. Residual lifetime (t_f) for internally pressured pipe estimated in dependence of initial defect size (a_o=0.01-0.5) for two different hoop stress levels.

The second important phenomena is the decrease of the creep crack grow rates close to the threshold value and the effect of the threshold itself. Unfortunately, from the experimental data of our particular material it is not possible to estimate the threshold value of the stress intensity factor. The influence of the threshold values for the creep crack growth rate can be express by a modified exponential relationship:

$$\frac{da}{dt} = A\left(K_I^{\ m} - K_{th}^{\ m}\right) \qquad (7)$$

where K_{th} is a threshold value of the stress intensity factor. Then residual lifetime of the structure can be calculated by integration of this modified relationship:

$$t = \int_{a_o}^{a_f} \frac{da}{A\left(K_I^{\ m} - K_{th}^{\ m}\right)} \qquad (8)$$

When assuming an initial defect of the size 0.1 mm the threshold of the stress intensity factor have to be smaller than the stress intensity factor computed for the same crack length in order to be sure that crack will grow from that initial defect. It means that in our case, the threshold value of the stress intensity factor is smaller than 0.07 MPa $m^{1/2}$.

The influence of the threshold region is significant and due to the strong decrease of the creep crack growth rate leads to higher residual lifetime (see Fig. 11). So in order to get a realistic estimation of pipe lifetime the experimental input parameters are of essential importance.

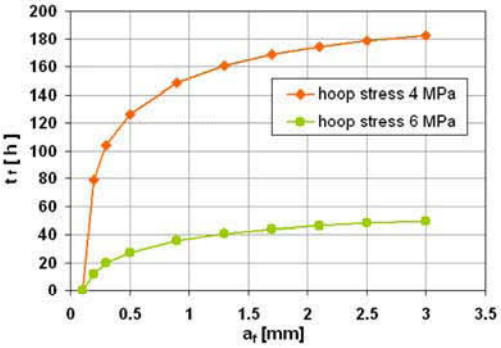

Figure 11. Residual lifetime estimation for internally pressured pipe for two different hoop stress levels obtained from 3D model. Initial defect size (a_o) is assumed 0.1 mm and threshold value of the stress intensity factor is assumed 0.07 MPa $m^{1/2}$.

Soil loads

The most relevant loading situation for real polymer pipe systems is not only internal pressure but also soil loads, bending or different kinds of point loads. The advantage of the presented numerical model is the possibility to easily add different loading conditions and estimate residual lifetime for various loading configurations.

The effect of soil embedding is possibly most important from a practical point of view. Because of that, the model presented in Fig.3, was used for estimation of the residual lifetime of the pressured pipe with additional external pressure. The effect of the soil embedding was simplified as external pressure p = 0.6 MPa according to experimental observations and literature data [6].

The value of the stress intensity factor obtained by 3D calculation with additional external pressure of 0.6 MPa is shown in Fig. 12. As in previous cases calculation of residual lifetime was done using equation 6 (see Fig. 13).

Generally, it can be concluded that soil embedding has a positive effect on the residual lifetime of the pipe systems. For hoop stress 6 MPa the increase of the residual lifetime due to the soil embedding is more than 400 %. Same effect for hoop stress 4 MPa multiply residual lifetime more than 25 times. Also important it is

to note that as a result of soil embedding the stress intensity factors for small initial defects are smaller than 0.02 MPa $m^{1/2}$, which possibly is below the threshold value K_{th} of used polymer material. In this case, soil embedding can arrested small cracks in pipe structure and final damage due to slow crack growth will not occur.

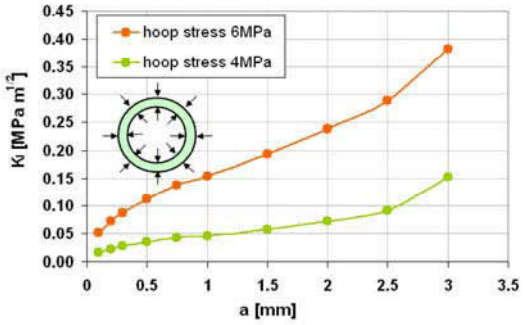

Figure 12. Stress intensity factor as a function of the crack length obtained from 3D calculation of the internally pressured pipe with additional external pressure 0.6 MPa

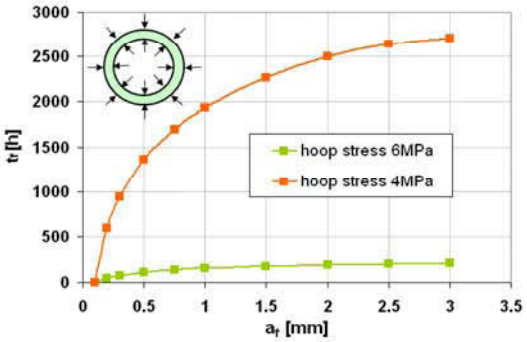

Figure 13. Residual lifetime estimation for internally and externally pressured pipe for two different hoop stress levels obtained from 3D FE model. Initial defect size (a_o) is assumed 0.1 mm

Effect of bending

The stress distribution around the crack tip can be affected by additional bending of the polymer pipe. The bending load used for following numerical simulations corresponds to a tensile strain equal to 3% in peripheral fiber of the pipe. This is an extreme value permitted by Austrian regulations for pressure pipes [7]. Final values of the stress intensity factors versus crack length are shown in Fig.14.

The stress intensity factor values are similar for internally pressured pipes and internally pressured pipes with additional bending load. Therefore, residual lifetime is also similar for the pressured pipes with and without bending load. This result can be explained by the parallel crack orientation against the maximal tensile stress induced by the bending. This tensile stress in this case has no influence on the opening stress of the crack faces, therefore the effect on the stress intensity factor in the loading mode I is negligible. The bending load is dangerous mainly for radial cracks in the pipe system.

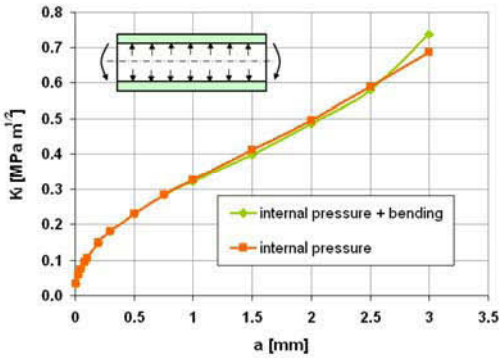

Figure 14. Stress intensity factor as a function of the crack length obtained from 3D calculation with and without additional bending loads (hoop stress 6 MPa)

Conclusions

A new approach that combines numerical simulation of lifetime of pressured pipes with additional loads with linear elastic fracture mechanics testing of the polymer materials is introduced. In a case study simulated lifetimes were compared with experimental results from internally pressured pipes. Taking into account that crack initiation times were not considered in the model, on the one hand, a good correlation could be found but also, on the other hand, essential parameters affecting the simulated lifetimes could be identified (defect size, near threshold crack growth, etc.). Moreover the implementation of additional loads (soil loads, bending) into the model and lifetime assessment was successful. In a next step in the ongoing project the effect of point loads will be studied with the established model.

Acknowledgements

The research work of this paper was performed at the Polymer Competence Center Leoben GmbH (PCCL, Austria) within the framework of the K_{plus}-program of the Austrian Ministry of Traffic, Innovation and Technology with contributions by the University of Leoben, AGRU Kunststofftechnik GmbH (Austria), Borealis Polyolefine GmbH (Austria), OMV Exploration & Production GmbH (Austria), Österreichische Vereinigung für das Gas und Wasserfach (Austria) and SABIC Europe (Netherlands).

The PCCL is funded by the Austrian Government and the State Governments of Styria and Upper Austria.

References

1 R.W. Lang, A. Stern, G. Doerner, Die Angewandte Makromolekulare Chemie, **247,** 131(1997).
2 R.W. Lang, G. Pinter, W. Balika, A Novel Qualification Concept for Lifetime and Safety Assessment of PE Pressure Pipes for Arbitrary Installation Conditions. Plastics Pipes XIII, Washington DC, USA. (2006).
3 EN ISO 9080 (2003) Plastics piping and ducting systems - Determination of the long-term hydrostatic strength of thermoplastics materials in pipe form by extrapolation.
4 T.L. Anderson, (1991) Fracture Mechanics – Fundamentals and Application, CRC Press Inc., Boca Raton, Florida, USA. (1991).
5 A. Stern, Dissertation, University of Leoben, Austria (1995).
6 G. Kiesselbach, 3R international, **36** 2/3, 136 (1997).
7 ÖVGW Richtlinie G52 (2001).

Key Words: PE pipes, lifetime assessment, linear elastic fracture mechanics, numerical modeling

I-4 Prediction of the Remaining Lifetime of Polyethylene Pipes after up to 30 Years in use

A. Frank, G. Pinter, R.W. Lang

Polymer Testing 28 (2009), 737–745.

Polymer Testing 28 (2009) 737–745

Contents lists available at ScienceDirect

Polymer Testing

journal homepage: www.elsevier.com/locate/polytest

Product Performance

Prediction of the remaining lifetime of polyethylene pipes after up to 30 years in use

A. Frank [a,*], G. Pinter [b], R.W. Lang [b]

[a] Polymer Competence Center Leoben GmbH, 8700 Leoben, Austria
[b] Institute of Materials Science and Testing of Plastics, University of Leoben, 8700 Leoben, Austria

ARTICLE INFO

Article history:
Received 30 April 2009
Accepted 18 June 2009

Keywords:
Polyethylene
Fatigue
Pipe
Slow crack growth
Lifetime prediction
Ageing

ABSTRACT

Plastics pipes made of polyethylene (PE) play an outstanding role in gas and water supply. While for modern pipe grades typical lifetimes of 50 years are taken for granted and service times of 100 years are discussed, pipes made of PE with a lower performance have been used for decades. As the repair and rehabilitation of existing pipe systems involve immense costs, the question of their qualitative condition has to be considered. In this paper, four different pipes used in the gas and water distribution in Austria with an age up to 30 years have been investigated. After a morphological and mechanical study, particular attention was paid to material stabilization, which is essential for long-term applications. Fracture mechanics tools have been used to gain information on the resistance to crack initiation and slow crack growth. Furthermore, a fracture mechanics extrapolation procedure has been applied to predict the remaining lifetime of the pipes. The results have indicated that all the pipes investigated are still in a very good condition and are likely to be sufficiently safe to remain in use.

1. Introduction

Pressurized plastics pipes have been used successfully for several decades and, especially, pipe systems made of polyethylene (PE) are widely used in fuel gas and water supply as well as in sewage systems [1–3]. In 2007, the worldwide demand for pipes made of polyethylene with high density (PE–HD) was about 3.7 million tons and a growth rate of six percent per year up to 4.9 million tons is expected in 2012 [4]. Based on results from internal pressure tests, the standard extrapolation method described in EN ISO 9080 [5] classifies these pipe grades by their minimum required strength (MRS) to ensure service times of at least 50 years. Nowadays, modern materials with the classification PE 100 (MRS = 10 MPa) and above are available. Knowledge of the long-term failure behavior is essential for the lifetime and safety assessment of these pipes, and the commonly accepted failure mechanisms thereof are characterized by crack initiation and slow crack growth (SCG) [1,6–10]. To gather information on the resistance to these failure mechanisms, modern methods of linear elastic fracture mechanics (LEFM) are used.

In long-term applications of plastics pipe systems, the ageing behavior of the material has to be considered as well. Physical or chemical ageing may change material properties by influencing the morphology (crystallinity) and molecular mass (crosslinking or degradation), both of which certainly have an effect on the mechanical properties of the pipes and on the resistance to crack initiation and SCG.

Modern PE pipe grades seem to guarantee a lifetime of 50 years and more. However, pipes made of PE grades with lower performance have been used for gas and water transportation for decades and, as the repair and rehabilitation of buried pipes is associated with high technical effort and immense costs, the reliability of these pipe systems is of substantial interest. Unfortunately, there are

* Corresponding author. Tel./fax: +43 3842 42962 26.
E-mail address: andreas.frank@pccl.at (A. Frank).

0142-9418/$ – see front matter © 2009 Elsevier Ltd. All rights reserved.
doi:10.1016/j.polymertesting.2009.06.004

only a few scientific publications which focus on the investigation of the remaining lifetime of used pipe systems [11–13]. The objective of this paper is to conduct an extensive study of four different gas and water supply pipes which have been in use for up to 30 years in Austria with an emphasis on a systematic investigation of the structure, morphology and stabilization of the pipe materials. Furthermore, fracture mechanics tests have been performed in order to evaluate the resistance to crack initiation and SCG. Based on an extrapolation procedure by means of cyclic fatigue tests, a fracture mechanics prediction of the remaining lifetime has been made.

2. Background

The failure mechanisms of internally pressurized pipes can be divided into three characteristic regions [1] depending on the load level, schematically shown in Fig. 1. Failure region A appears at a relatively high hoop stress σ_{hoop} and at relatively short times t_f, and is dominated by ductile failure along with large scale plastic deformation. Usually, plastics pipe systems are designed to operate below region A. With a decreasing σ_{hoop}, a transition knee into the quasi-brittle region B is passed and the failure is characterized by creep crack growth initiation, creep crack growth, and only small scale crack tip plasticity. It is generally accepted that this failure region determines the lifetime of long-term applications [1,6–10]. The brittle failure region C is nearly load-independent and is a result of large scale material ageing and polymer degradation [14].

Crack initiation and slow crack growth heavily depend on the molecular structure and morphology of the material such as the molecular mass, the molecular mass distribution, the positioning, the concentration and the length of short chain branches, and the crystallinity. With improvements in the polymerization process of PE and controlled variation of these material parameters, the raw material suppliers were able to achieve a significant increase in the resistance to crack initiation and slow crack growth [15,16]. During the service time of buried pipes over several decades, changes in the morphology can lead to physical ageing. However, sufficient and effective material stabilization inhibits molecular degradation and oxidation processes. The concentration and the type of the stabilizer may significantly affect the lifetime of pressurized pipes in the quasi-brittle and in the brittle failure regions. Likewise, the concept of local crack tip ageing can be used to explain crack growth mechanisms depending on different stabilizer systems [17].

To investigate the quasi-brittle failure region B in highly crack-resistant modern PE pipe grades, a number of accelerated laboratory tests using fracture mechanics considerations have been developed; among which are the Notched Pipe Test (NPT), the Pennsylvania Notch Test (PENT) and the Full Notch Creep Test (FNCT) [9,18]. Besides these test methods, fatigue tests with cyclic loads are used for accelerated characterization of the resistance to crack initiation and SCG, and a number of studies prove the correlation of fatigue and SCG in high density PE as well as in medium density PE [19–23]. Especially, fatigue tests with circumferentially cracked round bar (CRB) specimens show a high potential for quick material ranking [24,25]. By measuring the kinetics of fatigue crack growth at different loading ratios, an extrapolation to the kinetics of creep crack growth at static loading is possible [27–30].

The crack growth kinetics da/dt for static loading is usually shown in a double logarithmic diagram as a function of the stress intensity factor (SIF) K_I, and often results in a S-shaped relationship (see Fig. 2). The region of stable crack growth can be described by the equation by Paris and Erdogan Paris law, Equation (1) [31], in which A and m are parameters depending on the material, the temperature and the loading conditions.

$$\frac{da}{dt} = A \cdot K_I^m \tag{1}$$

When knowing the crack kinetics under static loading conditions (creep crack growth, CCG) and the material constants of the Paris law, a fracture mechanics lifetime prediction is possible. By integrating Equation (1), the time for the creep crack growth t_{CCG} from an initial starter defect with size a_{ini} to a final defect size a_f can be calculated (Equation (2)). The overall failure time t_f consists of the sum

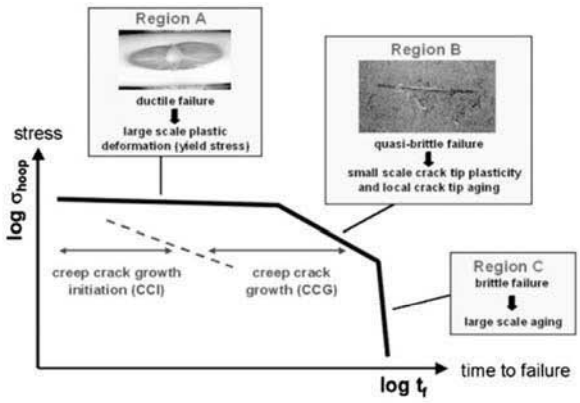

Fig. 1. Schematic illustration of the failure behavior of pressurized PE pipes [1].

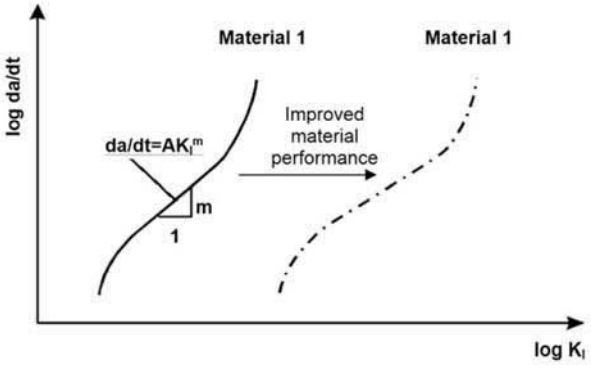

Fig. 2. Schematic illustration of the crack growth kinetics da/dt as a function of the stress intensity factor K_I [26].

of the time until the crack initiation t_{ini} and t_{CCG} (Equation (3)). The evaluation of t_{ini} was not part of this study, which means that all calculated lifetime predictions in this paper are on the conservative side as they only take an already growing crack into account.

$$t_{CCG} = \frac{1}{A} \cdot \int_{a_{ini}}^{a_f} \frac{1}{K_I^m} \cdot da \tag{2}$$

$$t_f = t_{tot} \approx t_{in} + t_{CCG} \tag{3}$$

3. Experimental

Four different pipes with unknown polyethylene pipe grades and of different ages (1976–1988) have been investigated: a black water pipe from 1988 (DN160 SDR11) and three yellow pipes transporting gas from 1987 (DN110 SDR11), 1981 (DN160 SDR11), and 1976 (DN160 SDR17). Since the origin of the materials of the old pipes was unknown, two typically available polyethylene pipe materials with hexene comonomer from the early 1990s, GM5010T2 (Hoechst AG, 1991) for a high density polyethylene (PE 80-HD) and Finathene 3802B (Atofina, 1993) for a medium density polyethylene (PE 80-MD), have been used as a reference in their virgin form. Their density was measured by means of density gradient columns (Davenport, UK) across the entire wall thickness (ISO 1183–2). The melt flow rates MFR 190/5 and MFR 190/21.6 (ISO 1133) were determined with a Zwick 4106/4103 (Zwick, GER). An elemental analysis was conducted by Wavelength Dispersive X-ray Fluorescence (WDXRF) with a Bruker S4 pioneer (Bruker AXS GmbH, GER). The molecular structure was investigated by means of gel permeation chromatography (GPC) with an Alliance GPC 2000 (Waters Corp., USA) with trichlorbenzole as a solvent. Infrared (IR) spectroscopy and Fourier transform-IR-spectroscopy (FTIR) were carried out with a Bruker Vertex 70 (Bruker AXS GmbH, GER).

For the morphological characterization, specimens were taken from inner, middle, and outer positions of the pipe wall with a microtome (Jung, GER). The temperature-dependent storage modulus and the loss factor were determined by means of dynamic mechanical analysis (DMA) with a DMA/SDTA861e (Mettler Toledo GmbH, CH) at a heating rate of 3 K/min in a displacement controlled mode. The results were compared to specimens from a modern PE 100 pipe (Hostalen CRP 100, Basell Polyolefine GmbH). The crystallinity was measured by dynamic scanning calorimetry (DSC) with a DSC822 (Mettler Toledo GmbH, CH) at a heating rate of 10 K/min. The oxidation induction time (OIT) was measured near the inner pipe wall position with a DSC of the type 2920 (TA Instruments, USA). Additives were detected by high performance liquid chromatography (HPLC) with an Agilent Technologies Series 1200 (Agilent Technologies, USA).

For the estimation of residual stresses in the circumferential direction, ring segments of 80 mm in length were prepared. In the axial direction, strips with a thickness of 5 mm and a length of 250 mm were prepared [3,32,33]. To correlate the deformation of these specimens with residual stresses, the creep modulus under bending conditions (ISO 899–2) was measured with a Zwick 010 (Zwick, GER).

The resistance to crack initiation and slow crack growth was determined by full notch creep tests (FNCT) and cyclic fatigue tests on CRB specimens. For the FNCT (ISO 16770), specimens with a cross-section of 10 × 10 mm were milled out of the pipes and an initial crack of 1.6 mm was inserted with a razor blade. The tests were performed at a temperature of 80 °C in a medium of 2% aqueous Arkopal N110. The CRB specimens of the old pipes were milled and drilled out with a diameter of 10 mm and a circumferential initial crack of 1 mm in depth was inserted with a razor blade. The cyclic fatigue tests were executed on a servo-hydraulic closed-loop testing system MTS Table Top (MTS Systems GmbH, GER) with sinusoidal loading at a frequency of 10 Hz at 23 °C. All tests were performed at an R-ratio (minimum/maximum load) of 0.1. To compare the results of the FNCT and the fatigue tests of the old pipe materials, two typical pipe grades of those times (compression-molded plates) were also tested: Finathene 3802B (Atofina, 1993) for a medium density polyethylene (PE 80-MD) and Daplen CE4664 (Borealis Polyolefine GmbH) for a high density polyethylene (PE 80).

For the prediction of the remaining lifetime, an extrapolation methodology was applied with a procedure based on material-specific and specimen-specific compliance having been used for the direct measurement of the crack kinetics [24,26–30,34]. To develop a compliance calibration curve, the material-specific compliance (ΔC) was measured with CRB specimens with different initial crack lengths a_{ini} between 0.0 and 4.0 mm. Following the determination of the ΔC calibration curve, the crack kinetics could be measured in a single CRB fatigue test. For the measurement of ΔC, a larger diameter of the CRB specimens was necessary. Only the walls of the pipes from 1981 and 1988 were thick enough to prepare CRB specimens with a diameter of 13.8 mm. The initial crack length of 1.5 mm was inserted with a razor blade. For the lifetime prediction procedure, the crack kinetics was measured at different R-ratios ($R = 0.1$, 0.3, and 0.5) and was afterwards extrapolated to $R = 1.0$, which represents static loading conditions. From this "synthetic" CCG curve, the relevant material constants A and m were obtained. To predict the remaining lifetime of the pipes, the stress intensity factor for a pressurized pipe with an initial defect on the inner pipe surface was chosen from literature [35] and the time for the creep crack growth t_{CCG} was calculated with Equation (2).

4. Results and discussion

Table 1 summarizes some basic material properties of the old pipes. Values from virgin PE–HD and PE–MD are also listed in this table as reference values. While for the yellow gas pipes the density was found below 945 kg/m^3, the black water pipe from 1988 shows the highest density with 947.5 kg/m^3. Compared to the two reference materials, the density of all the pipe materials was lower than the virgin material. The melt flow rates are in a typical range for PE–MD of this time. However, the value for the pipe from 1988 is comparable to PE–HD. The pipe from 1988 has the

Table 1
Basic properties of old pipes compared to typical pipe materials.

	1988	1976	1981	1987	GM5010T2, 1991	Finathene 3802B, 1993
Color	Black	Yellow	Yellow	Yellow	Black	Black
Pipe dimension	160SDR11	160SDR17	160SDR11	110SDR11	Pellets	pellets
Density 23 °C [kg/m^3]	947.5	944.9	940.4	942.2	954	949
MFR 190/5 [g/10 min]	0.47	1.42	1.05	0.84	0.43	0.95
MFR 190/21.6 [g/10 min]	9.21	29.37	22.3	16.9	12.7	18.2
MFRI 21.6/5	20	21	21	20	30	19
M_w [g/mol]	190000	111800	114000	185000	334000	218000
M_n [g/mol]	14051	15900	13950	10500	14000	21000
PDI	13.5	7	8.2	17.7	23.6	10.6

highest weight average molecular mass M_w. The molecular mass of the pipes from 1976 and 1981 is very similar, while the values of the pipes from 1988 and 1987 are comparable. However, for all old pipes, M_w is lower than the molecular mass of the reference materials, which could be a result of polymer degradation or crosslinking (crosslinked molecules have not been detected in GPC). The ratio of M_w and the average molecular weight M_n represent the polydispersity index (PDI) as a characteristic indicator of the broadness of the molecular mass distribution. While the pipes from 1976 and 1981 show a relatively narrow distribution, the pipes from 1988 and 1987 have a broader one.

The results of the FTIR in Table 2 show that the molecular structure of the old pipe materials did not significantly differ from the values of the reference materials. All materials could be identified as chromium-based catalyst PE with hexene for the pipe materials from 1988, 1976, and 1981 and butene for the pipe material from 1987 as comonomer. Likewise, the density of short chain branches is within a typical range.

To characterize the thermomechanical properties of the old pipes, DMA was used to investigate the temperature-dependent storage modulus E′ and the damping tanδ. With respect to the processing history, samples near the inner and outer pipe wall surface and the middle of the pipe wall were tested. Fig. 3 shows the results for the youngest pipe from 1988 and the oldest pipe from 1976. In both materials, the specimen from the outer pipe wall position shows a lower E′ across the entire temperature range than specimens from the middle and inner pipe position. This is an effect of the cooling process during the extrusion, due to which the crystallization on the outer pipe surface is retarded by a higher cooling rate. A similar behavior was found in the damping behavior, in which an increase in tanδ from the inner pipe wall position to the outer pipe wall position was noticed. Depending on the pipe wall position, the values of E′ at a temperature of 23 °C in the pipe from 1988 varied between 700 and 950 MPa. In the pipe from 1976, the storage modulus was slightly lower, between 670 and 870 MPa. These values are within a typical range for PE pipe materials and can be compared to the result of a compression-molded plate of a modern PE 80-MD (E′ = 1100 MPa at 23 °C). The results for the old pipes from 1987 and 1981 are very similar to the data discussed, yet for a better illustration their curves have not been included in Fig. 3.

The crystallinity α was investigated with DSC at three different pipe wall positions near the inner and the outer surface and at the middle of the pipe wall. The results in Fig. 4 again show the influence of the cooling of the pipe during processing. For all pipes, the lowest α was found at the outer pipe wall position. With an increasing distance from the cooled surface, the material had more time to crystallize. While for the pipe materials from 1976, 1981, and 1987 α varies between 46 and 51%, the crystallinities for the pipe from 1988 are slightly higher (52–59%). The increase of α from the outer to the inner pipe wall position is in agreement with the results from the DMA, according to which materials with a higher crystallinity result in a higher storage modulus and lower damping.

Residual stresses in plastics materials highly depend on their processing history. The faster the product (e.g. the pipe) has been cooled, the higher are the internally frozen stresses in the component. The residual stresses of the old pipes were measured in two directions, circumferentially and axially. The results summarized in Fig. 5 have been compared to previous experiments [32], in which a typical

Table 2
Molecular structure of the old pipes compared to typical pipe materials.

		1988	1976	1981	1987	GM5010T2, 1991	Finathene 3802B, 1993
CH_3	/100 C	3.8	8.5	8.1	8.6	4.3	9.1
CO	/100 C	0	0	0	0	0	0
-^-	/100 C	0.03	0.04	0.07	0.1	0.12	0.08
-=	/100 C	1.02	0.9	0.98	1.19	1.6	1.04
=<	/100 C	0.1	0.14	0.16	0.16	0.21	0.19
Comonomer		1.1% C6	3.6% C6	3.2% C6	1.4% C4	C6	C6

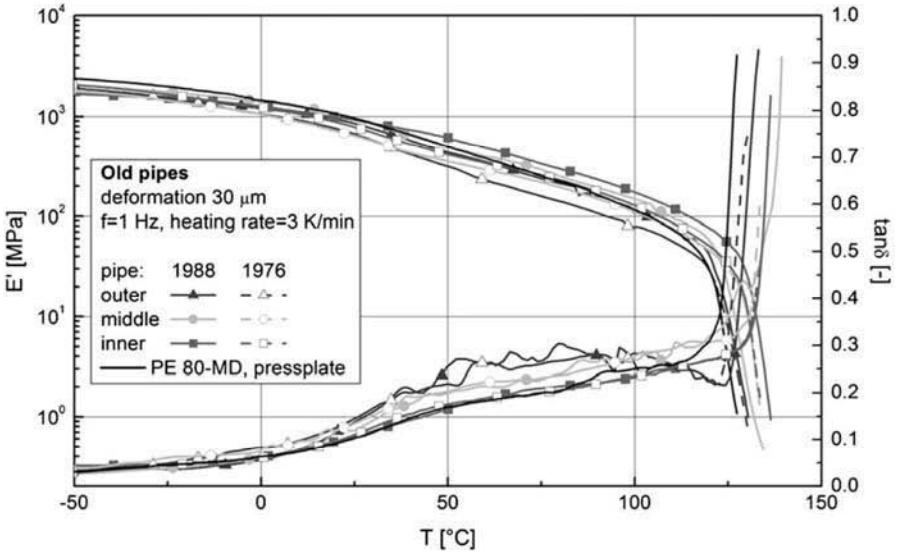

Fig. 3. Storage modulus E' and loss factor tanδ at different pipe wall positions as a function of the temperature for the pipes from 1988 and 1976 and the compression-molded plate from PE 80–MD.

range of residual stresses in the circumferential direction $\sigma_{r,c}$ was found between approx. 1.9 and 5.0 MPa and in the axial direction $\sigma_{r,a}$ between approx. 1.5 and 6.4 MPa. The amount of residual stresses for all pipes, except for the pipe from 1981, was within this typical range between 3 and 4 MPa. The lowest values with $\sigma_{r,c} = 1.9$ MPa and $\sigma_{r,a} = 1.6$ MPa were found for the pipe from 1981, which may suggest a relatively low cooling rate during the processing. Not enough material had been left from the pipe from 1988 which is why the residual stresses in the axial direction could not be measured.

To study the effectiveness of the material stabilization and the extent of material ageing, the old pipes were investigated with OIT, additive analysis and IR-spectroscopy. Apart from the general stabilizer consumption, it can be expected that stabilizers are eluted especially near the inner pipe wall under the influence of media so that samples near the inner pipe wall position were tested. The OIT's measured at 210 °C in an oxygen atmosphere (see Table 3) vary between 15 and 36 min. Although the pipes have been in use for up to 30 years, the materials measured still show a distinct resistance of more than 15 min. The findings of the additive analysis summarized in Table 3 complement the results from the OIT, as packages of classical phenolic and phosphitic antioxidants were detected in all materials, even in the oldest pipe from 1976. In the material from 1981, the antioxidants may be included in the unknown peak.

Fig. 6 shows the results of the IR-spectroscopy for samples near the inner pipe wall position of the old pipes and the PE 80-MD reference material, with the transmission T being a function of the wave number ν. As this method is also useful for material identification, typical characteristics of PE could be seen such as hydrocarbon bands at wave numbers of 2925, 2850, and 1470 cm^{-1}. Typical ageing products are carbonyl groups with bonds at wave numbers between 1700 and 1740 cm^{-1}. The measurements of the old pipes show only small peaks in the range of 1735–1740 cm^{-1}, which matches aldehyde and

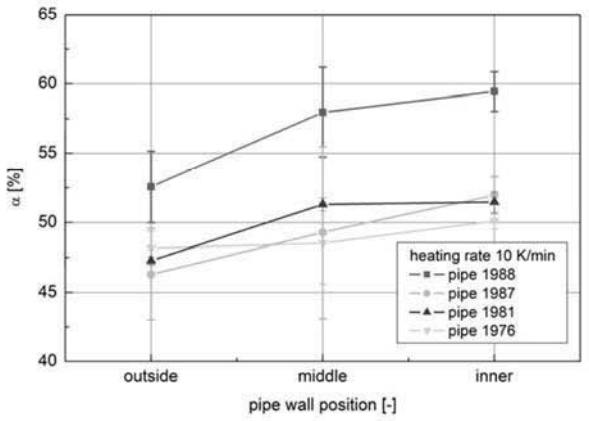

Fig. 4. Crystallinity α depending on the pipe wall position for the pipes from 1988, 1987, 1981, and 1976.

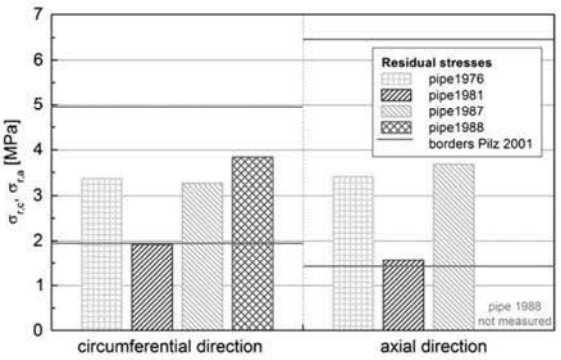

Fig. 5. Residual stresses in the circumferential and axial direction for the pipes from 1988, 1987, 1981, and 1976 compared to reference data [32].

Table 3
Oxidation–induction times and additive analysis of old pipes.

	Values in [ppm]	1988	1987	1981	1976
OIT [mm]		15	36	15	25
Phenol	IRGANOX 1010	35	730	–	–
Phenol	IRGANOX 1076	–	90	–	–
Phenol	IRGANOX 1330	350	–	–	–
Phenol	BHT	–	–	–	85
Phosphite	IRGAFOS 168	–	825	–	–
Phosphite	IRGAFOS 168OX	890	285	–	–
Phosphite	ULTRANOX 626	–	–	–	150
UV-absorber	Chimasorb 81	–	–	–	1790
	Unknown peak	–	–	1535	–
UV (HALS)	TINUVIN 770	–	–	1290	–

ester groups as products of restricted material ageing. The indications for all materials at wave numbers between 1500 and 1700 cm^{-1} and 3000 and 3500 cm^{-1} could be assigned to the stabilizer systems found in the additive analysis.

The results presented so far indicate that the old pipes are still in very good condition. Unfortunately, an exact identification of the origin PE type was not possible. The melt flow rates, the weight average molecular mass M_W, and the crystallinities indicate that the materials of the pipes from the years 1976, 1981, and 1987 are most likely to be PE–MD pipe grades, which were widely used for gas pipes at the respective times. The higher density and crystallinity of the pipe from 1988 rather matches PE–HD pipe grades, which are typically used for water pipe applications. All materials show a relatively low M_W compared to the reference materials. The DMA results show that the stiffness and damping behavior of all the old pipes is in the region of virgin polyethylene. The different crystallinities, depending on the pipe wall thickness, indicate that no post-crystallization at the outer pipe wall position has taken place and the residual stresses have obviously not been released over the years either. It can be concluded from these results that the mechanical material properties of the PE pipes have been almost unaffected. The investigation of the ageing of the old pipes shows that there is only a slight amount of carbonyl groups which indicate ageing. However, distinct OIT values and clearly detectable amounts of stabilizer systems found in the additive analysis ascertain that the pipes are sufficiently stable to stay in service, even after 30 years in use.

Fracture mechanics tests are typically used to rank pipe grades by their resistance to crack initiation and SCG. Fig. 7 shows the results of the FNCT at 80 °C in 2% Arkopal N110 for the old pipes and for a PE 80 reference material (Daplen CE4664), with the failure times t_f being plotted as a function of the stress level σ_0. The shortest failure times by far, which were lower than 10 h, were found for the oldest pipe from 1976. With decreasing pipe age, t_f also increased correspondingly. The pipes from 1987 and 1988 are nearly the same age; however, t_f for the pipe from 1987 is the highest around $\sigma_0 = 4$ MPa. The time interval between the pipe in the worst and in the best condition is about a decade. In this test, all failure times were shorter than the time of the PE 80 reference material.

A possibility to obtain an accelerated material ranking is to conduct fatigue tests with cyclic loads on CRB specimens. On the one hand, the major advantage of this method is that the tests are performed at an ambient temperature of 23 °C, which is much closer to the application temperature of real pipes than is the case with internal pressure tests, FNCT, or other fracture mechanics tests. On the other hand, fatigue tests on CRB specimens are carried out without any additional stress-cracking liquids. Fig. 8 shows the failure times t_f of the old pipes in the cyclic fatigue tests at $R = 0.1$ at a temperature of 23 °C as a function of the initial stress intensity factor difference ΔK_I and the initial maximum ligament stress $\sigma_{max,ini}$, respectively. For comparison, the PE 80 material (Daplen CE4664) was tested again as well as the PE 80-MD reference pipe grade. The shortest failure times were determined for the oldest pipe from 1976. The

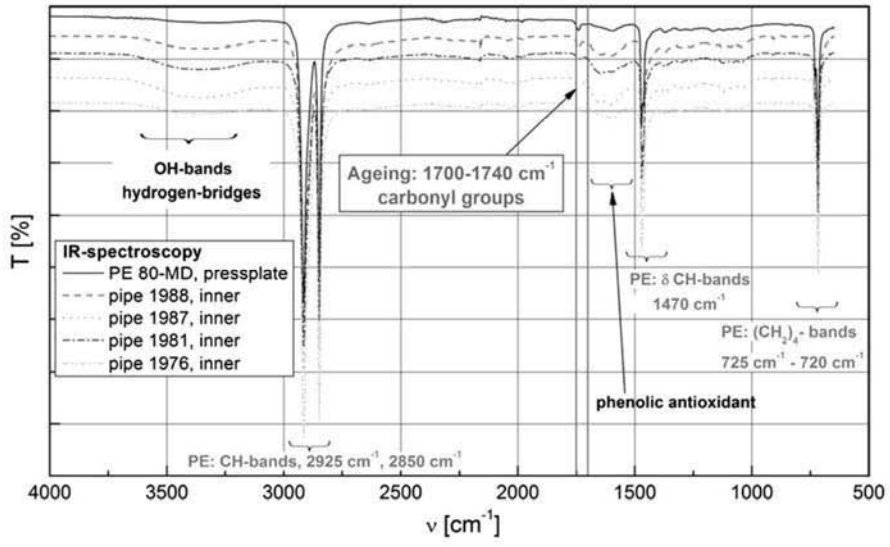

Fig. 6. Infrared spectroscopy for the pipes from 1988, 1987, 1981, 1976, and the compression-molded plate from PE 80–MD.

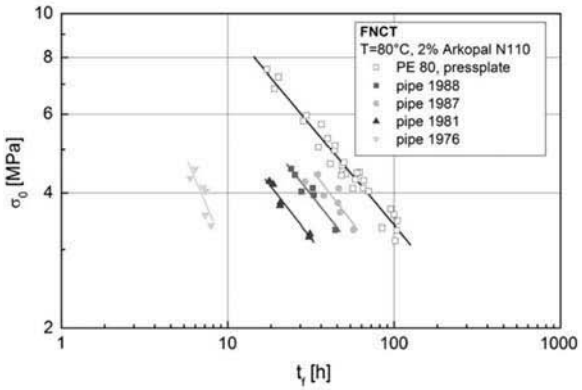

Fig. 7. Failure time t_f as a function of the stress level σ_0 in FNCT for the pipes from 1988, 1987, 1981, and 1976 and the compression-molded plate from PE 80.

failure time t_f increased with decreasing pipe age and at stress levels of $\sigma_{max,ini} = 8$ MPa the youngest pipe from 1988 showed the best performance, what is in contrast to the FNCT results at 4 MPa. In previous studies, fatigue tests on CRB specimens proved to differ from one PE type to another and even within the same pipe grade [24,25]. The results in Fig. 8 show that the best PE–MD pipe from 1987 quite well matches the virgin PE 80-MD reference material. The pipe from 1988, identified as a PE–HD type, even had slightly longer failure times than the PE 80 reference material, which could be attributed to different processing histories. In the GPC measurements, the pipes from 1976 and 1981 were identified as the materials with the lowest molar mass, which is of course the main reason for their reduced crack growth resistance. However, it could also be noticed that the PE–MD materials have a lower gradient than the PE 80 pipe from 1988 and the PE 80 reference material, which implies a crossover of the failure times with decreasing loads, which is an indication of a higher crack growth resistance of PE–MD at low stress levels.

Compared to the FNCT with failure times up to 60 h, the testing times of the cyclic CRB tests between a few hours up to a day emphasize the potential of this approach as a quick ranking method [24,25]. Although the rankings of both methods are comparable, the FNCT is performed at elevated temperatures far beyond the applied service temperatures and the specimens are embedded in an aggressive stress-cracking liquid. Regarding the different rankings of the pipe from 1987 and the pipe from 1988, the question has to be raised as to whether the same micro-mechanics effects are responsible for crack initiation and SCG in the FNCT as in the fatigue tests at 23 °C.

A vital advantage of cyclic CRB tests is the possibility to gather deeper information on crack initiation and crack kinetics. Based on a fracture mechanics extrapolation procedure [27,30,34], a prediction of the creep crack growth (CCG) is possible with cyclic tests at different R-ratios. If the crack kinetics under static loading conditions is known, a fracture mechanics lifetime prediction of components is possible. Fig. 9 shows the compliance calibration curve for the materials of the pipes from 1981 and 1988, with the difference of the compliance ΔC being a function of the crack length a_c. For the pipe from 1988, the calibration curve is clearly lower than for the pipe from 1981, which indirectly reflects the higher stiffness of the PE–HD material in the pipe from 1988. For the mathematical fitting of the data, a second order polynomial function was used and then transformed to express the crack length a_c of a single CRB test as a function of ΔC, which enables the determination of the crack kinetics da/dt.

In Fig. 10, the crack kinetics da/dt as a function of the maximum stress intensity factor $K_{I,max}$ for the two pipe materials is shown for R-ratios of 0.1, 0.3, and 0.5. With an increasing R-ratio, the kinetic lines are shifted to the right side to higher stress intensity factors. The kinetics of the pipe from 1981 has a steeper slope than the one of the pipe from 1988. Although the kinetics for the pipe from 1981 is slightly faster than the kinetics of the pipe from 1988, at lower stress intensity factors the lines seem to cross one another, which proves the failure times in Fig. 8, in which the crack resistance of PE–MD is higher at lower loads. While the slope of the material from 1981 is nearly constant at all R-ratios, it gets slightly steeper for the pipe material from 1988. The "synthetic" CCG curve at $R = 1.0$ was developed with an exponential extrapolation and the material constants were $A = 6.41 \times 10^{-8}$ and $m = 5.02$ for the pipe material from 1981 and $A = 4.49 \times 10^{-8}$ and $m = 4.68$ for the pipe from 1988.

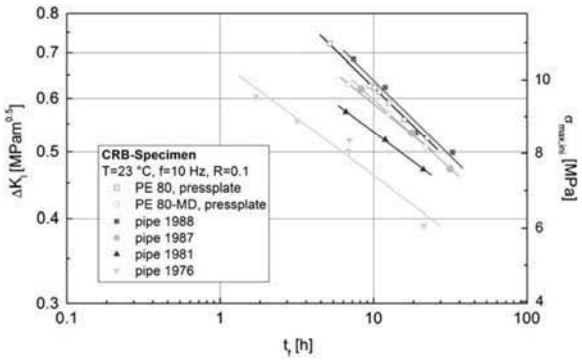

Fig. 8. Failure time t_f as a function of the stress intensity factor ΔK_I of cyclic fatigue tests on CRB specimens at $R = 0.1$ for the pipes from 1988, 1987, 1981, and 1976 and the compression-molded plates from PE 80 and PE 80–MD.

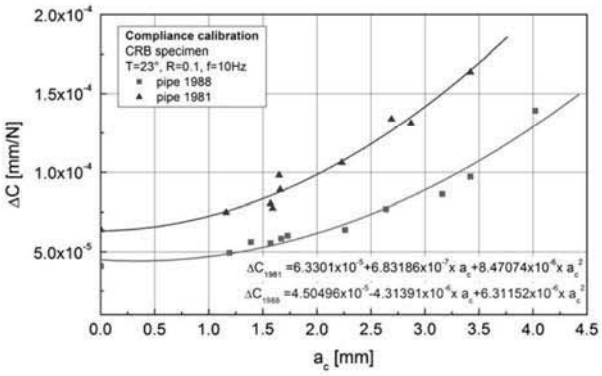

Fig. 9. Compliance calibration curves ΔC as a function of the crack length a_c for the pipes from 1981 and 1988.

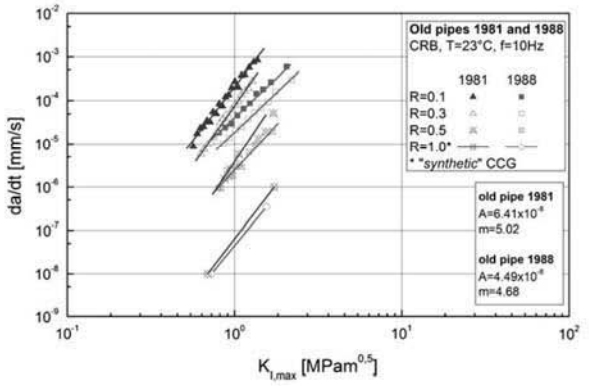

Fig. 10. Crack kinetics of the materials of the pipes from 1981 and 1988 at $T = 23$°C at $R = 0.1$, 0.3, and 0.5 and extrapolated "synthetic" creep crack growth (CCG) curves ($R = 1.0$) to obtain the material constants A and m.

The remaining lifetime to achieve an overall service time of 50 years for the pipe from 1981 is 23 years, and 30 years for the pipe from 1988. For calculating the stress intensity factor in an internally pressurized pipe with defects on the inner pipe surface, different solutions are available [34,36]. For this study, the stress intensity factor by Murakami [35] was used. Fig. 11 shows the predicted remaining lifetimes of the pipes from 1981 and 1988, calculated with Equation (2) and the material constants A and m from the "synthetic" CCG curves. The results show a very high dependency on the size of the initial defect. A typical defect size a_{ini} for the initiation of quasi-brittle cracks was found to be between 100 and 400 μm [1,37,38]. Using a hoop stress level of $\sigma_v = 8$ MPa (MRS in a PE 80 pipe grade) as a reference, both pipes seem to remain intact for the required service time of 50 years and even longer. Considering that the crack initiation time is neglected in this calculation, these pipes can be expected to remain in good order should they stay in use.

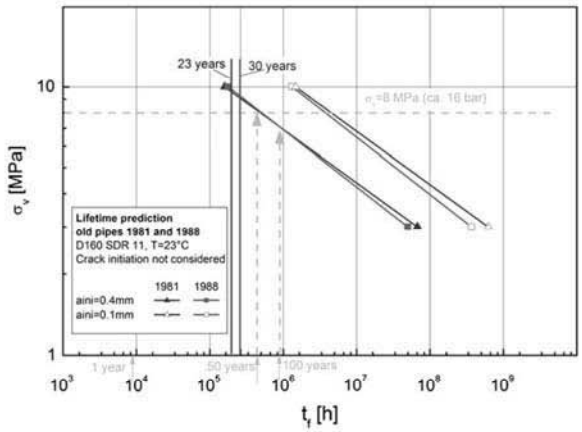

Fig. 11. Predicted remaining lifetime of the pipes from 1981 and 1988 at $T = 23$ °C for estimated initial defect sizes a_{ini} between 0.1 and 0.4 mm. Failure times t_f as a function of the hoop stress σ_v only include crack propagation time; crack initiation time has not been considered.

5. Conclusions

Four different used polyethylene pipes for gas and water supply with an age of up to more than 30 years have been investigated with respect to molecular and morphological changes. Furthermore, special focus has been put on the characterization of the remaining resistance to slow crack growth. It was not possible to identify the original materials by means of extensive molecular, morphological and fracture mechanics characterization, yet it could be found that the materials were still in a very good condition. The molecular analysis did not show any significant polymer degradation as an indication of ageing of the materials. Moreover, the thermomechanical behavior delivered comparable values to the reference materials. The absence of post-crystallization on the outer pipe wall and a still existing typical amount of residual stresses showed that the mechanical material properties have been almost unaffected. Distinct OIT values and clearly detectable amounts of stabilizers in the pipes ensure a sufficient stability for a continuation of the service. However, the fracture mechanics investigations indicated a decrease in failure times along with an increase in the age of the pipes. Using an extrapolation concept to predict the creep crack growth by means of fatigue tests, a prediction of the remaining lifetime was made for two pipes. Although the time for the crack initiation had not been considered, both pipes showed sufficient stability to prevent a quasi-brittle failure to remain in good order for 50 years.

Acknowledgments

The research work of this paper was performed at the Polymer Competence Center Leoben GmbH (PCCL, Austria) within the framework of the K_{plus}-program of the Austrian Ministry of Traffic, Innovation and Technology with contributions by the University of Leoben (Austria), AGRU Kunststofftechnik GmbH (Austria), Borealis Polyolefine GmbH (Austria), OMV Exploration & Production GmbH (Austria), Österreichische Vereinigung für das Gas und Wasserfach (Austria) and SABIC Europe (Netherlands). The PCCL is funded by the Austrian Government and the State Governments of Styria and Upper Austria.

References

[1] R.W. Lang, A. Stern, G. Doerner, Die Angewandte Makromolekulare Chemie 247 (1997) 131–137.
[2] H. Brömstrup, PE 100 Pipe Systems, Vulkan Verlag, Essen, Germany, 2004.
[3] L.E. Janson, Plastics Pipes for Water Supply and Sewage Disposal, Borealis, Sven Axelsson AB/Fäldts Grafiska AB, Stockholm, Sweden, 1999.
[4] G. Brescia, Proceedings of Plastics Pipes XIV, Budapest, Hungary (2008).
[5] DIN EN ISO 9080, Plastics piping and ducting systems - Determination of the long-term hydrostatic strength of thermoplastics materials in pipe form by extrapolation, 2003.
[6] E. Gaube, H. Gebler, W. Müller, C. Gondro, Zeitstandfestigkeit und Alterung von Rohren aus HDPE, Kunststoffe 75 (7) (1985) 412–415.
[7] M. Ifwarson, Gebrauchsdauer von Polyethylenrohren unter Temperatur und Druckbelastung, Kunststoffe 79 (6) (1989) 525–529.
[8] M.B. Barker, J.A. Bowman, M. Bevis, The performance and cause of failure of polyethylene pipes subjected to constant and fluctuating internal pressure loadings, Journal of Materials Science 18 (1983) 1095–1118.

[9] N. Brown, X. Lu, Proceedings of the 12th Plastic Fuel Gas Pipe Symposium, Boston, Massachusetts, USA (1991).
[10] N. Brown, X. Lu, Proceedings of the 13th Plastic Fuel Gas Pipe Symposium, San Antonio, Texas, USA (1993).
[11] U. Schulte, J. Hessel, Remaining service life of plastic pipes after 41 years in service, 3R International 45 (9) (2006) 482–485.
[12] J. Hessel, 100-years service-live for polyethylene pipes. Review and prospects, 3R International 46 (4) (2007) 242–246.
[13] S. Chung, T. Kosari, T. Li, K. Oliphant, P. Vibien, J. Zhang, Proceedings of ANTEC 2007, Cincinnati, Ohio, USA (2007).
[14] B.-H. Choi, A. Chudnovsky, R. Paradkar, W. Michie, Z. Zhou, P.-M. Cham, Polymer Degradation and Stability 94 (5) (2009) 859–867 May 2009.
[15] N. Brown, X. Lu, Y. Huang, I.P. Harrison, N. Ishikawa, The fundamental material parameters that govern slow crack growth in linear polyethylens, Plastics, Rubber and Composites Processing and Applications 17 (4) (1992) 255–258.
[16] G. Pinter, R.W. Lang, Creep crack growth in high density polyethylene, in: D.R. Moore (Ed.), The Application of Fracture Mechanics to Polymers, Adhesives and Composites, Elsevier Science Ltd., ESIS, New York, 2004, pp. 47–54.
[17] G. Pinter, R.W. Lang, Effect of stabilization on creep crack growth in high density polyethylene, Journal of Applied Polymer Science 90 (2003) 3191–3207.
[18] M. Haager. Fracture mechanics methods for the accelerated characterization of the slow crack growth behavior of polyethylene pipe materials, Doctoral Dissertation, Institute of Materials Science and Testing of Plastics, University of Leoben, Austria (2006).
[19] A. Shah, E.V. Stepanov, G. Capaccio, A. Hiltner, E. Baer, Correlation of fatigue crack propagation in polyethylene pipe specimens of different geometries, International Journal of Fracture 84 (1997) 159–173.
[20] A. Shah, E.V. Stepanov, M. Klein, A. Hiltner, E. Baer, Study of polyethylene pipe resins by a fatigue test that simulates crack propagation in real pipe, Journal of Materials Science 33 (1998) 3313–3319.
[21] A. Shah, E.V. Stepanov, G. Capaccio, A. Hiltner, E. Baer, Stepwise fatigue crack propagation in polyethylene resins of different molecular structure, Journal of Polymer Science Part B: Polymer Physics 36 (1998) 2355–2369.
[22] M. Parsons, E.V. Stepanov, A. Hiltner, E. Baer, Correlation of stepwise fatigue and creep slow crack growth in high density polyethylene, Journal of Materials Science 34 (1999) 3315–3326.
[23] M. Parsons, E.V. Stepanov, A. Hiltner, E. Baer, Correlation of fatigue and creep slow crack growth in a medium density polyethylene pipe material, Journal of Materials Science 35 (2000) 2659–2674.
[24] M. Haager, G. Pinter, R.W. Lang, Proceedings of ANTEC 2006, Charlotte, North Carolina, USA (2006).
[25] G. Pinter, M. Haager, W. Balika, R.W. Lang, Cyclic crack growth tests with CRB specimens for the evaluation of the long-term performance of PE pipe grades, Polymer Testing 26 (2) (2007) 180–188.
[26] A. Saxena, S.J. Hudak, Review and extension of compliance information for common crack growth specimens, International Journal of Fracture 14 (5) (1978) 453–468.
[27] R.W. Lang, G. Pinter, W. Balika, Qualification concept for lifetime and safety assessment of PE pressure pipes for arbitrary installation conditions, 3R International 44 (1-2) (2005) 33–41.
[28] Frank, W. Freimann, G. Pinter, R.W. Lang. A fracture mechanics concept for the accelerated characterization of creep crack growth in PEHD pipe grades. Engineering Fracture Mechanics, Under Review (2009).
[29] G. Pinter, R.W. Lang, M. Haager, A test concept for lifetime prediction of polyethylene pressure pipes, Chemical Monthly 138 (2007) 347–355.
[30] A. Frank, G. Pinter, R.W. Lang, Proceedings of ANTEC 2008, USA (2008).
[31] P.C. Paris, F. Erdogan, A critical analysis of crack propagation laws, Journal of Basic Engineering 85 (1963) 528–534.
[32] G. Pilz. Viscoelastic Properties of Polymeric Materials for Pipe Applications, Doctoral Dissertation, Institute of Materials Science and Testing of Plastics, University of Leoben, Austria (2001).
[33] A. Frank, G. Mannsberger, G. Pinter, R.W. Lang, Proceedings of ANTEC 2008, Milwaukee, Wisconsin, USA (2008).
[34] A. Frank, G. Pinter, R.W. Lang, Proceedings of Plastics Pipes XIV, Budapest, Hungary (2008).
[35] Y. Murakami, Stress Intensity Factors Handbook, Pergamon Press, Oxford, Great Britain, 1990.
[36] S.I. Krishnamachari, Applied Stress Analysis of Plastics: an Engineering Approach, Van Nostrand Reinhold, New York, USA, 1993.
[37] A. Gray, J.N. Mallinson, J.B. Price, Fracture behaviour of polyethylene pipes, Plastics and Rubber Processing and Applications 1 (1981) 51.
[38] G. Pinter. Rißwachstumsverhalten von PE-HD unter statischer Belastung, Doctoral Dissertation, Institute of Materials Science and Testing of Plastics, University of Leoben, Austria (1999).

I-5 Lifetime Prediction of Polyethylene Pipes Based on an Accelerated Extrapolation Concept for Creep Crack Growth with Fatigue Tests on Cracked Round Bar Specimens

A. Frank, G. Pinter, R.W. Lang
in proceedings: ANTEC 2009, Chicago, Illinois, USA 2009), 2169-2174.

LIFETIME PREDICTION OF POLYETHYLENE PIPES BASED ON AN ACCELERATED EXTRAPOLATION CONCEPT FOR CREEP CRACK GROWTH WITH FATIGUE TESTS ON CRACKED ROUND BAR SPECIMENS

Andreas Frank, Polymer Competence Center Leoben, Austria (frank@pccl.at)
Gerald Pinter, University of Leoben, Austria
Reinhold W. Lang, University of Leoben and Polymer Competence Center Leoben, Austria

Abstract

Fracture mechanics lifetime and safety assessment of pressurized polyethylene (PE) pipes is based on the knowledge of material specific creep crack growth (CCG). However, with common test methods the investigation of this failure mechanism is not possible in modern PE-pipe materials in a feasible time. For an accelerated generation of CCG an extrapolation concept based on fatigue tests with cracked round bar (CRB) specimens was developed. In the present work this concept was applied to a common PE-pipe material to generate the material specific CCG-data within a few weeks. To evaluate these data a fracture mechanics lifetime prediction of the CRB test was compared to results from static tests. With the integration of the data into a lifetime prediction model for pressurized pipes a simulation of a real pipe was possible.

Introduction

For lifetime prediction of long term applications like pressurized pipes made of polyethylene (PE) it is generally accepted, that crack initiation and slow crack growth (SCG) are the critical failure mechanisms. Hence, the knowledge of material specific crack kinetics is of essential interests for a reliable safety assessment [1-7]. The standard approach for the determination of the long term behavior and lifetime estimation of pressurized pipes is based on internal pressure test [8] and EN ISO 9080 [9] describes an extrapolation method to ensure operating times of at least 50 years.

However, this time consuming procedure is expansive and no longer useful to obtain information about SCG of modern PE pipe grades even at elevated temperatures. Essentially improvements in the raw material, particularly the bimodal molecular mass distribution and the controlled implementation of short chain branches, have lead to materials with increased resistance against crack initiation and SCG. Today materials with minimum required strengths (MRS) of 10 MPa and above, that are classified in PE 100 grades [10, 11], are available and the increased resistance against crack initiation and SCG create needs for new accelerated characterization methods.

To fulfill this new requirements a number of test methods using fracture mechanics considerations were developed for an accelerated characterization of the resistance against SCG, like the Notche Pipe Test (NPT), the Pennsylvenia Notch Test (PENT) or the Full Notch Creep Test (FNCT) [7, 13]. These methods are widely used for material ranking, however, they are not satisfactory concerning short testing times and information about material specific crack kinetics.

One possibility to reduce testing times is the use of fatigue tests under cyclic loads and the implementation of fracture mechanics concepts for data evaluation [4, 12]. Moreover, the choice of suitable specimen geometries influences the testing time and especially cracked round bar (CRB) specimens show very promising results, even at service near temperatures and without any stress cracking liquids [13-15].

An extrapolation concept for the transformation of cyclic fatigue tests with CRB specimens into the case of static loading conditions and a procedure to describe SCG has already been proposed [16-20]. One essential step in this procedure is the determination of the crack kinetics at several R-ratios (ratio of minimum to maximum loading) and the extrapolation of this fatigue kinetics to static loading conditions. The present work demonstrates the application of this procedure to a commercially available PE 80 pipe grade. After the determination of the material specific crack kinetics at static loadings the lifetime for CRB specimens was predicted and correlated to results of static tests to evaluate the results of the extrapolation concept. Finally the lifetime of a pressurized pipe was predicted and correlated to data form internal pressure tests.

Background

The failure behavior of pressurized pipes is well investigated and is divided into characteristic regions depending on the stress level (Figure 1, right) displayed in a double logarithmic diagram [1]. At relatively high stress levels the failure is dominated by ductile deformation with large plastic zones. At lower loadings the failure mechanism passes a transfer knee and change to quasi-

brittle failure. In this region the failure time consists of the fractions of crack initiation and slow crack growth (SCG) and can be described with concepts of the linear elastic fracture mechanics (LEFM). It is very well accepted, that for long term applications this region characterizes the critical failure mechanisms. After very long times a nearly load independent third region is reached that is caused by ageing processes and polymer degradation.

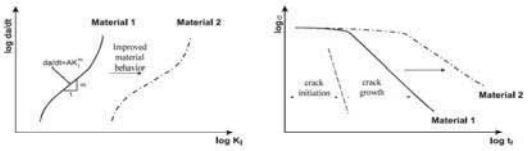

Figure 1: Relationship between creep crack growth behavior and failure behavior of internally pressurized pipes [17].

Basic requirements for the applicability of the LEFM are that global loadings are in the range of linear viscoelasticity and the formation of plastic zones at the crack tip is only small. In general the stress distribution in the vicinity of the crack tip is described by the stress intensity factor (SIF) K_I [21-23] that is a function of the global loading σ, the crack length a and a geometric factor Y that is known for several specimens or can be derived by simulation programs (Equation 1).

$$K_I = \sigma \cdot \sqrt{a} \cdot Y \tag{1}$$

The crack growth kinetics da/dt for static loading and da/dN for cyclic loading, respectively, usually is shown in a double logarithmic diagram as a function of the SIF K_I and the difference of the maximum and minimum SIF $\Delta K_I = K_{I,max} - K_{I,min}$ respectively, and often gives an S-shaped relationship (Figure 1, left). The region of stable crack growth rate under static and cyclic loads can be described by the equation of Paris and Erdogan (Equation 2 and 3) [24] where the constants A and m are material constants depending on the temperature and loading parameters like the R-ratio (ratio of minimum to maximum loading).

$$\frac{da}{dt} = A \cdot K_I^{\,m} \tag{2}$$

$$\frac{da}{dN} = A' \cdot \Delta K_I^{\,m'} \tag{3}$$

Figure 1 also illustrates the potential for material ranking. A higher crack growth resistance results in a shift of the crack kinetics to higher SIF and accordingly the failure of the specimen or component occur after longer times.

To extrapolate fatigue crack growth (FCG) from cyclic tests to the case of static loading an already proposed procedure is used [16-20] (Figure 2). Therefore the crack kinetics of cyclic tests with CRB specimens at different R-ratios are cut at constant crack growth rates da/dt. After transforming the points of intersection into a diagram where the SIF is a function of the R-ratio, the constant crack growth rates are extrapolated to R=1 what represents static loading. Finally the SIF's at R=1 are transformed back into the kinetics diagram to generate a "synthetic" creep crack growth (CCG) curve and the material and temperature dependent material constants A and m can be obtained.

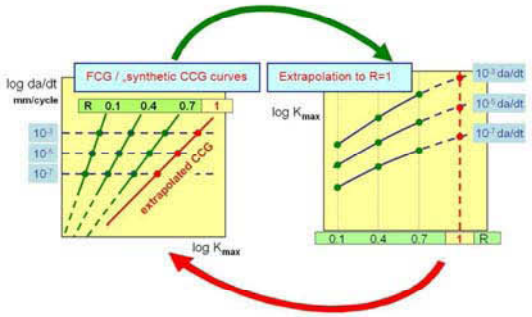

Figure 2: Methodology to generate "synthetic" creep crack growth curves for static loading (R=1.0) based on cyclic experiments with CRB specimens [16-20]

A fracture mechanics lifetime prediction is possible by the knowledge of the crack kinetics, that delivers the material parameters A and m, and the function of the SIF. By solving the equation of Paris and Erdogan to Equation 4 the time for creep crack growth t_{CCG} from an initial start defect with the size a_{ini} to a final defect size a_f can be calculated. The overall failure time t_f consists of the sum of time until crack initiation t_{ini} and t_{CCG} (Equation 5). The evaluation of t_{ini} is not part of this work so that all calculated lifetime predictions in this paper are on the conservative side as they only take into account an already growing crack.

$$t_{CCG} = \frac{1}{A} \cdot \int_{a_{ini}}^{a_f} \frac{1}{K_I^{\,m}} \cdot da \tag{4}$$

$$t_f = t_{tot} \approx t_{in} + t_{CCG} \tag{5}$$

Experimental

The CRB specimens were manufactured from compression moulded plates made of a commercially available PE 80 pipe grade with a diameter of 13.8 mm

and a length of 100 mm. The circumferential initial crack a_{ini}=1.5 mm was inserted with a razor blade. All fatigue tests were executed on a servo-hydraulic closed-loop testing system MTS Table Top (MTS Systems GmbH, GER) with a sinusoidal loading at temperatures of 23 °C and a frequency of 10 Hz. Static tests on CRB specimens with an initial crack length of a_{ini}=1.5 mm were performed on a static test device at temperatures of 23°C.

Due to the specimen geometry and the tendency of eccentric crack growth a reliable direct measurement of the crack kinetics da/dN on a CRB specimen is difficult [13, 18]. Nevertheless a determination of the crack kinetics is possible by using the specimen compliance C that is defined as the ratio of the crack opening displacement COD and the applied load F [25]. As displayed in Figure 3 the specimen compliance also depends on the crack length a, which means, that with increasing crack length C increases respectively.

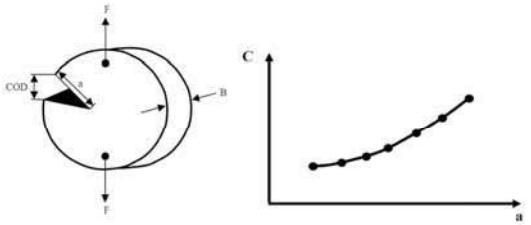

Figure 3: Left: Schematic illustration of crack opening displacement COD. Right: Dependence of compliance C from crack length [19].

For the indirect determination of the crack kinetics a crack length depending compliance calibration curve was developed. Therefore the COD of CRB specimens with different initial crack lengths from 1.0 to 3.0 mm was measured with three extensometers (Type 632.13-20, MTS Systems GmbH, GER) that were equally distributed around the crack. It was important to guarantee that during these tests no crack initiation took place and the loads were chosen in the linear viscoelastic range. Because the loads in fatigue tests change between a minimum and a maximum value the crack opening displacement was measured as the difference ΔCOD of minimum and maximum COD. Analog the specimen compliance was calculated to ΔC. The compliance calibration curve could then be used to calculate crack lengths in a single cyclic CRB tests and to generate the R-specific crack kinetic curve.

Several studies prove that a ranking based on results of fatigue tests are in good accordance to internal pressure tests [4, 12, 14, 15]. Provided that the failure mechanisms in the cyclic tests are the same as in the static test the data can be correlated by Equation 6 [26, 27].

$$\frac{da}{dt} = f \cdot \frac{da}{dN} \tag{6}$$

For the determination of the SIF in CRB specimens several equations are available. Analytic calculations from literature [28-30] are compared to values from simulation with ABAQUS (Version 6.8.0.2, Simulia, Providence, USA). The SIF of a pressurized pipe with a crack at the inner surface was calculated with SIF from literature [29].

Results and discussion

The compliance calibration curve for CRB specimens of the PE 80 pipe grade at a temperature of 23 °C is shown in Figure 4 where the compliance ΔC is a function of the crack length a_c. The calibration curve was determined at R=0.1 at test relevant loads and ΔC was recorded after a few thousand cycles, so that starting effects are eliminated, and before crack initiation (Figure 5). The clear correlation between ΔC and a_c. can be fitted by a polynomial function. For constant temperature ΔC is only dependent on the material and the specimen geometry what is proven by the fatigue tests at R=0.1, 0.3 and 0.5 where the overlap of the compliance is indicating load independency.

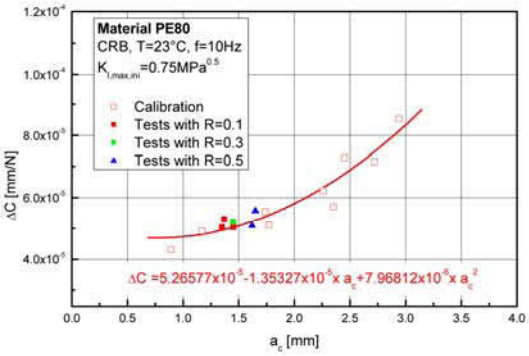

Figure 4: Compliance calibration curve ΔC at 23 °C as a function of the crack length a_c for CRB specimens of PE 80.

Figure 5 shows the typical signals of the three equally distributed extensometers, where ΔCOD and the associated ΔC values of a single fatigue test are displayed as a function of cycle numbers N. After starting effects at very low N the values of ΔCOD and ΔC are constant. The crack growth starts at the first step in these signals where crack initiation is detected. By continuing the test an increase of ΔCOD and ΔC indicates crack growth and the very typical stepwise characteristic of quasi-brittle crack growth in PE can be noticed. To the end of the test the fast

rise of ΔCOD and ΔC reflects instable crack growth and ductile failure of the specimen.

One additional benefit of using three equally distributed extensometers is a very sensitive detection of the crack initiation. For all executed cyclic tests it was found, that the fraction of crack initiation is about 30 to 40 % of the total failure time [19, 20].

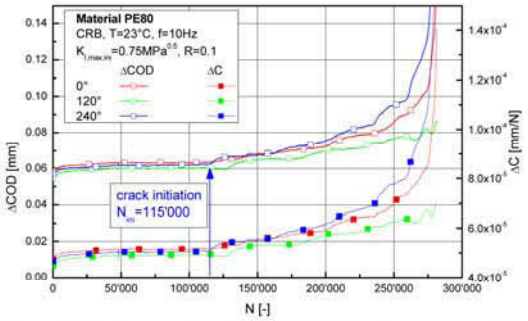

Figure 5: Extensometer signals ΔCOD and corresponding specimen compliance ΔC as a function of cycles N. The first step in the curves indicates crack initiation.

With the help of the polynomial fitting function of the compliance calibration it was possible to generate the crack kinetics from a single CRB test. Figure 6 shows the crack kinetics da/dt at 23 °C determined at R=0.1, 0.3 and 0.5 as a function of the maximum SIF $K_{I,max}$. With increased R-ratio the kinetic lines are shifted to higher SIF what denotes a decrease in the crack growth rate. Each kinetic line includes R-specific values for the material parameters A and m. Based on the described extrapolation procedure [16-20] the "synthetic" CCG curve at R=1 (representing static loading) was calculated and included in this diagram. The material and temperature specific material constants for R=1 were obtained as $A=1.404 \times 10^{-6}$ and m=6.33.

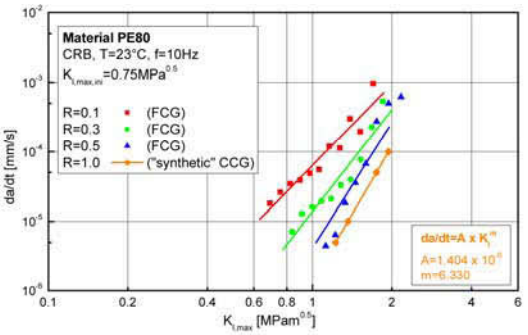

Figure 6: Crack kinetics da/dt of PE 80 at R=0.1, 0.3 and 0.5 and extrapolated "synthetic" CCG curve (R=1).

For the calculation of SIF's in CRB specimens different mathematics solutions are available. Figure 7 shows the calculations of the SIF K_I by Benthem and Koiter [28], G.E. Dieter [30] and an ABAQUS simulation as a function of the normalized crack length a/R, where R is the radius of the CRB specimen. At short crack lengths a very good correlation of the three functions exists. While the SIF by G.E. Dieter shows the lowest values at higher crack lengths above a/R=0.7 the SIF of the ABAQUS simulation shows clearly the steepest gradient above a/R=0.5. The relevant crack length in a CRB test is in the range of 0.22<a/R<0.58. The quick increase of the SIF with growing crack length is one of the typical characteristics that make the CRB specimen useful for accelerated fatigue tests.

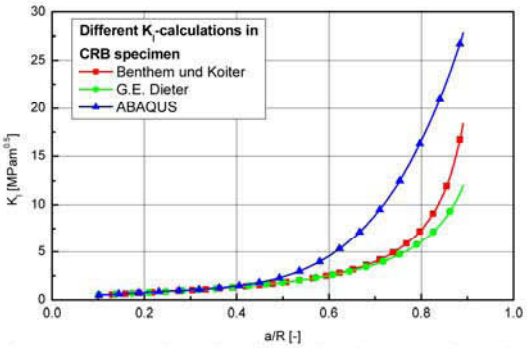

Figure 7: Stress intensity factor in CRB specimen by Benthem and Koiter [28], G.E. Dieter [30] and ABAQUS simulation as a function of the normalized crack length a/R.

In Figure 8 cycle numbers for slow crack growth N_{SCG} until failure of the CRB test at R=0.1, 0.3 and 0.5 are displayed as a function of the maximum SIF $K_{I,max}$. N_{SCG} was calculated by subtracting the cycle numbers until crack initiation (detected by the three extensometers) from the total cycle number until failure. Furthermore, test results from static tests (R=1) on CRB specimens are included in this diagram. The correlation of these static tests to cyclic tests was done by Equation 6. The total failure cycle number N_{tot} was reduced by an estimated fraction for crack initiation of 40 %.

To evaluate the generated material constants A and m from the extrapolation procedure a lifetime prediction of the CRB test was done by using Equation 4 and applying the SIF by Benthem and Koiter as well as the SIF of the ABAQUS simulation. Like in a real CRB test the initial crack length a_{ini} was chosen with 1.5 mm (a/R=0.22), slow crack growth was supposed until a_f=4.0 mm (a/R=0.58). Using the R-specific values for the material constants A and m the simulated failure cycle numbers for slow crack growth N_{SCG} fit quite well to the real test data. Due to the

higher gradient in the SIF the ABAQUS simulation results in a little lower cycle numbers than the calculation with the SIF by Benthem and Koiter. At R=0.1 and 0.3 testing data are closer to the simulated values of ABAQUS, whereas at R=0.5 both simulations are applicable. However, the cycle numbers N_{SCG} for the test results at R=1.0 are slightly higher than simulation. This might be a hint, that the estimated fraction of crack initiation at static loading is higher than 40 %. Nevertheless, the simulation of slow crack growth at static loading with material constants A and m generated by the extrapolation procedure of fatigue tests results in a reasonable matching.

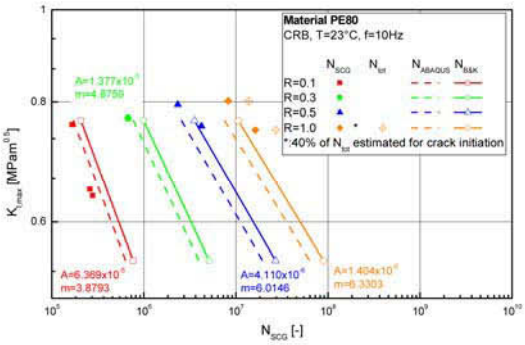

Figure 8: Number of cycles for slow crack growth N_{SCG} until failure compared to simulated lifetimes (creep crack growth) by Benthem and Koiter [28] $N_{B\&K}$ and ABAQUS simulation N_{ABAQUS}.

As the parameters A and m in the fracture mechanics calculation of the crack kinetics are material specific constants, it is possible to calculate lifetimes for any structure just by adjusting the SIF K_I in Equation 4. The SIF of pressurized pipes with cracks at the inner surface was subject to several studies and different calculations are available [21, 29, 31]. Fracture mechanics lifetime prediction for a pipe was done with the material constants A and m at 23 °C obtained from the extrapolation procedure and the SIF by Murakami [29]. The initial size a_{ini} of the defect at the inner pipe surface was estimated between 100 and 400 µm [32].

Figure 9 shows data from internal pressure tests of the investigated PE 80 pipe grade at different temperatures of 20, 60 and 80 °C based on EN ISO 9080 for pipes with the dimensions D40 SDR 11. The results at 80 °C show ductile failure at relatively high stress levels σ_v and a transition knee to the region of quasi-brittle failure with decreasing σ_v, as it was shown in Figure 1 schematically. At lower temperatures the failure curves are shifted to higher stress levels and the transition knee to longer testing times. Because the tests were stopped after 10'000 hours the region of quasi-brittle failure was not detectable at temperatures of 60 °C and below.

The simulated failure times of a pressurized pipe of the dimensions D40 SDR 11 shown in Figure 9 reflect a strong dependency on the initial defect size a_{ini}. However, at an operating pressure of 10 bars and below, sufficient resistance against failure by CCG is ensured for more than 100 years. Additional safety time is given, as crack initiation time is not considered in this illustration.

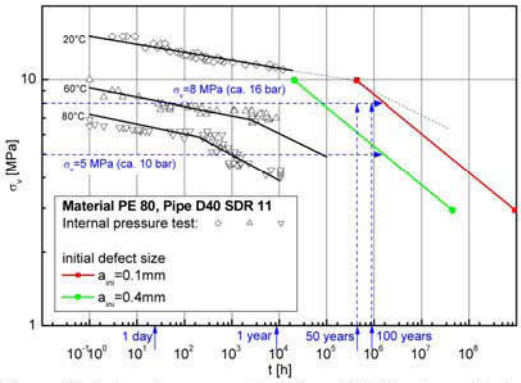

Figure 9: Internal pressure test for a PE 80 pipe with the dimensions D40 SDR 11 at different temperatures and simulated failure times at 23 °C with estimated initial defect size $100 < a_{ini} < 400$ µm. Crack initiation time is not considered in simulation.

Conclusion

In the present research work a new technique for a direct measurement of crack growth kinetics in cracked round bar (CRB) specimens made of polyethylene was demonstrated. An already proposed procedure was applied to extrapolate fatigue crack growth curves to static loading conditions to generate a "synthetic" creep crack growth (CCG) curve from which material constants were obtained. Stress intensity factors from literature and simulation tools were used to predict failure times of the CRB specimens and to verify the material constants of the extrapolation procedure. After this successful evaluation the material constants were used for a fracture mechanics lifetime prediction of a pipe. Although failure times are heavily dependent on the initial defect size, predicted lifetimes are in good correlation to experimental data. An additional safety for the lifetime assessment is given, as crack initiation times were not considered.

Acknowledgement

The research work of this paper was performed at the Polymer Competence Center Leoben GmbH (PCCL, Austria) within the framework of the K_{plus}-program of the Austrian Ministry of Traffic, Innovation and Technology with contributions by the University of Leoben, AGRU Kunststofftechnik GmbH (Austria), Borealis Polyolefine

GmbH (Austria), OMV Exploration & Production GmbH (Austria), Österreichische Vereinigung für das Gas und Wasserfach (Austria) and SABIC Europe (Netherlands). The PCCL is funded by the Austrian Government and the State Governments of Styria and Upper Austria.

Literatur

1. Lang, R.W., Stern, A., Doerner, G., (1997) Die Angewandte Makromolekulare Chemie, 247 (1997) 131.
2. Gaube, E., Gebler, H., Müller, W., Gondro, C. (1985) Kunststoffe 75(7), 412-415.
3. Ifwarson, M. (1989) Kunststoffe 79(6), 525-529.
4. Barker, M.B., Bowman, J.A., Bevis M. (1983) Journal of Materials Science 18, 1095-1118.
5. Brömstrup, H. (2004) Vulkan Verlag, Essen, Deutschland.
6. Brown, N. and X. Lu (1993) 13th Plastic Fuel Gas Pipe Symposium, San Antonio, Texas, USA.
7. Brown, N. and X. Lu (1991) 12th Plastic Fuel Gas Pipe Symposium, Boston, Massachusetts, USA.
8. Janson, L.E. (1999) Borealis, Sven Axelsson AB/ Fäldts Grafiska AB, Stockholm, Schweden.
9. EN ISO 9080 (2003) Plastics piping and ducting systems - Determination of the long-term hydrostatic strength of thermoplastics materials in pipe form by extrapolation
10. Brown, N., X. Lu, et al. (1992), Plastics, Rubber and Composites Processing and Applications 17(4): 255-258.
11. Pinter, G., Lang, R.W. (2004) D.R. Moore. Oxford, England, Elsevier Science Ltd. and ESIS. ESIS Publication 33: 47-54.
12. Parsons, M., Stepanov, E.V., Hiltner, A., Baer, E. (2000) Journal of Materials Science 35, 2659-2674.
13. Haager, M. (2006) Dissertation, Institute of Material Science and Testing of Plastics, University of Leoben, Austria.
14. Pinter, G., Haager, M., Lang, R.W. (2006) ANTEC 2006, Charlotte, North Carolina, USA, Society of Plastics Engineers.
15. Pinter, G., Haager, M., Balika, W., Lang, R.W. (2007) Polymer Testing, Volume 26, Issue 2, 180-188.
16. Lang, R.W., Pinter, G., Balika, W. (2005) 3R international, 44(1-2), 33-41.
17. Lang, R.W., Pinter, G., Balika, W., Haager, M. (2006) Plastics Pipes XIII, Washington DC, USA.
18. Frank, A., Pinter, G., Lang, R.W. (2008) ANTEC 2008, Milwaukee, Wisconsin, USA, Society of Plastics Engineers.
19. Frank, A., Freimann, W., Pinter, G., Lang, R.W. (2008) 5th International Conference on Fracture of Polymers, Composites and Adhesives, Les Diablerets, Switzerland, Elsevier Science Ltd. and ESIS.
20. Frank, A., Pinter, G., Lang, R.W. (2008) Plastics Pipes XIV, Budapest, Hungary.
21. Anderson, T.L. (1991) Fracture Mechanics – Fundamentals and Application, CRC Press Inc., Boca Raton, Florida, USA.
22. Kinloch, A.J., Young, R.J. (1983) Fracture Behaviour of Polymers, Applied Science Publ., London, England.
23. Dieter, G.E. (1988). Mechanical Metallurgy, McGraw-Hill Book Company, London, United Kingdom.
24. Paris, P.C., Erdogan, F. (1963) Journal of Basic Engineering 85, p. 528-534.
25. Saxena, A, Hudak, S.J. (1978) International Journal of Fracture, Vol. 14, No. 5, p 453-468.
26. v. d. Grinten, F., Wichers Schreur, P.W.M. (1996) Plastics, Rubber and Composites Processing and Applications 25 (6), 294.
27. Lang, R. W. (1984) Dissertation, Lehigh University (Bethlehem, PA), USA.
28. Benthem, J.P., Koiter, W.T. (1973) in "Method of Analysis and Solutions of Crack Problems", (Sih, G. C., ed.), 3, 131-178, Noordhoft International Publisching, Groningen, Netherlands.
29. Murakami, Y. (1990) Stress Intensity Factors Handbook, Pergamon Press, Oxford, Great Britain.
30. Dieter, G.E. (1988). Mechanical Metallurgy, McGraw-Hill Book Company, London, United Kingdom.
31. Krishnamachari, S.I. (1993) Applied Stress Analysis of Plastics – A Mechanical Engineering Approach, Van Nostrand Reinhold, New York, USA.
32. Pinter, G. (1999) Dissertation, University of Leoben, Austria.

Key Words: Polyethylene, fatigue, pipe, crack growth, lifetime prediction.

II-1 Characterization of the Effects of Preforming and Redeforming on Morphology and Thermomechanical Properties of Polyethylene Close-Fit Liners for Trenchless Pipe Rehabilitation

A. Frank, G. Mannsberger, G. Pinter, R.W. Lang

in proceedings: ANTEC 2008, Milwaukee, Wisconsin, USA (2008), 2251-2255.

CHARACTERIZATION OF THE EFFECTS OF PREFORMING AND REDEFORMING ON MORPHOLOGY AND THERMO-MECHANICAL PROPERTIES OF POLYETHYLENE CLOSE-FIT LINERS FOR TRENCHLESS PIPE REHABILITATION

Andreas Frank, Polymer Competence Center Leoben, Austria (frank@pccl.at)
Gernot Mannsberger, Polymer Competence Center Leoben, Austria
Gerald Pinter, University of Leoben, Austria
Reinhold W. Lang, University of Leoben and Polymer Competence Center Leoben, Austria

Abstract

Close-fit liners made of polyethylene (PE) are exposed to strong thermo-mechanical deformation during the preforming and redeforming process. In the present research work a morphological and thermo-mechanical characterization with different methods was carried out where the redeformed pipe was compared to its undeformed condition. It was shown, that with the used characterization methods no disadvantageous effects within the material occur and particularly the level of residual stresses was reduced significantly in the redeformed pipe.

Introduction

In our modern society buried pipes contribute an inconspicuous but very important part to maintenance of the infrastructure. Depending on the transported goods, their application varies in a wide range. Pressurized pipes made of polyethylene (PE) have been used successfully for more than 40 years, especially in fuel gas and water supply systems [1, 2]. The reliability of these pipe systems is of essential significance. However, usually these pipes have been installed for an operating time of at most 50 years, so that many pipe systems needs to be replaced or rehabilitated. Especially in urban regions, repairing and rehabilitation of old or defect pipes (especially made of cast-iron and asbestos-cement) is associated with high technical efforts and extensive costs.

Since the late eighties several methods for trenchless pipe rehabilitation, also called no-dig techniques, were developed for time saving and cost reducing renovation of existing pipe systems [3]. One important technique is the close-fit lining system. In this technology usually a standard PE-pipe is preformed by folding, so that its effective diameter is reduced by approx. 30 %. Afterwards the folded pipe is inserted into an existing pipe. With a defined temperature and pressure program (hot steam) the folded pipe restores back to its original shape and forms a close fit with the original pipe. In this redeformation process the memory-effect of thermoplastic materials plays an important role.

To ensure best material performance and high crack resistance, the material used for close-fit liners are modern PE-pipe grades with a bimodal molecular weight distribution. Although there are a large number of publications dealing with morphology and the thermo-mechanical behavior of PE pipes, unfortunately there is rather less information about the influence of the preforming and redeformation process on morphology. Hence, the main objective of this research work is the characterization of the influence of the preforming and redeformation on the material behavior. Therefore a pipe was manufactured and separated into two parts. The first one was left in its initial state whereas the second one was preformed to a close-fit liner and afterwards restored to its final shape. In this work the focus of the characterization was given on the comparison of thermo mechanical and dynamic-mechanical values between the original pipe and the restored pipe. Also it was elaborated, if thermo oxidative degradation of the material appears during the forming processes. Finally, the residual stresses in axial and circumferential direction of both pipes were investigated and compared to each other.

Background

After their extrusion conventional pipes are folded to the preformed close-fit liners with special deformation tools at elevated temperatures. By continuous processing it is possible to produce pipes in a length of 600 m or more [3] that can be stored on coils. After insertion into an existing pipe system, the redeformation process can usually be split into three main phases:

- At first the heating of the pipe is performed. Therefore compressed hot steam with temperatures less than 130 °C is inserted into one end, whereas the material temperature is measured at the other pipe end. A temperature of at least 80 °C is held for two hours. During this phase the memory-effect restores the preformed pipe back to its original circle profile.

- In the second phase the steam is pressurized continuously to about 1.5 bar within 30 minutes whereby the pipe temperature rises again. Then the pressure is increased stepwise depending on the pipe diameter (approx. 3 bar for SDR17).
- In the final phase the maximum pressure is held constant for at least 8 hours and the material temperature decreases by passive cooling.

Regarding this redeformation process changes in the morphological structure are possible. Especially the preforming of the pipe to the close-fit liner is a process, where the typical folding points are exposed to high mechanical loadings. It must be assumed, that orientation of molecular chains takes place, depending on the deformation grade of the pipe. During the redeformation process heating to temperatures of 80 °C and above for several hours correspond to an annealing process, that will reverse the orientation of the chains at least to a certain extent. But generally, thermal annealing of PE also causes changes in the crystallinity and density. However, a degradation of the residual stresses is expected too [4].

Experimental

The investigated pipe was processed with a commercial PE100-pipe grade with a minimum required stress (MRS) of 10 MPa. The diameter was 180 mm and the wall thickness was 10 mm. The preforming and redeforming process was done as described above.

Dynamic mechanical analysis (DMA) was used to determine the temperature dependent modulus and damping behavior. Tensile specimens with the dimensions 6x0.3x19.5 mm were investigated with a maximum displacement of 30 µm in a temperature range from -100 to 125 °C with a heating rate of 3 K/min on a DMA/SDTA861e from Mettler Toledo GmbH (Switzerland). To analyze crystallinity differential scanning calorimetry (DSC) was performed with a DSC822 from Mettler Toledo GmbH (Switzerland) in a temperature range from 25 to 180 °C and a heating rate of 10 K/min. The calculation of the crystallinity α was done with equation 1, where ΔH_m is the melt enthalpy of the material, and ΔH_m^0 is the melt enthalpy of 100 % crystalline PE (ΔH_m^0=293 J/g) [5].

$$\alpha = \frac{\Delta H_m}{\Delta H_m^0} \cdot 100 \qquad (1)$$

The degree of orientation of the material was characterized by measuring thermal extension using thermo-mechanical analysis (TMA). Specimens with dimensions of 4x4x6 mm were tested in a temperature range from 25 to 120 °C with a heating rate of 2 K/min with a TMA/SDTA840 from Mettler Toledo GmbH (Switzerland). As a result of entropic elasticity oriented polymer chains will try to recoil with increasing temperature during this test leading even to negative thermal extension in the direction of orientation [6].

For the detection of possible ageing as a result of the thermal treatment of the pipes two tests were applied. On the one hand oxygen inductivity time (OIT) at 220 °C in air was measured with the DSC mentioned above. On the other hand infrared (IR) spectroscopy was used to detect carbonyl groups, the typical ageing products in PE, in a the range of 1700 to 1740 cm^{-1}. These tests were performed with a spectroscope of the type Spektrum GX (Perkin Elmer, Germany) in attenuated total reflection mode.

Considering the folding process of the pipe to the close-fit liner, five characteristic positions were defined for characterization, what is illustrated schematically in Fig. 1. Hence, position 1 describes the point of the highest bending. At each of these positions of the redeformed pipe pieces were milled out. In order to consider also effects over the pipe wall thickness specimens were cut out from the inner, the middle and the outer wall position with a microtome (R. Jung, Germany). For TMA specimens were milled out not only in axial but also in circumferential direction.

Residual stresses in circumferential direction were detected by ring deformation tests [2, 7]. Therefore pipe samples with a length of 80 mm were cut free at the defined positions. The deformation of these segments was recorded as a function of time. In axial direction the residual stresses were investigated by strip deformation tests [8]. At each defined position a strip with the length of 250 mm was milled out of the pipe. The bending of the strips was recorded by time. In both cases the deformation of the segments was used for the calculation of residual stresses [2, 8]. The time dependent creep-bending modulus needed for both calculations was taken from an existing data sheet [9].

Results and discussion

No effect of pipe position could be detected on the results of the DMA and DSC measurements. Therefore only the results of Pos. 1 of the redeformed pipe are compared to the undeformed pipe (Fig. 2). The storage modulus E' is slightly higher for the redeformed pipe, what can be explained by the higher crystallinity of the redeformed pipe (see DSC results); the loss factor tanδ agrees well for both conditions. For both pipes, E' at the outer wall position is slightly lower than at the middle and inner wall position. These results can be explained by the slightly lower crystallinity at the outer pipe surface as a result of the higher cooling rate during pipe processing (see next paragraph).

In Fig. 3 the crystallinity α of the undeformed and redeformed pipes are illustrated. For the undeformed pipe an increase of α from the outer wall position (52 %) to the middle and inner wall position (58 %) could be detected. Keeping in mind the extrusion process of a pipe, this result makes sense. High cooling rates at the outer pipe surface reduces the time for crystallization, so that a higher amount of amorphous phase remains in the material. During the redeformation process post crystallization takes place and α is increasing for about 4 to 5 % at all pipe wall positions.

In Fig. 4 and 5 the thermal extension is shown. As for the inner and the middle wall position no differences were detected, only the results for the outer wall position are shown at the different pipe positions. In axial direction the results for the undeformed pipe differ only slightly from the redeformed pipe (Fig. 4) and there are also no differences between the different circumferential positions. However, the thermal extension in circumferential direction is quite different. Comparing to the undeformed pipe, position 1 of the redeformed pipe has the lowest thermal extension that indicates a higher orientation still existing at this point. Also for positions 2 and 3 a small tendency for higher molecular orientation is visible. This, of course, is consistent with the assumptions based on the deformation of the original pipe.

The OIT results in Fig. 6 show similar values for the undeformed pipe and the redeformed pipe. The longer times at the redeformed pipe may be a result of the very local nature of this characterization method. Nevertheless the results show, that no antioxidants are lost during the redeformation process. With IR-spectroscopy no peaks in the range of carbonyl groups were detected and it can be assumed, that no ageing of the pipe material occurs during the redeformation process.

Residual stresses in a pipe have their origin in processing and are dependent on the cooling gradient after extrusion. Typical values are in the range of 4 MPa in circumferential and 5.5 MPa in axial direction [7]. As shown in Fig. 7 the residual stresses remaining in circumferential direction of the undeformed pipe are about 2.5 MPa. After redeformation the stresses are relaxing to values lower than 1 MPa. In axial direction the residual stresses of the undeformed pipe were found between 5 to 6 MPa (see Fig. 8). After the redeformation process the residual stresses are decreasing to values of 1 MPa and less. Relating to the MRS of 10 MPa for this PE-pipe grade a significant degradation of the residual stresses takes place during the redeformation process.

Conclusion

The main goal of this work was a morphological and thermo-mechanical comparison of a conventionally manufactured pipe and a preformed and redeformed close-fit liner used for trenchless pipe rehabilitation. DSC shows that crystallinity in the redeformed pipe increases by about 4 to 5 % as a result of post crystallization. This, of course, effects the modulus in the DMA measurements, giving slightly higher values for the redeformed pipe. Induced by the preforming process, orientation only at the outer wall position in circumferential direction of the redeformed pipe could be detected. Although the pipe is exposed to high temperatures during redeformation, no thermo oxidative ageing takes place. Residual stresses are reduced to a great extent as a result of the redeformation process that can be seen as an annealing process. Summarizing based on the used methods no negative effect of the preforming and redeforming process could be detected. Nevertheless additional investigations are necessary for the evaluation of the long-term failure behavior of the redeformed close-fit liners.

Acknowledgements

The research work of this paper was performed at the Polymer Competence Center Leoben GmbH (PCCL, Austria) within the framework of the Kplus-program of the Austrian Ministry of Traffic, Innovation and Technology with contributions by the University of Leoben. The PCCL is funded by the Austrian Government and the State Governments of Styria and Upper Austria.

References

1. Brömstrup, H. (2004) PE 100 Pipe Systems, Vulkan Verlag, Essen, Germany.
2. Janson, L.E. (1999) Plastics Pipes for Water Supply and Sewage Disposal, Borealis, Sven Axelsson AB/ Fäldts Grafiska AB, Stockholm, Sweden.
3. Glanert, R., Schulze, S. (2002) U-Liner – Der Klassiker für die Sanierung von Reuckrohren, Rohrbau congress 2002, Weimar, Germany.
4. Choi, S. and L. J. Broutman (1997). "Residual Stesses in Plastic Pipes and Fitting - IV. Effect of Annealing on Deformation and Fracture Properties." Polymer (Korea) 21(1): 93-102.
5. Lohmeyer, S. (1984) Die speziellen Eigenschaften der Kunststoffe, Expert Verlag, Grafenau, Germany.
6. Menges G., et al. (2002) Werkstoffkunde Kunststoffe, Hanser, München, Germany.
7. Pilz, G. (2001) Viscoelastic Properties of Polymeric Materials for Pipe Applications, Dissertation, Institute of Materials Science and Testing of Plastics, University of Leoben, Austria.

8. König, G. (1989) Stand der Technik auf dem Gebiet der Eigenspannungsmessungen, Seminar über Eigenspannungsmessungen, Miskolc, H
9. www.basell.com, 15.05.2007.

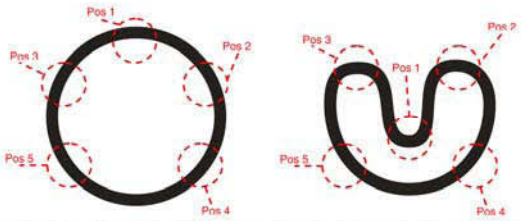

Figure 1: Characteristic circumferential positions on the pipe, considering the preforming of a pipe to a close-fit liner. Pos. 1: Position with highest bending.

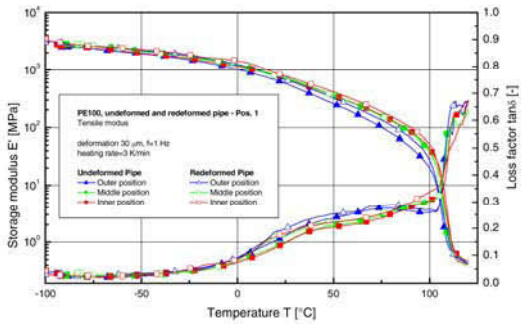

Figure 2: Storage modulus E' and loss factor tanδ of the undeformed and the redeformed pipe (pos. 1) at the inner, middle and outer wall position.

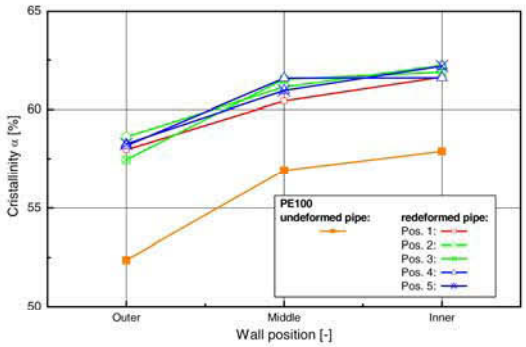

Figure 3: Crystallinity of the undeformed and the redeformed pipe at the inner, middle and outer wall position.

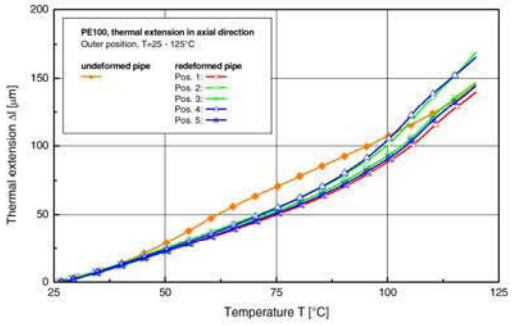

Figure 4: Thermal extension of the undeformed and the redeformed pipe in axial direction, outer wall position.

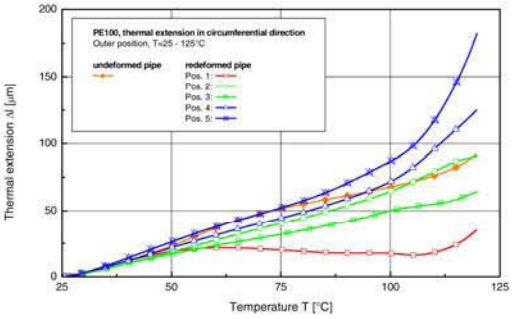

Figure 5: Thermal extension of the undeformed and the redeformed pipe in circumferential direction, outer wall position.

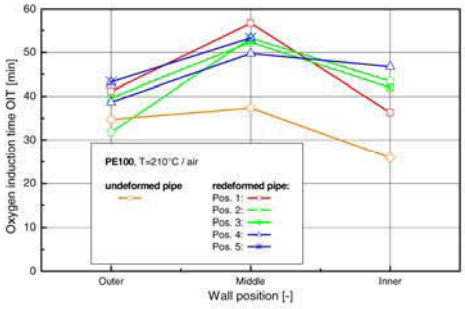

Figure 6: Oxidation induction time at 210 °C/air of the undeformed and the redeformed pipe at the inner, middle and outer wall position.

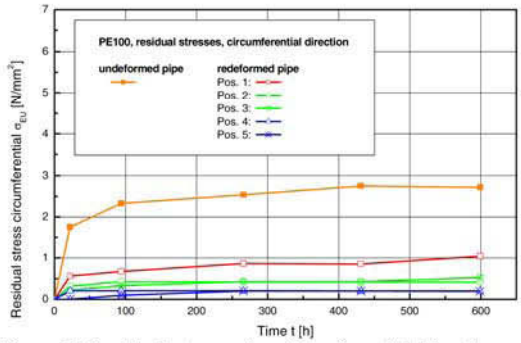

Figure 7: Residual stresses in circumferential direction as a function of time for the undeformed and the redeformed pipe.

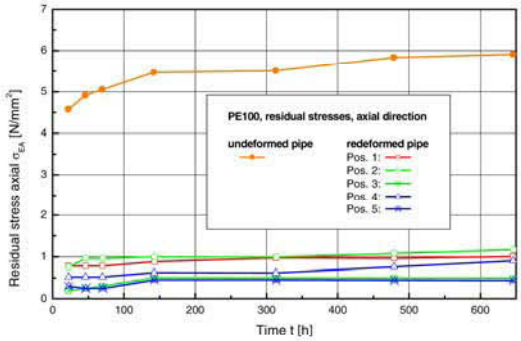

Figure 8: Residual stresses in axial direction as a function of time for the undeformed and the redeformed pipe.

Key Words: PE, pipe, residual stresses, close-fit liner

II-2 Close-Fit Liner – Verfahrensbe dingte Beeinflussung der Werkstoffei - genschaften und des Rohrlangzeitverhaltens

A. Frank, M. Haager, A. Hofmann, G. Pinter

3R international 48 (11) (2009), 639-645.

Close-Fit-Liner – Verfahrensbedingte Beeinflussung der Werkstoffeigenschaften und des Rohrlangzeitverhaltens[1)]

Close-Fit-Lining – Process-related changes of material properties and long-term failure behavior[1)]

Von A. Frank, M. Haager, A. Hofmann, G. Pinter

Der Einsatz von Close-Fit-Linern aus Polyethylen stellt bereits seit vielen Jahren ein effizientes Verfahren zur raschen und kostengünstigen Sanierung von Altrohrsystemen dar. Im Rahmen der vorgestellten Arbeit erfolgte eine umfangreiche werkstoffkundliche Charakterisierung eines kommerziell erhältlichen PE 100-Close-Fit-Liners, wobei stets der Vergleich der Eigenschaften vor der Faltung zum Close-Fit-Liner mit jenen des Endproduktes des installierten Rohres im Mittelpunkt stand. Die präsentierten Ergebnisse zeigen durchweg, dass relevante Eigenschaften im Rohrmaterial durch die für das Close-Fit-Liner-Verfahren typischen Deformationsprozesse und zusätzlichen thermischen Belastungen nicht negativ beeinflusst werden. Die Verringerung des Eigenspannungszustandes im installierten Endzustand des Rohres bewirkt sogar eine Verbesserung im Widerstand des Materials gegenüber Rissinitiierung und langsamem Risswachstum, so dass insgesamt von einer verbesserten Langzeiteigenschaft des rückverformten Close-Fit-Liners ausgegangen werden kann.

For many years the Close-Fit-Relining technology with polyethylene pipes has been an established and efficient technology for a quick and cost-saving rehabilitation of old pipe systems. Within the current study a comprehensive material characterization of a commercially PE 100 Close-Fit-Liner was done, in which the main focus always was given on a correlation of the material properties of the pipe before the deformation to the Close-Fit-Liner and those of the final pipe. The presented results show, that the typical deformation processes and the additional thermal treatment have no negative effect on the relevant material properties. The reduction of the residual pipe stresses in the final pipe even results in an increase of the resistance of the pipe material against crack initiation and slow crack growth, so that all in all an improved long-term failure behavior can be expected.

Einleitung

Unterirdisch verlegte Rohrleitungen spielen eine unauffällige, jedoch sehr wichtige Rolle in der Sicherstellung unserer modernen Infrastruktur und unseres hohen Lebensstandards. In Abhängigkeit zu den auftretenden Belastungen und den zu transportierenden Medien kommen eine Reihe unterschiedlicher Materialien zum Einsatz und speziell im Bereich der Gas- und Wasserversorgung sowie im Abwassertransport werden Rohre aus Polyethylen (PE) bereits seit mehr als 50 Jahren erfolgreich eingesetzt [1-4].

Aufgrund ihrer langen Betriebszeiten sowie der unmittelbaren Nähe zu stark bewohnten Regionen ist die Zuverlässigkeit der Rohrsysteme gegen relevante Versagensmechanismen für alle verwendeten Werkstoffkategorien von wesentlicher Bedeutung. Viele seit Jahrzehnten verwendete Rohrleitungen nähern sich jedoch dem Ende ihres geplanten Einsatzes und müssen renoviert oder erneuert werden. Speziell in städtischen Regionen sind solche Sanierungs- oder Reparaturarbeiten alter Rohrsysteme mit enormem technischen Aufwand und beträchtlichen Kosten verbunden. Aus diesen Gründen entwickelten sich bereits in den späten Achtzigerjahren verschiedenste Methoden zur grabenlosen Rohrsanierung, die eine deutliche Einsparung von Zeit und Kosten bei der Sanierung von Altrohrsystemen ermöglichten [5]. Eine wichtige und etablierte Technologie stellt dabei das Close-Fit-Lining mit PE-Rohren dar. Dabei wird ein konventionell hergestelltes PE-Rohr nach dem Extrudieren zur Querschnittsreduktion gefaltet, in das zu sanierende Altrohr eingezogen und anschließend durch Erwärmung und unter Nutzung des für Kunststoffe typischen Memory-Effektes und zusätzlichem Überdruck wieder rückdeformiert. Das installierte Rohr legt sich dabei spaltfrei an das Altrohr an („close-fit").

Im Gegensatz zu konventionell extrudierten und verlegten PE-Rohren stellen die fertigungstechnischen Schritte der Faltung des PE-Rohres zum Close-Fit-Liner und die spätere Rückdeformation zum Ursprungsquerschnitt beträchtliche zusätzliche thermische und mechanische Beanspruchungen des Rohrmaterials dar. Es ist davon auszugehen, dass sich Veränderungen in morphologischen

1) Der Beitrag basiert auf einem Vortrag des Erstautors am Symposium Grabenlos 2009 der ÖGL (Österreichische Vereinigung für grabenloses Bauen und Instandhalten von Leitungen) am 20./21. Oktober 2009 in Loipersdorf (Österreich).

The paper is based on a presentation of the first author at the Symposium Grabenlos 2009 of the ÖGL (Österreichische Vereinigung für grabenloses Bauen und Instandhalten von Leitungen), October 20./21, 2009, in Loipersdorf (Austria).

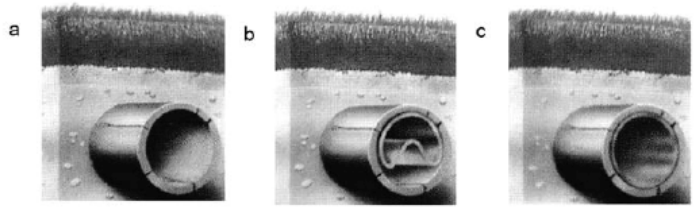

Bild 1: Schematische Darstellung der Installation eines CFL: a) Altrohr, b) Altrohr mit eingezogenem CFL, c) Altrohr mit rückdeformiertem CFL [6]

Fig. 1: Schematically illustration of the installation of a CFL: a) Old pipe, b) Old pipe with inserted CFL, c) Old pipe with redeformed CFL [6]

Eigenschaften wie Kristallinität, Orientierungen, in der Stabilisierung des Materials hinsichtlich thermisch bedingter Alterung, in den mechanischen Eigenschaften und Eigenspannungen oder dem Widerstand gegen Rissinitiierung und langsames Risswachstum einstellen. Unter dem Aspekt, dass mit dem sanierten Rohr Betriebszeiten von 50 Jahren und mehr sichergestellt werden sollen, ist die Frage, wie sich der Rohrwerkstoff durch diese Verfahrensschritte verändert, daher mehr als berechtigt.

Um die Anforderungen bezüglich Materialeigenschaften und vor allem Rissbeständigkeit zu erfüllen, kommen heute in erster Linie moderne PE-Rohrmaterialien mit bimodaler Molmassenverteilung zum Einsatz. Obwohl eine Vielzahl an Studien über morphologische und thermomechanische Eigenschaften von PE für Rohranwendungen existiert, gibt es keine Informationen über die Auswirkungen der beim Close-Fit-Liner-Verfahren typischen Deformationsvorgänge auf die entsprechenden Materialeigenschaften, weshalb das Hauptziel der vorliegenden Arbeit in einer ausführlichen Charakterisierung des Einflusses der Deformation und der späteren Rückdeformation eines Rohres auf die Eigenschaften des Close-Fit-Liners lag. Dabei wurden morphologische Veränderungen wie Kristallinitätsgrad und Orientierungen ebenso untersucht, wie Veränderungen im Eigenspannungszustand der Rohre oder in der Stabilisierung gegen oxidative Alterung sowie im, für die Lebenszeitabschätzung kritischen, Langzeit-Versagensverhalten der Rohre.

Grundlagen

Für die Herstellung des Close-Fit-Liners (CFL) wird ein konventionelles Rohr üblicherweise direkt in der Extrusionslinie unter kontrollierten Temperatur- und Belastungsbedingungen gefaltet, wodurch eine Querschnittsreduktion von etwa 30 % erreicht wird. Die gefalteten Rohre werden dann auf Haspeln gerollt, wo sie bis zur Installation zwischengelagert werden.

Bei der Installation des CFL (**Bild 1**) werden nach dem Einziehen in das Altrohr beide Enden verschlossen und am Rohranfang (A-Station) Wasserdampf mit einer Temperatur von ca. 110 °C eingeleitet. Ziel ist es, eine Rohraußenwandtemperatur am Rohrende (B-Station) von ca. 80 °C zu erreichen und diese für ca. 2 Stunden lang aufrecht zu halten. Um eine gleichmäßige Temperierung der gesamten Rohrstrecke sicherzustellen, wird während der gesamten Prozedur die Temperatur an der B-Station gemessen und an der A-Station geregelt. Aufgrund der im Material eingefrorenen Orientierungseigenspannungen relaxiert der CFL und erhält annähernd seinen kreisrunden Querschnitt zurück (Memory-Effekt). Anschließend erfolgt ein dimensionsabhängiger Druckaufbau, wodurch eine eng anliegende Passung an das stützende Altrohr gewährleistet wird. Nachdem ein dimensions- und temperaturspezifischer Druck erreicht wurde, wird mit der schrittweisen Kühlung begonnen. Dazu wird Kompressorluft in die Haltung eingeleitet und der Druck, in Abhängigkeit von der Temperatur, bis zu einem dimensionsabhängigem Maximalwert gesteigert. Unter diesem Druck wird der Liner weiter abgekühlt [6].

Basierend auf den beschriebenen zusätzlichen Deformationsprozessen muss mit Änderungen in verschiedenen Materialeigenschaften gerechnet werden. Speziell an den Umfaltungspunkten treten beim Falten des konventionellen Rohres hohe mechanische Kräfte auf, die in Abhängigkeit des Deformationsgrades zu unterschiedlich ausgeprägten Orientierungseffekten führen können. Die lange thermische Belastung von 80 °C über mehrere Stunden [6] stellt im weitesten Sinn einen Tempervorgang dar, der einerseits Orientierungen ebenso abbauen lässt wie produktionsbedingte Rohreigenspannungen [7]. Andererseits verändert ein nachträgliches Tempern in der Regel die Kristallinität im Material und wegen der langen thermischen Belastung weit oberhalb der eigentlichen Anwendungstemperatur muss auch die Stabilisierung gegen thermo-oxidative Materialalterung berücksichtigt werden. Alle Eigenschaften spielen in weiterer Folge eine wesentliche Rolle im Langzeiteinsatz der Rohrleitungen und im Widerstand gegenüber den kritischen Versagensmechanismen der Rissinitiierung und des langsamen Risswachstums.

Experimentelles

Um den Einfluss der Deformationsprozesse auf die untersuchten Eigenschaften zu ermitteln, wurden unterschiedliche Zwischenzustände des CFL hergestellt. Ein Rohr, das in seinem konventionellen Zustand belassen wurde, diente als Referenz sowohl für den Zwischenzustand eines deformierten CFL, als auch für den Endzustand des rückdeformierten CFL. Die Rohre, die aus einem handelsüblichen PE 100-Rohrmaterial mit einer erforderlichen Mindestfestigkeit („minimum required strength“, MRS) von 10 MPa hergestellt wurden, wiesen eine Dimension von DN 180 mm, SDR 17 auf. Die Herstellung der Rohre und die Deformation zum CFL erfolgte durch AGRU Kunststofftechnik GmbH (Bad Hall, Österreich). Die installationsgerechte Rückdeformation erfolgte durch RABMER Bau- und Installations GesmbH & Co.KG (Altenberg, Österreich).

Unter Berücksichtigung der während des Faltungsprozesses am meisten beanspruchten Positionen wurden entsprechend **Bild 2** fünf charakteristische Punkte zur Prüfkörperentnahme definiert. Position 1 ist demnach der Bereich, an dem die Rohrwand bei der Faltung quasi nach außen umgeklappt wird und wo somit die stärksten geometrischen Änderungen auftreten. Die symmetrischen Positionen 2 und 3 stellen Scheitelpunkte dar, bei denen sich der Rohrradius während der Faltung stark verringert. Die ebenfalls symmetrischen Positionen 4 und 5 hingegen sind von den mechanischen Faltvorgängen nahezu unbeeinflusst. Aus den definierten Positionen wurden durch temperaturschonendes Fräsen Quader entnommen, aus denen in weiterer Folge je nach Charakterisierungsmethode die Prüfkörperfertigung erfolgte.

Für die Bestimmung des Kristallinitätsgrades [8] wurden an unterschiedlichen Wandtiefenpositionen mit einem Mikrotom (R. Jung, D) Schichten von ca. 30 µm Dicke von der Rohraußenseite, der Rohrmitte und der Rohrinnenseite entnommen. Der Kristallinitätsgrad α wurde mittels dynamischer Differenzkalorimetrie (DSC) mit einem Messgerät vom Typ DSC822 (Mettler Toledo GmbH, CH) in einem Temperaturbereich von 25 bis 180 °C und einer Aufheizrate von 10 K/min gemessen, wobei die Berechnung von α mit einem Literaturwert für die Enthalpie eines PE mit einer theoretischen Kristallinität von 100 % von ΔH_{m0}=293 J/g [8, 9] erfolgte.

Die Bestimmung von Orientierungseffekten erfolgte über die Messung der linearen thermischen Wärmeausdehnung Δl, wofür ein Dilatometer vom Typ TMA/SDTA840 (Mettler Toledo GmbH, CH) verwendet wurde. Hierfür wurden durch temperaturschonendes Fräsen an der Außen- und der Innenseite der Rohre Quader von 4 x 4 x 6 mm entnommen, wobei die lange Dimension in Umfangsrichtung lag, in der die Messung von $\Delta l(T)$ in einem Temperaturbereich von 25 bis 120 °C bei einer Aufheizrate von 2 K/min erfolgte [10].

Die thermo-oxidative Materialalterung bzw. die Charakterisierung des Stabilisierungszustandes des Rohrmaterials erfolgte über die Messung der Oxidations-Induktionszeit (OIT) und Infrarot (IR)-Spektroskopie. Die Prüfkörperherstellung erfolgte analog zu jener der DSC. Die Bestimmung der OIT erfolgte bei einer Temperatur von 210 °C in Luft mit dem oben erwähnten DSC-Prüfgerät [11]. Die IR-Spektroskopie wurde an einem Gerät vom Typ Spektrum GX (Perkin Elmer, D) im ATR-Verfahren („attenuated total reflection", abgeschwächte Totalreflexion) durchgeführt.

Die Bestimmung der Rohreigenspannungen in Umfangsrichtung $\sigma_{E,u}$ erfolgte über das Ringschlitzverfahren [2, 7, 12]. Hierfür wurden Rohrsegmente mit einer Länge von 80 mm freigeschnitten und aus der unbehinderten Deformation die Eigenspannung berechnet. Die Messung der Rohreigenspannungen in Axialrichtung $\sigma_{E,a}$ wurde mit dem Streifenkrümmungsverfahren [12, 13] durchgeführt, wofür Streifen von 250 mm Länge und 5 mm Breite durch temperaturschonendes Fräsen aus der Rohrwand entnommen wurden. Der für beide Verfahren notwendige zeitabhängige Biegekriechmodul wurde aus dem Werkstoffdatenblatt entnommen.

Die Charakterisierung des Widerstandes gegen langsames Risswachstum erfolgte mit zyklischen Ermüdungsversuchen an zylindrisch gekerbten Prüfkörpern („cracked round bar", CRB), die temperaturschonend zu einer Dimension von ϕ10 x 80 mm gedreht wurden. Die Kerbe in Umfangsrichtung von 1 mm Tiefe wurde mit einer Rasierklinge eingebracht. Die Ermüdungsversuche wurden auf einer servohydraulischen Prüfmaschine vom Typ MTS Table Top 858 (MTS Systems, D) bei Raumtemperatur von 23 °C mit einer Prüffrequenz von 10 Hz durchgeführt. Für eine zuverlässige bruchmechanische Bewertung musste sichergestellt sein, dass die globalen Belastungen am Prüfkörper die Kriterien der linear-elastischen Bruchmechanik erfüllten [14, 15]. Die Belastungsamplitude, die durch das R-Verhältnis (minimale/maximale Belastung) definiert wird, betrug für alle Versuche R = 0,1.

Ergebnisse und Diskussion

Die Charakterisierung von Orientierungseffekten erfolgte über die Messung der linearen Wärmeausdehnung in Umfangsrichtung der Rohre. Molekülorientierungen sind wegen der bei der Verarbeitung von thermoplastischen Werkstoffen vorhandenen Scherströmung und raschen Abkühlung in nahezu jedem Bauteil eingefroren. Bei einer nachträglichen Erwärmung des Materials erhöht sich die Beweglichkeit der Molekülketten, die dann danach streben, den Zustand der günstigsten Entropie bzw. höchsten Unordnung einzunehmen (Entropieelastizität). Erhöhte Orientierungen bewirken eine Verringerung der linearen Wärmeausdehnung in Orientie-

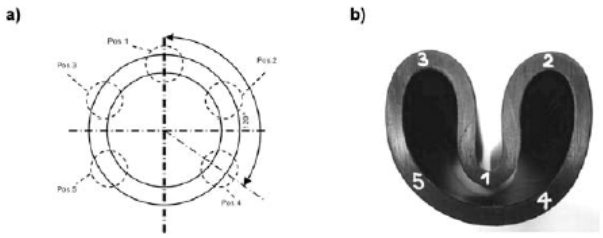

Bild 2: Definition der Positionen 1 bis 5 für die Prüfkörperentnahme: a) Schematische Darstellung, b) Gefalteter Zwischenzustand des deformierten CFL

Fig. 2: Definition of positions 1 to 5 for the specimen preparation: a) Schematically illustration, b) Folded intermediate state of the deformed CFL

rungsrichtung, die bei sehr starker Ausprägung sogar negativ sein kann [16].

Wird ein fertiges Bauteil bei einer definierten Temperatur deformiert und die auftretenden Molekülorientierungen eingefroren, so bewirkt die Entropieelastizität bei einer neuerlichen Erwärmung auf diese Temperatur eine Rückbildung zur ursprünglichen geometrischen Form (Memory-Effekt). In **Bild 3** sind die linearen Wärmeausdehnungen ΔI in Umfangsrichtung der Position 1 für das konventionelle undeformierte Rohr, den Zwischenzustand des deformierten CFL und den rückdeformierten CFL dargestellt. Im Vergleich zum undeformierten Rohr ist im deformierten CFL an der Rohraußenseite ein starker Anstieg in ΔI und an der Rohrinnenseite hingegen eine deutliche Verringerung zu negativen Werten für ΔI erkennbar. Im Endzustand des rückdeformierten CFL sind diese starken Wärmeausdehnungen wieder verschwunden. Die Wärmeausdehnungen sind im Endzustand deutlich geringer als im konventionellen undeformierten Rohr, was eine allgemeine Entspannung im Orientierungszustand des Materials widerspiegelt.

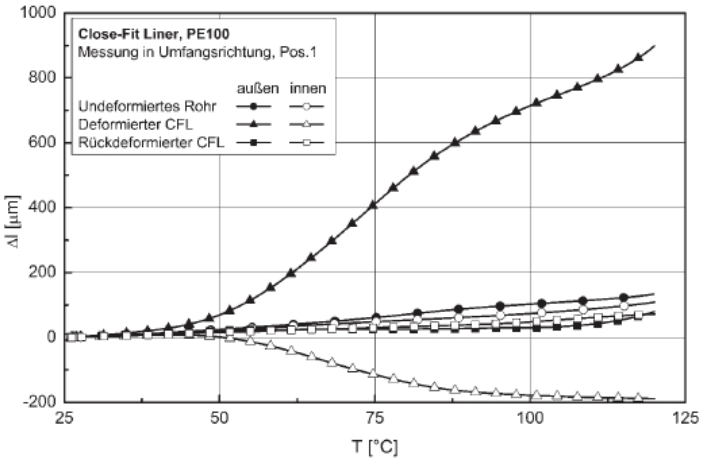

Bild 3: Lineare thermische Längenänderung DI an der Pos.1 im undeformierten Rohr, im deformierten CFL und im rückdeformierten CFL

Fig. 3: Linear thermal expansion DI at Pos.1 in the undeformed pipe, the deformed CFL and the redeformed CFL

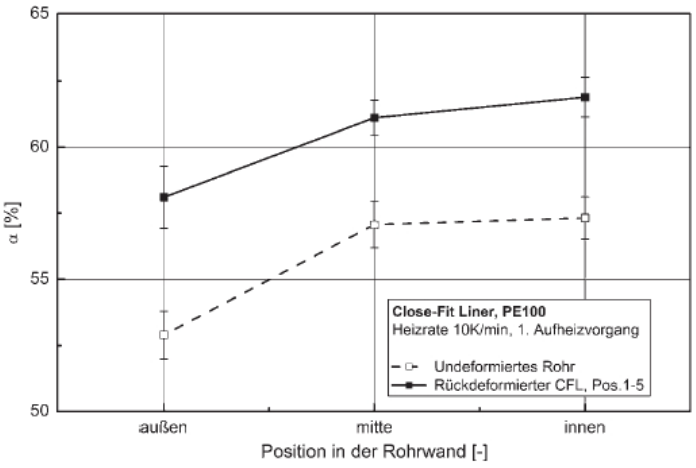

Bild 4: Kristallisationsgrad α in verschiedenen Rohrwandtiefen im undeformierten Rohr und im rückdeformierten CFL

Fig. 4: Crystallinity α at different pipe wall positions in the undeformed pipe and the redeformed CFL

In **Bild 4** sind die Resultate für den Kristallinitätsgrad α zusammengefasst. Dabei ist zu erkennen, dass an der Rohraußenseite eine deutlich niedrigere Kristallinität besteht als in der Mitte und der Rohrinnenseite. Dieser Effekt ist auf den Herstellungsprozess bei der Extrusion zurückzuführen, bei dem das Rohr von außen gekühlt wird und dem Material an der Oberfläche weniger Zeit zur Kristallisation gegeben wird als im Inneren der Rohrwand.

Im undeformierten Rohr betrug die Kristallinität an der Rohraußenseite ca. 53 %, in der Rohrmitte und an der Rohrinnenseite wurden etwa 4 % höhere Werte für α gemessen. Im rückdeformierten CFL ergaben sich über die gesamte Wandtiefe um ca. 4–5 % gleichmäßig erhöhte Werte für α. Dies ist ein Hinweis dafür, dass durch die zusätzliche Temperierung bei der Deformation zum CFL bzw. der Rückdeformation bei der Installation eine Nachkristallisation auftrat, die zu Kristallisationsgraden von bis zu 62 % führte. Eine Abhängigkeit von α von den unterschiedlichen Umformgraden an den Positionen 1 bis 5 wurde nicht festgestellt.

Eine Erhöhung der Kristallisation bedeutet im Allgemeinen einerseits eine Zunahme des E-Moduls und der Steifigkeit des Materials sowie eine höhere Härte. Andererseits kann die verringerte Zähigkeit der Werkstoffes den Widerstand gegen Rissinitiierung und langsamem Risswachstum beeinflussen.

Zur Beurteilung der Stabilität des Materials gegen thermo-oxidativen Materialabbau wurden Messungen der OIT und des IR-Spektrums durchgeführt. In **Bild 5** sind die OIT-Werte für das undeformierte Rohr und den rückdeformierten CFL bei unterschiedlichen Wandtiefen dargestellt. Im undeformierten Rohr betrugen die Zeiten zwischen 25 und 37 min, wobei an der Rohrinnenseite die kürzesten Zeiten auftraten. Eine Abhängigkeit von der Umfangsposition wurde nicht festgestellt. Interessanterweise stiegen im rückdeformierten Rohr die OIT-Werte gleichmäßig um durchschnittlich

50 % auf Zeiten zwischen 42 und 53 min an. Die Erhöhung der OIT-Werte lässt sich einerseits damit erklären, dass die Beweglichkeit der in den amorphen Phasen des PE eingebetteten Stabilisatorsysteme nach der zusätzlichen Temperierung während der Deformationsprozesse deutlich verbessert wurde. Andererseits spiegelt dieses Resultat den relativ lokalen Charakter dieser Messmethode wider. Die Messungen zeigen jedenfalls, dass während der Umformvorgänge keine Stabilisatoren verbraucht werden bzw. nach der Rückdeformation mehr aktiver Stabilisator zur Verfügung steht. Der Vollständigkeit halber wird darauf hingewiesen, dass die OIT nicht dazu geeignet ist, verschieden stabilisierte Werkstoffe hinsichtlich ihrer Langzeitstabilität zu vergleichen oder gar eine Lebenszeitabschätzung durchzuführen [17, 18].

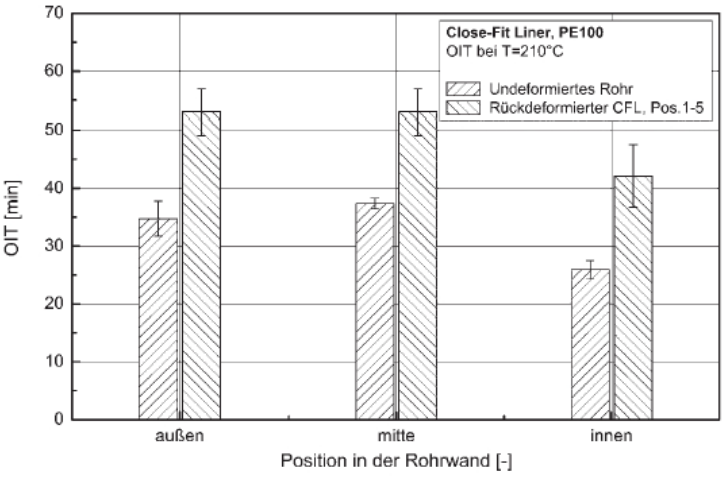

Bild 5: Oxidations-Induktionszeit OIT bei T = 210 °C in verschiedenen Rohrwandtiefen im undeformierten Rohr und im rückdeformierten CFL

Fig. 5: Oxidation-induction time OIT at T=210°C at different pipe wall positions in the undeformed pipe and the redeformed CFL

Die Ergebnisse der IR-Spektroskopie für das undeformierte Rohr und den fünf definierten Umfangspositionen des rückdeformierten CFL sind in **Bild 6** abgebildet, wobei die Transmission T als Funktion der Wellenzahl ν dargestellt wird. Da die längste und größte Temperaturbeanspruchung während der Installation im Inneren des Rohres auftritt, wurde speziell die Rohrinnenseite untersucht. Die auftretenden Absorptionspeaks bei ν zwischen 2925 und 2850 cm^{-1}, bei 1470 cm^{-1} und zwischen 725 und 720 cm^{-1} sind charakteristisch für PE und werden von CH-Banden und $(CH_2)_4$-Banden verursacht. Auf ein intaktes Stabilisatorsystem weisen die Signale im Wellenzahlbereich zwischen 3000 und 3500 cm^{-1} (OH-Banden) und zwischen 1500 und 1700 cm^{-1} (phenolische Antioxidantien) hin [19-21].

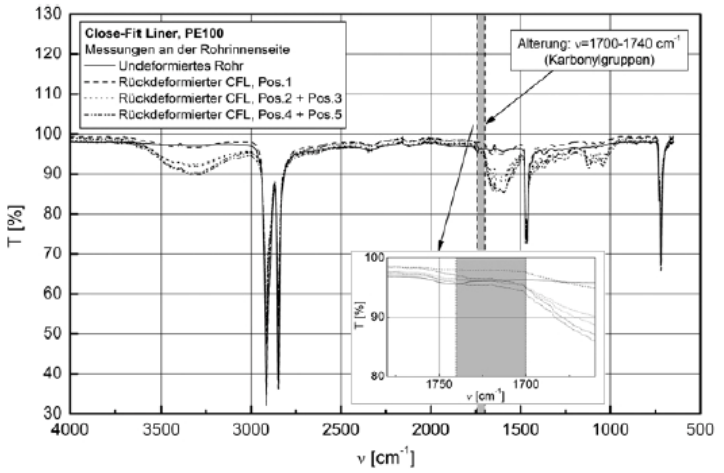

Bild 6: IR-Spektroskopie an der Rohrinnenseite des undeformierten Rohres und des rückdeformierten CFL

Fig. 6: IR-spectroscopy at the inner pipe wall position of the undeformed pipe and the redeformed CFL

Im Vergleich zum undeformierten Rohr sind die Signale für das Stabilisatorsystem im rückdeformierten Rohr deutlich stärker ausgeprägt. Auffallend ist, dass die Signale umso stärker sind, je geringer das Material an den Deformationsprozessen beteiligt war (Pos. 4 und Pos. 5). Dies kann – analog zur OIT – wiederum auf eine Erhöhung der Beweglichkeit der für die Materialstabilisierung verantwortlichen Moleküle durch den Tempervorgang erklärt werden. Bei thermo-oxidativer Materialalterung werden Carbonylgruppen in den Molekülketten gebildet, die Infrarotwellen im Wellenzahlbereich zwischen 1700 und 1740 cm^{-1} absorbieren. Nachdem in diesem Bereich keine Peaks auftreten, ist davon auszugehen, dass die thermische Belastung der Deformationsprozesse keine Schädigung hinsichtlich vorzeitiger Alterung verursacht. Eine quantitative Beurteilung der Wirksamkeit von Stabilisatorsystemen lässt sich aus der IR-Spektroskopie nicht ableiten, jedoch zeigt sich, dass das Stabilisatorpaket noch intakt ist.

Eigenspannungen in Kunststoffrohren haben ihren Ursprung im Extrusionsprozess, wo die Rohraußenseite relativ rasch abgekühlt wird, während die Temperaturen an der Rohrinnenseite aufgrund der schlechten Wärmeleitung nur langsam abnehmen. Als Faustregel gilt, dass an der zuerst gekühlten Seite Druck- und an der zuletzt gekühlten Seite Zug-Eigenspannungen auftreten. In PE-Rohren können in Abhängigkeit von den Prozessparametern bei der Verarbeitung durchaus Eigenspannungswerte von 4 MPa in Umfangsrichtung und 6 MPa in Axialrichtung auftreten [12]. Für ein PE 100-Rohrmaterial mit einem MRS-Wert von 10 MPa bedeutet dies, dass Eigenspannungen bei der Auslegung der Betriebsbelastung von Rohrsystemen durchaus beachtet werden müssen.

In **Bild 7** sind die Eigenspannungen in Umfangsrichtung $\sigma_{E,u}$ und in Axialrichtung $\sigma_{E,a}$ für das undeformierte Rohr und den rückdeformierten CFL zusammengefasst und mit typischen Eigenspannungswerten $\sigma_{E,u}^{ref}$ und $\sigma_{E,a}^{ref}$ gegenübergestellt [12]. Das undeformierte Rohr liegt mit Werten von ca. 2,7 MPa für $\sigma_{E,u}$ und 5,9 MPa für $\sigma_{E,a}$ im Bereich vergleichbarer Messungen. Für das rückdefor-

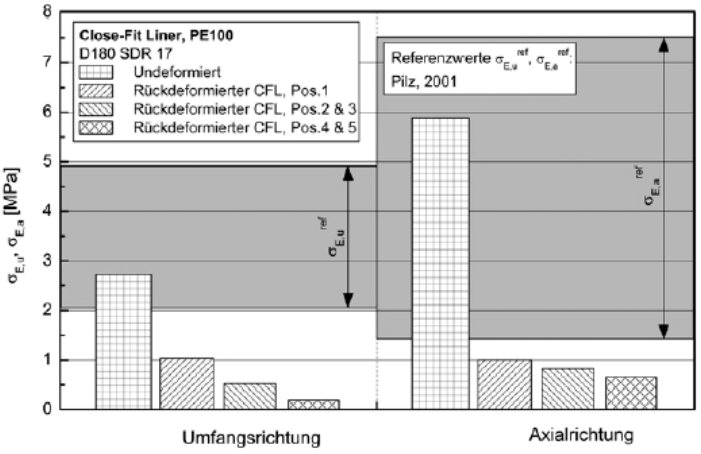

Bild 7: Rohreigenspannungen $\sigma_{E,u}$ und $\sigma_{E,a}$ in Umfangs- und Axialrichtung im undeformierten Rohr und im rückdeformierten CFL

Fig. 7: Residual pipe stresses $\sigma_{E,u}$ and $\sigma_{E,a}$ in circumferential and axial direction of the undeformed pipe and the redeformed CFL

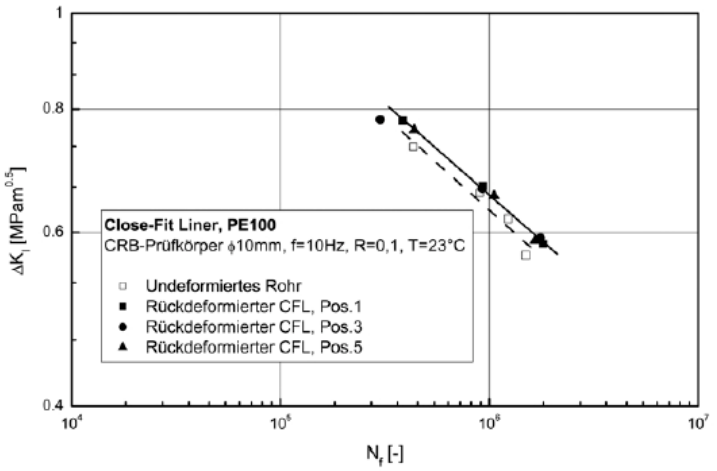

Bild 8: Zyklenzahlen bis zum Versagen N_f von CRB Prüfkörper als Funktion des Spannungsintensitätsfaktors ΔK_I bei einer Temperatur von 23 °C für das undeformierte Rohr und die Positionen 1, 3 und 5 des rückdeformierten CFL

Fig. 8: Failure cycle number N_f of CRB specimens as a function of the stress intensity factor ΔK_I at a temperature of 23 °C for the undeformed pipe and the positions 1, 3 and 5 of the redeformed CFL

mierte Rohr wurde hingegen in Abhängigkeit der Position des Freischneidens eine deutliche Verringerung der Rohreigenspannungen aufgrund der zusätzlichen Temperaturbelastungen gemessen. Für die Position 1 (d.h. Ringsegment bzw. Streifen wurde an der Position 1 freigeschnitten bzw. entnommen) sanken sowohl $\sigma_{E,u}$ als auch $\sigma_{E,a}$ auf etwa 1 MPa und nahmen an den weiteren Umfangspositionen noch weiter ab.

Die für das CFL-Verfahren notwendigen zusätzlichen Verfahrensschritte stellen somit einen Tempervorgang dar, der vor allem eine signifikante Reduktion der im Rohr vorhandenen Eigenspannungen bewirkt. Dadurch erhöht sich einerseits die Sicherheitsreserve des Materials zum jeweiligen MRS-Wert, andererseits ist mit einer deutlichen Verbesserung des Langzeit-Versagensverhaltens beim rückdeformierten CFL zu rechnen [7].

Zur Charakterisierung des Langzeit-Versagensverhaltens wurden Ermüdungsversuche an CRB-Prüfkörpern durchgeführt. Die Zyklenzahlen N_f bis zum Versagen durch Rissinitiierung und sprödem Risswachstum sind in **Bild 8** als Funktion der Differenz des minimalen und maximalen Spannungsintensitätsfaktors ΔK_I dargestellt. In doppelt-logarithmischer Darstellung ergibt sich sowohl für das undeformierte Rohr als auch den rückdeformierten CFL ein typischer linearer Zusammenhang, wobei mit Verringerung von ΔK_I ein Anstieg von N_f auftritt.

Die CRB-Prüfkörper aus dem rückdeformierten CFL versagten bei etwas höheren Zyklenzahlen als jene aus dem undeformierten Rohr. Dies kann vor allem auf die deutlich verringerten Eigenspannungen in den CRB-Prüfkörpern aus dem rückdeformierten CFL zurückgeführt werden, die einen maßgeblichen Einfluss auf das Langzeit-Versagensverhalten haben. Eine Abhängigkeit von der Umfangsposition wurde nicht festgestellt. Die mit der DSC gemessene geringfügige Erhöhung der Kristallinität, die zu einer Verringerung der Zähigkeit des Materials führen kann, wirkt sich nicht negativ auf das Langzeit-Versagensverhalten aus.

Zusammenfassung

Im Rahmen der gegenständlichen Arbeit erfolgte eine umfangreiche Studie über den Einfluss der prozessbedingten Deformationsprozesse auf Materialeigenschaften bei der Installation von Close-Fit-Liner (CFL)-Rohren. Dabei stand jeweils der Vergleich der untersuchten Eigenschaften im konventionell extrudierten, undeformierten Rohr mit jenen des Endzustandes des rückdeformierten CFL im Vordergrund. Die Charakterisierung von Orientierungseffekten mittels linearer thermischer Längenänderung vertiefte das Verständnis über den bei diesem Verfahren typischen Memory-Effekt. Dabei wurde gezeigt, dass die bei der temperaturbegleiteten Faltung künstlich eingebrachten Molekülorientierungen so stark ausgeprägt sind, dass sie bei neuerlicher Erwärmung der Deformation entgegenwirken und somit maßgeblich an der Rückführung des CFL in seine ursprüngliche Rohrgeometrie beteiligt sind.

Diese, im Vergleich zum undeformierten Rohr, zusätzlichen Temperaturbelastungen bewirken dabei einen gleichmäßigen Anstieg des Kristallisationsgrades im Material von ca. 4 bis 5 %, der im Allgemeinen eine geringe Erhöhung in der Steifigkeit bewirkt. Die Ergebnisse der Oxidations-Induktionszeit und der Infrarotspektroskopie ergaben keinerlei Hinweise auf eine vorzeitige, thermisch bedingte oxidative Materialalterung.

Eine wesentliche Veränderung wurde hingegen im Eigenspannungszustand des rückdeformierten CFL festgestellt. Sowohl in

Umfangs- als auch in Axialrichtung bewirkten die zusätzlichen Temperaturbelastungen während der Deformationsprozesse eine Verringerung der Eigenspannungen auf etwa 1 MPa und darunter. Da an der Rohrinnenseite stets von Zug-Eigenspannungen auszugehen ist, die an eventuell vorhandenen Defekten eine rissöffnende Wirkung haben, ist dies als deutliche Verbesserung des Rohrzustandes anzusehen. Ein weiterer Folgeeffekt von reduzierten Eigenspannungen ist die Erhöhung des Widerstandes gegen Rissinitiierung und langsames Risswachstum, was durch zyklische Ermüdungsversuche an CRB-Prüfkörpern nachgewiesen wurde. Eine Beeinflussung des Versagensverhaltens durch den geringfügig erhöhten Kristallinitätsgrad wurde hingegen nicht beobachtet.

Zusammenfassend kann festgehalten werden, dass mit den angewandten Charakterisierungsmethoden keinerlei negative Auswirkungen auf das Rohrmaterial festgestellt wurden, die auf die für das Close-Fit-Liner-Verfahren typischen Deformations- und Rückdeformationsprozesse zurückzuführen sind. Der deutliche Abbau der Eigenspannungen und folglich die Erhöhung des Widerstandes gegen Rissinitiierung und langsamem Risswachstum stellen sogar eine deutliche Verbesserung gegenüber dem konventionellen Rohr dar und unterstreichen die Zuverlässigkeit von derart installierten Rohrleitungen.

Danksagung

Die vorliegende Forschungsarbeit wurde an der Polymer Competence Center Leoben GmbH im Rahmen des Kompetenzzentren-Programms K_{plus} des Bundesministeriums für Verkehr, Innovation und Technologie unter Beteiligung der Montanuniversität Leoben, AGRU Kunststofftechnik GmbH und Rabmer Rohrtechnik GmbH & Co. KG durchgeführt und mit Mitteln des Bundes und der Länder Steiermark und Oberösterreich gefördert.

Literatur

[1] Brömstrup, H. (2004): PE 100 Pipe Systems, Vulkan Verlag, Essen, Germany

[2] Janson, L.E. (1999): Plastics Pipes for Water Supply and Sewage Disposal, Borealis, Sven Axelsson AB/ Fäldts Grafiska AB, Stockholm, Sweden

[3] Richard, K.; Gaube, E.; Diedrich, G.: (1959). Trinkwasserrohre aus Niederdruckpolyäthylen, Kunststoffe 49 (10): 516-525

[4] Hessel, J. (2006): 50 Jahre Rohre aus PE, 3R International 45 (2006) Nr. 3-4, S. 128-133

[5] Glanert, R.; Schulze, S. (2002). U-Liner – Der Klassiker für die Sanierung von Reuckrohren, Rohrbau congress 2002, Weimar, Deutschland

[6] Rabmer Bautechnologie GesmbH & Co. KG (2009). „Arbeitsanweisung, Heizanleitung Close Fit Rohr", Altenberg, Österreich

[7] Choi, S.; Broutman, L. J. (1997): Residual Stesses in Plastic Pipes and Fitting – IV. Effect of Annealing on Deformation and Fracture Properties. Polymer (Korea) 21(1): 93-102

[8] ISO 11357-3:1999 (E) „Plastics-Differential scanning calorimetry (DSC), Part 3: Determination of temperature and enthalpy of melting and crystallization"

[9] Lohmeyer, S. (1984): Die speziellen Eigenschaften der Kunststoffe, Expert Verlag, Grafenau, Deutschland

[10] ISO 11359-2:1999 (E) "Plastics-Thermomechanical analysis, Part 2: Determination of coefficient of linear thermal expansion and glass transition temperature"

[11] ISO 11357-6:2002 (E) „Plastics-Differential scanning calorimetry (DSC), Part 6: Determination of oxidation induction time"

[12] Pilz, G. (2001): Viscoelastic Properties of Polymeric Materials for Pipe Applications, Dissertation, Institute of Materials Science and Testing of Plastics, University of Leoben, Austria

[13] König, G. (1989): Stand der Technik auf dem Gebiet der Eigenspannungsmessungen, Seminar über Eigenspannungsmessungen, Miskolc, Ungarn

[14] Haager, M.; Pinter, G.; Lang, R.W. (2006): Ranking of PE Pipe Grades by Cyclic Crack Growth Tests with Cracked Round Bar Specimen, Proceedings of ANTEC 2006, Charlotte, North Carolina, USA, Society of Plastics Engineers, 2475-2479

[15] Pinter, G.; Haager, M.; Balika, W.; Lang, R.W. (2007): Cyclic crack growth tests with CRB specimens for the evaluation of the long-term performance of PE pipe grades, Polymer Testing 26 (2), 180-188

[16] Menges, G.; Haberstroh, E.; Michaeli, W.; Schmachtenberg, E. (2002): Werkstoffkunde Kunststoffe, Hanser, München, Deutschland

[17] Grob, M. (2005): Moderne Additivierung – ein effektiver Alterungsschutz für Kunststoffe. Korrosion von Kunststoffen, Frankfurt, Deutschland, Gesellschaft für Korrosionsschutz e.V.

[18] Schulte, U. (2004): HDPE Pipes are More Resistant to Oxidation than the OIT Indicates. Plastics Pipes XII, Baveno, Italien

[19] Allen, N.S.; Hoang, E.; Liauw, C.M.; Edge, M.; Fontan, E. (2001): Influence of processing aids on the thermal and photostabilisation of HDPE with antioxidant blends, Polymer Degradation and Stability 72, 367

[20] Gulmine, J.V.; Janissek, P.R.; Heise, H.M.; Akcelrud, L. (2003): Degradation profile of polyethylene after artificial accelerated weathering, Polymer Degradation and Stability 79, 385

[21] Mendes, L.C.; Rufino, E.S.; de Paula, F.O.C.; Torres Jr, A.C. (2002): Mechanical, thermal and microstructure evaluation of HDPE after weathering in Rio de Janeiro City, Polymer Degradation and Stability 79, 371

Autoren:

A. Frank
Polymer Competence Center Leoben GmbH, Leoben, Österreich

M. Haager
AGRU Kunststofftechnik GmbH, Bad Hall, Österreich

A. Hofmann
Rabmer Rohrtechnik GmbH & Co KG, Altenberg, Österreich

G. Pinter
Institut für Werkstoffkunde und Prüfung der Kunststoffe, Montanuniversität Leoben, Österreich